

CANADIAN THESES ON MICROFICHE

I.S.B.N.

THESES CANADIENNES SUR MICROFICHE



National Library of Canada
Collections Development Branch

Canadian Theses on
Microfiche Service

Ottawa, Canada
K1A 0N4

Bibliothèque nationale du Canada
Direction du développement des collections

Service des thèses canadiennes
sur microfiche

NOTICE

The quality of this microfiche is heavily dependent upon the quality of the original thesis submitted for microfilming. Every effort has been made to ensure the highest quality of reproduction possible.

If pages are missing, contact the university which granted the degree.

Some pages may have indistinct print especially if the original pages were typed with a poor typewriter ribbon or if the university sent us a poor photocopy.

Previously copyrighted materials (journal articles, published tests, etc.) are not filmed.

Reproduction in full or in part of this film is governed by the Canadian Copyright Act, R.S.C. 1970, c. C-30. Please read the authorization forms which accompany this thesis.

THIS DISSERTATION
HAS BEEN MICROFILMED
EXACTLY AS RECEIVED

AVIS

La qualité de cette microfiche dépend grandement de la qualité de la thèse soumise au microfilmage. Nous avons tout fait pour assurer une qualité supérieure de reproduction.

S'il manque des pages, veuillez communiquer avec l'université qui a conféré le grade.

La qualité d'impression de certaines pages peut laisser à désirer, surtout si les pages originales ont été dactylographiées à l'aide d'un ruban usé ou si l'université nous a fait parvenir une photocopie de mauvaise qualité.

Les documents qui font déjà l'objet d'un droit d'auteur (articles de revue, examens publiés, etc.) ne sont pas microfilmés.

La reproduction, même partielle, de ce microfilm est soumise à la Loi canadienne sur le droit d'auteur, SRC 1970, c. C-30. Veuillez prendre connaissance des formules d'autorisation qui accompagnent cette thèse.

LA THÈSE A ÉTÉ
MICROFILMÉE TELLE QUE
NOUS L'AVONS REÇUE



National Library of Canada

Bibliothèque nationale du Canada

Canadian Theses Division

Division des thèses canadiennes

Ottawa, Canada
K1A 0N4

60239

PERMISSION TO MICROFILM — AUTORISATION DE MICROFILMER

• Please print or type — Ecrire en lettres moulees ou dactylographier

Full Name of Author — Nom complet de l'auteur

SHU-MING ALBERT LAI

Date of Birth — Date de naissance

7 AUG 1956

Country of Birth — Lieu de naissance

HONG KONG

Permanent Address — Résidence fixe

20B, NASSAU STREET, 17/F MEI FOO SUN CHEN, KOWLOON,
HONG KONG

Title of Thesis — Titre de la thèse

GEOMETRIC NON-LINEARITY IN MULTISTOREY FRAMES

University — Université

UNIVERSITY OF ALBERTA

Degree for which thesis was presented — Grade pour lequel cette thèse fut présentée

Ph. D.

Year this degree conferred — Année d'obtention de ce grade

FALL, 1982

Name of Supervisor — Nom du directeur de thèse

James G. MacGregor

Permission is hereby granted to the NATIONAL LIBRARY OF CANADA to microfilm this thesis and to lend or sell copies of the film

The author reserves other publication rights, and neither the thesis nor extensive extracts from it may be printed or otherwise reproduced without the author's written permission

L'autorisation est, par la présente, accordée à la BIBLIOTHÈQUE NATIONALE DU CANADA de microfilmer cette thèse et de prêter ou de vendre des exemplaires du film

L'auteur se réserve les autres droits de publication, ni la thèse ni de longs extraits de celle-ci ne doivent être imprimés ou autrement reproduits sans l'autorisation écrite de l'auteur

Date

Aug 11, 1982

Signature

THE UNIVERSITY OF ALBERTA

Geometric Non-Linearity in Multistorey Frames

by

Shu-Ming Albert LAI

(C)

A THESIS

SUBMITTED TO THE FACULTY OF GRADUATE STUDIES AND RESEARCH
IN PARTIAL FULFILMENT OF THE REQUIREMENTS FOR THE DEGREE
OF Doctor of Philosophy

Department of Civil Engineering

EDMONTON, ALBERTA

Fall 1982

MICRO

THE UNIVERSITY OF ALBERTA
RELEASE FORM

NAME OF AUTHOR Shu-Ming Albert LAI
TITLE OF THESIS Geometric Non-Linearity in Multistorey
 Frames
DEGREE FOR WHICH THESIS WAS PRESENTED Doctor of Philosophy
YEAR THIS DEGREE GRANTED Fall 1982

Permission is hereby granted to THE UNIVERSITY OF ALBERTA LIBRARY to reproduce single copies of this thesis and to lend or sell such copies for private, scholarly or scientific research purposes only.

The author reserves other publication rights, and neither the thesis nor extensive extracts from it may be printed or otherwise reproduced without the author's written permission.

(SIGNED) .. *Shu-Ming Lai*

PERMANENT ADDRESS:

.. 20 B. NASSAU STREET, 17/F. ..
.. MEI FOO SUN CHUEN, KOWLOON ..
.. HONG KONG

DATED .. *Aug. 4* .. 1982

THE UNIVERSITY OF ALBERTA
FACULTY OF GRADUATE STUDIES AND RESEARCH

The undersigned certify that they have read, and recommend to the Faculty of Graduate Studies and Research, for acceptance, a thesis entitled Geometric Non-Linearity in Multistorey Frames submitted by Shu-Ming Albert LAI in partial fulfilment of the requirements for the degree of Doctor of Philosophy.

..... *J. H. Mills*

Supervisor

..... *Peter J. Collins*

..... *Donald H. Bell*

..... *R. W. Murray*

..... *[Signature]*

..... *R. Green*

External Examiner

Date..... *Aug 4, 1982*

ABSTRACT

This investigation attempts to develop approximate methods for the second-order elastic analysis of multistorey frames. Because a frame under gravity and lateral loads can be analyzed as a non-sway frame and a sway frame with the final force resultants obtained by superposition, non-sway frames, sway frames and combination of both were investigated separately. Based on analysis of the behavior of elastic non-sway frames and a critical examination of the problems and rationale behind the ACI design method for non-sway slender columns, modifications in this method are suggested. Various approximate second-order analyses for elastic sway frames are derived and their assumptions are discussed in the light of the results of the behavioral study. The approximate analyses were compared to complete second-order analyses of frames to determine the range of application of the approximate methods. A rational method, which is more accurate than the current approaches, is proposed to combine the non-sway and sway moments in a column. Finally recommended procedures for the second-order elastic analysis of frames subjected to both gravity and lateral loads or gravity loads only are proposed, and modifications to the ACI Code design procedure for slender columns are suggested.

ACKNOWLEDGEMENTS

The author would like to express his sincere appreciation to Dr. James G. MacGregor, chairman of the supervisory committee, for his indispensable guidance and inspirational advice throughout all phases of this study. The author is grateful to Dr. Jostein Hellesland (visiting research engineer from Norway), who has given invaluable help to the author in understanding the subject at the early stages of this investigation.

The author also wishes to thank Dr. Roger Green (Professor of Civil Engineering, University of Waterloo), Dr. Donald G. Bellow (Professor of Mechanical Engineering), Dr. Peter F.G. Adams (Dean of Engineering), Dr. David W. Murray, and Dr. Sidney H. Simmonds for their helpful comments as members of the examining committee.

Financial aid provided by the National Research Council of Canada is acknowledged.

The author cannot fully express his appreciation to his fiancée, Henriette Kai-Yee Shen, for her sustaining encouragement during the author's stay in Canada. Finally, the author is greatly indebted to his parents, Mr. and Mrs. Kui-Sing Lai, for their sacrifices which make the author's studies in Canada possible, and to them this book is gratefully dedicated.

TABLE OF CONTENTS

| Chapter | Page |
|---|------|
| 1. INTRODUCTION | 1 |
| 1.1 Background | 1 |
| 1.2 Objectives and scope | 5 |
| 1.3 Outline | 5 |
| 2. BASIC THEORIES AND ASSUMPTIONS FOR ELASTIC FRAMES | 7 |
| 2.1 Introduction | 7 |
| 2.2 Basic equations | 8 |
| 2.3 Exact second-order elastic analysis | 17 |
| 2.4 Effects of axial forces in the beams | 23 |
| 2.5 Elastic critical load and failure load | 27 |
| 2.6 Non-sway and sway frames | 31 |
| 3. BEHAVIOR OF ELASTIC NON-SWAY FRAMES | 36 |
| 3.1 Geometric effects | 36 |
| 3.2 Pin-ended columns | 36 |
| 3.3 Single restrained columns | 42 |
| 3.4 Single-storey frames | 51 |
| 3.5 Multistorey frames | 57 |
| 3.6 Summary | 62 |
| 4. APPROXIMATE SECOND-ORDER ANALYSIS OF ELASTIC NON-SWAY FRAMES | 64 |
| 4.1 Pin-ended columns | 64 |
| 4.2 Effective length method for single restrained columns | 71 |
| 4.3 ACI method | 85 |
| 4.3.1 Single restrained columns | 85 |
| 4.3.2 Multistorey frames | 94 |

| | | |
|-------|--|-----|
| 4.4 | Wood's method | 100 |
| 4.5 | Discussion | 102 |
| 4.5.1 | Pin-ended columns | 102 |
| 4.5.2 | Single restrained columns | 104 |
| 4.5.3 | Multistorey frames | 110 |
| 4.5.4 | Concluding remarks | 112 |
| 5. | BEHAVIOR OF ELASTIC SWAY FRAMES | 103 |
| 5.1 | Geometric effects | 113 |
| 5.2 | Single-storey frames | 116 |
| 5.2.1 | An example frame | 116 |
| 5.2.2 | Individual column behavior | 120 |
| 5.3 | Multistorey frames | 129 |
| 5.4 | Summary | 132 |
| 6. | APPROXIMATE SECOND-ORDER ANALYSIS OF ELASTIC SWAY FRAMES | 134 |
| 6.1 | Iterative method | 134 |
| 6.2 | Modified iterative method | 140 |
| 6.2.1 | The method | 141 |
| 6.2.2 | Flexibility factor | 150 |
| 6.2.3 | Average flexibility factor | 162 |
| 6.3 | Modified negative brace method | 163 |
| 6.4 | Storey magnifier method | 167 |
| 6.5 | Overturning moment method | 170 |
| 6.6 | Frame magnifier method | 175 |
| 6.7 | ACI method | 177 |
| 6.8 | Moment-correction factors | 185 |
| 6.8.1 | Introductory remarks | 185 |
| 6.8.2 | AISC approach | 186 |
| 6.8.3 | Hellesland and MacGregor approach | 189 |
| 6.8.4 | Moment-correction factors for multistorey frames | 196 |
| 6.9 | Summary | 200 |

| | | |
|-------|--|-----|
| 7. | EVALUATION OF THE APPROXIMATE METHODS FOR SWAY FRAMES | 203 |
| 7.1 | Introduction | 203 |
| 7.1.1 | Problem statement | 203 |
| 7.1.2 | Method of evaluation | 204 |
| 7.2 | Single-storey structures | 205 |
| 7.2.1 | Supported sway columns | 205 |
| 7.2.2 | Assumption concerning inflection points | 208 |
| 7.3 | Low-rise multistorey structures | 211 |
| 7.3.1 | Problems | 211 |
| 7.3.2 | Structures studied | 211 |
| 7.3.3 | Results | 213 |
| 7.3.4 | Concluding remarks | 222 |
| 7.4 | High-rise multistorey structures | 223 |
| 7.4.1 | Problems and structures studied | 223 |
| 7.4.2 | Results | 230 |
| 7.4.3 | Concluding remarks | 238 |
| 7.5 | Proposed methods | 239 |
| 8. | PROCEDURES FOR SECOND-ORDER ELASTIC ANALYSIS | 241 |
| 8.1 | Introduction | 241 |
| 8.2 | Combination of non-sway and sway moments | 241 |
| 8.2.1 | Current approaches | 241 |
| 8.2.2 | Proposed approach | 244 |
| 8.3 | Deflections due to gravity load moments | 250 |
| 8.4 | Out-of-plumbs | 255 |
| 8.5 | Summary of the proposed procedures for second-order analysis | 256 |
| 8.5.1 | Introductory remarks | 257 |
| 8.5.2 | Storey magnifier method | 257 |
| 8.5.3 | Frame magnifier method | 262 |
| 8.5.4 | Modified iterative method | 263 |
| 8.5.5 | Modified negative brace method | 265 |
| 8.6 | Modifications to the ACI Code procedure | 266 |
| 8.6.1 | Modified formulae | 266 |
| 8.6.2 | Definitions of braced frames and unbraced frames | 269 |
| 9. | SUMMARY | 272 |

| | |
|------------|-----|
| REFERENCES | 275 |
| APPENDIX A | 282 |
| APPENDIX B | 284 |

LIST OF TABLES

| Table | | Page |
|-------|---|------|
| 2.1 | Load-deflection equations | 16 |
| 2.2 | Fixed-end moments | 16 |
| 6.1 | Formulae for the flexibility factor | 161 |
| 6.2 | Suggested values for the average flexibility factor | 164 |

LIST OF FIGURES

| Figure | | Page |
|--------|---|------|
| 1.1 | Procedure of approximation | 3 |
| 2.1 | Equilibrium of an element | 9 |
| 2.2 | Load-deflection relationship | 11 |
| 2.3 | Symbols and sign convention for the slope-deflection equation | 13 |
| 2.4 | Stability functions | 14 |
| 2.5 | Element stiffness matrix for a second-order elastic analysis | 19 |
| 2.6 | Element stiffness matrix for a second-order elastic analysis (virtual work approach) | 20 |
| 2.7 | Effects of axial forces in the beam | 24 |
| 2.8 | A frame subjected to any loading | 29 |
| 2.9 | Principle of superposition | 32 |
| 3.1 | Deformations and moments in a pin-ended column | 37 |
| 3.2 | Load-deformation relationship for a pin-ended column | 39 |
| 3.3 | Deflected shapes and bending moments of pin-ended columns under increasing compression | 40 |
| 3.4 | Maximum moment in a pin-ended column | 40 |
| 3.5 | Symbols and sign convention for a restrained column | 43 |
| 3.6 | Variation of internal end moments in symmetrically restrained columns under increasing compression | 44 |
| 3.7 | Bending moments and deflected shapes of symmetrically restrained columns under increasing compression | 46 |
| 3.8 | Effects of unsymmetrical restraints on the end moments | 48 |

| | | |
|------|--|----|
| 3.9 | Maximum moments in a restrained column | 49 |
| 3.10 | A single-storey frame | 52 |
| 3.11 | Horizontal interaction between columns for $r_0 = 0.6$ | 54 |
| 3.12 | Horizontal interaction between columns for $r_0 = -0.6$ | 55 |
| 3.13 | A simple two-storey frame | 58 |
| 3.14 | Variation of maximum moments in the top (strong) column of the frame shown in Fig. 3.13 | 60 |
| 3.15 | Variation of maximum moments in the bottom (weak) column of the frame shown in Fig. 3.13 | 61 |
| 4.1 | Comparison of theoretical C_m with approximate equations | 67 |
| 4.2 | Comparison of approximate with theoretical magnification factor | 70 |
| 4.3 | Comparison of approximate with theoretical magnification factor | 72 |
| 4.4 | Effective length method for single restrained columns | 73 |
| 4.5 | Required end moments in an equivalent pin-ended column | 77 |
| 4.6 | Examination of the effective length method for $K_1 = K_2$ and $r_0 = 1.0$ | 79 |
| 4.7 | Examination of the effective length method for $K_1 = K_2$ and $r_0 < 1.0$ | 82 |
| 4.8 | Examination of the effective length method for $K_1/K_2 = \infty$ and $r_0 < 1.0$ | 84 |
| 4.9 | Types of columns corresponding to upper and lower bounds of the maximum moments | 87 |
| 4.10 | Comparison of approximate with theoretical magnification factor for $r_0 = 1.0$ | 88 |
| 4.11 | Comparison of approximate with theoretical magnification factor for $r_0 = 0.5$ | 89 |

| | | |
|------|--|-----|
| 4.12 | Comparison of approximate with theoretical magnification factor for $r_0 = 0.0$ | 90 |
| 4.13 | Comparison of approximate with theoretical magnification factor for $r_0 = -0.5$ | 91 |
| 4.14 | Comparison of approximate with theoretical magnification factor for $r_0 = -1.0$ | 92 |
| 4.15 | A column isolated from a non-sway frame | 95 |
| 4.16 | Effective length factors for non-sway single columns | 101 |
| 4.17 | Inelastic columns | 106 |
| 5.1 | Geometric effects due to axial loads | 114 |
| 5.2 | Single-storey frame with rigid beams | 117 |
| 5.3 | A non-sway frame with imposed lateral deformation | 122 |
| 5.4 | Variation in B values with axial loads for a column with flexible restraints | 126 |
| 5.5 | Variation in B values with axial loads for a column with stiff restraints | 128 |
| 5.6 | Vertical interaction due to N-a effects | 131 |
| 6.1 | Sway forces in the iterative method | 136 |
| 6.2 | A frame with different column heights in the bottom storey | 138 |
| 6.3 | N-a shear of an inclined bracing member | 139 |
| 6.4 | Assumption in the modified iterative method | 142 |
| 6.5 | Vertical displacement of column distortion | 144 |
| 6.6 | The potential energy in a deformed bracing member | 148 |
| 6.7 | Upper limit of the flexibility factor | 152 |
| 6.8 | Column bent by end moments | 154 |
| 6.9 | A column isolated from the frame | 156 |
| 6.10 | Modified negative brace method | 165 |

| | | |
|------|---|-----|
| 6.11 | Loadings and deformation of a shear beam and a bending beam | 174 |
| 6.12 | A storey isolated from the frame (ACI method) | 178 |
| 6.13 | Concept in AISC approach for B_{max} | 188 |
| 6.14 | Approximate values for B_{max} and B_2 | 195 |
| 6.15 | A laterally deformed non-sway multistorey frame | 197 |
| 6.16 | Major assumptions in the approximate methods of second-order analysis for sway frames | 201 |
| 7.1 | Supported sway column | 206 |
| 7.2 | Evaluation of the approximate methods for a single-storey structure | 209 |
| 7.3 | Low-rise structures studied | 212 |
| 7.4 | Approximate vs. exact results for a low-rise structure with strong beams | 214 |
| 7.5 | Evaluation of the moment correction factor for a 3-storey frame with strong beams | 216 |
| 7.6 | Approximate vs. exact results for a low-rise structure with weak beams | 217 |
| 7.7 | Deflection and moment magnification from a 3-storey frame with weak beams | 219 |
| 7.8 | Approximate vs. exact results for a low-rise shear wall | 221 |
| 7.9 | Structure A: A frame with weak beams at the bottom | 224 |
| 7.10 | Structure B: A frame with a flexible shear wall of constant stiffness | 225 |
| 7.11 | Structure C: A frame with a flexible shear wall of two discrete stiffnesses | 226 |
| 7.12 | Structure D: A frame with a flexible discontinuous shear wall | 228 |

| | | |
|------|--|-----|
| 7.13 | Structure E: A frame with very strong columns (weak beams) at the bottom | 229 |
| 7.14 | Approximate vs. exact solutions for Structure A | 231 |
| 7.15 | Approximate vs. exact solutions for the frame in Structure B | 232 |
| 7.16 | Bending moments in the shear wall of Structure B | 234 |
| 7.17 | Approximate vs. exact solutions for Structure C | 235 |
| 7.18 | Approximate vs. exact solutions for Structure D | 236 |
| 7.19 | Approximate vs. exact solutions for Structure E | 237 |
| 8.1 | Schematic development of the proposed approach for combining the non-sway and sway moments | 245 |
| 8.2 | Combination of the non-sway and sway moments | 248 |
| 8.3 | Holding shears in a non-sway frame with imposed displacements | 252 |

NOTATION

Roman letters, capital

| | |
|------------|--|
| B | moment (or shear) correction factor for sway columns |
| C | stability function in the slope-deflection equation (Eq. 2.3) |
| C_m | moment gradient correction factor |
| EI | flexural stiffness of a column |
| EI_B | flexural stiffness of a beam |
| G | ratio of column stiffness to beam stiffness defined in Eq. 6.16 |
| G_l | larger value of G for a given column |
| G_s | smaller value of G for a given column |
| H | horizontal load applied at the joint |
| H_s | sway force applied at the joint |
| K | rotational restraint stiffness at the end of a column |
| L | column length |
| L_B | beam length |
| M | moment in a column |
| M_t | external moment applied at the joint |
| $\sum M_H$ | sum of the overturning moments of the horizontal loads about the base of a structure |
| N | axial force in a column (positive for compression) |
| N_e | Euler load defined by $\pi^2 EI/L^2$ |
| N_{fs} | free-to-sway critical load of an elastic column |
| N_{ns} | non-sway critical load of an elastic column |
| S | stability function in the slope-deflection equation (Eq. 2.3) |
| V | shear at the end of a column |

Roman letters, lower case

- a sway deflection of the upper end of a column (or a storey) relative to the lower end
- e vertical displacement of the upper end of a column relative to the lower end due to flexural shortening of the column
- e_r vertical displacement of a rigid column due to the rigid body rotation of the column length
- f_s sway deflection magnifier defined by a/a_0
- g symbol in formulation of approximate equations for B.
- k_{fs} effective length factor of an elastic free-to-sway column
- k_{ns} effective length factor of an elastic non-sway column
- k_m modified effective length factor used in the effective length method for non-sway columns* to give exact solutions
- n total number of storeys
- r ratio of end-moments, $-M_1/M_2$
- r_0 ratio of first-order end-moments, $-M_{01}/M_{02}$

Greek letters

- α axial load index, N/N_e
- α_{fs} axial load index, N/N_{fs}
- α_{ns} axial load index, N/N_{ns}
- β $\pi\sqrt{N/N_e}$
- $\bar{\beta}$ $\pi\sqrt{N/N_{ns}}$
- δ moment magnification factor, M_{max}/M_2
- δ_1 δ corresponding to $r = 1.0$
- δ_{ns} moment magnification factor for a restrained non-sway column, M_{max}/M_{02}
- Δ horizontal displacement of a floor from the original position
- γ flexibility factor

$\bar{\gamma}$ average flexibility factor
 θ end-rotation of a column (except in Fig. 6.3 or 6.6)
 λ load factor
 λ_c critical load factor
 ψ ratio of column stiffness to beam stiffness defined in Fig. 5.3(d)

Subscripts

1, 2 indicate ends of a column
max maximum moment
ns non-sway column
0 first-order effects (for $N = 0$)
s sway column
t total
w wall

1. INTRODUCTION

1.1 Background

Two major difficulties in the analysis and design of slender reinforced concrete frames result from:

- the 'material non-linearity' caused by the inelastic properties of materials, and
- the 'geometric non-linearity' caused by the effects of displacement on the equilibrium of individual members and of the whole structure.

A structural analysis which includes these non-linearities is referred to as second-order inelastic analysis. A second-order elastic analysis, which includes the geometric non-linearity only, assumes elastic response of the structure. The simplest type of structural analysis is a first-order elastic analysis, which neglects both non-linearities.

The first-order elastic analysis is the most widely used technique in current design practice. As a result, the current design approaches for slender concrete columns are based on approximate methods to include the effects of the two non-linearities by modifying the first-order elastic analysis (MacGregor et al., 1970). This is because the modified first-order elastic analysis is currently much simpler and less time-consuming than the other two analyses, especially in a design situation where iteration, and trial and error are usually involved. A significant advantage of

the approximate methods is that the significant parameters affecting the end results are normally apparent during the calculations, allowing the designer more control over the final selection of dimensions and the final distribution of forces in the structure. This is seldom the case with complex analysis techniques.

In deriving the final approximate method, two distinct steps are generally involved, as shown in Fig. 1.1. In step 1, the stiffness parameter EI of individual members is considered. The EI values used in the second-order elastic analysis are selected in such a way that the results obtained are close to those from the second-order inelastic analysis corresponding to a defined limit state of ultimate strength. This modified EI of a particular member should be regarded as the effective EI for the entire length of that member, accounting for all the inelastic effects. This has been discussed by MacGregor (1972). In step 2, the first-order elastic analysis is modified to obtain results close to those from the second-order elastic analysis. Note that the effective EI values selected in step 1 are used in both analyses in step 2. As apparent from the above procedure, the effects of the two non-linearities are approximated independently of each other.

In step 1, it has been tacitly assumed that the inelastic structure behaves in a way that can be represented by the elastic behavior modified with the effective EI . In fact, this is the basic assumption in the present American

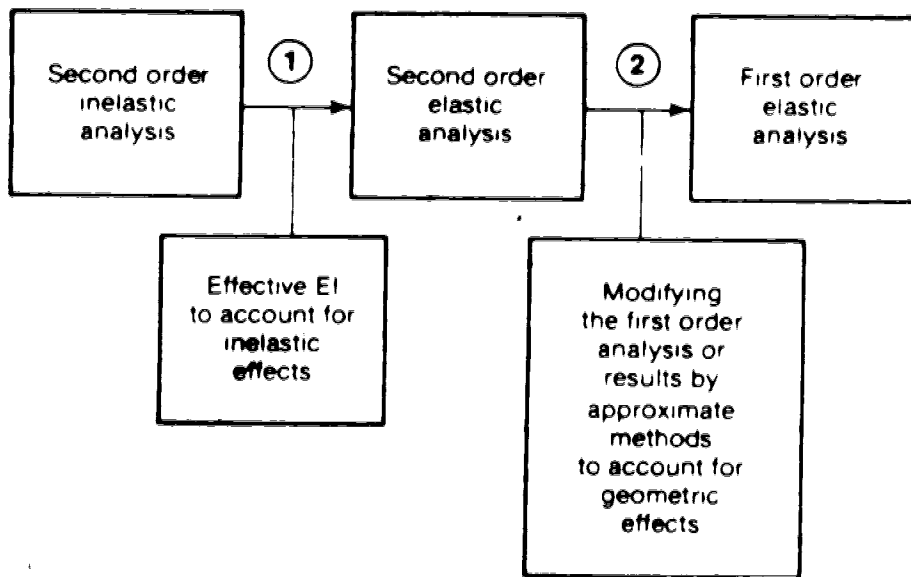


Fig. 1.1 Procedure of approximation

Concrete Institute Code (1977), which allows the use of elastic theory in analysis. The ultimate strength limit state, implicit in the ACI Code, is defined by the reaching of the first plastic hinge or the simultaneous occurrence of plastic hinges in several critical sections. It is generally believed that the elastic analysis is still reasonable at this limit state (or strictly speaking, immediately prior to the occurrence of this limit state).

Several investigators (Kordina, 1972; Hage, 1974; MacGregor, Oelhafen and Hage, 1975) have suggested simple expressions for the effective EI of concrete beams and columns. Wood and Shaw (1979) have suggested a more complicated approximate method to determine the effective EI for a restrained concrete column bent in symmetrical single-curvature. The results from their method were shown in excellent agreement with 'exact' analytical solutions.

The modification of the first-order analysis in step 2 (Fig. 1.1) is the primary objective of the present study. Here a number of approximate methods are available to account for the effects of the geometric non-linearity (or geometric effects), notably the traditional effective length factor approach in the current ACI Code (1977) procedure for designing slender columns. As a part of this investigation, the ACI Code approach and other current approaches are critically reviewed.

1.2 Objectives and scope

The present investigation is concerned with step 2 in Fig. 1.1, and thereby only elastic frames are considered.

The objectives of this study are:

- to analyze the geometric effects on the behavior of the elastic single and multi-storey frames,
- to develop approximate methods for the second-order analysis of elastic multi-storey frames.

The present study is limited to plane frames and static loads. Unless stated otherwise, the type of structures to be considered is as follows: The structure can include bracing elements which may be shear walls or inclined bracing elements such as diagonal braces. In general, no distinction will be made between a column and a shear wall unless stated otherwise. Inclined bracing elements are assumed to be pin-ended. A joint can be either rigid or pinned. All individual members must be prismatic.

Two types of loadings are considered - gravity loads and horizontal loads. The horizontal loads are assumed to be concentrated loads applied at the joints.

1.3 Outline

The theories and basic assumptions used to study the geometric effects in columns and frames are reviewed in Chapter 2. It will be shown in this chapter that a general frame can be decomposed into a non-sway frame subjected to external moments at the joints and column axial forces, plus

a sway frame subjected to lateral loads and column axial forces. The non-sway frame is studied in Chapters 3 and 4, and the sway frame is studied in Chapters 5, 6 and 7. The combination of the load effects from the non-sway and sway frames is studied in Chapter 8, which also concludes the investigation. The whole study is summarized in Chapter 9.

2. BASIC THEORIES AND ASSUMPTIONS FOR ELASTIC FRAMES

2.1 Introduction

The basic theories and assumptions used to study geometric effects in columns and frames are reviewed in this chapter. The standard assumptions and the basic equations for the elastic analysis of individual members and of a frame are presented in Sect. 2.2, which also includes the discussion of the principle of superposition. The 'exact' second-order elastic analysis is described in Sect. 2.3. In addition to the standard assumptions mentioned in Sec. 2.3, it will be assumed that the effect of axial forces in the beams can be neglected in the analysis. This is discussed in Sect. 2.4.

In the analysis of elastic frames, the terms 'elastic critical load' (or buckling load) and 'elastic failure load' are frequently encountered. Their relationship is discussed in Sect. 2.5. The theorem developed in Sect. 2.5 will serve as a basis for subsequent investigation on the behaviour of elastic frames. In Sect. 2.6, it will be shown that a frame under gravity and lateral loads can be analyzed as a non-sway frame and a sway frame with the final force resultants obtained by superposition. The study on elastic frames in subsequent chapters are based on this principle.

2.2 Basic equations

The basic equation for in-plane elastic analysis of a member subjected to axial loads and lateral loads is derived from an infinitesimal element as shown in Fig. 2.1. By taking the equilibrium of moments and forces, and using Eq. 2.1, Eq. 2.2 can be obtained (Timoshenko & Gere, 1961).

$$M = -EIy'' \quad (2.1)$$

$$(EIy'')'' + Ny'' = q \quad (2.2)$$

All the symbols have been defined in Fig. 2.1. The second term in Eq. 2.2 gives the effect of geometry on the moments and deflections. It is referred to as the geometric non-linearity. The application of the above equations in an analysis is often called a second-order analysis. A first-order equation would result if the contribution of the axial force N in the moment equilibrium, i.e., the geometric effect, were neglected (Fig. 2.1).

Several assumptions are required to derive Eqs. 2.1 and 2.2 (Chen & Atsuta, 1976):

1. Material is linearly elastic.
2. Shear deformations are neglected.
3. Effects of Poisson's ratio are neglected.
4. Deformations are assumed to be small.

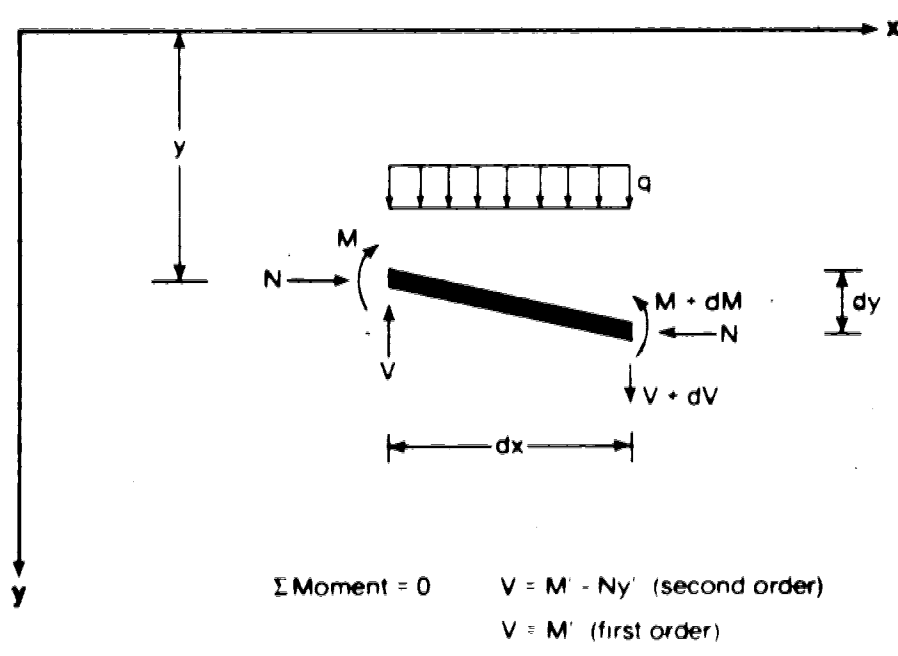
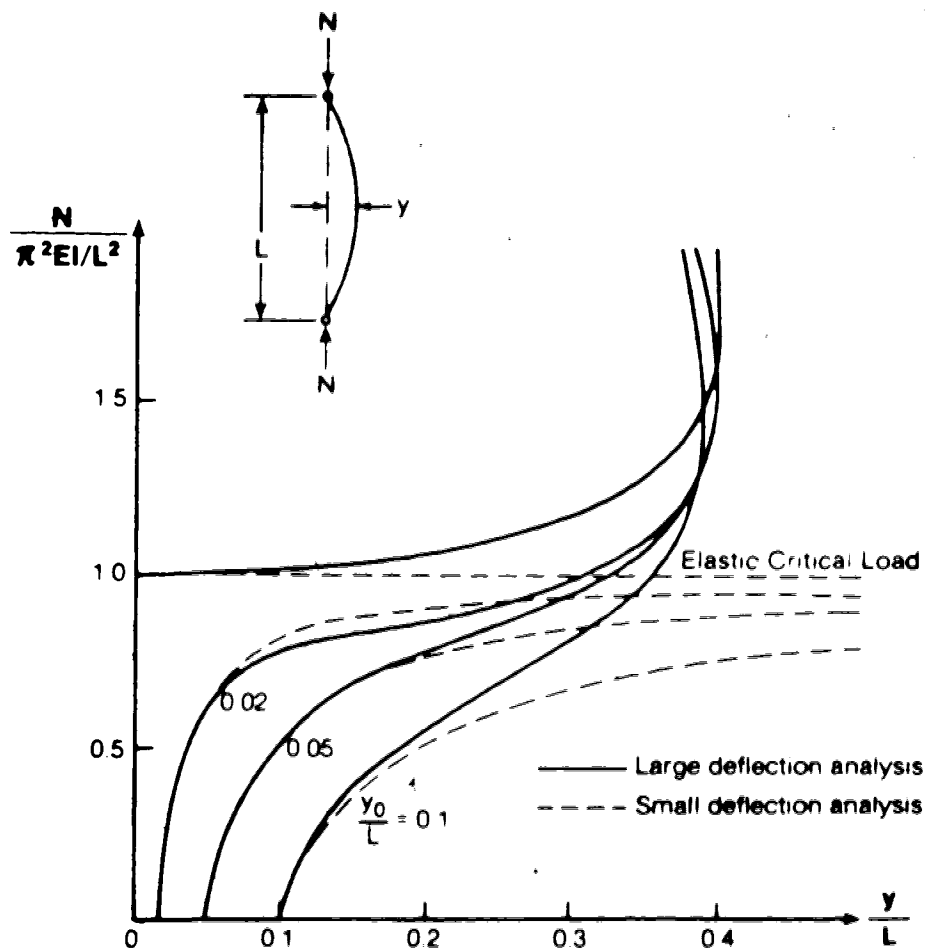


Fig. 2.1 Equilibrium of an element

Assumption 1 is the basic condition. Assumptions 2 and 3 are valid for elements with lateral dimensions that are small compared to their length. As to assumption 4, apparent conflicts occur when the elastic critical load elastic failure load of a structure is reached. The terms elastic critical load and elastic failure load refer to the values from the small-deflection analysis. Based on the small-deflection theory, the deflection of a straight column is indeterminate at the critical load. For an initially bent column the deflections become infinite when the elastic failure is reached. To examine this problem, a more exact analysis that takes into account the effects of large deflections is compared in Fig. 2.2 (from Chen & Atsuta, 1976) to the analysis based on Eq. 2.2. In this figure, the mid-height deflections of a pin-ended column with different magnitudes of initial imperfection are compared.

For an initially straight column, it is seen from the figure that the deflection is determinate in the large deflection analysis. When the load is only slightly in excess of the critical load, the deflections become extremely large, though the bent configuration is in stable equilibrium. For initially bent columns, it is apparent and shown from the figure that the small-deflection theory breaks down when the deflections are no longer small. Nevertheless, similar to the case of the initially straight column, the deflections at the elastic failure load are very large, although the column can remain stable for loads



**Fig. 2.2 Load-deflection relationship
(from Chen & Atsuta, 1976)**

higher than the failure load. The above observations suggest that the elastic critical load or elastic failure load serves as a good indicator of the load at which the structure undergoes very large deformations. In the following study on elastic columns, it is assumed that the deformations are small up to loads slightly less than the elastic failure load. Although the small-deflection analysis fails to predict the magnitudes of loading effects in the vicinity of the failure load, it is believed that the trends of behavior can be reasonably predicted and the failure load serves as a practical upper limit of the loading. In other words, the study of elastic columns will not be extended to the post-failure region.

When Eq. 2.2 is solved with appropriate end conditions, the slope deflection equation relating the end moments and deformations (Fig. 2.3) for a prismatic member can be derived (Bleich, 1952):

$$M_1 = \frac{EI}{L} [C(\theta_1 - \rho) + S(\theta_2 - \rho)] \quad (2.3)$$

The terms C and S are functions of N/N_e and referred to as stability functions. The term N_e is defined as $\pi^2 EI/L^2$. In a first-order analysis, the values of C and S are taken as 4 and 2, respectively, corresponding to $N = 0$.

The physical significance of the C and S functions can be shown using a member with a hinged end and a fixed end (Fig. 2.4). The term $C \cdot EI/L$ represents the rotational

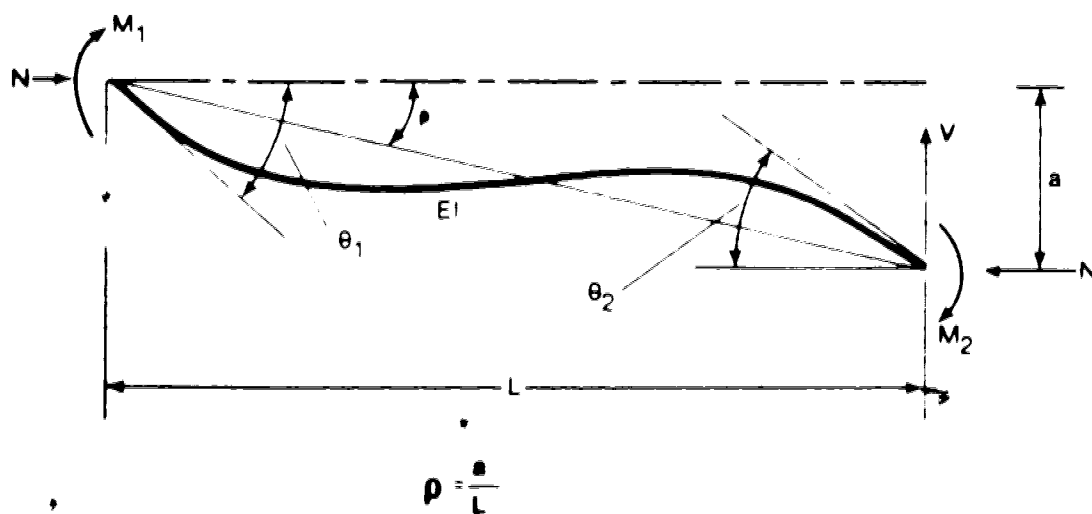
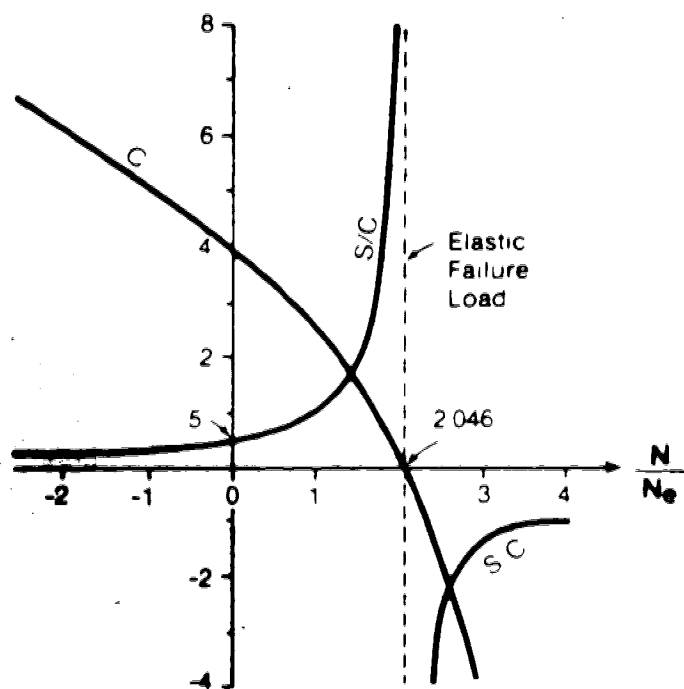
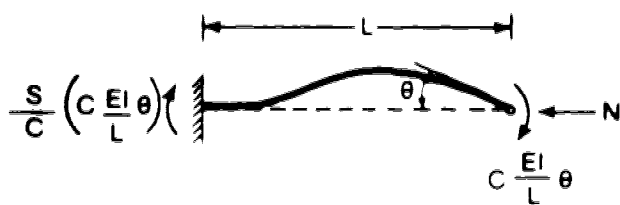


Fig. 2.3 Symbols and sign convention for the slope-deflection equation



$$C = \frac{c}{c^2 - s^2}$$

$$S = \frac{s}{c^2 - s^2}$$

$$N > 0 \quad c = \frac{1}{\beta^2} (1 - \beta \cot \beta) \quad s = \frac{1}{\beta^2} \left(\frac{\beta}{\sin \beta} - 1 \right)$$

$$N < 0 \quad c = \frac{1}{\hat{\beta}^2} (\hat{\beta} \coth \hat{\beta} - 1) \quad s = \frac{1}{\hat{\beta}^2} \left(1 - \frac{\hat{\beta}}{\sinh \hat{\beta}} \right)$$

$$\beta = \pi \sqrt{\frac{N}{N_e}} \quad \hat{\beta} = \pi \sqrt{\frac{-N}{N_e}}$$

Fig. 2.4 Stability Functions

stiffness for moment applied at the hinged end and S/C is the carry-over factor. These terms are plotted in Fig. 2.4. The figure shows that the stiffness at the hinged end of the member decreases with increase in compression and becomes zero at elastic failure, followed by an increase in negative stiffness. The negative stiffness implies that the end moment acts in the opposite direction to the end rotation. Such moment is often called restraining moment. For this to happen, the column has to be connected at its ends to other members capable of supplying the restraint. The carry-over factor S/C , however, increases with increasing compressive load and becomes infinite at failure. With increasing tensile load, the member stiffness is strengthened and the carry-over factor is reduced.

Table 2.1 shows the load-deflection equations for several loading cases which were developed by solving Eq. 2.1 or 2.2 with appropriate boundary conditions. All three equations indicate the linearity of the relationship between applied forces and deformation for a given location and a constant axial force N . This justifies the application of the principle of superposition to a sequence of operations provided the axial forces in the members are held constant in each operation. Therefore, a more general slope deflection equation which includes the effects of lateral loads acting between the ends is possible:

Table 2.1 Load-deflection equations (from Timoshenko & Gere, 1961)

| | |
|--|--|
| | $y = \frac{1}{N} \left[-M_1 + (M_1 + M_2) \frac{x}{L} + M_1 \cos \beta \frac{x}{L} - (M_1 \cos \beta - M_2) \sin \beta \frac{x}{L} / \sin \beta \right]$ |
| | $y = \frac{wL^2}{2N\beta^2} \left[-\beta \frac{x}{L} (\beta - \beta \frac{x}{L}) + \sin \frac{\beta x}{2L} \sin \frac{1}{2} (\beta - \beta \frac{x}{L}) \cos \frac{\beta}{2} \right]$ |
| | $y = \frac{PL}{N\beta} \sin \beta \frac{c}{L} \sin \beta \frac{x}{L} - \sin \beta - \frac{Pc}{NL} x$ <p style="text-align: center;">$0 < x < L - c$</p> |

Note $\beta = \pi \sqrt{\frac{N}{N_e}}$ where $N_e = \frac{\pi^2 EI}{L^2}$

Equations for axial tensions require changes from trigonometric to hyperbolic functions and occasional sign changes

Table 2.2 Fixed end moments (from Home & Merchant 1965)

| | |
|--|--|
| | $\frac{M_1}{wL^2/12} = \frac{3}{u^2} (1 - u \cot u)$ |
| | $\frac{M_1}{PL/8} = \frac{2(1 - \cos u)}{u \sin u}$ |

Note $u = \frac{\pi}{2} \sqrt{\frac{N}{N_e}}$

$$M_1 = M_{1f} + \frac{EI}{L} [C(\theta_1 - \rho) + S(\theta_2 - \rho)] \quad (2.4)$$

where M_{1f} is the fixed-end moment. The equations for two common loadings are shown in Table 2.2. The fixed-end moment increases with an increase in compression and theoretically becomes infinite at $N = 4N_e$. With an increase in tension, the fixed-end moment decreases gradually.

2.3 Exact second-order elastic analysis

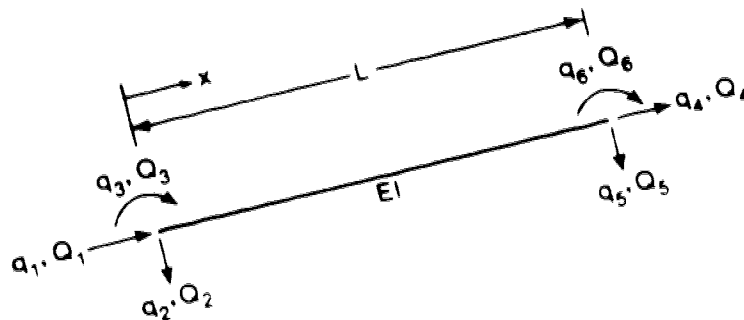
In this study, the second-order elastic frame analysis is based primarily on the slope-deflection equation (Eq. 2.4). The solution is obtained by considering force equilibrium and geometric compatibility at the joints. Furthermore, the shear equilibrium equations are formulated in the deformed configuration of the frame. The geometric effects due to the axial forces in the beams are neglected in the analysis. This will be shown to be a reasonable assumption in Sect. 2.4.

The load effects resulting from the above analysis are considered as exact solutions. The 'first-order' load effects are those from a first-order elastic analysis where $C = 4$ and $S = 2$ are used in the slope-deflection equation and where the formulation of shear equilibrium equations is based on the undeformed configuration of the frame. The term 'first-order' will always accompany the first-order load effects, and the symbol for any of these load effects will have a subscript 0 (implying $N = 0$).

When large multistorey frames are analyzed, a finite-element program will be used. The element stiffness matrix for a second-order elastic analysis can be derived using the slope-deflection equation (Eq. 2.3) and following the same standard procedure for a first-order element stiffness matrix except that the shear equilibrium is formulated in a deformed configuration. The matrix developed in this way is shown in Fig. 2.5. When the element axial force N is set equal to zero (i.e., $C = 4$, $S = 2$ also), it can be seen that the stiffness matrix becomes a first-order stiffness matrix.

A second approach to determine the stiffness matrix is to make use of the virtual work principle and to assume a third-degree polynomial for the deflection. (Note that the third-degree polynomial is only exact for the first-order deflection.) The matrix so obtained is composed of a first-order element stiffness matrix $[K_0]$ and a geometric element stiffness matrix $[K_G]$ which is a function of the element axial load N , as shown in Fig. 2.6. When the axial load equals zero, the geometric matrix vanishes. The stiffness matrix from the latter approach (Fig. 2.6) is derived in Appendix A.

Although the first approach is 'exact', the second approach is used in this study for easier programming. Using simple elastic structures, Aas-Jakobsen (1973) has tested the second approach. It was found that the solutions are converged to very accurate results when a member is divided into two elements for analysis. In this study, a



Local nodal displacements and forces

$$[K] \{q\} = \{Q\}$$

$$[K] = \begin{bmatrix} \frac{EA}{L} & & & & & \\ 0 & \frac{2(C+S)EI}{L^3} - \frac{N}{L} & & & & \\ 0 & \frac{(C+S)EI}{L^2} & \frac{CEI}{L} & & & \\ -\frac{EA}{L} & 0 & 0 & \frac{EA}{L} & & \\ 0 & -\frac{2(C+S)EI}{L^3} + \frac{N}{L} & -\frac{(C+S)EI}{L^2} & 0 & \frac{2(C+S)EI}{L^3} - \frac{N}{L} & \\ 0 & \frac{(C+S)EI}{L^2} & \frac{SEI}{L} & 0 & -\frac{(C+S)EI}{L^2} & \frac{CEI}{L} \end{bmatrix} \quad \text{(SYM.)}$$

Note: the axial force N is positive for compression (ie $N = Q_1$)

Fig. 2.5 Element stiffness matrix for a second order elastic analysis

$$[K] = [K_0] + [K_G]$$

$$[K_0] = \begin{bmatrix} \frac{EA}{L} & & & & & & \\ 0 & \frac{12EI}{L^3} & & & & & \\ 0 & \frac{6EI}{L^2} & \frac{4EI}{L} & & & & \\ -\frac{EA}{L} & 0 & 0 & \frac{EA}{L} & & & \\ 0 & -\frac{12EI}{L^3} & -\frac{6EI}{L^2} & 0 & \frac{12EI}{L^3} & & \\ 0 & \frac{6EI}{L^2} & \frac{2EI}{L} & 0 & -\frac{6EI}{L^2} & \frac{4EI}{L} & \end{bmatrix} \quad (\text{SYM.})$$

$$[K_G] = N \begin{bmatrix} 0 & & & & & & \\ 0 & -\frac{6}{5L} & & & & & \\ 0 & -\frac{1}{10} & -\frac{2L}{15} & & & & \\ 0 & 0 & 0 & 0 & & & \\ 0 & \frac{6}{5L} & \frac{1}{10} & 0 & -\frac{6L}{5} & & \\ 0 & -\frac{1}{10} & \frac{L}{30} & 0 & \frac{1}{10} & -\frac{2L}{15} & \end{bmatrix} \quad (\text{SYM.})$$

Note the axial force N is positive for compression (ie, $N = Q_1$)

Fig. 2.6 Element stiffness matrix for a second order elastic analysis (virtual work approach)

member is divided into four elements for analysis, which should guarantee sufficiently accurate results. For simplicity, the results from such analysis are also referred to as 'exact' values. The finite-element program for the second-order elastic analysis was obtained by modifying a first-order elastic analysis program for plane frames developed by EL-Zanaty and Murray (1980).

After obtaining the end-moments and axial forces from the exact second-order frame analysis, the method of determining the maximum moment in any member can be derived as follows: Solving Eq. 2.2 with a given set of end moments and end displacements and applying Eq. 2.1 gives an equation for the bending moment M at any point x along the column. The maximum moment M_{\max} , determined by setting $dM/dx = 0$, can be written in the form of (Galambos, 1968):

$$M_{\max} = \delta M_2 \quad (2.5)$$

and

$$\delta = \frac{1}{\cos\left(\beta \frac{\bar{x}}{L}\right)} \quad (2.6)$$

where \bar{x} is the location of M_{\max} and defined by

$$\tan\left(\beta \frac{\bar{x}}{L}\right) = \frac{r - \cos \beta}{\sin \beta} \quad (2.7)$$

The term δ is the magnification factor by which the numerically larger end moment M_2 is modified to obtain the maximum moment. The symbols r and β are defined by:

$$r = - \frac{M_1}{M_2}$$

$$\beta = \pi \sqrt{N/N_e}$$

The sign convention and other symbols have been defined in Fig. 2.3.

For $N < N_e$, it can be shown (Galambos, 1968) from Eq. 2.7 and some trigonometric manipulation that

$$\delta = \frac{+\sqrt{1 + r^2 - 2 r \cos \beta}}{\sin \beta} \quad (2.8)$$

Since \bar{x} may not be negative, the limit occurs when $r = \cos \beta$ as shown in Eq. 2.7. In other words,

$$\delta = 1.0 \quad \text{for } r < \cos \beta \quad (2.9)$$

and Eq. 2.8 is used when $r > \cos \beta$.

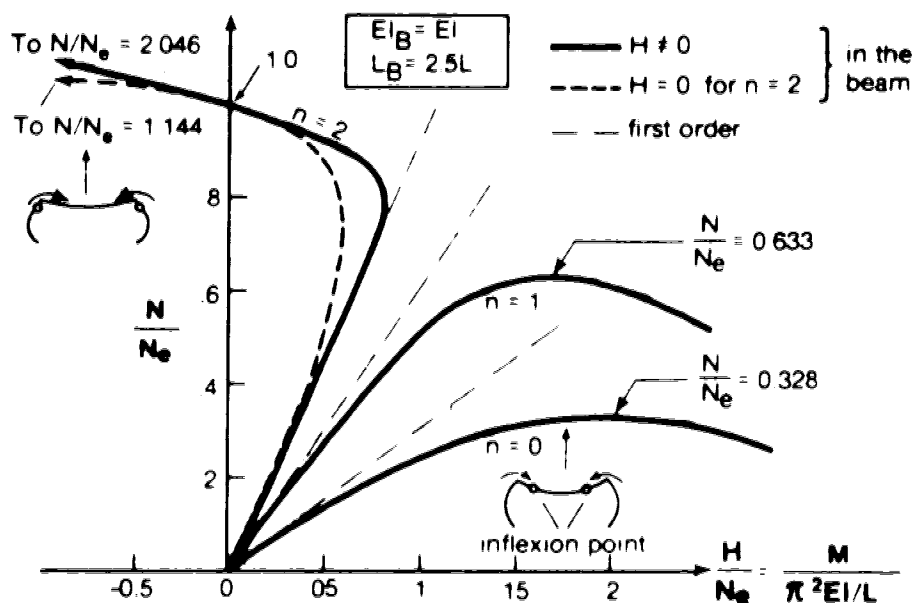
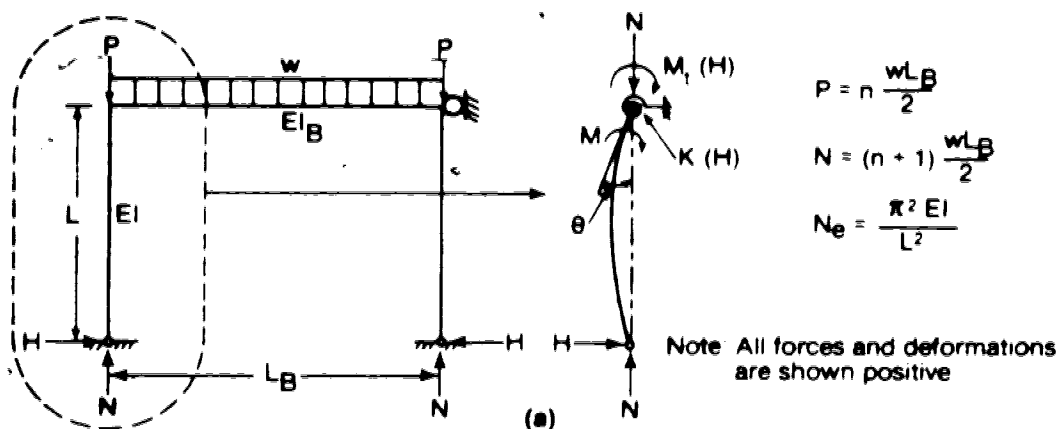
For $N > N_e$ it is possible to have more than one root in Eq. 2.6. Nevertheless, if $\frac{\pi}{2} < \beta \frac{\bar{x}}{L} < \pi$ is assumed, Eq. 2.8 will result. This has been shown graphically by Wood (1953). This assumption can be shown to be valid for $N < 4 N_e$ by a cumbersome calculation which computes all possible roots and determines the maximum one within the

region $0 < x < L$. Note that the limit given by Eq. 2.9 is not required for $N > N_e$.

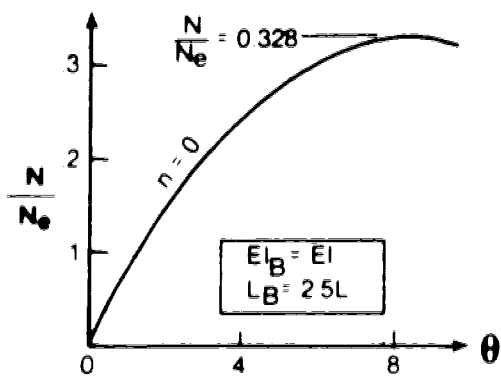
2.4 Effects of axial forces in the beams

In this study, the geometric non-linearities resulting from the axial forces in the beams are neglected in the analysis of elastic frames. The axial force in a beam is a function of the lateral and gravity loads. It is arbitrarily assumed that the lateral loads are not large enough to produce any significant axial forces in the beams. For the gravity loads, which not only produce axial forces in the columns but may also induce axial forces in the beams due to the gravity load moments, the problem is more complicated. (The first-order gravity load moments will be referred to as primary bending moments.) An attempt will be made to examine this problem by investigating the behavior of the simple elastic non-sway frame shown in Fig. 2.7(a) under several conditions. A similar problem has been discussed by Masur et al. (1956), Lu (1961), Horne and Merchant (1965), and McGuire (1968).

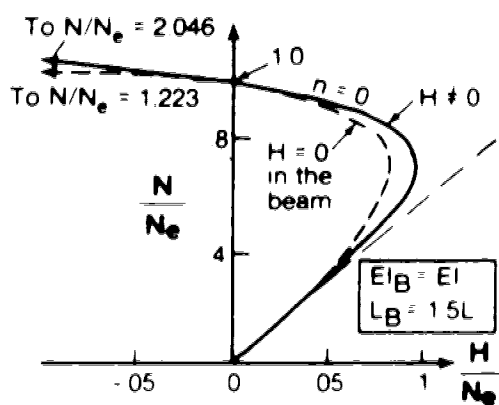
The non-sway portal frame in Fig. 2.7(a) is assumed to carry simultaneously a uniform distributed load w and concentrated loads P applied at the top of the columns. The concentrated load is related to the distributed load by a proportional constant n defined in the figure. The parameter n attempts to simulate the number of storeys above the column ends. The results of the primary bending



(b)



(c)



(d)

Fig. 2.7 Effects of axial forces in the beam

moments become less dominant. Note that the column axial force N is also related to w (Fig. 2.7(a)).

Because the frame is a symmetrical structure with symmetrical loading, the framed column can be simplified to a single restrained column, also shown in Fig. 2.7(a). The elastic spring stiffness K and the externally applied moment M_e , which is equal to the fixed-end moment due to the distributed load, become non-linear functions of the axial force in the beam, which in turn is equal to the horizontal base reaction H .

Based on the single restrained column, the solution can be formulated using the slope-deflection equation (Eq. 2.3) and fixed-end moments (Table 2.2), considering force equilibrium and rotation compatibility at the joint. The solution obtained by iteration leads to the relationship between the column axial load N and the horizontal base reaction H or the end moment M , described in Fig. 2.7(b) for a low wide frame with a span 2.5 times the column height. The results are given for different values of n .

In Fig. 2.7(b), the curve for $n = 0$ indicates that the column axial force N reaches a peak value and then decreases as the axial force in the beam increases. In this case, the maximum load ($0.328 N_e$) is considerably less than the failure load ($1.144 N_e$) predicted by neglecting the axial force in the beam. Such a small maximum load is attributed to the rapid decrease of the beam stiffness caused by the significant compression of the beam due to the horizontal

reactions. The figure also shows that the column end-moment increases more rapidly than the first-order moment. This suggests that the column is in fact restraining the beam.

Fig. 2.7(c) presents the load-deformation relationship for the same frame and same loading condition ($n = 0$). The very large joint rotation at the maximum load implies an inconsistency with the small-deflection assumption in the analysis. Although this should not affect the trend of the behavior, a practical consideration is that the large deformation produced by the dominant bending moments would bring about a material failure long before the geometric effects become important.

A higher maximum load is obtained for $n = 1$ (Fig. 2.7(b)), since the primary bending moments become less significant. For $n = 2$, the end-moment M_2 initially increases slightly more than the first-order value but later drops rapidly due to a more rapid decrease in column stiffness than beam stiffness. It becomes zero at $N = N_e$. With further increase in N , the end moment changes direction and thus causes tension in the beam, thereby stiffening it. At the failure load, the end moment theoretically approaches infinity, and thus induces an infinitely large tension in the beam and hence an infinitely stiff beam. The failure load so obtained would be the same as that of a column with a fixed support at the upper end. This, however, is incorrect because the large-deflection analysis (Fig. 2.2) indicates that the internal forces (or deformations) never

approach infinity. It appears more reasonable to assume that the failure load is equal to that predicted by neglecting the beam axial force. Figure 2.7(b) also shows that when the beam axial force is neglected in the analysis for $n = 2$, the end-moment is underestimated before the moment changes direction. Better agreement is expected for higher values of n .

The results of an analysis of a frame with shorter span ($L_B = 1.5 L$) and $n = 0$ are shown in Fig. 2.7(d). Here the effect of the axial force in the beam is smaller since the beam is stiffer. The exact curve compares reasonably well with the one which ignores the axial force in the beam.

In conclusion, the above observations suggest that the geometric effects due to the axial forces in the beams can be neglected in the analysis except for very low wide frames with dominant primary bending moments. In such frames, the large deflections induced by the bending moments, however, would bring about a material failure long before the geometric effects become significant. Hence, the exceptional case should pose no practical problems.

2.5 Elastic critical load and failure load

The 'elastic critical load' is the load at which an elastic frame with initially straight members buckles (i.e., bifurcation of equilibrium). Such a frame must only carry concentrated loads at the joints in such a manner that the only internal forces acting, before buckling occurs, are

axial loads in the members. For a normal structure with deformations from the outset, the 'elastic failure load' is attained when the structure undergoes indefinitely large deformations. In this section, the relationship between the elastic failure load and the elastic critical load is examined.

Figure 2.8(a) illustrates a frame that may be subjected to any loading. The first-order deflection y_0 at any point of the frame can be expressed as an infinite series of the form:

$$y_0 = \sum_{i=1}^{\infty} C_{0i} \bar{y}_i \quad (2.10)$$

where \bar{y}_i is the elastic critical deflection mode i corresponding to critical load factor λ_{ci} . The coefficient C_{0i} is the magnitude of critical mode i . The critical load factors are obtained from the modified state of loading of the frame in which the only internal forces acting are the member axial forces, as shown in Fig. 2.8(b). The axial forces are related by a load factor λ such that when $\lambda = 1$, the axial loads in the members are equal to those in the original frame. The load factor is increased to λ_{ci} for buckling of the frame in critical mode i . Based on the orthogonality relationship of the critical modes, developed by Horne (1962), and the principle of minimum potential energy, it is found that the total deflection y of the frame under the action of both vertical and lateral loads

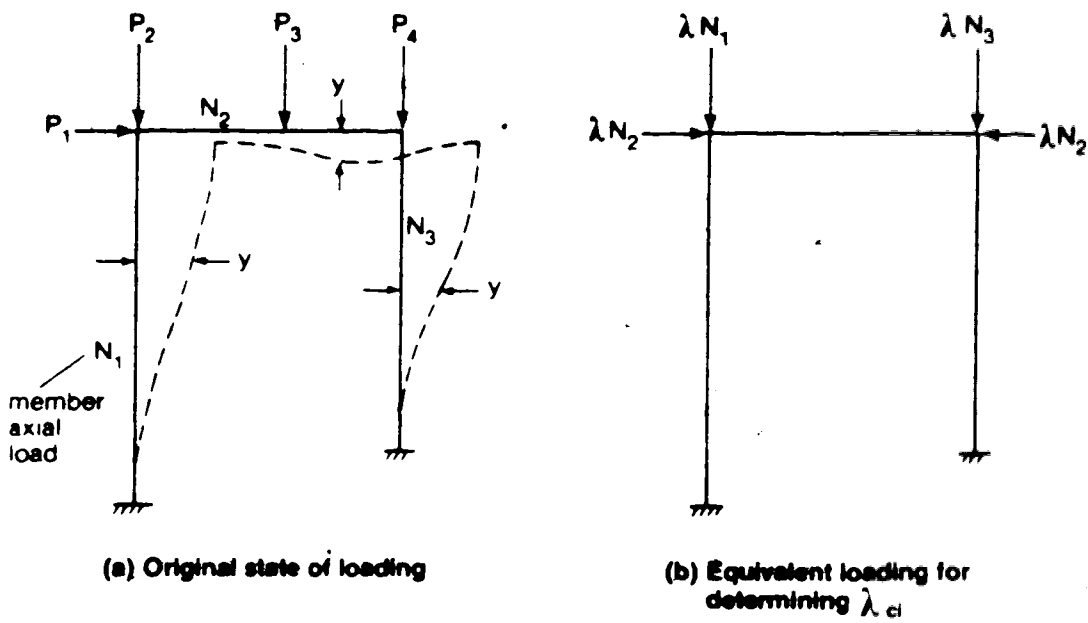


Fig. 2.8 A Frame subjected to any loading

(Fig. 2.8(a)) is equal to:

$$y = \sum_{i=1}^n \frac{C_{0i}}{1 - \frac{1}{\lambda_{ci}}} \bar{y}_i \quad (2.11)$$

The axial deformations of members are neglected in the derivation of the above equation. The complete derivation is shown in Appendix B.

Equation 2.11 indicates that the elastic failure load of a frame is defined by the corresponding lowest critical load λ_{ci} which makes y equal to infinity. Furthermore, the elastic failure mode is equal to the lowest critical mode since the first term in Eq. 2.11 will predominate.

To explain more specifically for a single column, regardless of the type of loading imposed on the structure, the elastic failure load is equal to the lowest critical load of the column. The failure mode will reach the lowest critical mode, regardless of the initial deformation produced by the first-order load effects.

For a multi-column frame, the critical load factors in Eq. 2.11 also become a function of the ratio of the axial loads in the members (Fig. 2.8(b)). In other words, the elastic failure load is equal to the lowest critical load that corresponds to the ratio of the axial forces in the members at the elastic failure of the frame. Suppose that the beam axial forces are neglected and the ratio of the column axial thrusts is held constant as the column axial loads increase; the critical load for a given frame and a

given ratio of the column axial loads is a constant quantity. In this way, the above conclusion for a single column also applies to a multi-column frame, that is, the elastic failure load and the failure mode of the frame are the same as the lowest critical load and the lowest critical mode, respectively, regardless of the initial condition of loading and deformation.

In the following chapters, the elastic failure load of a single column will be referred to as the elastic critical load (the lowest one is implied) since it is understood that they are equal. For a frame with a given ratio of column axial loads, the term elastic critical load will also be used in place of the term elastic failure load.

2.6 Non-sway and sway frames

Any frame sustaining gravity loads and lateral loads can be decomposed into a non-sway frame which carries the gravity loads only, and a sway frame which resists the original lateral loads plus the holding forces from the non-sway frame, as shown in Fig. 2.9(a). Furthermore, the non-sway frame can be decomposed into a non-sway frame with supports which are fixed against rotation at the joints, and a non-sway frame with external joint moments equal to the unbalanced fixed-end moments due to the gravity loads. This is illustrated in Fig. 2.9(b). According to the principle of superposition (Sect. 2.2), the axial forces N in the members of the sway and non-sway frames must be equal to

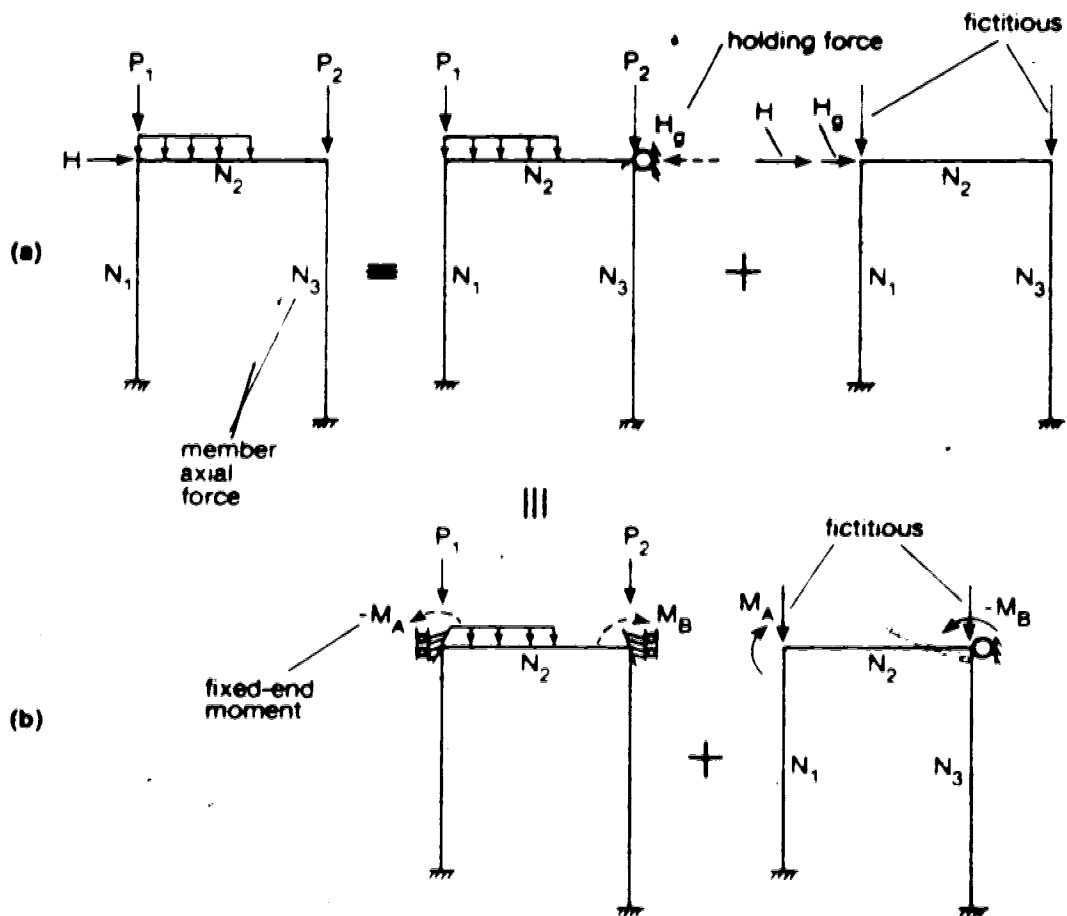


Fig. 2.9 Principle of superposition

those of the original frame as indicated in the figure. Consequently, the holding force becomes a non-linear function of the axial loads in the members, in addition to being a linear function of the gravity loads. Similarly, the external joint moment in the non-sway frame is a non-linear function of the corresponding axial forces in the beams. The total load effects for the columns are equal to the sum of those from the non-sway frame with external joint moments and those from the sway frame. These two types of frames are those to be investigated in following chapters. For simplicity, the non-sway frame subjected to external joint moments is termed the non-sway frame.

The geometric effects due to axial forces in the beams are neglected in this study. This assumption also implies that the external moments in the non-sway frame become independent of the geometric effects. Note that this assumption has been discussed in Sect. 2.4.

It should be noted that the concentrated vertical loads at the joints of the sway frame indicated in Fig. 2.9 are only diagrammatic indications that the column axial loads N should be considered in the analysis for the geometric non-linearity, but N should not be used for calculating the axial deformations of the columns. If the effects of deformation are included in the analysis, such as for the compatibility relationship, the axial deformations should be calculated based on the column axial loads arising from the shear forces in the beams, similar to a first-order analysis

of a frame that only carries lateral loads. Similarly, in the non-sway frame with the external moments, the concentrated vertical loads are fictitious too. It is apparent from Fig. 2.9 that the actual vertical loads are placed on the non-sway frame with the supports fixed against rotation at the joints. The fixed-end moments could include the effect of the axial deformations due to the actual vertical loads.

In the following chapters, the effects of the axial deformation in columns and beams are neglected in the analysis of elastic non-sway and sway frames. This is considered a valid assumption for two reasons. First, the load effects are non-dimensionalized by dividing by the first-order load effects, and therefore the errors of neglecting the axial deformations in both load effects are offsetting. Second, the axial deformations produced by the 'actual' column axial loads arising from the beam shear forces resulting from the geometric effects are relatively insignificant.

The next five chapters discuss the geometric behavior and approximate second-order analysis of non-sway and sway frames. In these chapters, the load effects will be non-dimensionalized by dividing by the corresponding first-order load effects (as mentioned before), so that the results are independent of the magnitudes of the external moments in the non-sway frame, or the lateral loads (including the holding

forces) in the sway frame. The combination of the non-sway and sway load effects will be discussed in Chapter 8.

3. BEHAVIOR OF ELASTIC NON-SWAY FRAMES

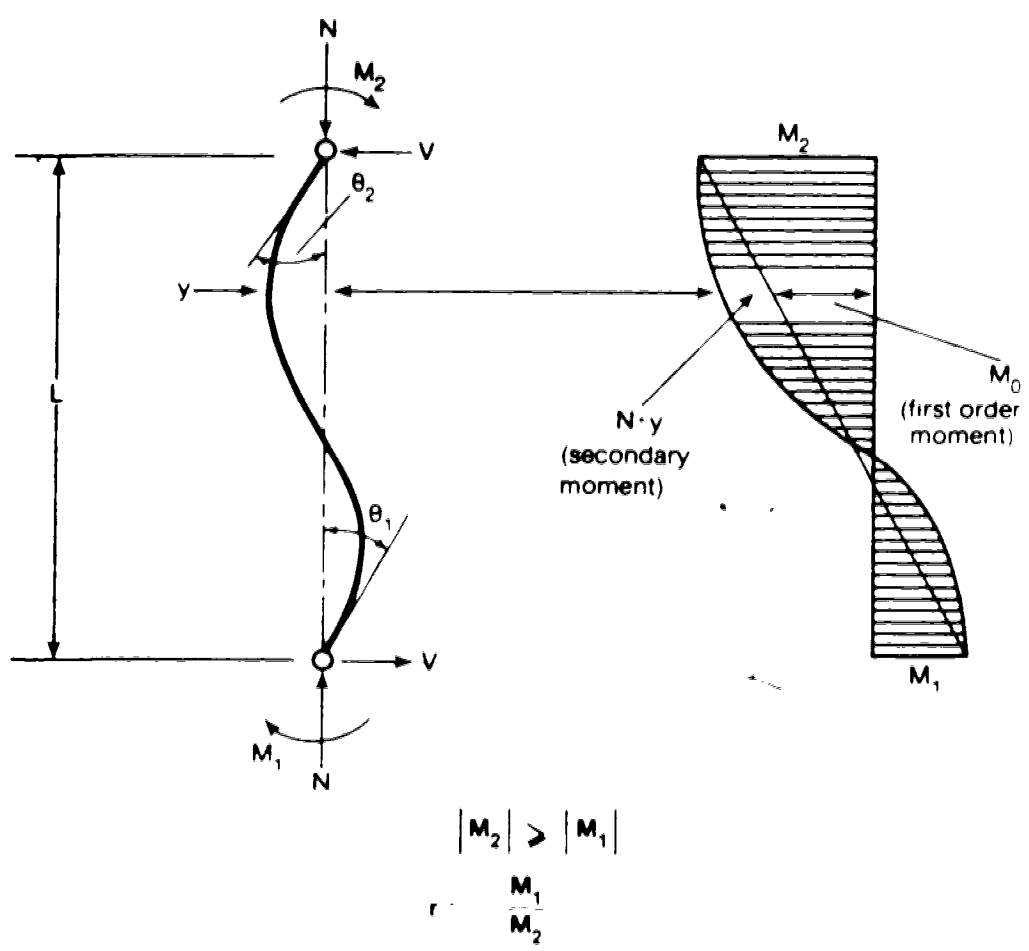
3.1 Geometric effects

In a non-sway elastic frame, the deformations along the length of a column, which are caused by the primary bending moments, introduce secondary bending moments contributed by the axial load. The secondary bending moments readjust the deflections and redistribute the end-moments at a joint. The redistribution of end-moments also affects the column deformations. The new deformations, in turn, bring about new secondary bending moments, and possibly a change in the axial load. This process continues until equilibrium is achieved. Instability occurs when equilibrium is not attainable (small-deflection theory). It can be seen that the whole process is complicated by the redistribution of internal end-moments, which is reflected by the stability functions, C and S , in the slope-deflection equation (Eq. 2.3).

An attempt will be made in this chapter to examine the above problem by investigating the behavior of simple elastic structures.

3.2 Pin-ended columns

Figure 3.1 shows a pin-ended column subjected to constant end-moments M_1 and M_2 , where M_2 is the numerically larger end-moment. The total bending moment in the column is the sum of the first order moment, M_0 , and the secondary



Note: All forces and deformations are shown positive

Fig 3.1 Deformations and moments in a pin-ended column

moment which is equal to the product of the axial compression and the deflection. Since the moment in the column is magnified by the secondary moment, the deformations increase at a faster rate than the load and hence become a non-linear function of the axial force N (Fig. 2.2). The same is true of all the other functions of N : end-rotations, bending moments and shears.

According to the theorem in Sect. 2.5, the failure load of an elastic pin-ended column is equal to its critical load, i.e., the Euler load N_e , and regardless of the initial deformations, the failure mode is the critical mode of symmetrical single-curvature. The process of the change from initial mode to the critical mode is shown in Figs. 3.2 and 3.3 for different ratios of end-moments, r ($= -M_1/M_2$). The ratio r may vary from $+1$ (symmetrical single-curvature) to -1 (antisymmetrical double-curvature). It should be noted for the special case of $r = -1$, the anti-symmetrical end-moments force the column to bend into two identical half waves for which the elastic critical load is $4 \cdot N_e$. From Eq. 2.11 in Sect. 2.5, it can be seen that a minute imperfection of the antisymmetry (i.e., $C_{01} \neq 0.0$) will cause failure at N_e , representing a bifurcation of equilibrium. This is illustrated by the curve for $r = -0.99$ in Fig. 3.2.

Figure 3.2 shows the change in end rotations of a hinged column as the axial load approaches the critical load, N_e . Based on Fig. 3.2, the deflected shapes under increasing compression are shown schematically in Fig. 3.3.

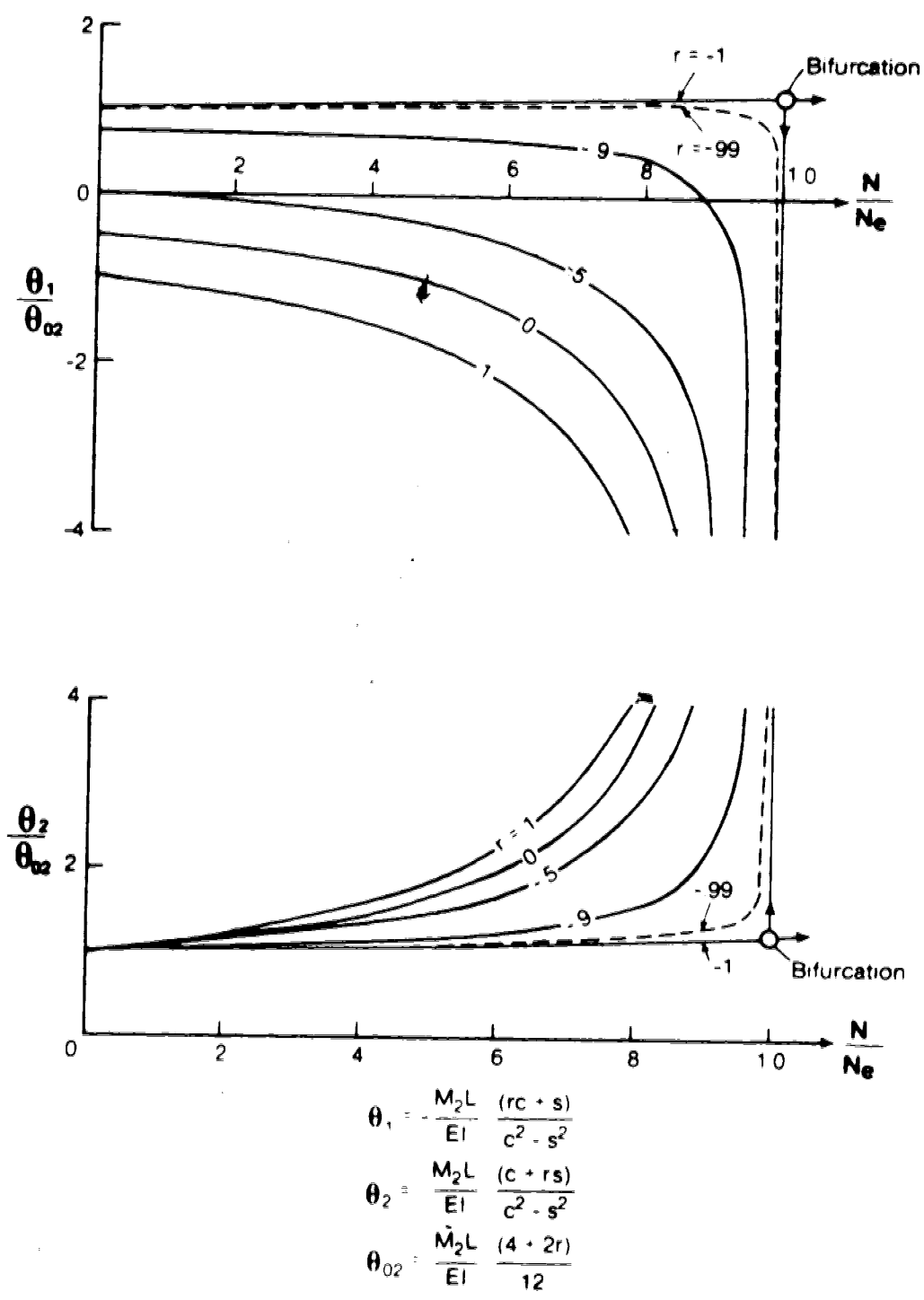


Fig. 3.2 Load-deformation relationship for a pin-ended column

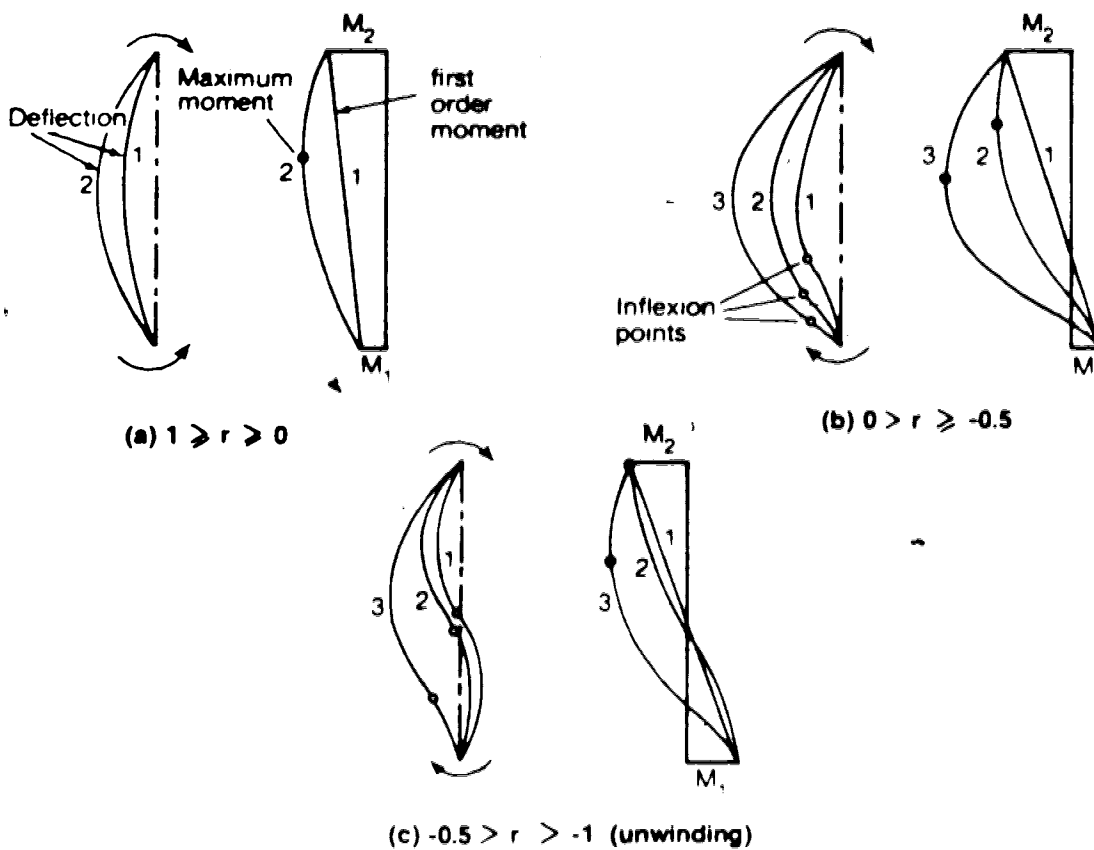


Fig. 3.3 Deflected shapes and bending moments of pin-ended columns under increasing compression

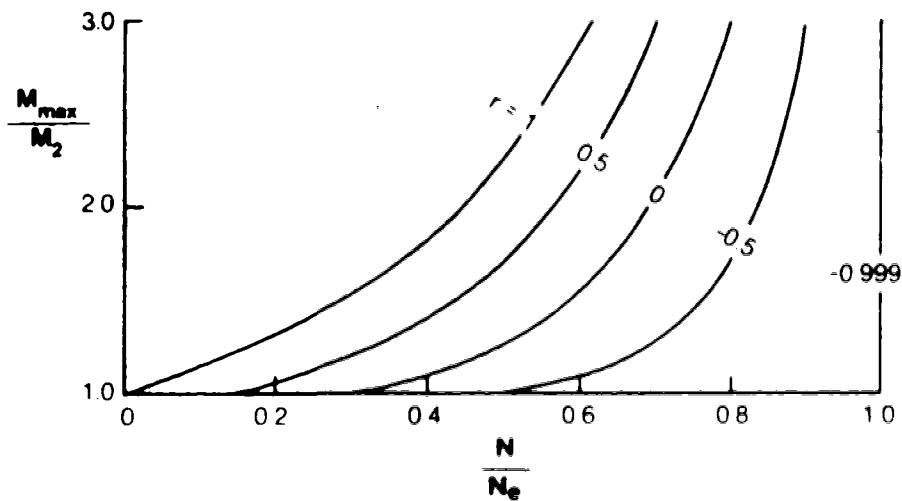


Fig. 3.4 Maximum moment in a pin-ended column

The left-hand parts of Figs. 3.3(a), (b) and (c) represent the deflections, the right-hand parts the moment diagrams. It should be noticed that for any values of r , the end rotation θ_2 always increases in the same direction as M_2 .

For $1 > r > 0$ (Fig. 3.3(a)), θ_1 and θ_2 both increase in the same direction as the end moments. For $0 > r > -0.5$ (Fig. 3.3(b)), the member deflects to one side of the line joining the two ends although there is an inflection point in the column. As the compression increases, θ_1 increases in the direction opposite to M_1 and the inflection point shifts towards the nearest end. When the critical load is reached, the deformations are so large that the inflection point is in effect at the end. As a result, the column fails in single curvature.

For $-0.5 > r > -1$ (Fig. 3.3(c)), the column is initially bent into reversed curvature. As the compression increases, θ_1 decreases (except for r close to -1 where θ_1 initially increases very slightly but later drops rapidly) until it reverses direction and increases in the direction opposite to M_1 . The inflection point moves towards the nearest end, and finally the deflection changes to single curvature at failure. The change of reversed curvature to single curvature is often referred to as unwinding (Ketter, 1961). For r close to -1 , unwinding occurs quite suddenly.

When the column is being compressed, the maximum moment in the column may also shift away from the end (Fig. 3.3).

For $r = 1$, the maximum moment is always located at mid-span. For other values of r , the maximum moment starts to differ from M_2 at a particular load level, as shown by the maximum moment curves, M_{\max}/M_2 , in Fig. 3.4. The curves also show that the maximum moment increases most rapidly when $r = 1$, although all curves approach infinity at the critical load. For any value of r , the location of the maximum moment tends to approach mid-span as the compression increases.

3.3 Single restrained columns

Figure 3.5 shows a single restrained column subjected to externally applied joint moments M_{t1} and M_{t2} , and axial compression N . The linearly elastic springs represent the rotational restraints at the ends. The related symbols and sign convention are also defined in the figure.

Figure 3.6 describes the changes of column end-moments, M_1 and M_2 , under increasing compression for different values of r_0 for a symmetrically restrained column with a non-sway effective length factor, k_{ns} , equal to 0.75. The ratio r_0 and the effective length factor k_{ns} are defined by:

$$r_0 = - \frac{M_{01}}{M_{02}}$$

$$N_{ns} = \frac{\pi^2 EI}{(k_{ns} L)^2}$$

where M_{01} and M_{02} are the first-order end-moments of the

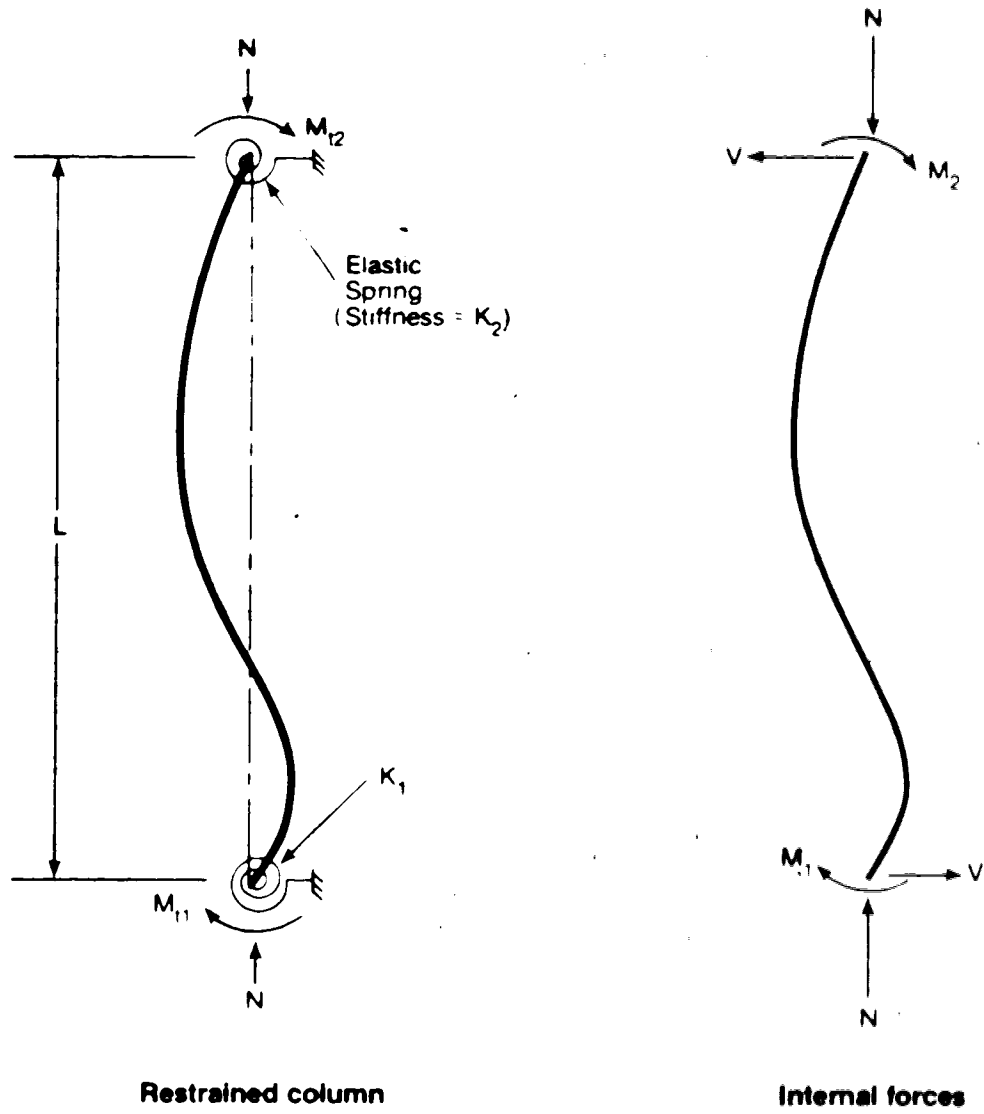


Fig. 3.5 Symbols and sign convention for a restrained column

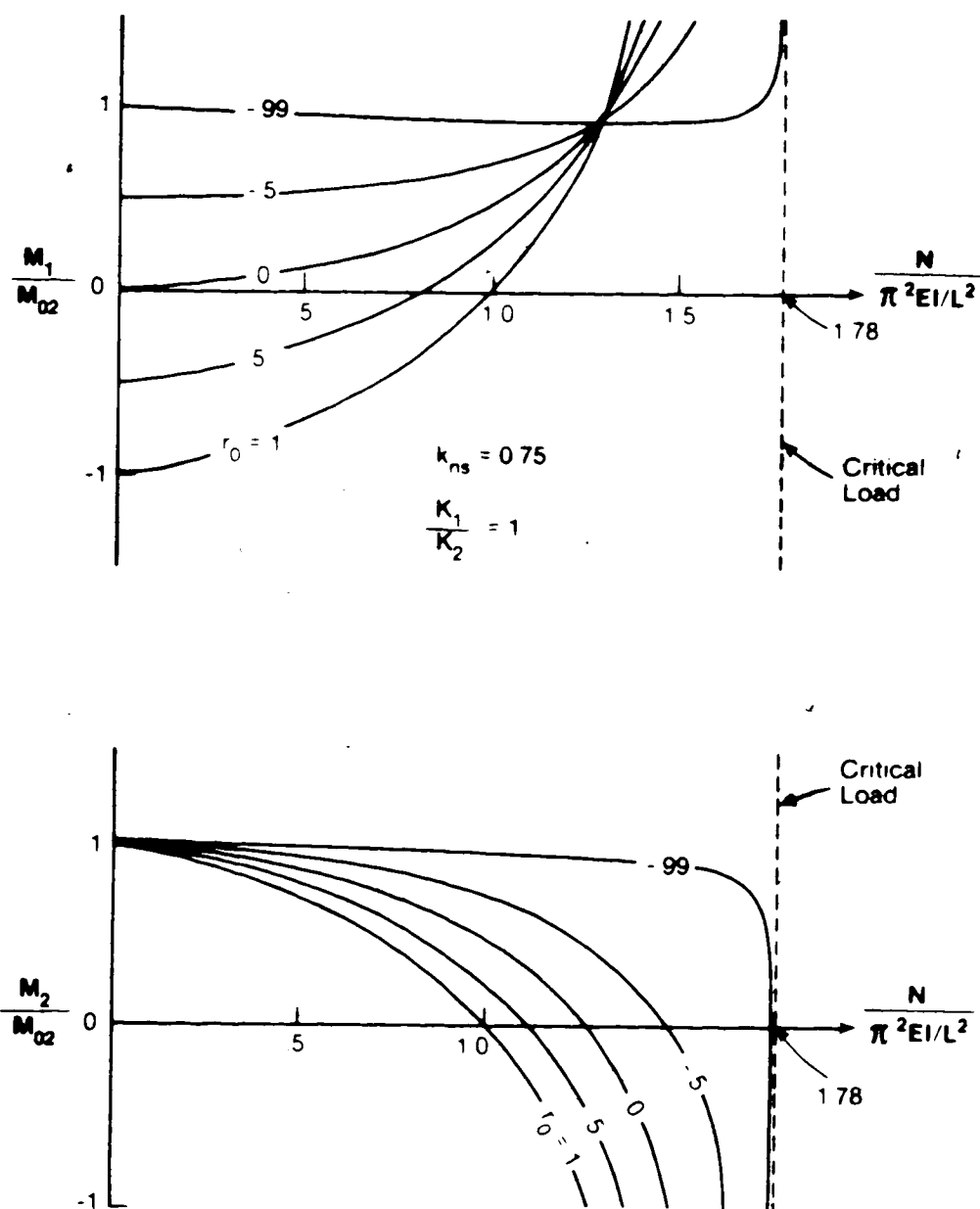


Fig. 3.6 Variation of internal end moments in symmetrically restrained columns under increasing compression

column, and M_{02} is the numerically larger one. The term N_{ns} is the non-sway critical load of the restrained column. Note that k_{ns} is a function of the end-restraints only, and therefore the value of k_{ns} also defines the magnitude of the equal end-restraints. Although r_0 may vary from +1 to -1, -0.99 is used as the lower limit in Fig. 3.6 to introduce small imperfections, as discussed previously.

Based on Fig. 3.6, the variation of moments and deflections with increasing compression is schematically described in Fig. 3.7. As already stated in Sect. 2.5, the deflection mode of a single restrained column will ultimately change to its critical mode as the compressive force is increased. The critical mode for a column restrained at both ends is triple curvature, i.e., two inflection points occur between the ends. The process to attain to the final mode is described below.

For $1 > r_0 > 0$ (Fig. 3.7(a)), M_1 and M_2 both decrease from the beginning and then reverse direction and increase negatively. For $0 > r_0 > -0.9$ (the value of -0.9 is approximate as it would depend on the magnitude of the end-restraints, but it is expected to be close to -1), M_1 increases with increasing axial load while M_2 decreases at the outset (Fig. 3.7(b)). After a change of direction, M_2 starts to increase in that direction. For $-0.9 > r_0 > -1$ (Fig. 3.7(c)) both M_1 and M_2 decrease gradually at the beginning. As the critical load is approached, M_1 rapidly increases, and M_2 rapidly decreases, changes direction and

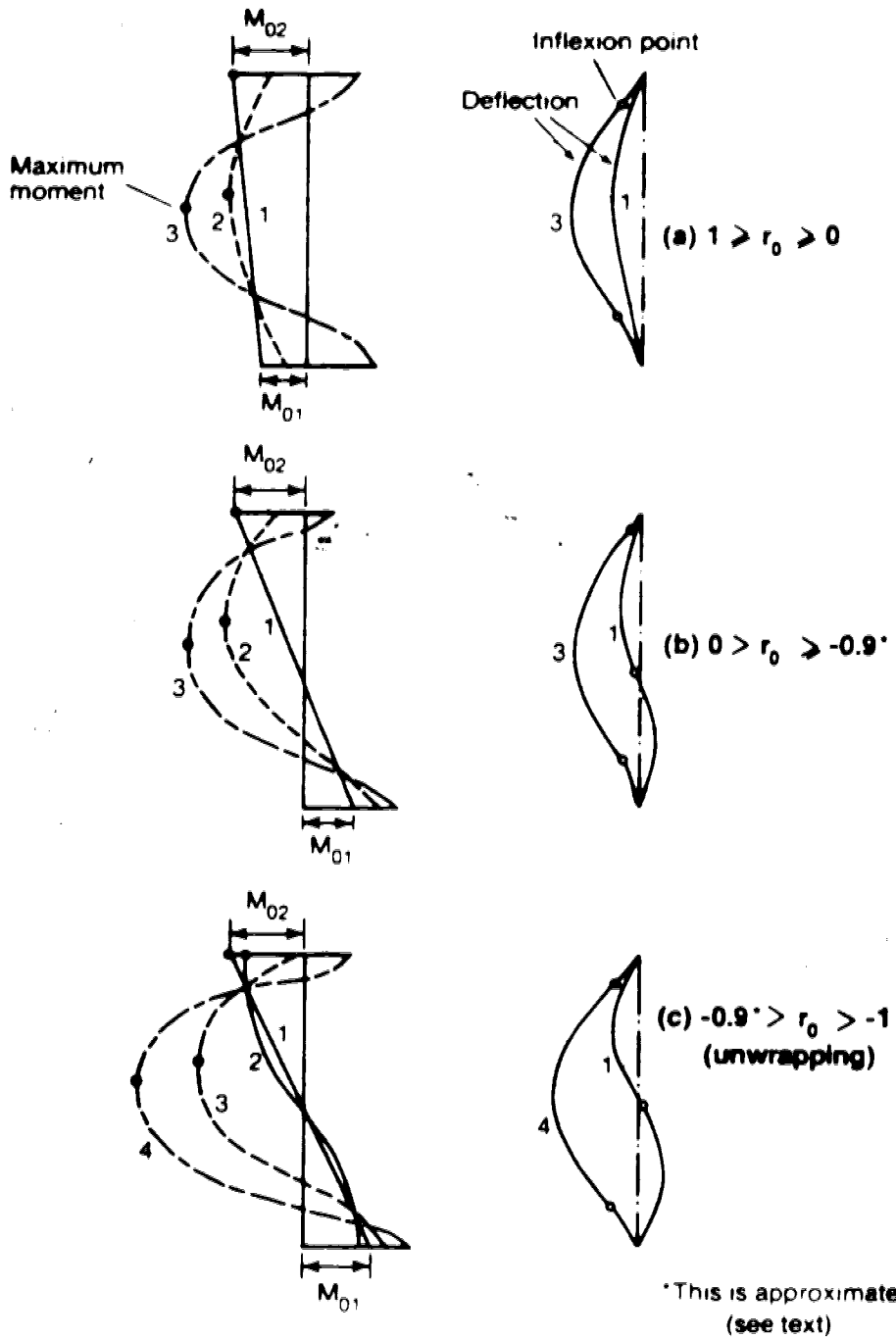


Fig. 3.7 Bending moments and deflected shapes of symmetrically restrained columns under increasing compression

increases in the negative direction. This drastic change from double curvature to triple curvature is often referred to as 'unwrapping' (Baker et al., 1956). The phenomenon is analogous to the unwinding of a pin-ended column.

Figure 3.8 shows the effects of unequal end-restraints ($K_1 \neq K_2$). Compared to the case of equal end-restraints for the same r_0 and k_{ns} , the end-moments at the stronger restraints change more rapidly under increasing compression, while the moments at the weaker restraints change less rapidly. In the extreme case of a hinged end, the end-moment does not change.

The variations of end-rotations with increasing compression for the cases shown in Fig. 3.6 are similar to those for the pin-ended column shown in Fig. 3.2 except that the critical load should be compatible with the restrained column. A closer comparison of Figs. 3.2 and 3.6 reveals the restraining effects offered by the elastic restraints. As the axial load is increased, the end moments change in the opposite direction to the change of end rotations for the same r_0 (or r in Fig. 3.2). In other words, the change of end-moments restrains the column deformations, as shown schematically in Fig. 3.7. Hence the restraining action results in a larger critical load for a restrained column than for a pin-ended column.

Because of the restraining action, the maximum moment in a restrained column is less than if it were unrestrained. The solid lines in Fig. 3.9(a) describe the variation of

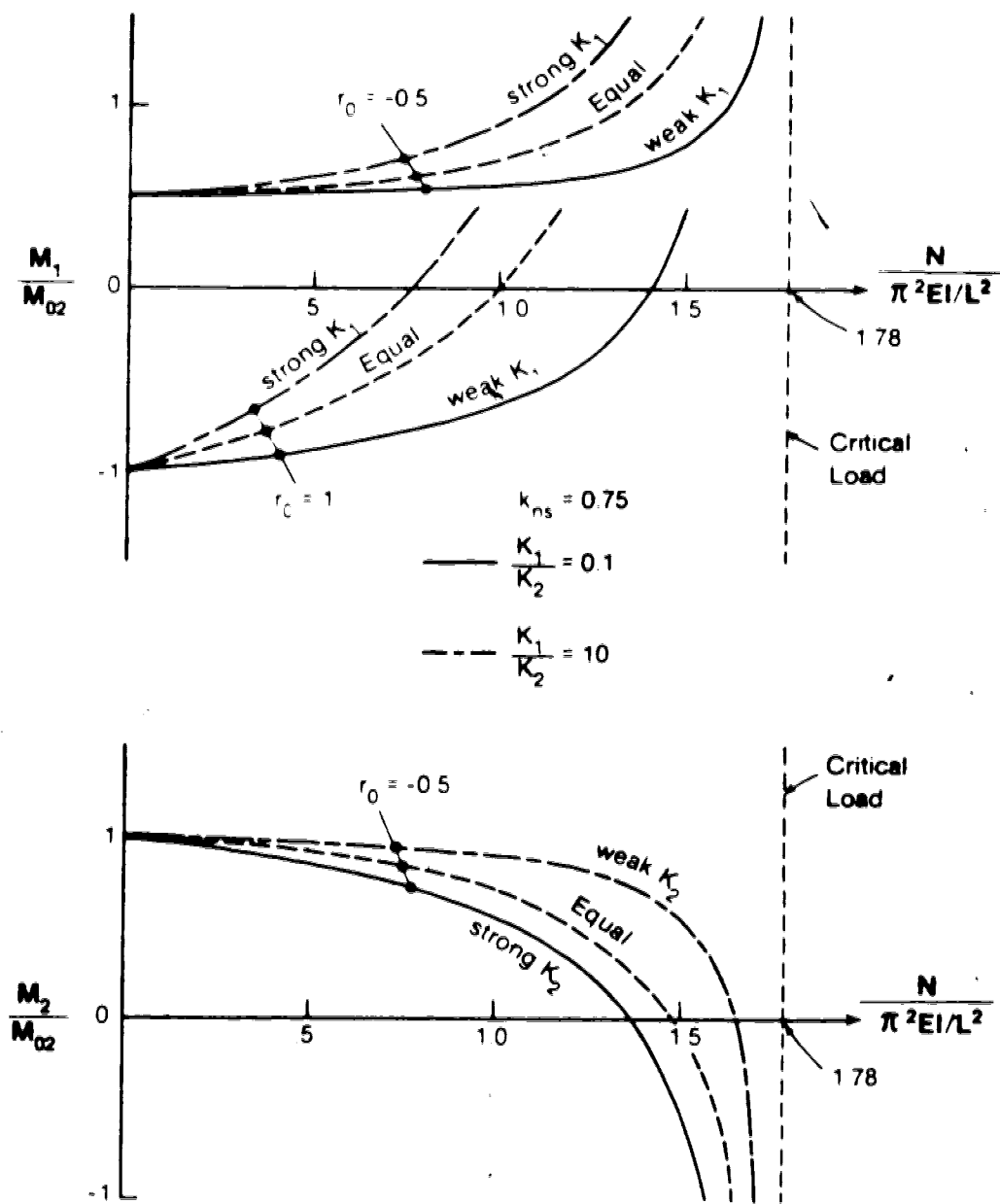
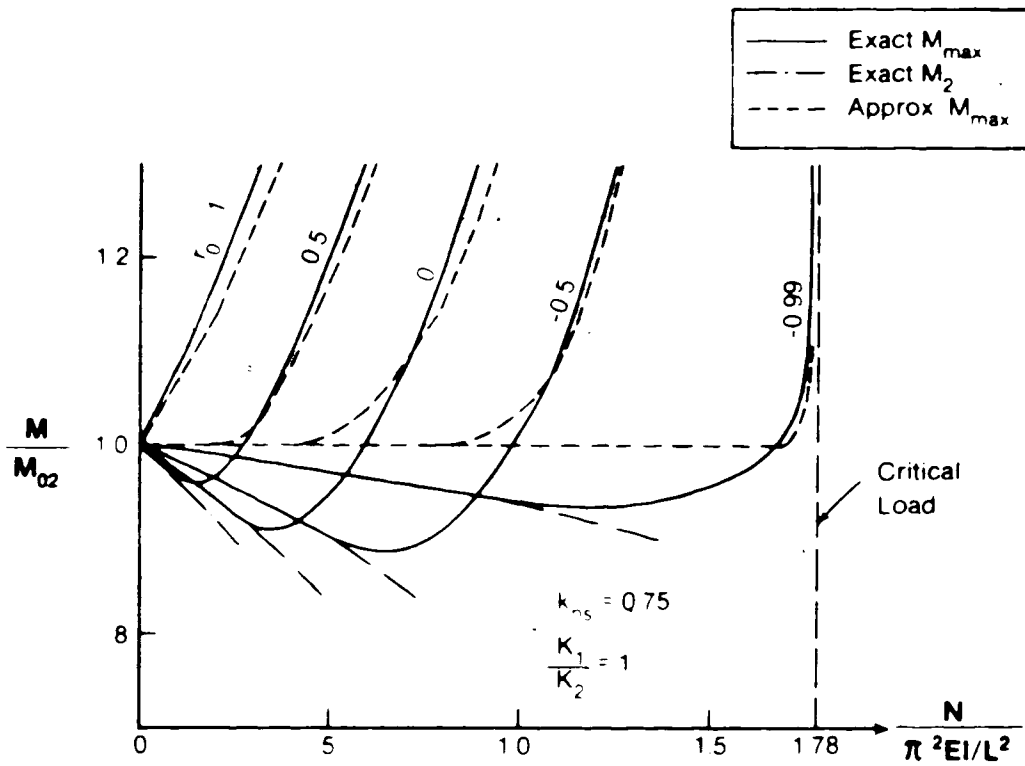
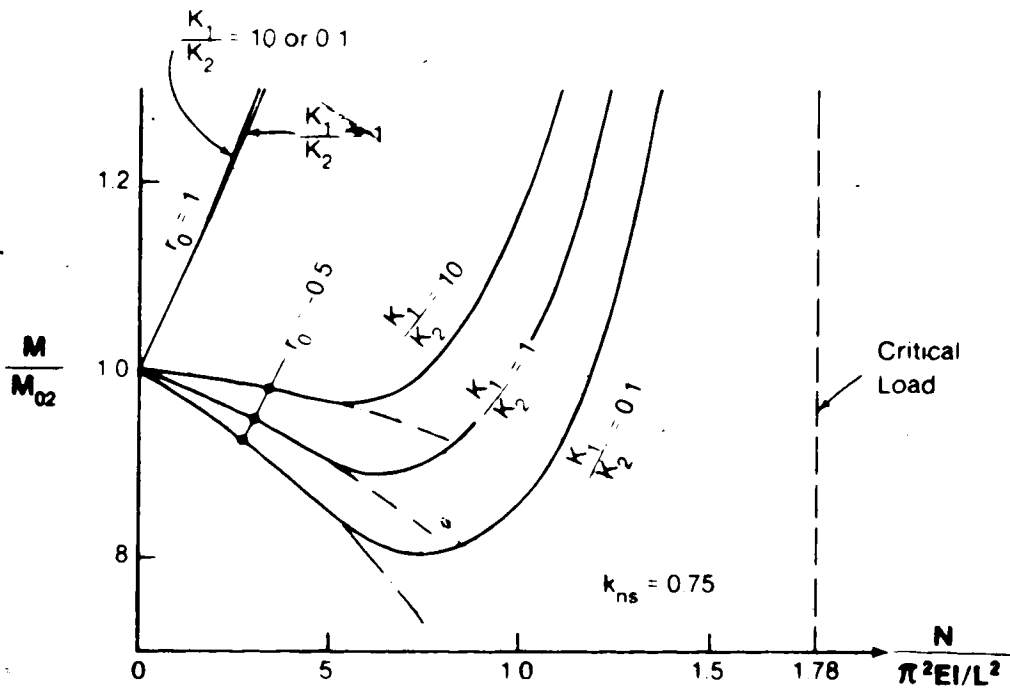


Fig. 3.8 Effects of unsymmetrical restraints on the end-moments



(a)



(b)

Fig. 3.9 Maximum moments in a restrained column

maximum moments in a symmetrically restrained column. (The dotted lines will be discussed in Sect. 4.2.) For $r_0 = 1$, the maximum moment begins to increase at the start of loading although the end-moments are decreasing, as shown in Fig. 3.9(a). For other values of r_0 , the maximum moment, initially equal to M_2 , decreases at lower load levels, but later departs from M_2 and increases thereafter. For smaller values of the first-order moment ratio, r_0 , a higher axial load is necessary to cause the maximum moment to move away from the end. Note that the maximum moment always maintains the same sign and the point of maximum moment tends to approach mid-height of the symmetrically restrained column (Fig. 3.7).

For columns having the same non-sway effective length k_{ns} , the effects of unequal end-restraints on the maximum moment are illustrated in Fig. 3.9(b). The effects are negligible for $r_0 = 1$. The curves for two different values of stiffness ratio follow very closely. This continues up to the critical load, though not shown in the figure. The effects of unequal end-restraints are more significant for $r_0 = -0.5$. Compared to the curve of equal restraints at the same load level, the maximum moment in the column is smaller when K_2 is stronger than K_1 (see Fig. 3.5 for definitions of K_1 and K_2), but it is larger when K_2 is weaker than K_1 . This is because M_2 decreases less rapidly with an increase in axial load for the case of weaker K_2 . It is shown that the maximum moment is not only a function of r_0 and k_{ns} but

also a function of the relative values of K_1 and K_2 .

3.4 Single-storey frames

The study of single restrained columns in the previous section assumes that the stiffness of an end-restraint remains constant as the axial load increases. When a column is a component of a frame, the end-restraints of any column may become a function of the deflected shape of the beams resulting from interaction between the columns. To shed some light on the effects of horizontal interaction between the columns, the behavior of the simple symmetrical frame shown in Fig. 3.10(a) is investigated for two different cases.

In the first case, the frame is subjected to symmetrical external moments so that the beams are bent into symmetrical single-curvature, as shown in Fig. 3.10(b), and the ratio of first-order end-moments, r_0 , for each column is equal to 0.6. In the second case, the external moments are antisymmetrical (Fig. 3.10(c)) so that the beams are bent into antisymmetrical double-curvature. The ratio r_0 for each column is -0.6. In both cases, one column is lightly loaded (strong column) and the other one is heavily loaded (weak column). The ratio between the two axial loads is kept constant during loading with $N_2 = 1.5N_1$ as shown in Fig. 3.10(a).

As stated in Sect. 2.5, for a given frame and a given ratio of column axial forces, the elastic failure mode is

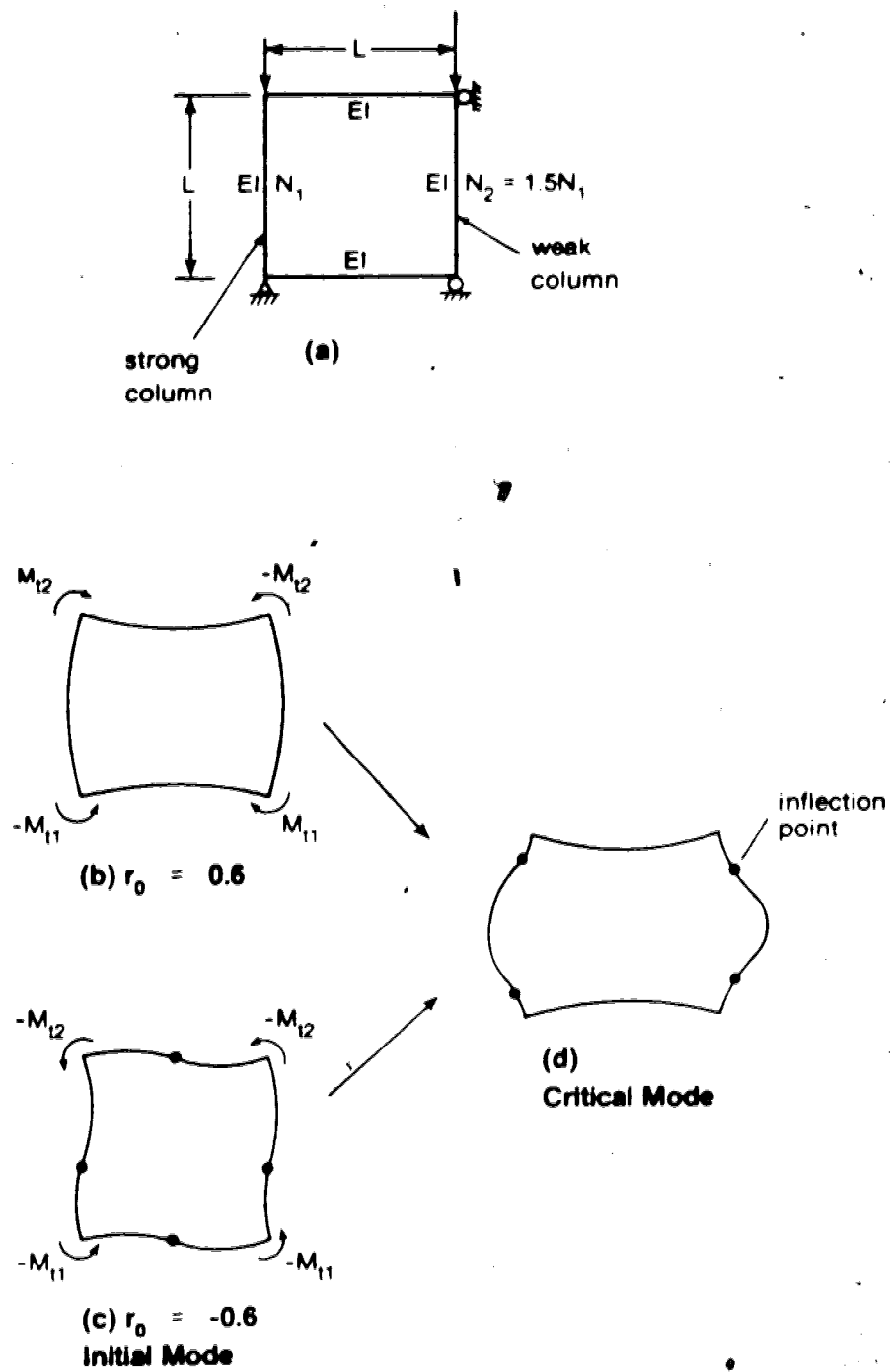


Fig. 3.10 A single-storey frame

identical to the elastic critical mode. This critical mode is independent of the initial deflected shape. As a result, the critical mode for both cases is the same and is shown in Fig. 3.10(d). It can be seen that in the first case, the stiffnesses of end-restraints do not change as much as in the second case. The process of the changes is shown in Fig. 3.11 for the first case and Fig. 3.12 for the second case. In both cases the exact moments, shown by solid lines, are compared to those obtained by assuming constant end-restraints equal to $2EI/L$ for single curvature and $6EI/L$ for antisymmetric curvature. In this way, the change in the end-restraints and the corresponding effects on moments can be observed.

In Fig. 3.11 for $r_0 = 0.6$, the end-restraints remain quite stationary until fairly high load levels, as shown by the close correspondence of the M_2 curves. For the stronger column, the maximum moment increases more rapidly than the one estimated using the first-order end-restraints. In effect, the strong column is losing end-restraints. On the other hand, the weak column is gaining end-restraints. This indicates that the strong column is assisting the weak column through the mechanics of horizontal interaction. The overall trend of the behavior is essentially the same as that predicted by assuming constant end-restraints, however.

For the antisymmetric loading case, $r_0 = -0.6$, the moments plotted in Fig. 3.12 indicate that the first-order values of the end-restraints closely approximate the exact

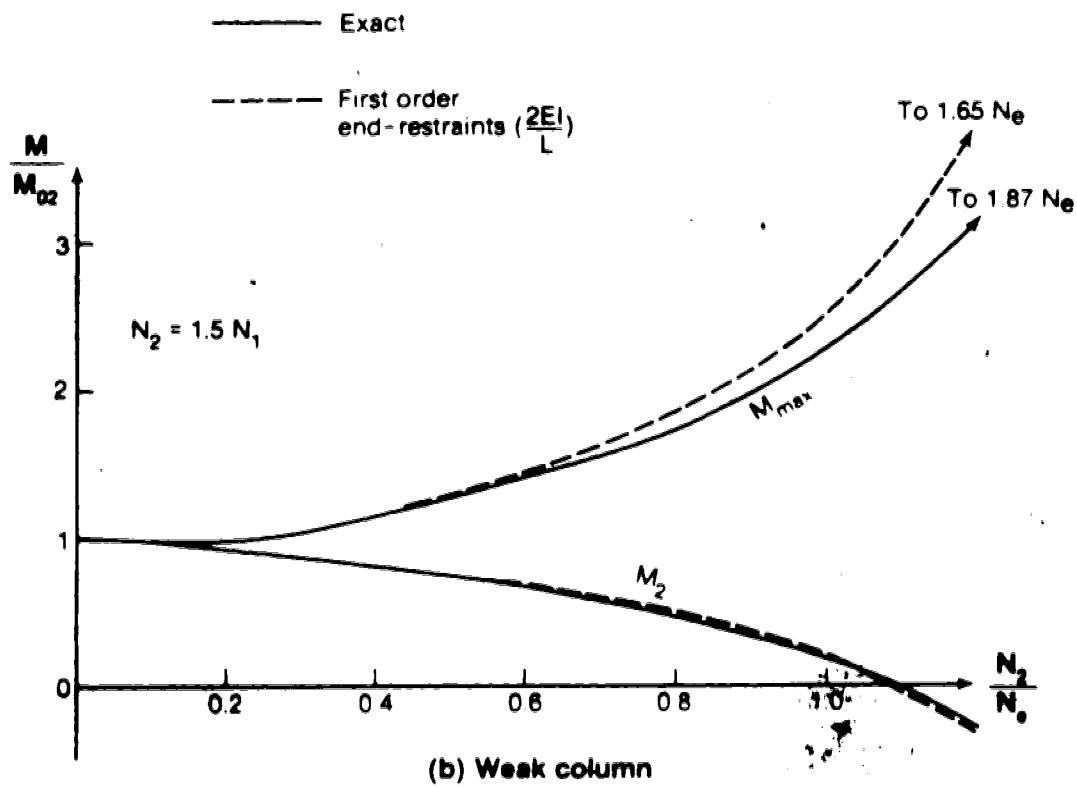
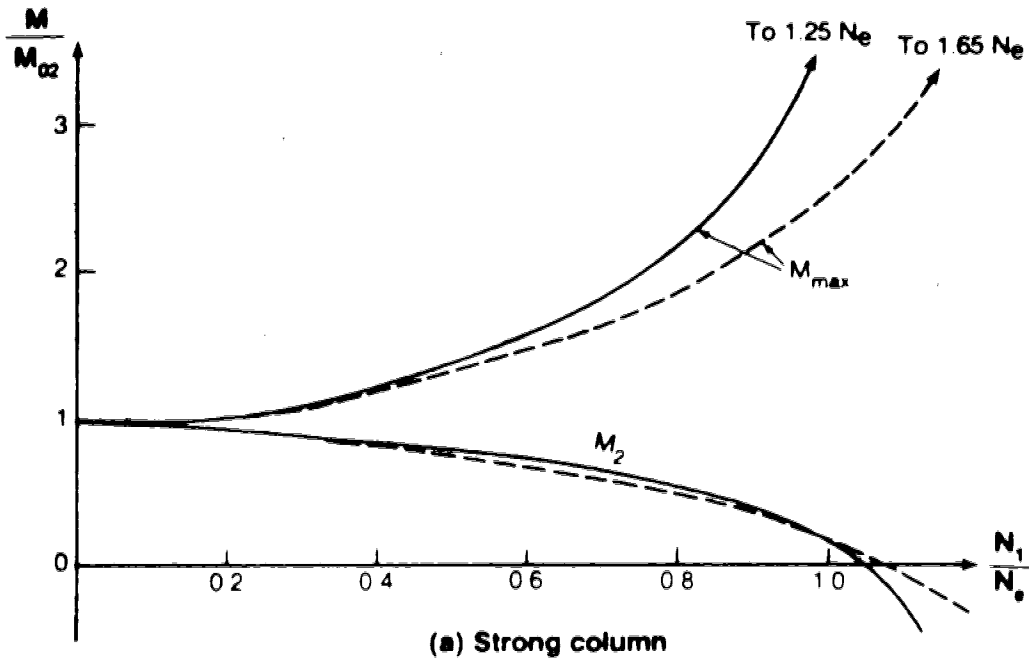


Fig. 3.11 Horizontal interaction between columns for $r_0 = 0.6$

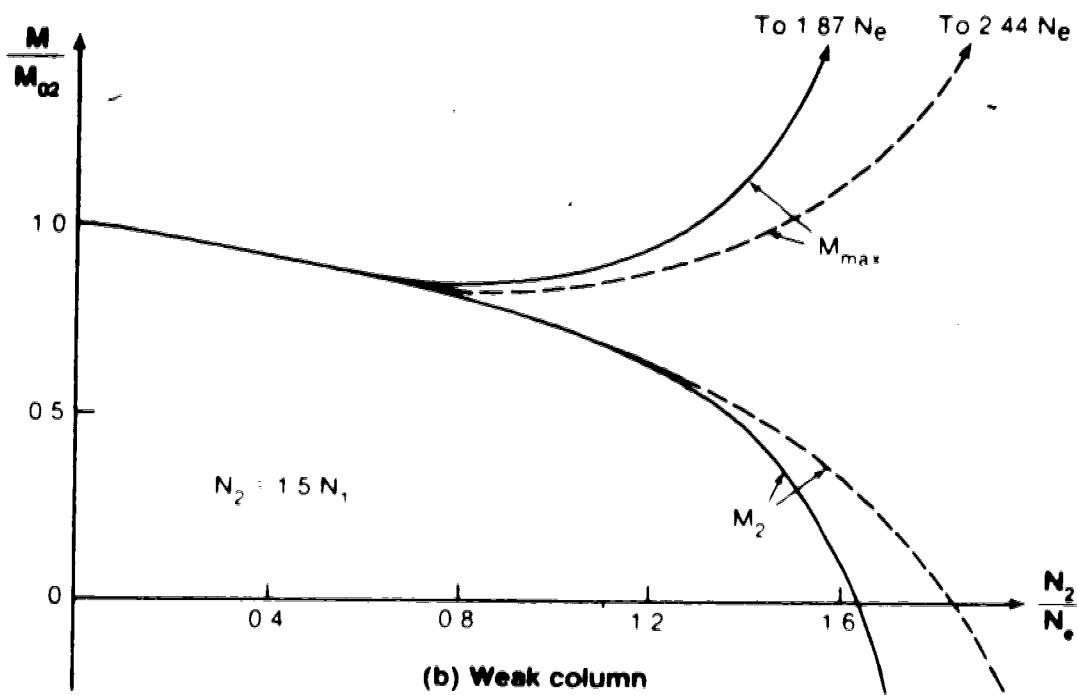
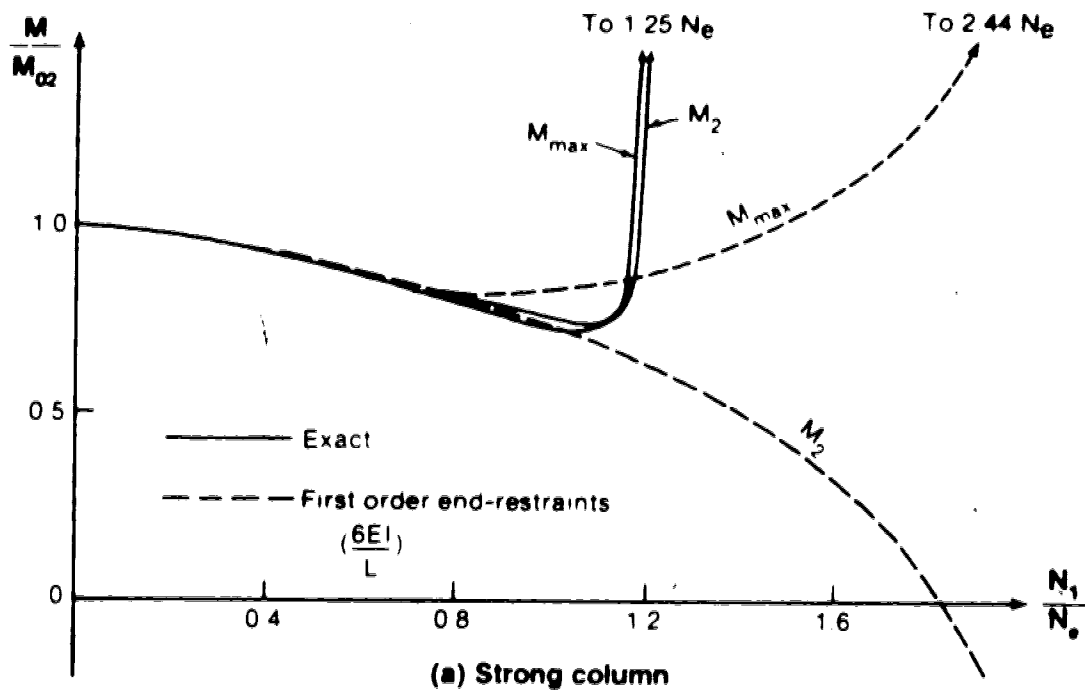


Fig. 3.12 Horizontal interaction between columns for $r_0 = 0.6$

restraints until N/N_e approaches 1.0. In this case, however, both columns ultimately lose end-restraints^{*} because the change from the initial anti-symmetric mode to the approximately symmetrical critical mode brings about a drastic decrease in the effective stiffness of the beams (from double to single curvature). The changes in the behavior of the weak column develop gradually and the trend of behavior does not differ from that predicted by assuming constant end-restraints. For the strong column, the changes are insignificant until a drastic change of behavior occurs as the elastic critical load of the frame is approached. This rapid change is brought about by the extremely large end-moments in the weak column, or in other words, the elastic failure of the whole frame is initiated by the elastic failure of the weak column. In an actual structure, these extremely large moments will not occur since the members will fail by material failure, and consequently the snap-through change of deflected shape of the strong column will stop short before there are any significant differences from the curves based on constant end-restraints.

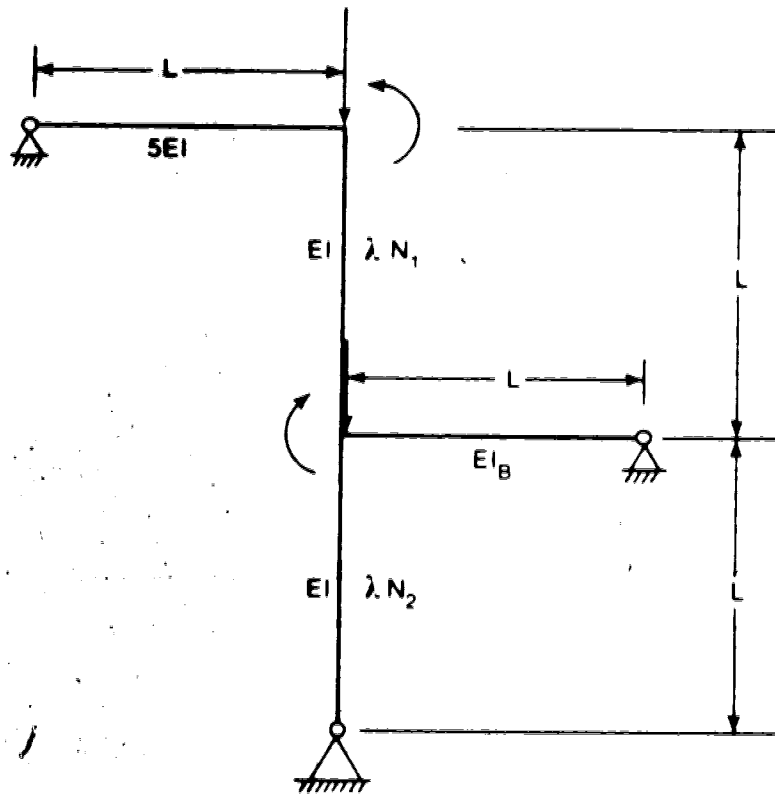
In summary, the above two cases suggest that even in a frame with mixed strong and weak columns (the words 'strong' column refer to one having a high EI/L or stiff end restraints or low N/N_e ratio, 'weak' column means vice versa), the end-restraints of any column are quite insensitive to the geometric action, except when the column is carrying a high axial load. At the high load levels at

impending elastic failure, the behavior of an individual column becomes complicated, as it is a function of the difference between the deflected shape of the end-restraints at elastic failure and the initial condition of the end-restraints.

3.5 Multistorey frames

In a multistorey structure where continuity of columns exists between storeys, the vertical interaction of columns due to geometric effects is a function of the relative stiffnesses of columns and the stiffnesses of the beams that connect the storeys. As the axial loads alter the relative stiffnesses of columns, they also affect the distribution of moments between columns. However, if the beams are stiff relative to the columns, any changes in the end-moments of a column will be absorbed primarily by the beams and therefore will not affect significantly the columns above or below. On the other hand if the beams are very flexible, any changes in one column will affect directly the other storeys through the continuous columns.

An attempt is made in this section to observe the significance of the above two factors, but for beams of intermediate stiffnesses which are considered to be more typical. The horizontal interaction of columns is neglected. The simple two-storey frame shown in Fig. 3.13 is the model to be examined. The bottom column of the frame is a distinctly weaker column than the upper column, because



$$N_2 = 1.5 N_1$$

$$r_0 = 0.0 \text{ (both columns)}$$

$$\text{Stiff Beam } EI_B = 2EI$$

$$\text{Flexible Beam } EI_B = 0.4 EI$$

Fig. 3.13 A simple two-storey frame

not only is it less restrained but also because the axial load it carries is 1.5 times that in the top column. Two cases will be studied. The beam that separates the two storeys in the first case is 5 times that in the second case, as shown in Fig. 3.13. In both cases, the first-order ratio of end-moments r_0 is equal to zero for both the upper and lower columns, and the column end-moments at the mid-height of the structure are equal.

The variation of the maximum moments with increasing axial loads are shown in Fig. 3.14 for the top (strong) column for both cases, and in Fig. 3.15 for the bottom (weak) column. In all the figures, the maximum moments are also compared to those obtained by assuming first-order (constant) end-restraints. Since the first-order column end-moments are distributed equally at the mid-height, the corresponding first-order end-restraint is equal to half of the effective stiffness of the beam. Note that λ is the load factor (Fig. 3.13), and λ_c is the critical load factor of the frame.

From the two figures, it is seen that the strong column is assisting the weak column as the axial loads increase. This phenomenon is more pronounced for the frame with the flexible beam between the storeys. It should be noted that this effect became quite appreciable even at early stages of loading.

In a multistorey frame where both vertical and horizontal interaction of columns may occur, it is likely

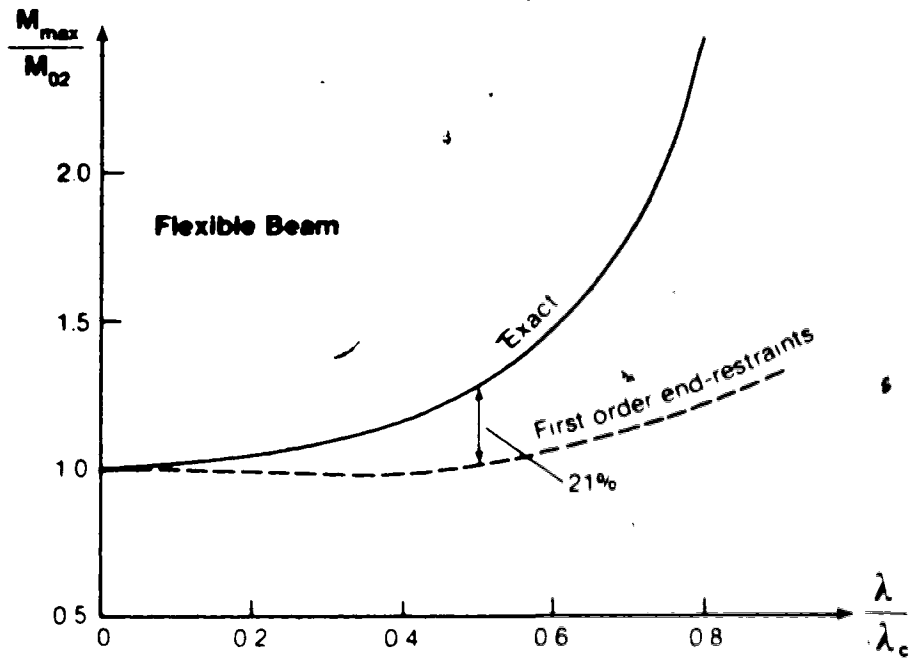
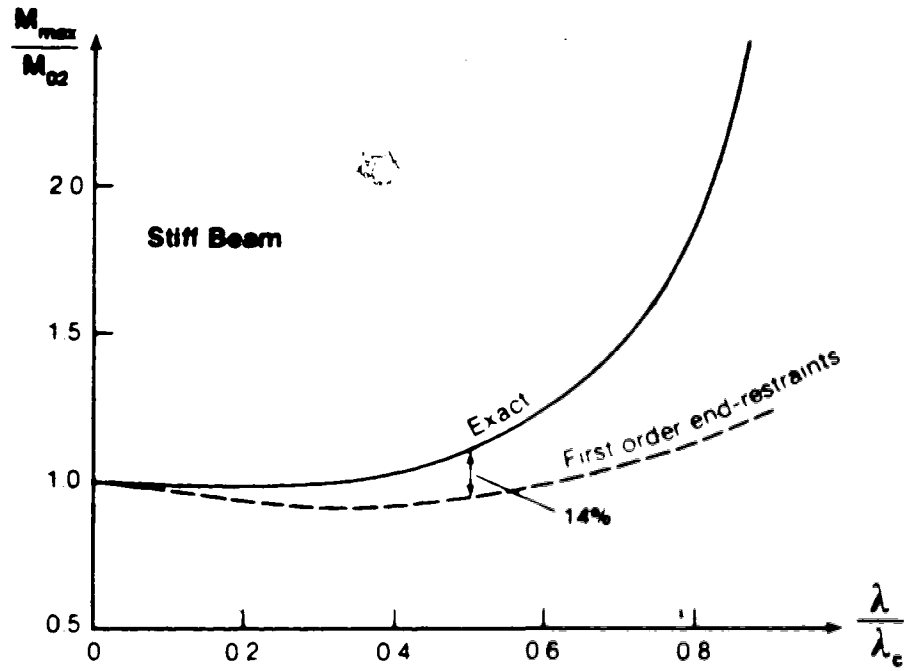


Fig. 3.14 Variation of maximum moments in the top (strong) column of the frame shown in Fig. 3.13

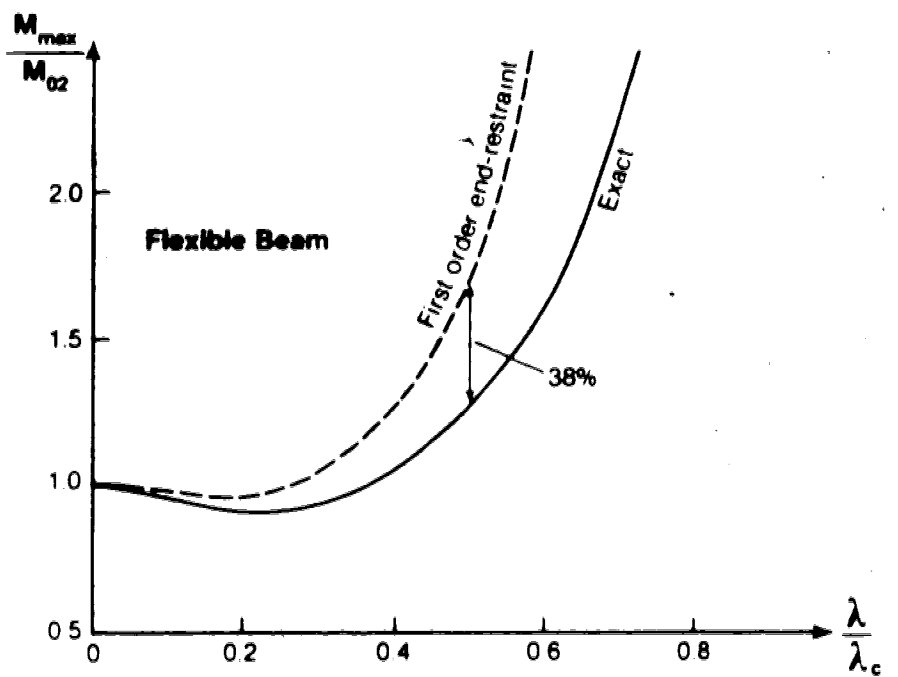
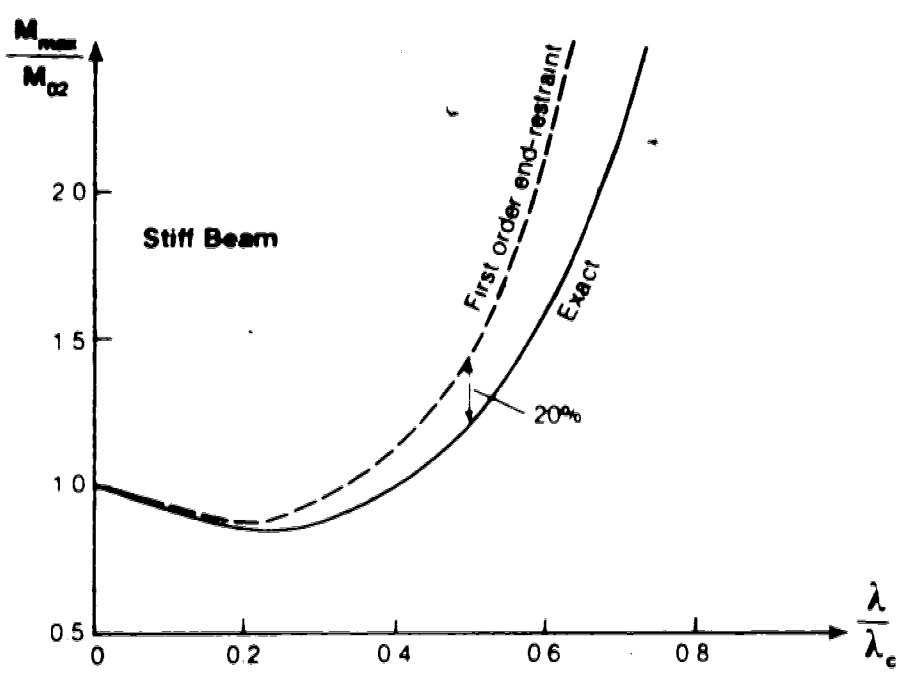


Fig. 3.15 Variation of maximum moments in the bottom (weak) column of the frame shown in Fig. 3.13

that the vertical interaction would play a more significant part. The significance is, obviously, a function of the factors discussed previously. In the case that the effects of both interactions are significant, it seems that the combined effects are too complicated to be traced in a general discussion.

3.6 Summary

The change of the deflected shape of a pin-ended column from its initial mode to its critical mode has been described. As the critical load is approached, the inflection point (if any) in the pin-ended column moves to the nearest end, while the point of maximum moment moves to mid-height of the column.

The changes in the end-moments of a symmetrically restrained column due to increasing compression have been described. These show how the column changes from its initial mode to its critical mode of triple curvature, and how the change of end-moments restrains the column deformations resulting in a larger critical load than if the column were unrestrained. The differences between the behavior of columns having unequal end-restraints and equal end-restraints have also been discussed.

Increasing axial compression will reduce the maximum moment in a restrained column if the maximum remains at the end of the column. With further increase in the compressive force, the maximum moment will be forced away from the end,

and the maximum moment will increase thereafter. The process depends on the first-order moment ratio (r_0), the load level and the magnitudes of the end-restraints.

The horizontal interaction of columns has been discussed with the help of two illustrations. They suggest that even in a single-storey frame with mixed strong and weak columns, the end-restraints of a given column are quite insensitive to the geometric action, except at impending elastic failure of the frame.

The two cases illustrating the vertical interaction between columns indicated that stronger columns assist weaker columns as the load levels increase. This phenomenon is more pronounced for a frame with more flexible beams between the storeys.

4. APPROXIMATE SECOND-ORDER ANALYSIS OF ELASTIC NON-SWAY FRAMES

4.1 Pin-ended columns

The maximum moment M_{\max} in an elastic pin-ended column can be written in the form:

$$M_{\max} = \delta M_2 \quad (4.1)$$

where M_2 is the numerically larger end-moment and δ is the magnification factor which is generally separated into two terms:

$$\delta = C_m \delta_1 \quad (4.2)$$

where δ_1 is the value of δ corresponding to symmetrical end-moments ($r = 1.0$), and C_m is the correction factor employed to account for $r \neq 1.0$. The unsymmetrical end-moments can be visualized as being replaced by equivalent symmetrical end-moments equal to $C_m M_2$, which will give rise to the same maximum moment as occurs under the actual loading. From Eq. 2.8 and some trigonometric operations:

$$\delta_1 = \sec \frac{\beta}{2} \quad (4.3)$$

and

$$C_m = +\sqrt{\frac{1 + r^2 - 2 r \cos \beta}{2 (1 - \cos \beta)}} \quad (4.4)$$

For a column subjected to end-moments, Eq. 4.3 can be approximated by (Wang and Salmon, 1973):

$$\delta_1 = \frac{1 + 0.23 \alpha}{1 - \alpha} \quad (4.5)$$

where $\alpha = N/N_e$. The approximation is derived by assuming a sine curve for the deflected shape of the column and applying the conventional moment-area method. Another approximation of δ_1 , similar to Eq. 4.5, can be obtained by using the energy method considering only one sine term of the Fourier series (Galambos, 1968):

$$\delta_1 = \frac{1 + 0.27 \alpha}{1 - \alpha} \quad (4.6)$$

When the average of Eqs. 4.5 and 4.6 (given in Eq. 4.7) is compared to the exact solution given by Eq. 4.3, the errors are within +0.2% and -0.1% for $N < 0.5 N_e$, and -2% for $N < N_e$. Therefore it may be concluded that Eq. 4.7 is a very good approximation for δ_1 .

$$\delta_1 = \frac{1 + 0.25 \alpha}{1 - \alpha} \quad (4.7)$$

In the design codes AISC (1978) and ACI (1977), it is implied that Eq. 4.3 can be approximated by:

$$\delta_1 = \frac{1}{1 - \alpha} \quad (4.8)$$

(discussed in the Guide ed. Johnston, 1976 and MacGregor et al., 1970). This approximation is unconservative and the error can be as high as -11% for $N = 0.5 N_e$. This will be discussed further in Sect. 4.5.1.

Due to the limitation on δ imposed by Eq. 2.9, the values of C_m for $N < N_e$ have an upper bound which is obtained by substituting $r = \cos \beta$ into Eq. 4.4. The lower bound is determined corresponding to $N = N_e$. These two bounds are plotted in Fig. 4.1 together with curves for different values of N/N_e computed using Eq. 4.4. An approximation for C_m , neglecting the dependence on N/N_e , was suggested by Austin (1961):

$$C_m = 0.6 + 0.4 r \quad \text{for} \quad 1.0 > r > -0.5$$

and (4.9)

$$C_m = 0.8 + 0.8 r \quad \text{for} \quad -0.5 > r > -1.0$$

Equation 4.9 is also plotted in Fig. 4.1. The equation is applicable for the case of in-place bending. Massonnet (1959) developed a similar relationship for the case of elastic lateral-torsional buckling of an I-shaped, bi-symmetrical, pin-ended column. The column is eccentrically loaded at the ends to produce bending about the strong axis

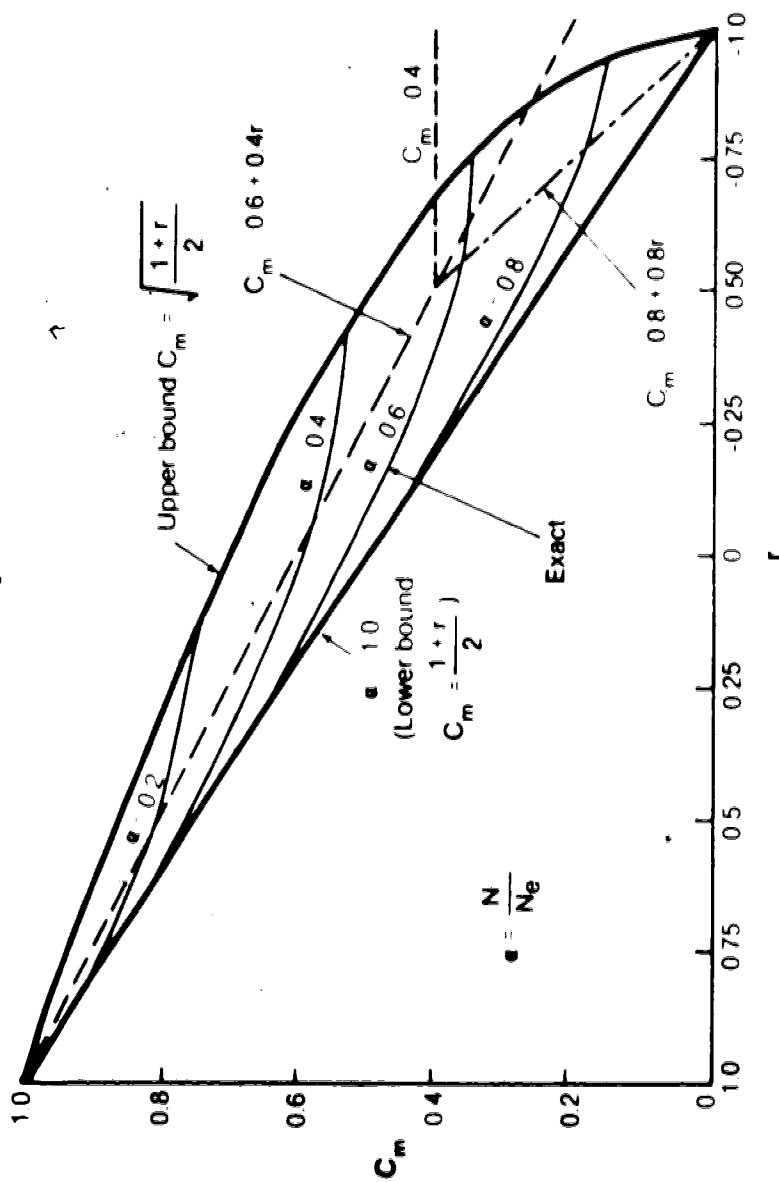


Fig. 4.1 Comparison of theoretical C_m with approximate equations

and assumed to fail by combined bending and twisting. The unequal end-moments are replaced by equivalent symmetrical end-moments M_{eq} which will give rise to the same lateral-torsional buckling load as occurs under the actual loading. Using the energy method, Massonnet expressed M_{eq} as follows:

$$\frac{M_{eq}}{M_2} = \sqrt{0.3 + 0.4 r + 0.3 r^2} \quad (4.10)$$

Equation 4.10 is approximate in the sense that the dependence on the axial load and some torsional parameters are neglected. (The derivation of Eq. 4.10 and the assumptions involved are thoroughly described by McGuire, 1968.) The soundness of this equation has been corroborated by Horne (1956) and Salvadori (1956) although they based their solutions on different assumptions.

In order to extend Eq. 4.9 to include the case of lateral-torsional buckling, Austin (1961) proposed the following equation (adopted by the current ACI (1977) and AISC (1978) Codes):

$$C_m = 0.6 + 0.4 r > 0.4 \quad (4.11)$$

which closely approximates Massonnet's equation (Eq. 4.10). With the limitation of $C_m > 0.4$, Eq. 4.11 becomes overly conservative for values of r close to -1 for in-plane bending (Fig. 4.1). On the other hand, for $r > -0.5$, the equation may underestimate C_m by up to 20% (Fig. 4.1). The

unconservative errors can be considerably reduced, however, if the approximate magnification factor, $\delta = C_m \delta_1$, is limited to values greater than or equal to 1.0. This will be shown in the following paragraphs.

If Eqs. 4.8 and 4.11 are combined with the limit of $\delta > 1.0$, the approximate magnification factor becomes:

$$\delta = \frac{C_m}{1 - \alpha} > 1.0$$

and (4.12)

$$C_m = 0.6 + 0.4 r > 0.4$$

which is the basic equation for calculating the maximum moment in a non-sway slender column specified in the ACI Code (1977). The errors in Eq. 4.12, compared to the exact elastic solution (Eqs. 2.8 and 2.9), are shown in Fig. 4.2. The approximate equation appears significantly unconservative in many cases because Eq. 4.8 itself is unconservative. If Eq. 4.7 and 4.11 are used instead such that:

$$\delta = C_m \frac{1 + 0.25 \alpha}{1 - \alpha} > 1.0$$

and (4.13)

$$C_m = 0.6 + 0.4 r > 0.4$$

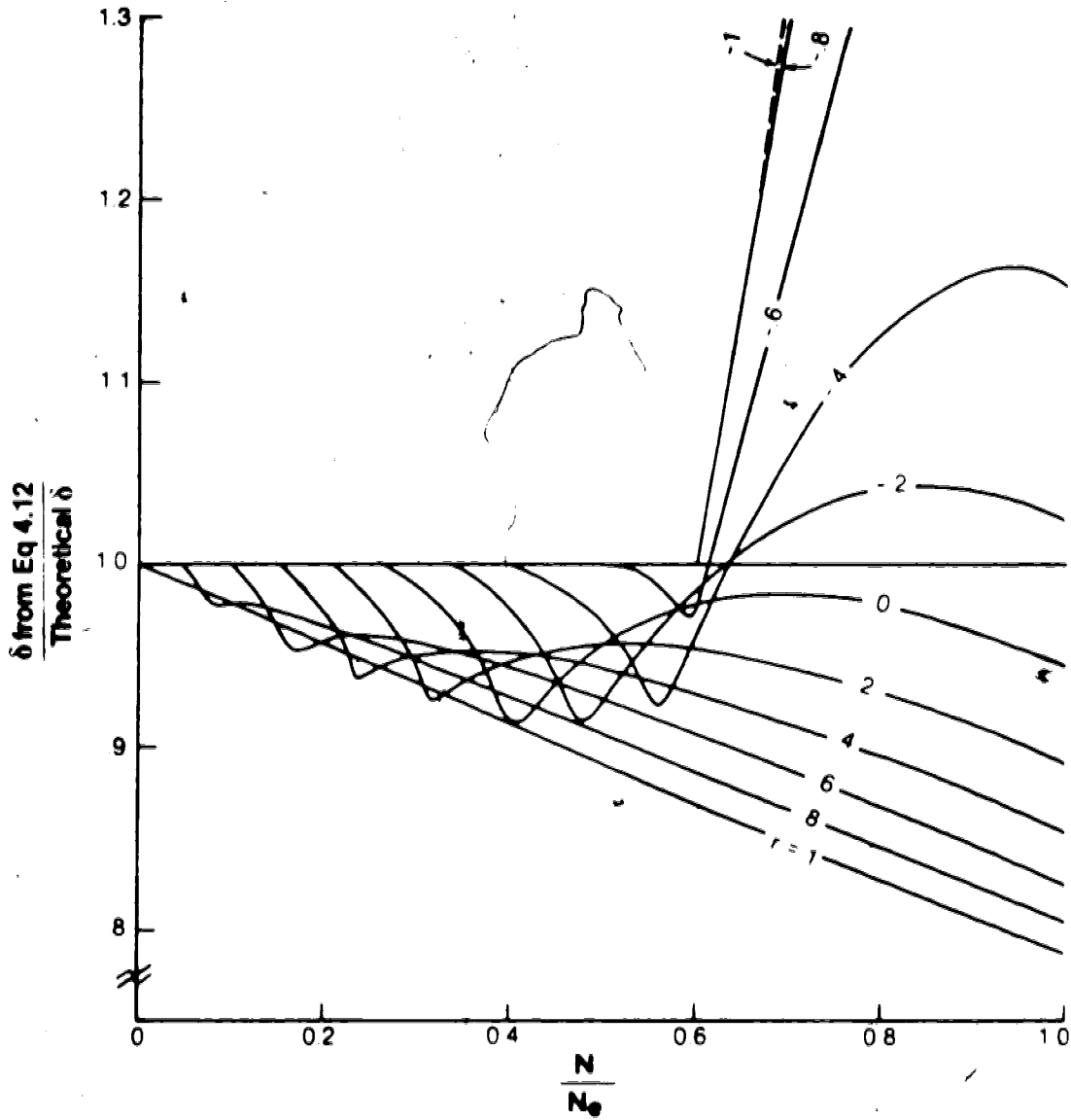


Fig. 4.2 Comparison of approximate with theoretical magnification factor

the unconservative errors are considerably reduced, as shown in Fig. 4.3. The error is always less than 4% on the unconservative side for $N < N_e$. For $N < 0.5 N_e$, the error is within +8% and -4%. For $N > 0.5 N_e$, Eq. 4.13 becomes increasingly conservative. It should be noted that for design purposes, the overconservative estimates at very high axial compressions are not of practical importance because the magnitudes of the design moment would be very small, as reflected by the moment-axial load interaction relationships of steel or reinforced concrete columns. The errors can be reduced yet still remain conservative, if the lower limit of 0.4 is deleted. It appears reasonable to neglect the lower limit if lateral/torsional buckling is not a consideration such as in the design of reinforced concrete columns. This will be discussed further in Sect. 4.5.

4.2 Effective length method for single restrained columns

The current design approach in the United States (AISC, ACI) and Canada (CSA) for restrained non-sway beam-columns proceeds as follows: The restrained beam-column is replaced by an equivalent pin-ended beam-column whose length is equal to the effective length of the real restrained column, $k_{ns}L$ (Fig. 4.4(a)). This equivalent pin-ended column is then analyzed for the axial compression plus the first-order internal end-moments of the real column. The use of k_{ns} is intended to take into account the effects of the end restraints on the end moments discussed in Sect. 3.3.

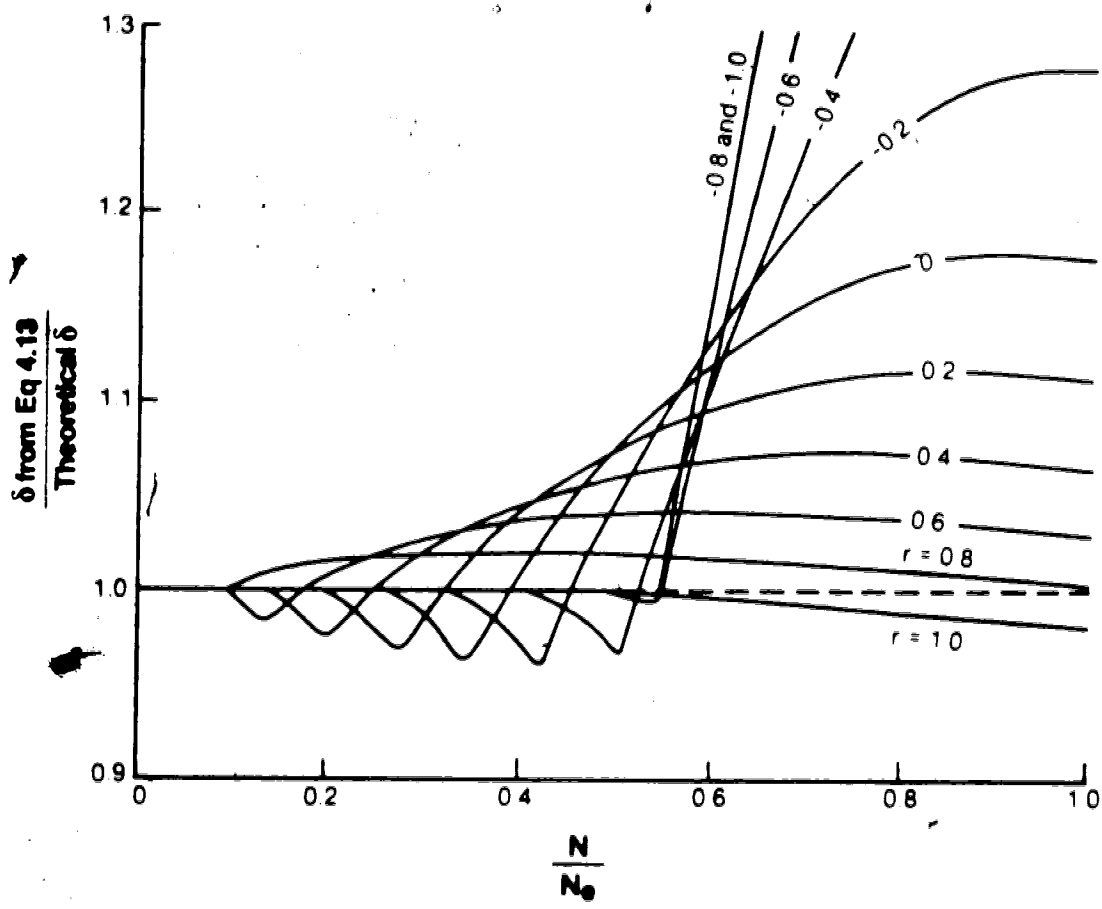


Fig. 4.3 Comparison of approximate with theoretical magnification factor

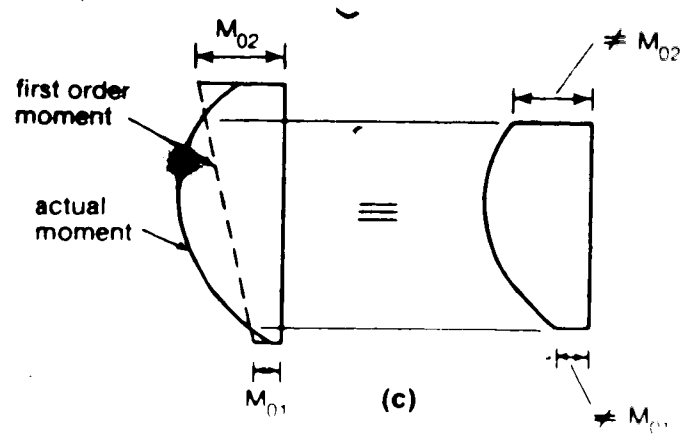
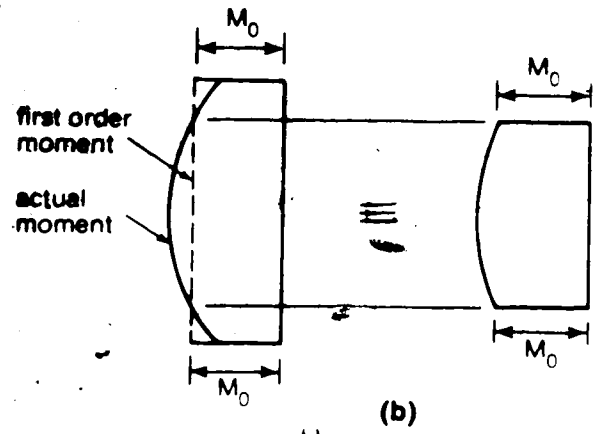
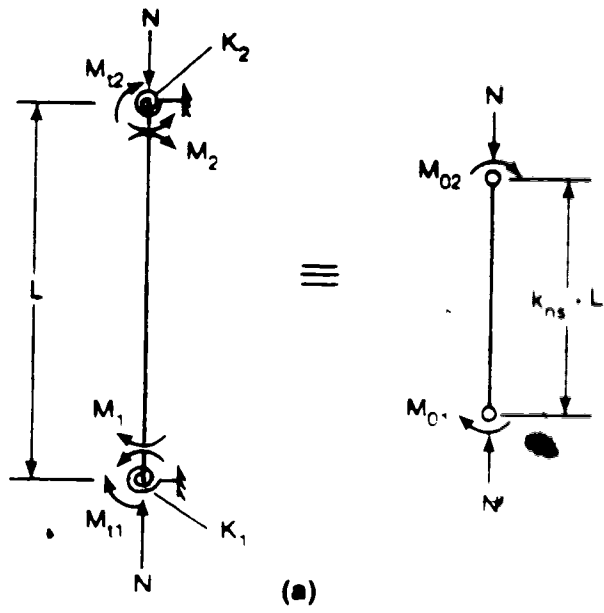


Fig. 4.4 Effective length method for single restrained columns

This method appears to have little theoretical basis except in the case of a column subjected to uniform first-order moment shown in Fig. 4.4(b). With increasing axial load the end moments decrease as shown in Fig. 3.7(a). The actual moment curve intersects the first-order moment at two points where the actual moments are identical to the first-order end-moments. The column can then be considered as a pin-ended column subjected to end-moments equal to the first-order end-moments of the real restrained column, with a column length equal to the distance between the two intersection points. The assumption that the intersection length is equal to the effective length is questionable, however, as will be studied later in this section. In the case of non-uniform first-order moment (Fig. 4.4(c)) where the moments at the intersection points are different from the first-order end-moments, the method loses its rationality. Therefore, in general, the effective length method can only be justified on an empirical basis.

The application of the effective length method to beam-columns was proposed by Winter (1954) based on the work of Lee (1949) and Bijlaard et al. (1953). Lee (1949) suggested that the maximum moment in a restrained elastic column with equal end-restraints and symmetrical joint moments can be approximated using the effective length method. Bijlaard et al. (1953) extended Lee's approach with some modification to determining the collapse load of an inelastic column with elastic restraints. Since this section deals with elastic

aspects of column behavior, discussion of Bijlaard's and Winter's papers is given in Sect. 4.5.2.

The following summarizes the development of Lee's method (1949). The restrained column studied, and the definition of related symbols have been shown in Fig. 3.5. For a restrained column with equal end-restraints K and symmetrical joint moments M_t , the internal end-moment, M , acting on the column can be obtained using the slope-deflection equation (Eq. 2.3), considering force equilibrium and rotation compatibility at the joints, and is given by

$$\frac{M}{M_t} = \frac{1}{1 + \frac{K}{EI/L} \frac{\tan(\beta/2)}{\beta}} \quad (4.14)$$

where

$$\beta = \pi \sqrt{N/N_e}$$

$$N_e = \frac{\pi^2 EI}{L^2}$$

From Eq. 4.3, the maximum moment M_{\max} in the column is equal to:

$$\frac{M_{\max}}{M_t} = \frac{\sec(\beta/2)}{1 + \frac{K}{EI/L} \frac{\tan(\beta/2)}{\beta}} \quad (4.15)$$

If the restrained column is replaced by an equivalent pin-ended column with a length equal to the effective length $k_{ns}L$, then, also from Eq. 4.3, the maximum moment is equal

to:

$$\frac{M_{\max}}{\bar{M}} = \sec \frac{\bar{\beta}}{2} \quad (4.16)$$

where

$$\bar{\beta} = \pi \sqrt{N/N_{ns}}$$

$$N_{ns} = \frac{\pi^2 EI}{(k_{ns} L)^2}$$

The fictitious end-moments \bar{M} that should be applied at the ends of the equivalent pin-ended column can be obtained by equating Eqs. 4.15 and 4.16:

$$\frac{\bar{M}}{M_t} = \frac{\sec(\beta/2)}{\sec(\bar{\beta}/2) \left(1 + \frac{K}{EI/L} \frac{\tan(\beta/2)}{\beta}\right)} \quad (4.17)$$

The effective length factor k_{ns} is used in Eq. 4.16 (though not explicitly stated by Lee), so that Eq. 4.16 gives the same elastic critical load as that of the real restrained column. The value of \bar{M} for different magnitudes of end-restraints (or k_{ns}) under increasing compression are plotted in Fig. 4.5 (from Lee's thesis, 1949). The end-moment \bar{M} increases gradually except in the vicinity of the buckling load at which \bar{M} drops abruptly to zero. Lee (1949) suggested that for simplicity, one may consider \bar{M} as a constant equal to M_0 which is the value of \bar{M} when the column axial thrust is equal to zero. That is, M_0 is the internal

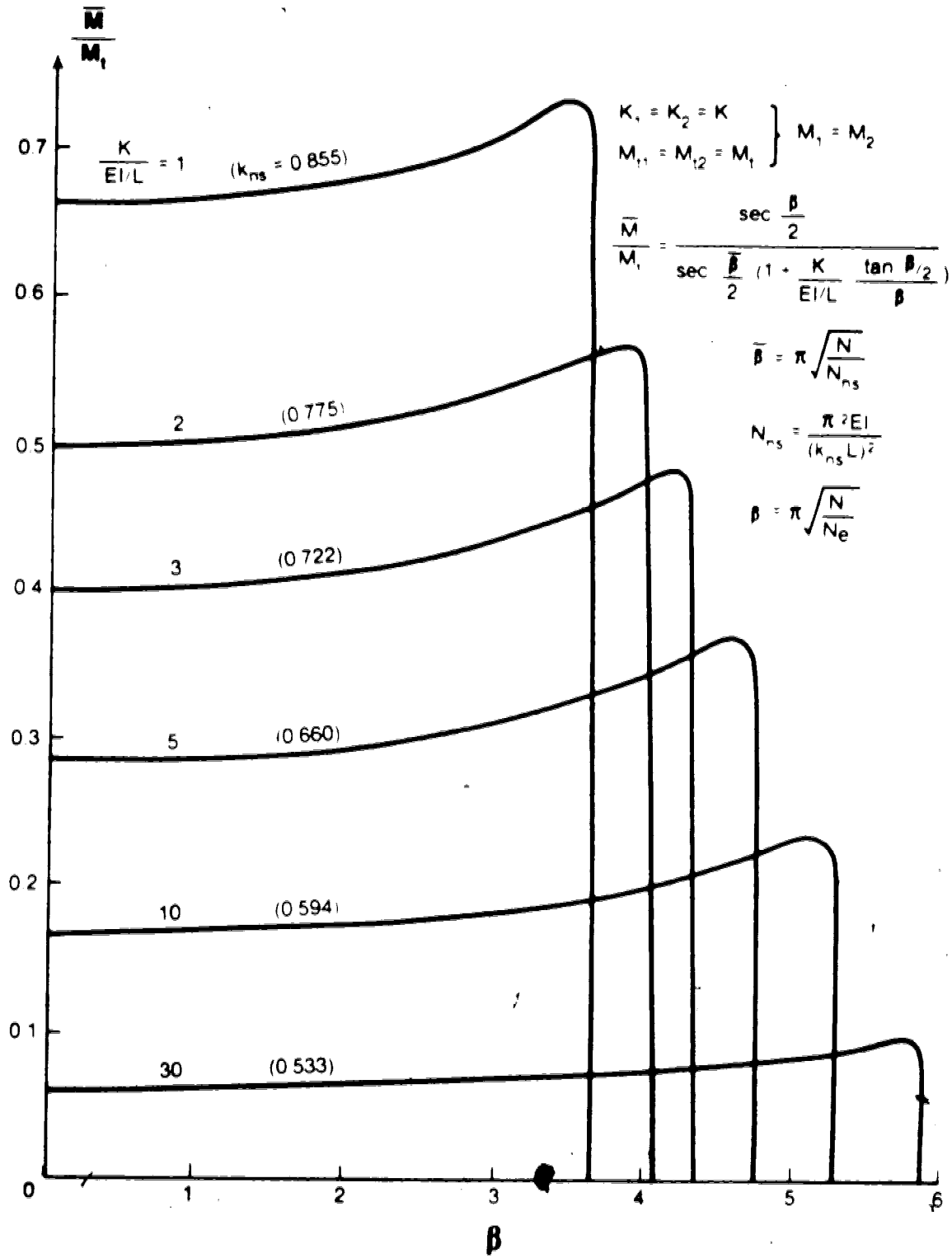


Fig. 4.5 Required end moments in an equivalent pin-end column

end-moment of the real restrained column determined from a first-order analysis. The maximum moment is therefore approximated by

$$\frac{M_{\max}}{M_0} = \sec \frac{\bar{\beta}}{2} \quad (4.18)$$

The errors introduced by Eq. 4.18 for different values of k_{ns} are shown in Fig. 4.6 as a function of the axial compression N divided by the critical load N_{ns} . It should be noted that although both the approximate value given by Eq. 4.18 and the theoretical value from the exact analysis become infinite at $N = N_{ns}$, mathematically speaking, they are not equal, as shown in Fig. 4.6. From the figure, the effective length method is shown to be unconservative for this case. The errors increase with increasing axial compression. With stronger restraints (or lower k_{ns}), the errors are larger at a given N/N_{ns} . For instance, the error at $N = 0.5N_{ns}$ for $k_{ns} = 0.85$ is approximately -4% and for $k_{ns} = 0.75$ is -8%. For lower values of k_{ns} , which may be regarded as uncommon in practice, the errors are considerably larger.

A modified effective length factor k_m which gives exact values of the maximum moment when used in Eq. 4.18 is plotted in Fig. 4.6(b). Because the first-order bending moment is uniform along the column, $k_m L$ is identical to the intersection length according to the previous discussion (Fig. 4.4(b)). Figure 4.6(b) shows that with increasing

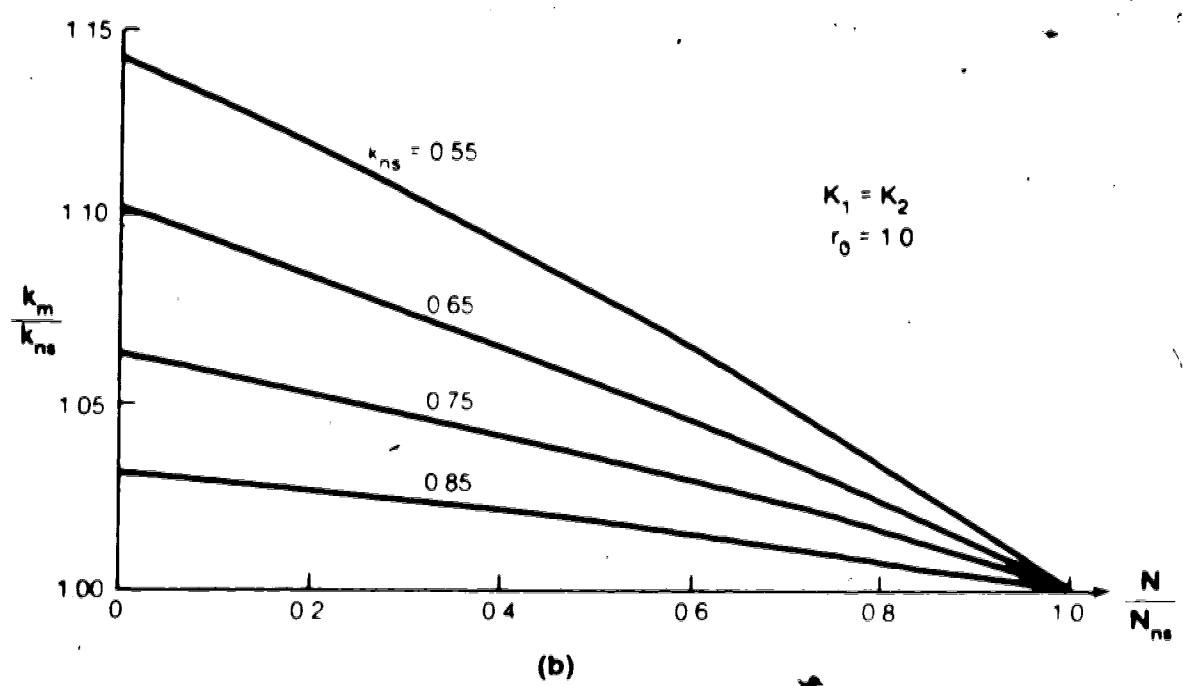
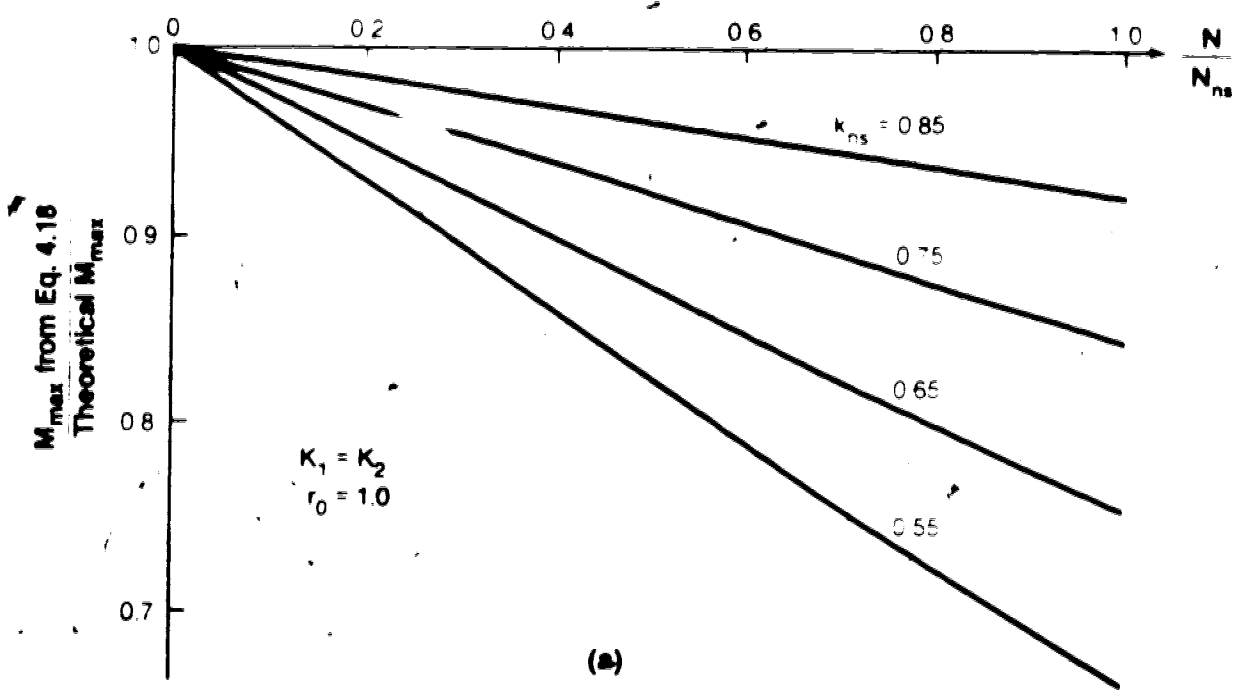


Fig. 4.6 Examination of the effective length method for $K_1 = K_2$ and $r_0 = 1.0$

compression, k_m approaches the value of k_{ns} , and is extremely close to k_{ns} at the critical load. The ratio k_m/k_{ns} varies from approximately 1.06 to 1.0 and 1.03 to 1.0 for $k_{ns} = 0.75$ and 0.85, respectively.

When Figs. 4.6(a) and 4.6(b) are examined together, they indicate that although k_{ns} becomes a more accurate approximation at higher axial loads, the resultant errors in the maximum moment increase. This is also indicated in the extreme condition of $N = N_{ns}$, at which the ratio k_m/k_{ns} is extremely close to 1.0 (Fig. 4.6(b)), while the difference in the moments is still distinct (Fig. 4.6(a)). This is because the maximum moment given by Eq. 4.18 increases very rapidly with increasing compression (Fig. 3.4), and hence the change in M_{max} becomes more sensitive to the change in N/N_{ns} (i.e., k_{ns}) when the axial load is larger.

The above observation suggests that a small overestimation of k_{ns} can eliminate the unconservative errors in the maximum moment for some particular cases. An example of $k_{ns} = 0.75$ shows that if the value of k_{ns} is overestimated by about 3.5% (Fig. 4.6(b)), the maximum moment for $N = 0.5N_{ns}$ can be accurately determined using the effective length method (Eq. 4.18). On the other hand, if k_{ns} is underestimated, the maximum moment will be underestimated to a much larger degree.

The above results for columns with equal end restraints are also applicable to the unequal end restraints if the first-order moment is uniform. In Section 3.3 (Fig. 3.9) it

was shown that the maximum moments are essentially independent of the ratio of end-restraints for a given value of k_{ns} and uniform first-order moment.

When the effective length method is extended to non-uniform first-order moments ($r_0 \neq 1.0$), from Eqs. 2.8 and 2.9, the maximum moment is approximated by:

$$\frac{M_{\max}}{M_{02}} = \frac{1 + r_0^2 - 2 r_0 \cos \bar{\beta}}{\sin \bar{\beta}} \quad \text{for } r_0 > \cos \bar{\beta} \quad (4.19)$$

$$= 1.0 \quad \text{for } r_0 < \cos \bar{\beta}$$

Equal end-restraints are first studied for the case of $k_{ns} = 0.75$ in Fig. 4.7. The theoretical maximum moment is determined using the exact elastic analysis described in Sect. 2.3. For $r_0 < 1.0$, Eq. 4.19 gives conservative results up to a load level that depends on the value of r_0 , as shown in Fig. 4.7(a). For smaller values of r_0 , the method tends to be conservative up to a larger axial load. This can be explained by noting Fig. 3.9(a), which shows that the ratio M_{\max}/M_{02} for $r_0 < 1.0$ initially diminishes due to the axial load, whereas the value of M_{\max}/M_{02} determined by Eq. 4.19 (shown in Fig. 3.9(a) as dotted lines) is always greater than or equal to 1.0. When the ratio M_{\max}/M_{02} is equal to 1.0, the value of k_m which gives exact results when used in Eq. 4.19 becomes immaterial (Fig. 4.7(b)). As expected from Fig. 4.6, the case of $r_0 = 1.0$ (for equal end-restraints) gives unconservative values of

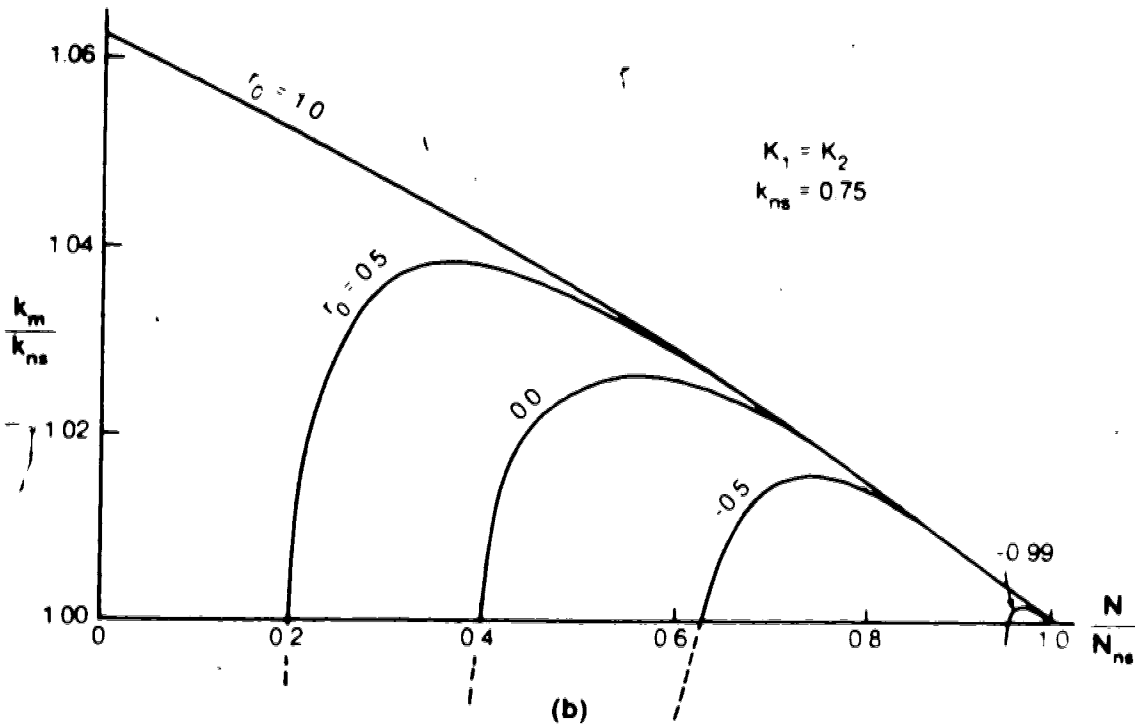
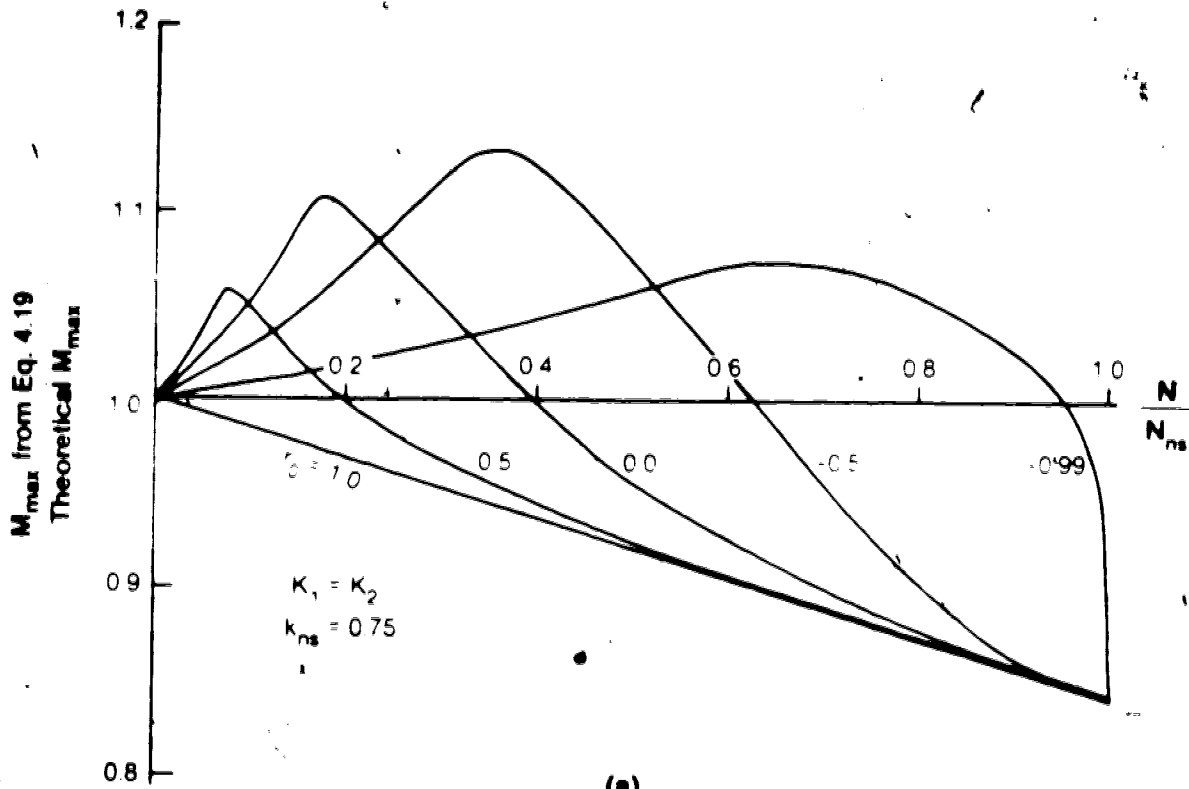


Fig. 4.7 Examination of the effective length method for $K_1 = K_2$ and $r_0 \leq 1.0$

moment for all values of axial load and forms a lower bound on the other curves. For restraint magnitudes other than $k_{ns} = 0.75$, the results are similar except that the magnitude of the errors will be larger for stronger restraints and smaller for weaker restraints.

For the case of the unequal end-restraints, Fig. 3.9(b) indicates that for a given k_{ns} , a column with weak restraint K_2 at the end where the moment M_2 acts and strong K_1 (symbols defined in Fig. 3.5) has the greatest maximum moment at any axial load for a given k_{ns} and r_0 value. The extreme case of $K_2 = 0.0$ (a hinge), shown in Fig. 4.8, indicates that for $r_0 < 1.0$ the maximum moment approximated by Eq. 4.19 is accurate up to a certain load level because the maximum moment occurs at the end ($M_{max} = M_2 = M_{02}$). When the maximum moment occurs between the ends of the column, the approximate values become unconservative. Unlike the previous case, the approximate values tend to be much more unconservative for smaller values of r_0 . This is also reflected by the values of k_m in Fig. 4.8(b).

In conclusion, the maximum moment in a column subjected to uniform first-order moment analyzed by the effective length method, which can only be considered empirical, is always less than the theoretical elastic value. For columns subjected to first-order moment gradient, with weak K_2 and strong K_1 , the errors could be even greater. On the other hand, the method may produce conservative results in cases where the actual maximum moment in a column is less than the

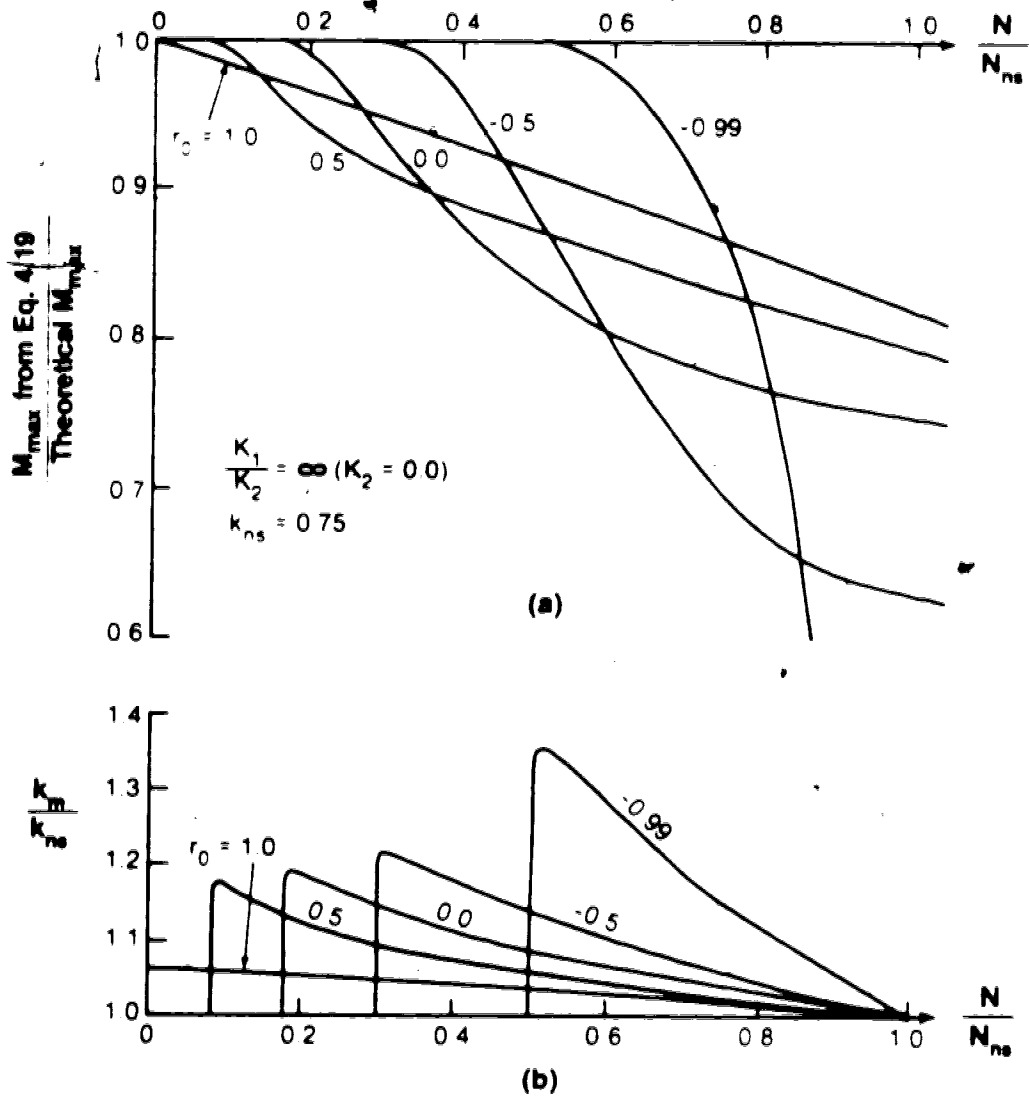


Fig. 4.8 Examination of the effective length method for $K_1/K_2 = \infty$ and $r_0 \leq 1.0$

larger first-order end-moment. (This condition cannot be predicted by the effective length method.) The errors increase with smaller k_{ns} and with larger axial load. In a design situation where the maximum moments need to be estimated, the above results suggest that a restrained elastic column analyzed by the effective length method may have a safety factor less than that implied for a pin-ended column.

4.3 ACI method

4.3.1 Single restrained columns

According to the current ACI Code (1977), the maximum moment (M_{max}) in a single restrained non-sway column with given internal first-order end-moments (M_{01} , M_{02}) can be determined by the following equation:

$$\delta_{ns} = \frac{C_m}{1 - \alpha_{ns}} > 1.0 \quad (4.20)$$

where

$$C_m = 0.6 + 0.4 r_0 > 0.4$$

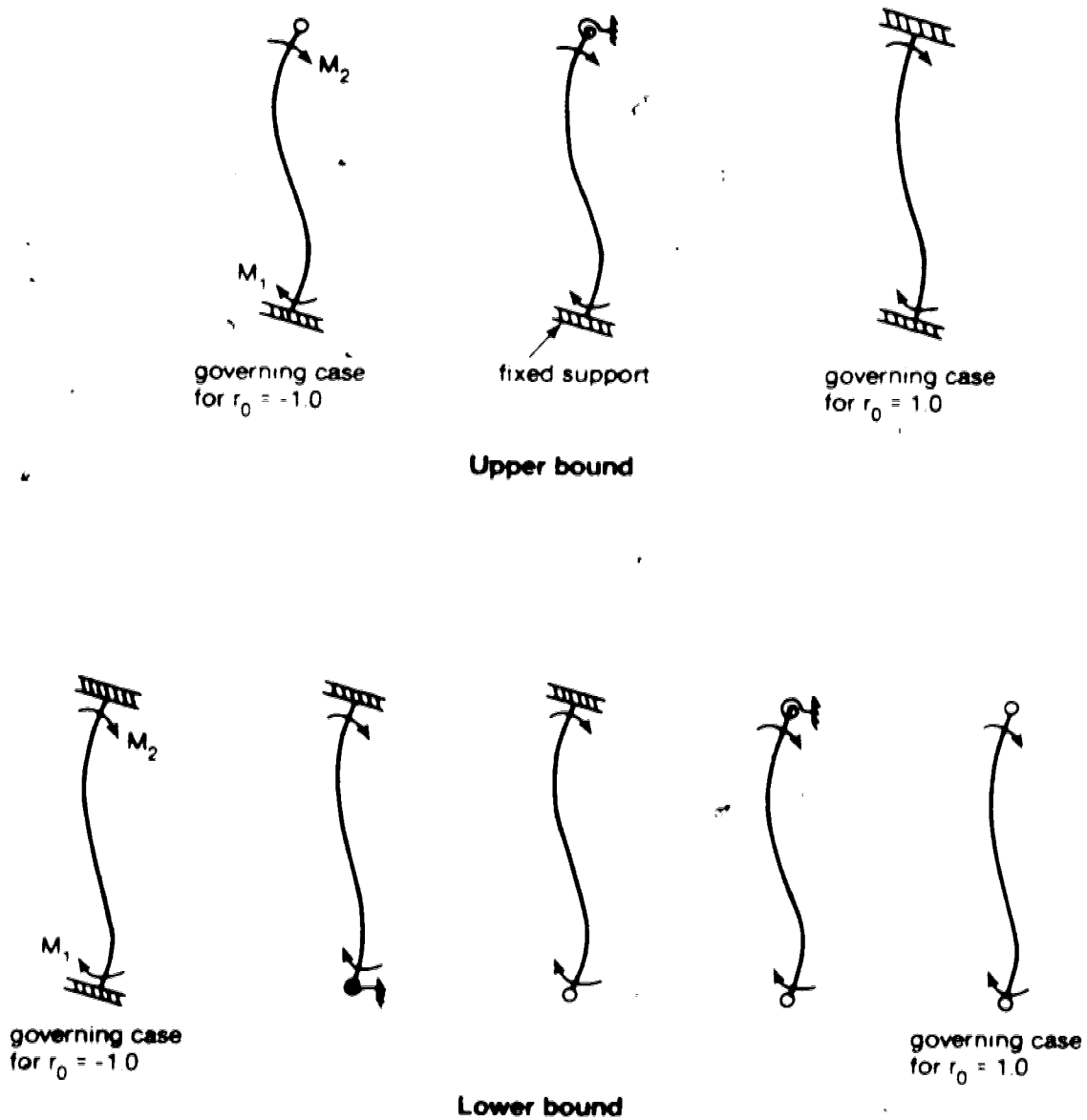
The moment magnifier δ_{ns} is defined as M_{max}/M_{02} , and α_{ns} is N/N_{ns} .

In the ACI Code N_{ns} is actually written as ϕN_{ns} where ϕ accounts for variability in N_{ns} . Since this discussion deals with ideal elastic members, ϕ will be taken equal to

1.0. The derivation of Eq. 4.20 is an approximation of the elastic solution based on a pin-ended column (Eq. 4.12 in Sect. 4.1) and it is extrapolated to a single restrained column by incorporating the effective length factor k_{ns} (Sect. 4.2, MacGregor et al., 1970).

The moment magnification from Eq. 4.20 is compared to the upper and lower bounds of M_{max}/M_{02} from the theoretical elastic solutions for a given N/N_{ns} in Figs. 4.10 to 4.14 for $r_0 = 1.0, 0.5, 0.0, -0.5, \text{ and } -1.0$, respectively. As mentioned in Sect. 3.3, for a given N/N_{ns} , the maximum moment in an elastic column is a function of k_{ns} and the relative magnitudes of the two end-restraints. Based on the observations made in Sects. 3.3 and 4.2, the upper and lower bounds of the maximum moments occur in the columns shown in Fig. 4.9. Each of the column types shown was studied, and the upper and lower bound values were selected.

For $r_0 = 1.0$, the upper bound on the maximum moments corresponds to columns with infinitely stiff beams at both ends, and the lower bound corresponds to columns with beams of zero stiffness (see Fig. 4.6(a)). A column with an infinitely stiff beam at one end and a hinge at the other end produces the upper bound values for $r_0 = -1.0$ (see Fig. 4.8(a)), whereas a column with infinitely stiff beams at both ends produces the lower bound values (see Fig. 3.9). For intermediate values of r_0 , the governing types of columns depend on the ratio r_0 as well as the magnitude of N/N_{ns} . In many cases, the column with an infinitely stiff



Note: The internal moments (M_1 , M_2) and deformations are arbitrarily shown according to the positive sign convention

Fig. 4.9 Types of columns corresponding to upper and lower bounds of the maximum moments

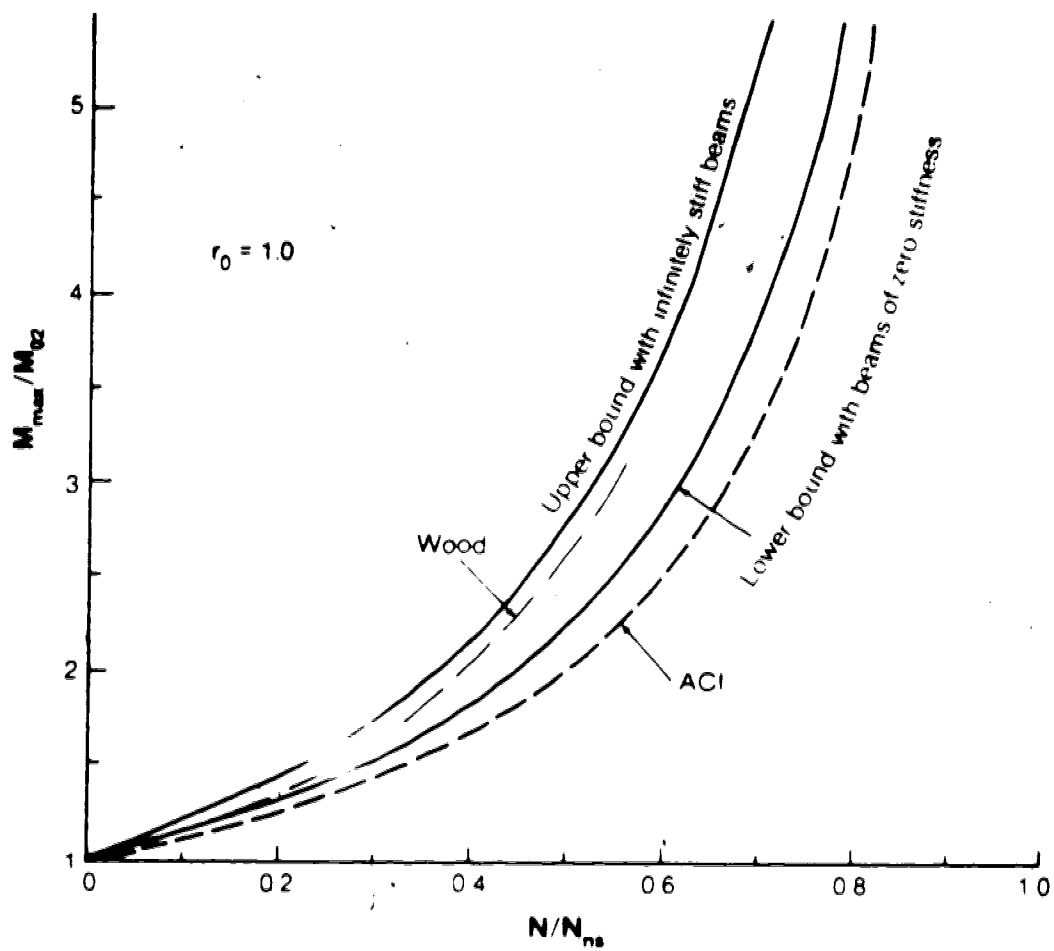


Fig. 4.10 Comparison of approximate with theoretical magnification factor for $r_0 = 1.0$

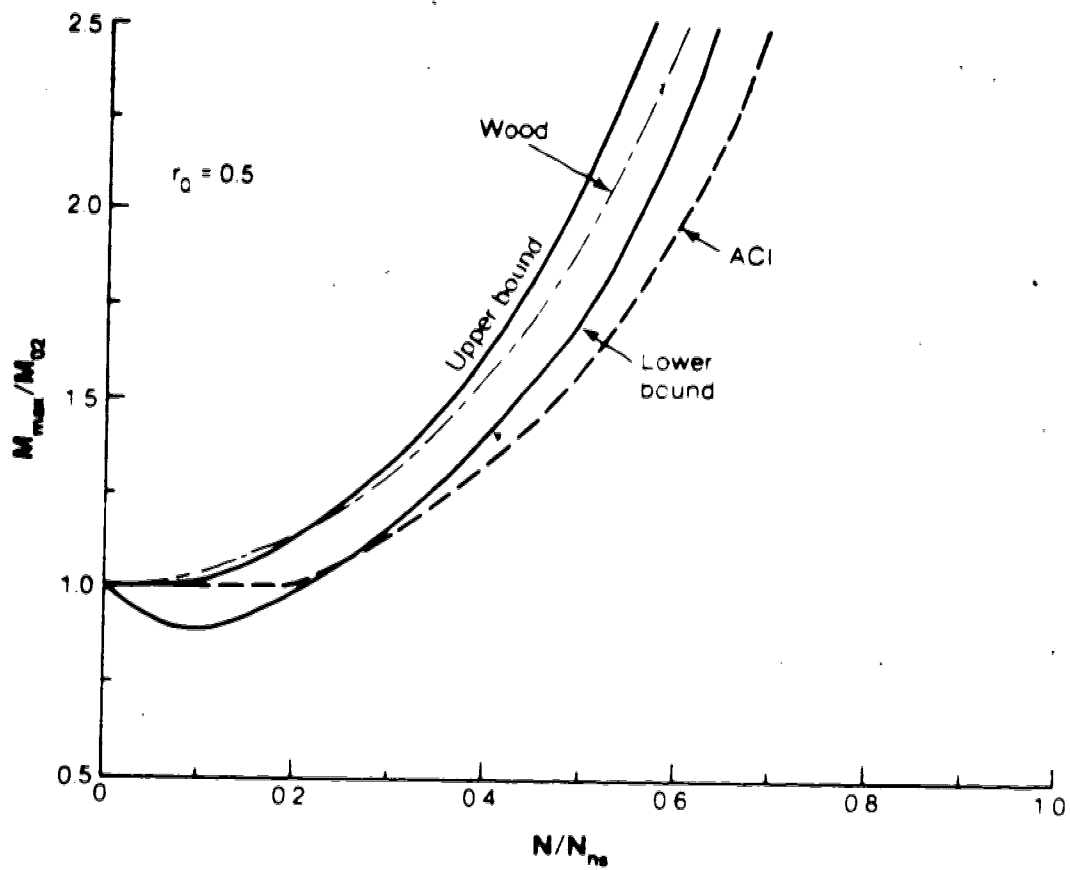


Fig. 4.11 Comparison of approximate with theoretical magnification factor for $r_0 = 0.5$

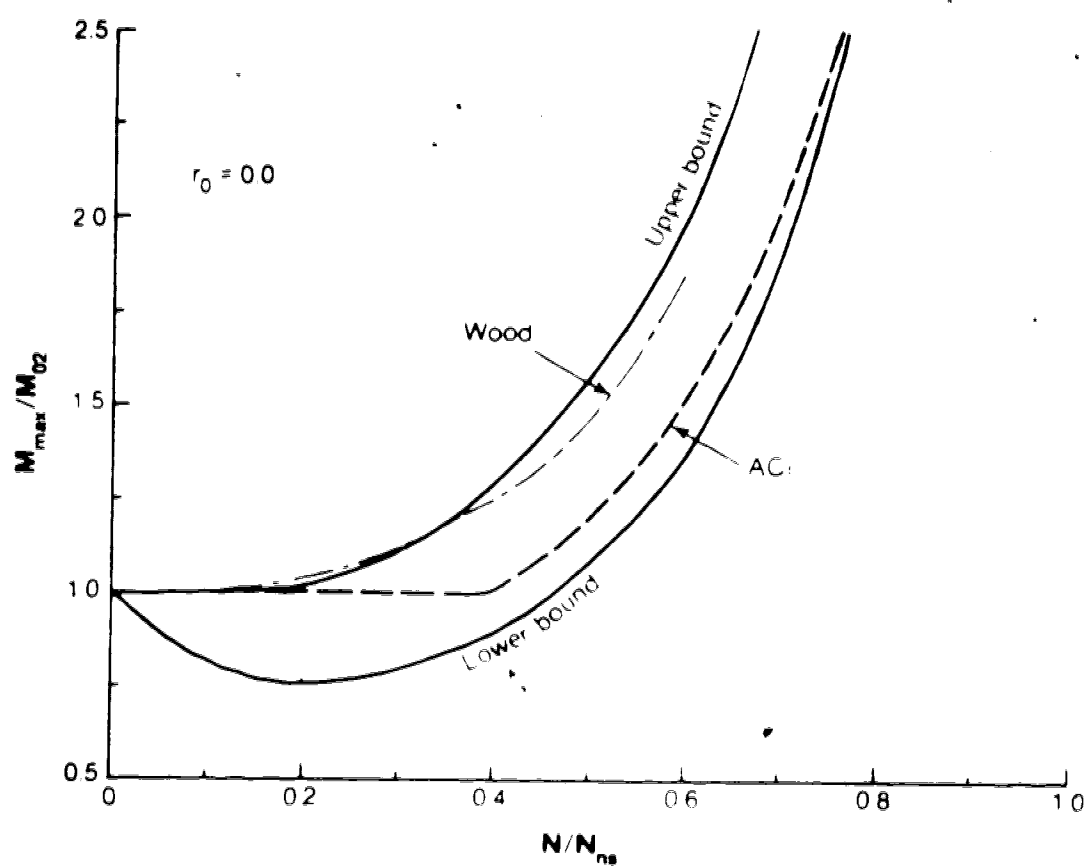


Fig. 4.12 Comparison of approximate with theoretical magnification factor for $r_0 = 0.0$

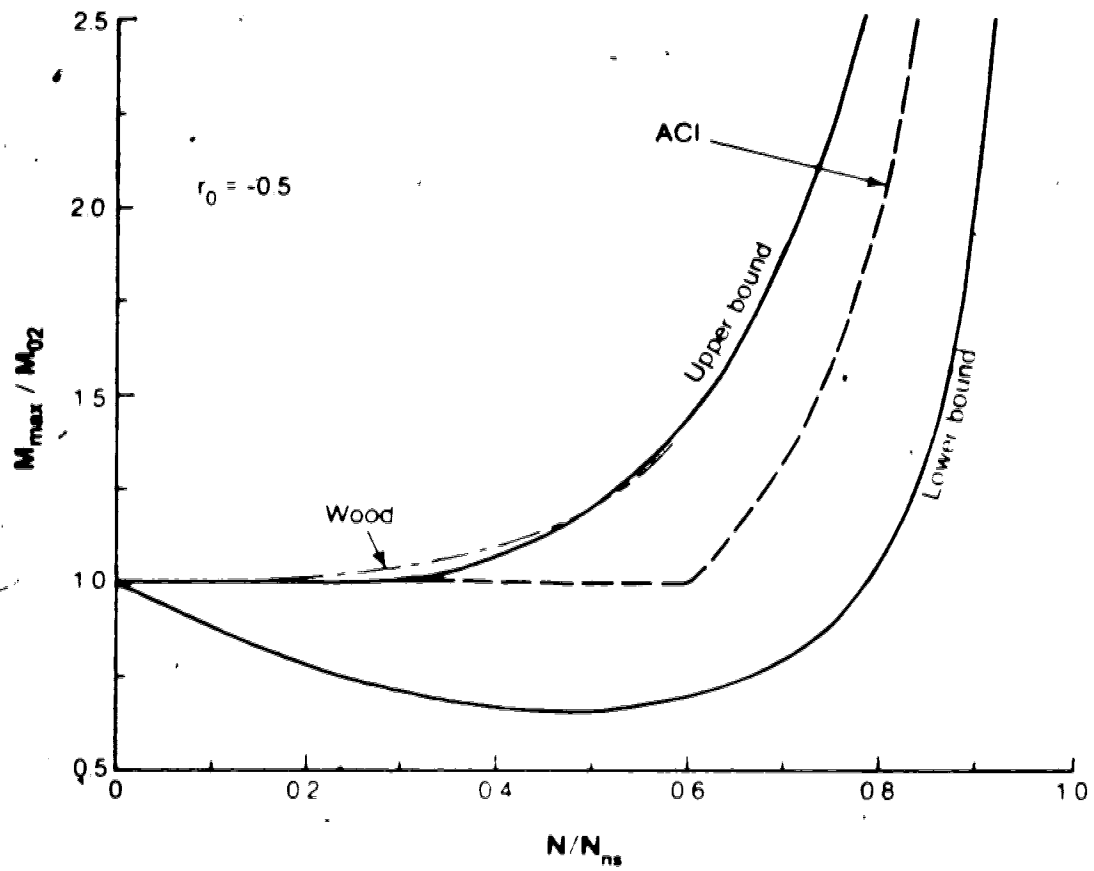


Fig. 4.13 Comparison of approximate with theoretical magnification factor for $r_0 = -0.5$

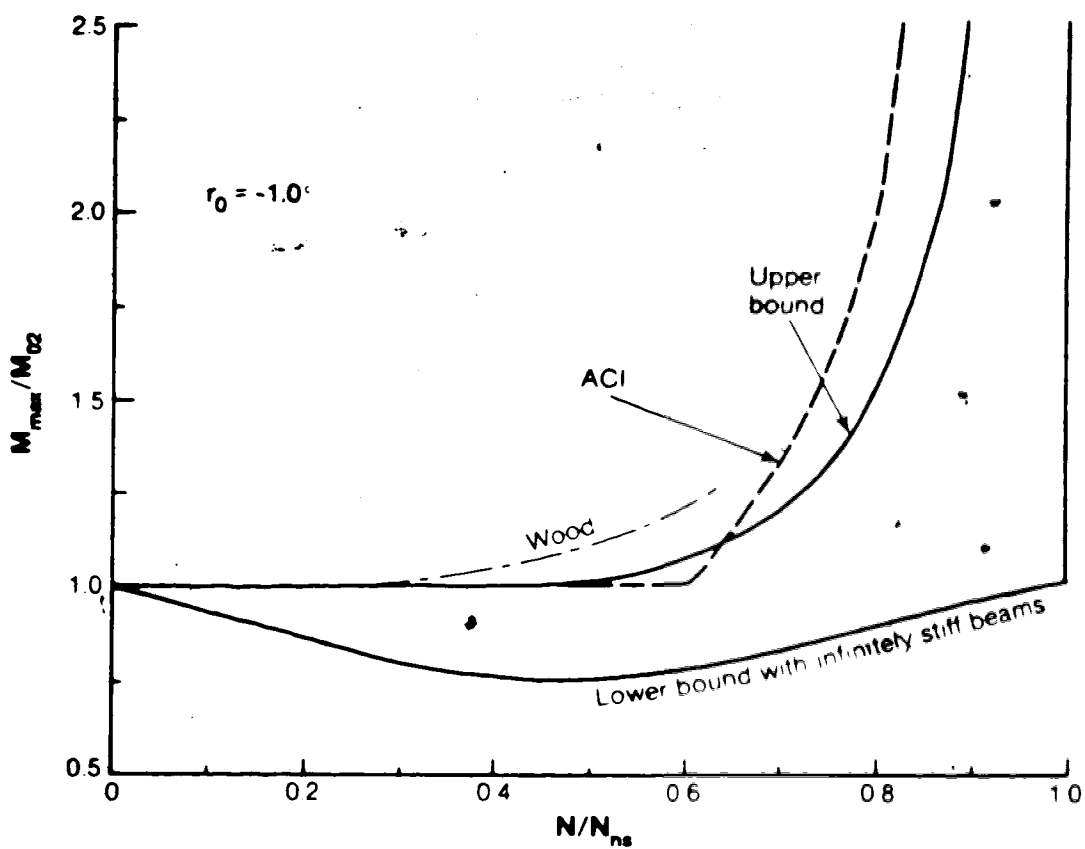


Fig. 4.14 Comparison of approximate with theoretical magnification factor for $r_0 = -1.0$

beam at one end and a hinge at the other end is the dominant case for upper or lower bound values. It should be noted that in determining the upper bound values, the larger first-order end-moment M_{02} is applied at the hinge (i.e., $M_2 = M_{02}$ for any values of N/N_{ns}), whereas for lower bound values, M_{02} is induced by the infinitely stiff beam (see Fig. 3.9(b)). From Figs. 4.10 to 4.14, it can be seen that the difference between the two bounds increases with increasing values of N/N_{ns} .

In the case of $r_0 = 1.0$, the maximum moments from Eq. 4.20 fall below the lower bound values for all values of N/N_{ns} because of the following two reasons. First, the term $[0.25 N/N_{ns}]$ has been neglected in Eq. 4.20 (see Eq. 4.7). If it were included, Eq. 4.20 would be almost the same as the lower bound curve. Second, the use of effective length method itself makes the solutions unconservative as discussed in Sect. 4.2. For smaller values of r_0 , Eq. 4.20 approaches to the lower bound and moves into the bounded region. This is because as r_0 decreases, Eq. 4.20, which is derived from the approximate equation (Eq. 4.12) for a pin-ended column, approaches closer to the theoretical equation for a pin-ended column as shown in Fig. 4.2. In addition, the effective length approach leads to conservative results up to certain load levels for lower bound cases as shown in Sect. 4.2. For $r_0 = -0.5$, Eq. 4.20 becomes virtually the mean curve of the two bounds. For $r_0 = -1.0$, Eq. 4.20 predicts values even higher than the upper bound at larger

axial loads due to the limit of $C_m > 0.4$ imposed on the equation.

4.3.2 Multistorey frames

As discussed in the previous sections, the current ACI Code (1977) method for calculating the maximum moment in a non-sway column (Eq. 4.20) is developed for single restrained columns whose magnitudes of end-restraints are unaffected by the geometric effects. In order to extend the method to restrained columns in a non-sway multistorey frame, it is necessary to assume that the end-restraints of any column in the frame remains unaffected by the geometric effects. As a result of this assumption, any column can be isolated from the frame, as shown schematically in Fig. 4.15, such that the end-restraints for the isolated column are equal to the first-order end-restraints.

In the Commentary to the ACI Code, the end-restraints are expressed in terms of the ratios of column to beam stiffnesses. The following analysis, based on the assumption in the above paragraph, is a necessary step preceding the method suggested in the ACI Commentary. The restraint offered by a beam is a function of the signs of the moments at its ends (Eq. 4.22, to follow), and the restraint is distributed to the upper and the lower column at a joint according to the relative values of the column end-moments at that joint. Thus the first-order end-restraints can be determined from the first-order moments.

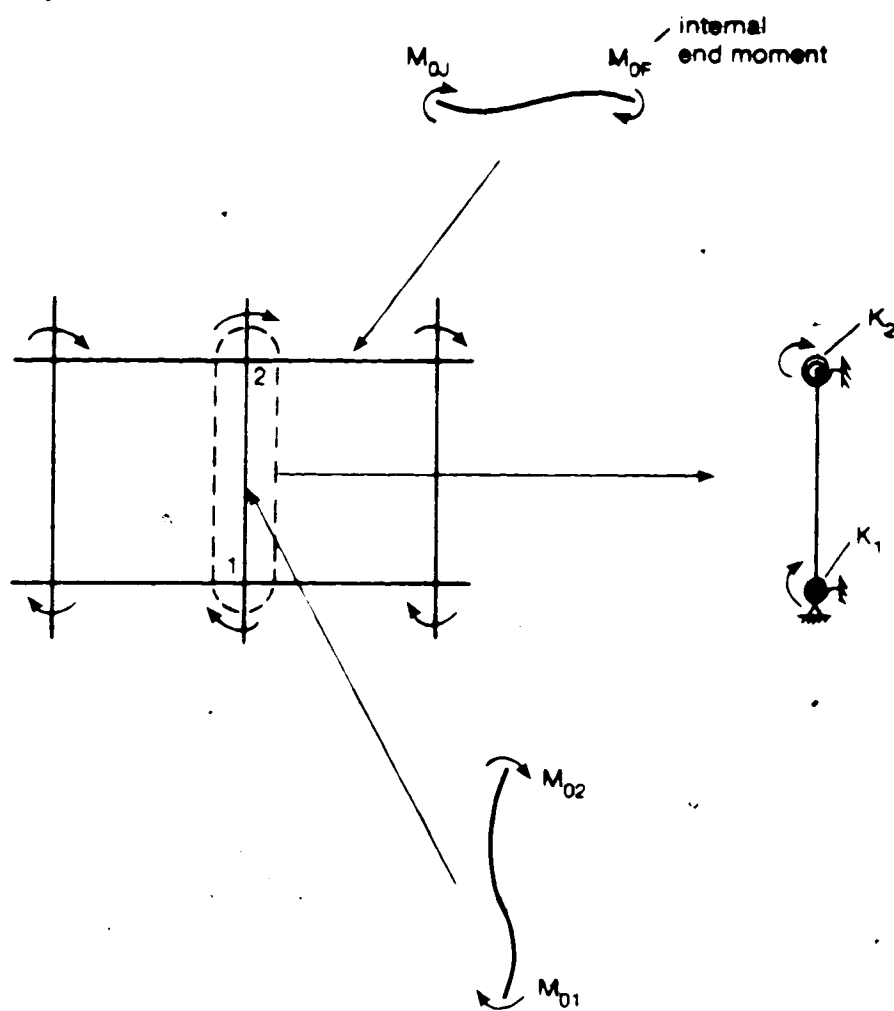


Fig. 4.15 A column isolated from a non-sway frame

The restraint stiffness K_2 at joint 2 of the isolated column (Fig. 4.15) obtained in this way is equal to:

$$K_2 = \frac{M_{O2}}{(\sum M_O)_{col}} \left(\sum m \frac{EI_B}{L_B} \right)_{beam} \quad (4.21)$$

where

$$m = \frac{3}{1 - \frac{1}{2} \frac{M_{OF}}{M_{OJ}}} \quad (4.22)$$

and $(\sum M_O)_{col}$ denotes the sum of first-order column end-moments at joint 2, M_{OJ} is the first-order beam moment at joint 2, and M_{OF} is the first-order moment at the far end of the beam (Fig. 4.15). The symbol $(\sum)_{beam}$ denotes summation for all beams rigidly connected to joint 2. Note that the first-order beam moments are those determined from the unbalanced fixed-end moments at the joints in the non-sway frame before the superposition of non-sway and sway effects (Fig. 2.9). The restraint stiffness K_1 at the other joint is given by the above equations with M_{O2} replaced by M_{O1} , and the summation of column moments and beam stiffnesses taken at joint 1.

Once a column has been isolated from the frame and the end-restraints are given by the above equations, the ACI Code treats it in the same way as discussed before for a single restrained column. In short, the effective length factor required in the ACI method for a restrained column in a multistorey frame should be determined based on the

corresponding first-order end-restraints. It is emphasized here that this assumption is a necessary step to extend the ACI Code design method to a column in a frame.

The assumption of constant end-restraints, i.e., neglecting the horizontal and vertical interaction of columns due to geometric effects, is reasonable for large regular multistorey frames where the member stiffnesses and axial loads of neighbouring columns do not vary appreciably (Sects. 3.4 and 3.5). In case the vertical interaction is significant, as discussed in Sect. 3.5, the assumption that a column can be isolated is conservative for weak columns (Fig. 3.15), but unconservative for strong columns (Fig. 3.14). For horizontal interaction, the further assumption introduced in the following paragraph will make the solution tend to be conservative.

The current ACI Commentary (1977) recommends a further step to simplify the determination of the constant end-restraints in calculating the effective length factor by making the following assumptions:

$$M_{0J} = - M_{0F} \quad (4.23)$$

$$\frac{M_{02}}{(\sum M_0)_{col}} = \frac{EI/L}{(\sum \frac{EI}{L})_{col}} \quad (4.24)$$

where $(\sum \frac{EI}{L})_{col}$ denotes summation of columns rigidly connected to that joint. By substituting Eq. 4.23 into Eq. 4.22, m becomes equal to 2.0. Substituting $m = 2$ and Eq.

4.24 into Eq. 4.21, Eq. 4.25 is obtained:

$$K_2 = \frac{2EI}{G_2 L} \quad (4.25)$$

where

$$G_2 = \frac{\left(\sum \frac{EI}{L}\right)_{\text{col}}}{\left(\sum \frac{EI_B}{L_B}\right)_{\text{beam}}}$$

Similarly K_1 is a function of G_1 . Consequently, the effective length factor for any column in the frame can be computed after obtaining the values of G_1 and G_2 . An effective length factor alignment chart, which is constructed according to the above assumptions and therefore is a function of G_1 and G_2 , is given in the ACI Commentary (1977), as well as in many other design codes.

The assumption in Eq. 4.23 that the beam effective stiffness is equal to $2 \cdot EI_B/L_B$ tends to be conservative and in fact safeguards the unconservative errors due to neglecting the horizontal interaction of columns (Sect. 3.4). The other assumption (Eq. 4.24) that the ratio of column end-moments at the joint is equal to the ratio of their stiffness parameters EI/L is reasonable if the far ends of the upper and the lower column are in similar condition. It can be seen that these two assumptions appear reasonable for a regular multistorey frame with regular loading pattern.

If the far end of the beam that is framed into the column under consideration is hinged ($M_{OF} = 0.0$), m becomes equal to 3. In order to use the alignment chart that is based on $m = 2$, the beam length should be multiplied by $2/3$ when calculating the value of G . Similarly for a beam with the far end fixed against rotation, the beam length should be multiplied by 0.5. This correction is mentioned in the AISC Commentary (1978) but not in the ACI Commentary (1977).

It should be noted that the derivation of the present form of the ACI method, as applied to multistorey frames, is unclear in the commentary, or the source paper (MacGregor, et al., 1970). It is believed the above description is a logical presentation of the assumptions involved.

The assumptions and simplifications involved in development of the ACI method suggest that it is not necessary to perform a rigorous elastic stability analysis for the whole frame to find the 'exact' effective length factors. (Of course, one would not do this in practice since a stability analysis is no simpler than an exact second-order analysis.) This point, however, is unclear in the present ACI Code and Commentary.

In the ACI Commentary, it is also suggested that the effective length factors used in the ACI method (Eq. 4.20) can be taken as the lesser of:

$$k_{ns} = 0.7 + 0.05 (G_1 + G_2) < 1.0$$

(4.26)

$$k_{ns} = 0.85 + 0.05 G_g < 1.0$$

where G_g is the smaller of G_1 and G_2 . This equation is a conservative empirical approximation for the effective length factors determined based on the previous assumptions (Eqs. 4.23-4.25). The formula was developed by Cranston (1972), and is recommended by the current British Code for concrete (CP 110, 1972).

The results from Eq. 4.26 are compared in Fig. 4.16 (from Cranston, 1972) with those from an exact analysis of a single restrained column with end-restraints given by Eq. 4.25 (i.e., the same results as those from the conventional effective length factor alignment chart). It is shown that the approximate equation (Eq. 4.26) always errs on the conservative side with errors ranging from 5% to 20%, mostly 10%, for $k_{ns} > 0.7$. Equation 4.26 has a lower limit of $k_{ns} > 0.7$, which will be discussed in Sect. 4.5.3.

4.4 Wood's method

In determining the maximum moment in a single restrained column from the first-order end-moments, Wood (1974) proposed to use empirical curves which depend only on N/N_{ns} for a given value of r_0 . The curves were intended to represent the mean values of the upper and lower bounds, but they tend to be closer to the upper bound curves, as shown in Figs. 4.10-4.14. These curves will be incorporated in the new British Code for steel design (BS 449, Roberts and

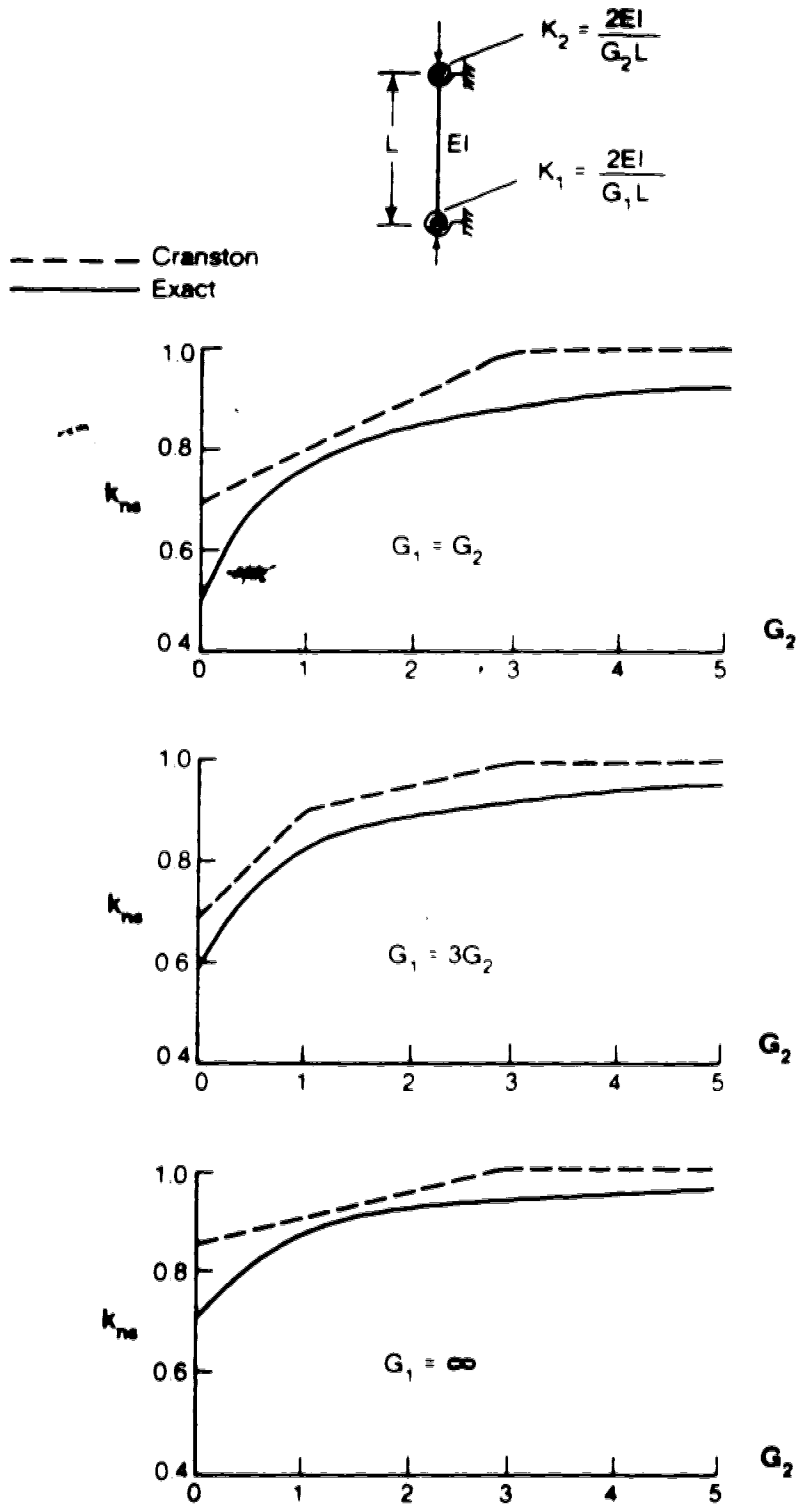


Fig. 4.16 Effective length factors for non-sway single columns

Yam, 1981). Such curves provide conservative results in almost all practical cases since the types of columns corresponding to the upper bound are rare in practice, but inevitably are overconservative in many cases.

For restrained columns in a multistorey frame, the assumptions in the ACI method are also followed except that the far ends of the beams are assumed fixed against rotation (i.e., $m = 4$ in Eq. 4.22) in determining the effective length factor (Wood, 1958, 1974). The different assumption is less conservative than the one in the ACI method, and appears unconservative in many practical loading cases when the beams are bent into single curvature (due to the unbalanced fixed-end moments).

4.5 Discussion

The major objective in this section is to discuss the accuracy of the ACI (1977) method in predicting the geometric non-linearity of non-sway columns. Since the ACI design rule is based on pin-ended columns, such columns will be discussed first. The discussion on the methods of extending the design rule for pin-ended columns to single restrained columns and restrained columns in multistorey frames will follow in the next two sections.

4.5.1 Pin-ended columns

The ACI (1977) design equation (Eq. 4.12) for pin-ended columns omits the term 0.25α included in the more accurate

Eq. 4.13. The omission of this term, however, has been shown in Fig. 4.2 to be unconservative. As discussed in Sect. 1.1, the derivation of the present ACI Code (1977) procedure for designing slender columns basically follows the procedure of approximation shown in Fig. 1.1 (MacGregor et al., 1970). That is, the inelastic effects and geometric effects are approximated independently of each other. If this assumption is strictly followed, it appears more reasonable to include the term 0.25α in the ACI equation.

As shown in Sect. 4.1, the limit of $C_m > 0.4$ in the ACI equation is theoretically unnecessary for in-plane bending, since this limit was derived for lateral-torsional buckling. In fact, this was realized by MacGregor et al. (1970) when developing the ACI (1977) design equation, but the limit was still employed because of "the uncertainty of frame action when values of r are between -0.5 and -1.0 ". The "uncertainty of frame action" referred to the unwinding problem mentioned in Sect. 3.2. Tests of pin-ended reinforced concrete columns bent in double curvature ($r = -1$) carried out by Martin et al. (1966) and MacGregor et al. (1966) have indicated that under high axial loads the column may unwind rather suddenly with the column collapsing in the instability mode. Since, in the derivation of the ACI (1977) equation, it was assumed that 'material failures' rather than 'stability failures' would occur, it appears advisable to retain the limit to safeguard against an instability mode of failure.

It can be seen that the limit of $C_m > 0.4$ is also applicable even if the exact elastic equations (Eqs. 2.8 and 2.9) are used to calculate the maximum moment. After all, this limit becomes effective only when the axial load in a column is greater than $0.6N_e$, which is a high axial load for a pin-ended column in practice, and as a result the limit should seldom have effect in design.

4.5.2 Single restrained columns

The discussion on single restrained columns is divided into four parts. In part (a), the question of whether a restrained column can be designed as a pin-ended column when the internal end-moments can be exactly determined at the onset of failure will be discussed. In part (b), the study of the effective length method carried out by Bijlaard et al. (1953) for steel beam-columns will be discussed. In part (c), a conservative estimate of the effective length factor using Cranston's equation (Eq. 4.26) will be suggested. In part (d), it will be suggested that the limit of $C_m > 0.4$ for restrained columns is still required.

(a) Equivalent pin-ended columns

Theoretically, a pin-ended column can be considered as a column with known end conditions provided the axial load is less than the critical load of a pin-ended column, and the maximum moment in the column can be computed.

Similarly, a restrained non-sway column can be treated in

the same way if the internal end-moments can be accurately determined at the onset of failure. It should be emphasized here that the end-restraints strengthen the column by changing its internal end-moments during loading to act in the opposite direction to the deflection caused by the increasing compression (Sect. 3.3). In other words, when the exact internal end-moments in a column at the onset of failure are used in the analysis, the restraining effects are also included automatically.

The above reasoning is based on a consideration of geometric effects only. This is not necessarily the case when the effect of inelastic action is taken into account, as discussed in the following. Figure 4.17(a) shows the moment-rotation curves for an inelastic column subjected to a given axial load N_1 and joint moments M_t . The moment M_t is resisted by M_B and M_C . Note that for an elastic column the moment-rotation relationship would be straight; the curve shown reflects inelastic action in the column. For the sake of discussion, the column is assumed to be symmetrically restrained and symmetrically loaded.

As shown in Fig. 4.17(a) the maximum applied joint moment, M_{tmax} , occurs when the internal end-moment of the column is equal to M_{C1} which is less than the peak value M_{Cmax} . If the column were unrestrained and subjected to end-moments M_{C1} , in general it would fail by instability at an axial load (N_2) different from N_1 , as shown in Fig. 4.17(b). (In order for the column to fail at N_1 , it should

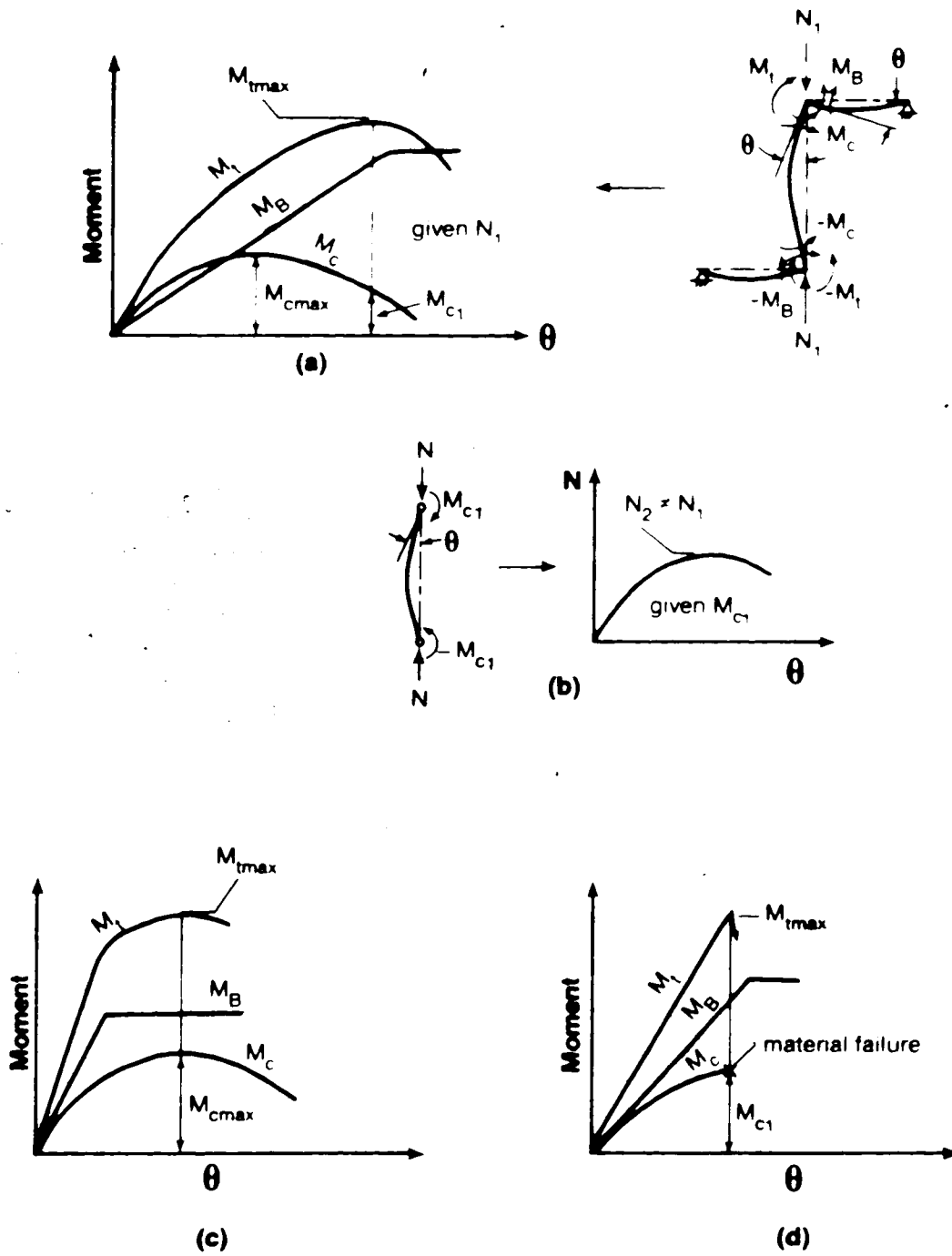


Fig. 4.17 Inelastic Columns

be subjected to end-moments M_{Cmax} .) The discrepancy occurs because the end-restraints allow the internal end-moments in the column to decrease after the maximum value M_{Cmax} is reached though the applied joint moments M_t are still increasing (Fig. 4.17(a)), whereas a pin-ended column fails at the maximum values of the end-moments. As a result, in this case a restrained column with known end-moments at the onset of failure cannot be treated as a pin-ended column subjected to those end-moments.

Figures 4.17(c) and (d) indicate cases where an inelastic column can still be treated like a pin-ended column if the internal end-moments at the onset of failure are known. In Fig. 4.17(c), the beam has yielded before the column end-moment M_C reaches the peak value M_{Cmax} . In this case the maximum joint moment, M_{tmax} , occurs when M_C is equal to M_{Cmax} . If this column were unrestrained and subjected to M_{Cmax} at both ends, it would also have the same maximum axial load as the actual restrained column. In Fig. 4.17(d), the maximum joint moment for the restrained inelastic column is reached at the material failure of the column. The corresponding end-moments M_{C1} , when applied to a similar but unrestrained column, would also lead to the same maximum axial load provided the unrestrained column also collapsed by material failure.

In the ACI design approach, the column is assumed to collapse by material failure (as mentioned earlier), thereby corresponding to Fig. 4.17(d). Following the above

reasoning and the assumptions made in Sect. 1.1 (Fig. 1.1), once the end-moments in the column have been obtained from a second-order elastic analysis (or other methods that take into account the geometric non-linearity) with appropriate effective EI values, the restrained reinforced concrete column can be designed as a pin-ended column using $k_{ns} = 1.0$ provided $N < N_e$. This approach is limited to $N < N_e$ because a pin-ended column can never sustain a load greater than N_e . The behavior of columns with $N > N_e$ has been discussed in Sect. 3.3.

(b) Work of Bijlaard et al. (1953)

Bijlaard et al. (1953) extended the effective length method (Sect. 4.2), derived for elastic columns, to inelastic non-sway steel beam-columns with symmetrical elastic end-restraints and symmetrical joint moments, and proposed that a reduced EI for the column should be used to account for the inelastic effects in calculating the first-order end-moments and the effective length factor k_{ns} . (Winter (1954) simplified further the method by suggesting that the gross EI, rather than the reduced EI, can be used, resulting in a conservative determination of end-moments and effective length factors in all cases for steel beam-columns.) The reduced EI was determined by assuming that a restrained column could be replaced by an equivalent pin-ended column with its length equal to the effective length of the real restrained column and subjected to the first-

order end-moments. The values of EI used in calculating the first-order end-moments and k_{ns} were selected in such a way that the ultimate axial load of the equivalent pin-ended column was equal to the exact ultimate axial load of the actual restrained column. The study was largely empirical, and it does not offer a theoretical or rational basis for the use of the effective length factor in the ACI design approach.

(c) Cranston's equation

The effective length method has been shown in Sect. 4.2 to be unconservative in many cases. On the other hand, Figs. 4.6 to 4.8 have shown that a small increase in the effective length factor can eliminate the unconservative errors inherent in the effective length method. As mentioned in Sect. 4.3.2, the effective length factor given by Cranston's equation (Eq. 4.26) is a conservative approximation for a single restrained column with restraint stiffness $K_1 = \frac{2EI}{G_1L}$ and $K_2 = \frac{2EI}{G_2L}$. For $k_{ns} > 0.7$, the effective length factor is overestimated by about 5% to 20%. As a result, the values of k_{ns} obtained from Cranston's equation, when used in the ACI equation, should yield conservative results in most cases provided the term $0.25\alpha_{ns}$ has also been included. Although Cranston's equation may appear too conservative in some cases, this conservatism appears to be justified when applied to columns in a multistorey frame, as discussed in the next section.

(d) C_m

The limit of $C_m > 0.4$ (in terms of r_0) is also required for restrained columns since unwrapping can occur near failure (Sect. 3.3, MacGregor and Barter, 1966), similar to the unwinding of a pin-ended column (Sect. 4.5.1).

4.5.3 Multistorey frames

For restrained columns in a multistorey frame, the assumption of constant end-restraints and further simplifying assumptions in determining the effective length factors are required in the ACI method. The relevant problems have been discussed in Sect. 4.3.2. In light of those problems plus the problems discussed in the following paragraphs, the use of Cranston's equation (Eq. 4.26), which may tend to be too conservative for single restrained columns, appears to be justified when applied to restrained columns in a multistorey frame.

In all the previous discussions, the use of the effective length factor in the ACI approach assumed that the beams maintain their assumed stiffness throughout the loading up to the instant of collapse of the restrained column. In order that the beam can be expected to behave this way, a designer needs to know the first-order column end-moments as well as the column ultimate end-moments. The ultimate end-moments, however, are unknown to the designer. Consequently, whether the beam can remain as stiff as assumed becomes uncertain. This situation is most

severe when the restraining beam is designed for moments which equilibrate the column moments, as may be the case for beams restraining the exterior columns in a frame or the columns in a single-storey frame. If in such a case the beam is designed to equilibrate the first-order end-moments of the columns, at the ultimate load a beam mechanism forms and the column end-moments remain equal to the first-order end-moments. In this case, the use of $k_{ns} < 1.0$ is unconservative and the use of $k_{ns} = 1.0$ is more reasonable.

For interior columns in a multibay multistorey frame, the column is designed assuming the worst load pattern. The beam, however, is designed assuming full gravity dead load plus live load acting on the beam; or even more conservatively based on a moment-envelope required in the ACI Code (1977). Consequently, the beam so designed can be adapted to considerable amount of change in the column end-moments before the beam would form a mechanism. The reserve of strength in the beam may justify the use of $k_{ns} < 1.0$.

It has been shown in Sect. 3.3 that when the axial load ratio N/N_e is close to or greater than 1.0, the column end-moments may reverse the direction and therefore induce beam moments in the opposite direction to the first-order values. Since this will not be accounted for in the design of beams, it seems advisable to safeguard against such an occurrence. Because axial loads as high as N_e can only happen in a column with very strong restraints, it is reasonable to limit the effective length factor. The

implicit limit of $k_{ns} > 0.7$ in Cranston's equation (Eq. 4.26) seems reasonable. The normal range of k_{ns} from 0.75 to 0.95 suggested by the ACI Commentary (1977) indicates that an actual value of $k_{ns} < 0.7$ should seldom be encountered in design.

4.5.4 Concluding remarks

The previous studies have described the rationale and problems behind the ACI method for restrained non-sway columns. The design procedure could be improved with respect to the geometric non-linearity if Eq. 4.20 were rewritten as follows:

$$\delta_{ns} = C_m \frac{(1 + 0.25\alpha_{ns})}{1 - \alpha_{ns}} > 1.0 \quad (4.27)$$

where

$$\delta_{ns} = \frac{M_{max}}{M_{02}}$$

$$\alpha_{ns} = \frac{N}{N_{ns}}$$

$$N_{ns} = \frac{\pi^2 EI}{(k_{ns} L)^2}$$

The term C_m is given in Eq. 4.20 including the lower limit of 0.4, and k_{ns} is given by Cranston's equation (Eq. 4.26).

5. BEHAVIOR OF ELASTIC SWAY FRAMES

5.1 Geometric effects

Figure 5.1(a) shows a column, which can be any column in a frame, subjected to internal forces acting at the ends. A straight line joining the ends of the column will form an angle equal to a/L with respect to the vertical. The symbols are defined in the figure. The axial load N may be replaced with its horizontal and inclined components (Fig. 5.1(b)). The first of these is equal to $N \cdot a/L$, the second one acts parallel to the line joining the ends of the column and, assuming small deformations, is equal to N . Consequently, the total shear acting at the end of the column is the sum of the original end-shear V resisting the external lateral loads and the $N \cdot a$ shear (Na/L) resulting from the moments induced by N acting through the deflection a . This is the system to be considered in this chapter for the sake of understanding the geometric effects.

Accordingly, the geometric effects due to the axial load can be decomposed into two types as shown in Fig. 5.1(c). First are effects due to the $N \cdot a$ shear which are termed the $N \cdot a$ effects. The $N \cdot a$ shear produces an overturning moment in the direction of lateral displacement, and therefore it tends to increase the lateral displacement. The second type of geometric effects occurs due to secondary moments produced by N times the displacements from the chord line. These will be termed the C and S effects because the

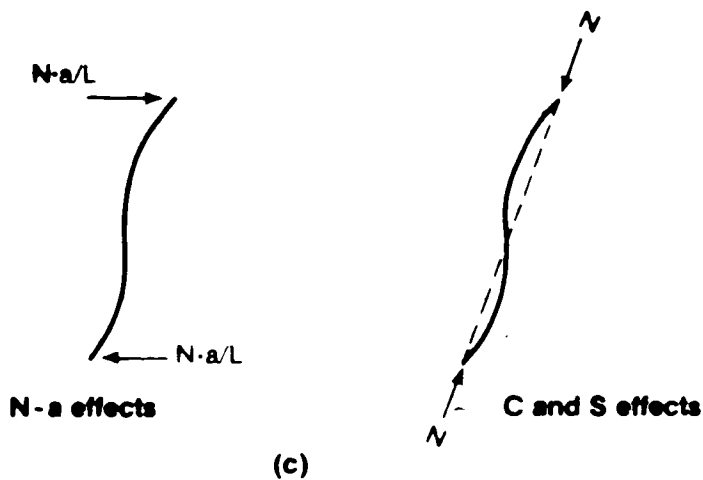
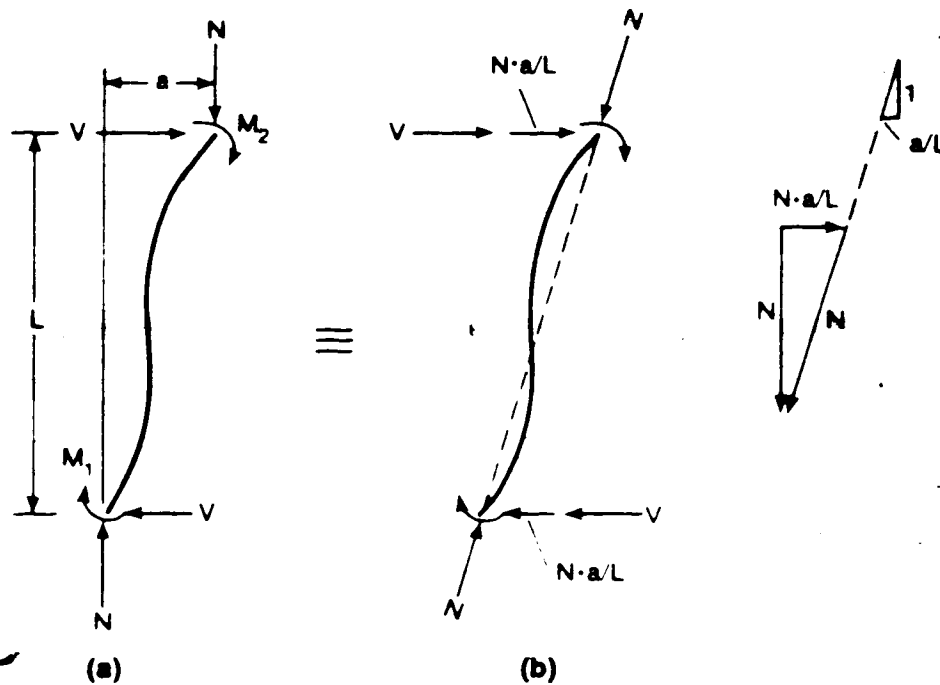


Fig. 5.1 Geometric effects due to axial loads

axial load N acting in this way changes the C and S values in the slope-deflection equation (Eq. 2.3). In effect, the values of C and S take into account the additional bending moments within a column contributed by the axial load (the inclined load N in this case). The geometric effects in this respect have been discussed in Sect. 3.1. The N - a effects take into account the additional moments at the ends of the column contributed by the vertical axial load. In a first-order analysis, both of these effects are neglected. An analysis including these two types of effects is called an exact second-order analysis (Sect. 2.3).

The two types of effects shown in Fig. 5.1(c) are interrelated. The C and S effects have been studied in detail in Chapter 3, where it was shown that the end-rotational stiffness of a column is a function of the axial load, and therefore the lateral stiffness is also affected by the axial load. The N - a shear increases the lateral deflection which is also a function of the column lateral stiffness.

The above relationships can be better understood by considering a storey in a multistorey frame. The total shear in that storey is the sum of the original storey shears due to the lateral loads plus the sum of N - a shears from each column. The total shear is distributed to each column in proportion to the relative lateral stiffnesses including the C and S effects. The moment at the end of a column in that storey is a function of the end-shear that is

distributed to that column and the end-rotational stiffness of that end relative to the other end, also including the C and S effects. Note that, in the final solution, the N-a shears should be compatible with the lateral displacement. In the case that the frame reaches elastic failure the N-a shears cannot attain equilibrium with the deflection, which therefore increases indefinitely (in small deflection theory).

To sum up, the axial load effects relative to the first-order effects occurring in a storey cause: (a) an increase in the overturning moment and the lateral deflection due to the N-a effects, and (b) cause a redistribution of the total shears (lateral load shears plus N-a shears) and column end-moments according to the changing stiffnesses of individual columns due to the C and S effects. Because of moment equilibrium at any joint, the end-moments of the beams connected to the joint are also changed accordingly.

5.2 Single-storey frames

5.2.1 An example frame

The mechanical behavior of geometric non-linearity discussed in Section 5.1 can be illustrated using a simple single-storey frame subjected to lateral and vertical loads (Fig. 5.2(a)). It is assumed that the axial load in a column is equal to the vertical load above it, the beam is rigid, and the stiffness parameter EI is constant for all

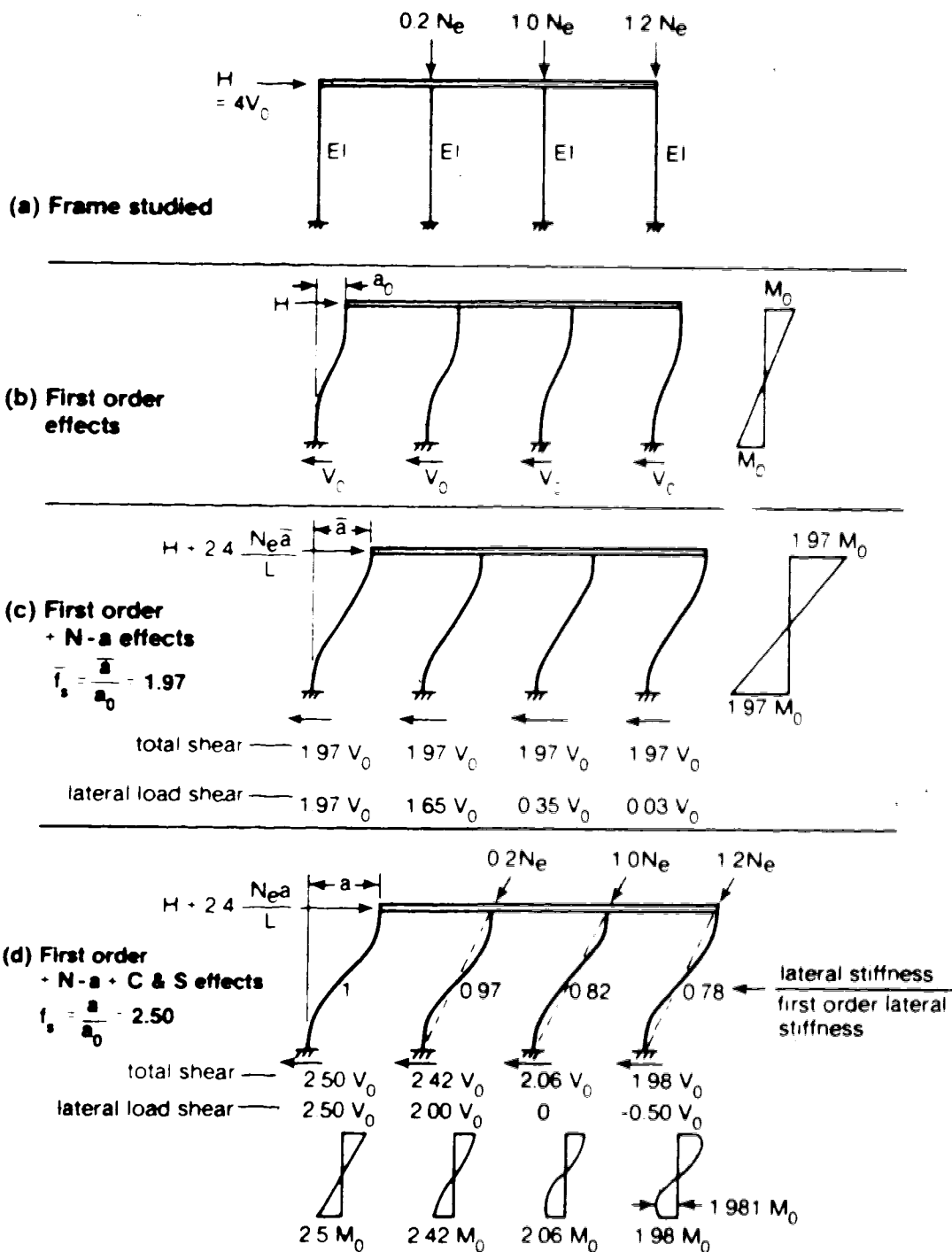


Fig. 5.2 Single-storey frame with rigid beams

the columns. The first-order lateral stiffness is therefore equal for all the columns. In the absence of vertical loads, i.e., first-order effects only, a lateral load $H = 4 \cdot V_0$ produces a shear of V_0 in each of the columns, and the frame undergoes a lateral deflection a_0 as shown in Fig. 5.2(b). The end-moment M_0 is equal in all the columns.

To study the N-a effects alone, the C and S effects are first neglected (i.e., $C = 4$ and $S = 2$ in the analysis). The vertical loads are replaced by a horizontal force equal to the sum of N-a shears from all the columns, as shown in Fig. 5.2(c). With this additional force, the sway of the frame is increased to $\bar{a} = \bar{f}_s a_0$. Since the lateral stiffness of each column remains unaffected, the shear resisting the total horizontal forces in each column becomes $\bar{f}_s V_0$, and the end-moment in each column is also equal to $\bar{f}_s M_0$. The shear resisting the lateral load H in each column, as presented in Fig. 5.2(b), can be obtained by subtracting the N-a shear for that particular column from the total shear $\bar{f}_s V_0$. As the N-a shear is different for each column, the lateral load shears have been redistributed, compared to the first-order shears in Fig. 5.2(b). Since the total shear $\bar{f}_s V_0$ in each column is the same, the capacity of a column to resist the lateral load becomes diminished with a higher axial load.

When the C and S effects are incorporated in the analysis, i.e., an exact analysis, the sway of the frame is increased further to $a = f_s a_0$ because the lateral

stiffnesses of those columns subjected to axial loads are reduced to the values shown in Fig. 5.2(d). The stiffness reduction increases with higher axial loads. Since the total horizontal forces are resisted by the columns in proportion to their relative lateral stiffnesses, the total shear in each column is different. The shear in the column without any axial load is equal to $f_g V_0$, whereas the total shear in each of the axially loaded columns is less than $f_g V_0$. The weakest column (i.e. the most highly loaded column) resists the least amount of shear. Similarly, the end-moment is equal to $f_g M_0$ for the column which is not axially loaded, and smaller for the others. The moment diagrams for the axially loaded columns are non-linear due to the C and S effects, compared to the linear moment distribution which results if only the N-a term is considered (Fig. 5.2(c)). In the most highly loaded column, the maximum moment occurs away from the end.

The lateral load shear in each column is also presented in Fig. 5.2(d). As stated earlier, the reduced stiffness of the axially loaded columns reduces their ability to resist the lateral loads. Consequently, more lateral load shear is added to the stronger columns. In fact, the columns with vertical loads equal to $1.0 N_e$ and $1.2 N_e$ would have failed, had they been free to sway independently of the other columns. However, elastic failure of these columns is prevented since all columns must undergo an equal lateral displacement a . In this process the lateral load shear in

the weaker columns will be redistributed to the stronger columns (Figs. 5.2(c) and (d)). For the column with a vertical load of N_e , the column does not offer any resistance to the lateral load, because N_e is equal to the free-to-sway critical load of that column. For the column with a vertical load greater than N_e , the lateral load shear has reversed direction, indicating that a negative shear is required to brace it from failing laterally. Hellesland and MacGregor (1982) have defined two types of columns: 'supporting sway columns' which contribute to resisting lateral loads and to bracing other columns, and 'supported sway columns' which need lateral support from the frame in order not to fail sideways.

The length of the above discussion for the simple structure in Fig. 5.2(a) reflects the complexity of the geometric effects. This arises primarily from the C and S effects which not only reduce the lateral stiffness of the whole frame, but also cause a redistribution of the moments and the total shears (the lateral load shears plus the N-a shears). The next section will elaborate on the latter phenomenon.

5.2.2 Individual column behavior

To study the moment and shear response of a column in a frame to the axial loads, the following simple method is used. The method employed originated from the work of Hellesland and MacGregor (1982).

A general frame subjected to vertical and lateral loads is shown in Fig. 5.3(a). Under the combined action of these loads, it undergoes a total displacement of $a = f_s a_0$, where a_0 is the first-order deflection caused by H and f_s is the 'deflection magnifier'. The frame can be assumed to reach equilibrium in the deflected shape in two stages. First, the frame is displaced laterally $a = f_s a_0$ in the absence of vertical loads (strictly speaking, in the absence of column axial forces), as shown in Fig. 5.3(b). A force R is required at the bracing point to hold the structure in this position. The moments and shears in a typical column increase from the values M_0 and V_0 due to H to $f_s M_0$ and $f_s V_0$ due to H + R, as shown by the moment diagram in Fig. 5.3(b). The total shear in all the columns equals $f_s H$ which is equivalent to H + R. In the second stage, the vertical loads P_1 to P_4 are applied to the structure held in the deflected position, as shown in Fig. 5.3(c). As the vertical loads are applied, the force R decreases to zero so that the final load effects in the Fig. 5.3(c) are identical to those in the frame in Fig. 5.3(a). The shears and moments in a typical column become:

$$V = B_v f_s V_0 \quad (5.1)$$

$$M_1 = B_1 f_s M_{01} \quad (5.2)$$

$$M_2 = B_2 f_s M_{02} \quad (5.3)$$

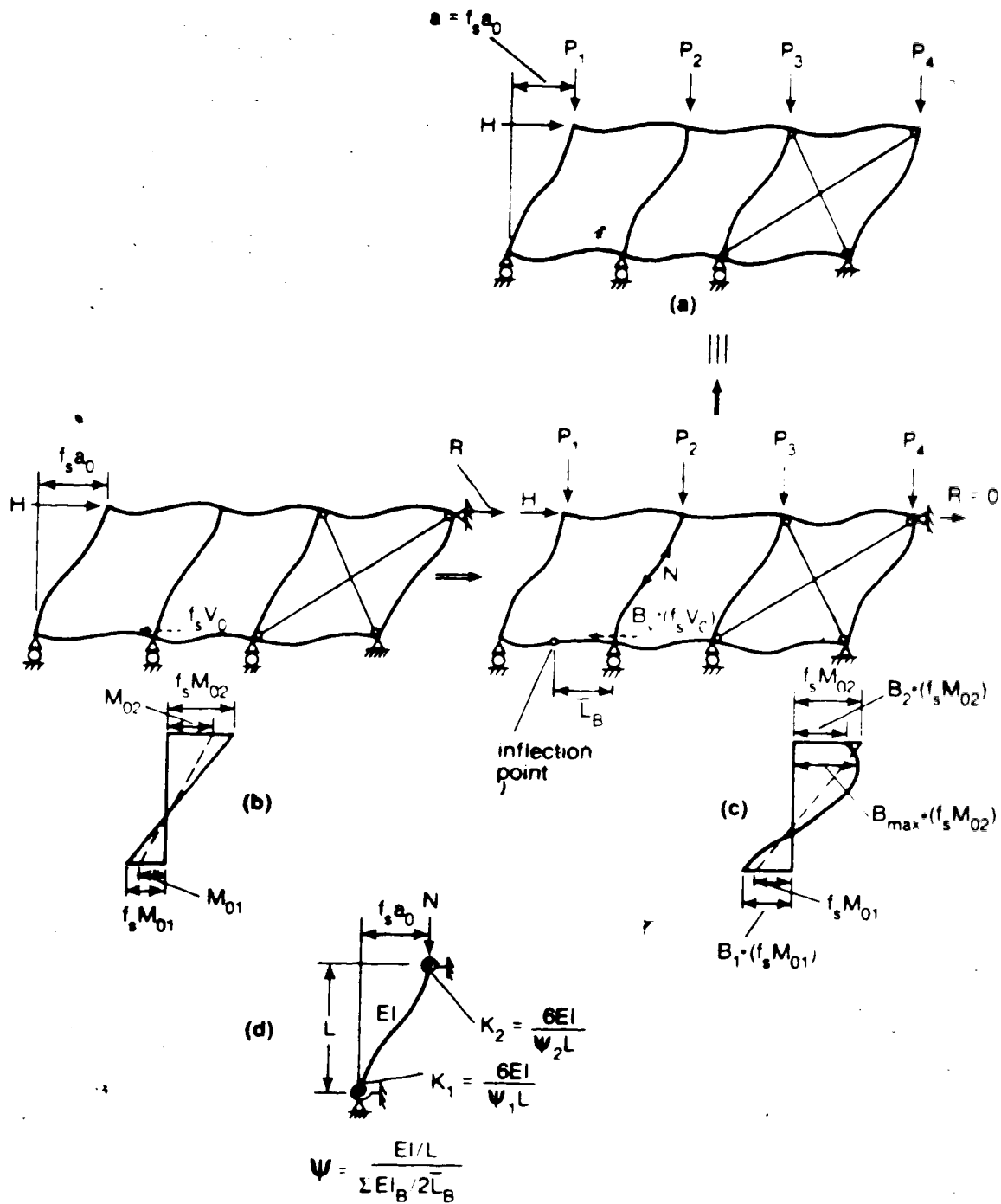


Fig. 5.3 A non-sway frame with imposed lateral deformation

$$M_{\max} = B_{\max} f_s M_{02} \quad (5.4)$$

where M_{02} is the numerically larger of the first-order end-moments in the column. As shown in Fig. 5.3(c), the bending moment distribution becomes non-linear and M_{\max} may occur between the ends of the column.

The deflection magnifier $f_s = a/a_0$ is equal for all columns in the frame. The values of B_v , B_1 , B_2 and B_{\max} for a particular column, in general different from those for other columns, reflect the changes induced by the vertical loads for a given constant end-displacement a . For a column which is not axially loaded, all the B values equal 1.0. Note that if the C and S effects are neglected, B_1 , B_2 and B_{\max} will also be equal to 1.0. If the lateral load shear V in Eq. 5.1 is replaced by the total shear (lateral load shear plus the N - a shear), B_v will also be equal to 1.0 when C and S effects are neglected (Fig. 5.2(c)). It can be seen that the redistribution of moments and shears due to the C and S effects (the change from Fig. 5.3(b) to Fig. 5.3(c)) is reflected by the coefficients B_1 through B_v .

The product of the terms B and f_s quantifies the geometric effects for the moments and shear in a particular column. It has been shown in Sect. 5.2.1 that the lateral deflection increased by the vertical loads is a function of the total vertical load and the lateral stiffness of the frame. The structure shown in Fig. 5.2 has demonstrated sufficiently the factors concerned. Henceforth, the

emphasis will be to examine the significance of the B coefficients, and the laterally deformed non-sway frame in Fig. 5.3(c) will be studied.

It is assumed that the end-rotational restraints of the columns remain unaffected by the geometric action. In other words, it is assumed that the inflection points in the beams remain stationary during loading. If this is done, a column in the deformed non-sway frame can be represented by a single non-sway column with known constant end-restraints and an imposed end-displacement a , as shown in Fig. 5.3(d). (The assumption of constant end-restraints will be discussed later.) The B values determined for the single column are only a function of the end-restraints and the axial load level. As a result, Eqs. 5.1 to 5.4 reflect that the shears and moments in an individual column are a function of both the behavior of the frame as a whole, as implied by f_s , and the behavior of the column itself, as implied by B .

In fact, the moments in the laterally deformed non-sway column shown in Fig. 5.3(d) behave identically to those in the non-sway column subjected to external joint moments studied in Chapter 3, provided the end-restraints and the first-order gradient r_0 are identical in both cases. By noting this restriction, the results and discussion in Chapter 3 can also be applied here for the B coefficients with the first-order end-moment M_0 in Chapter 3 being replaced by $f_s M_0$. Two particular cases are presented in the

following paragraphs to illustrate the effect of the B coefficients.

The B values determined for the single column shown in Fig. 5.3(d) are plotted as a function of the axial load in Fig. 5.4. This column has relatively flexible and unequal end-restraints, $\phi_1 = 6$ at end 1 and $\phi_2 = 2$. (The term ϕ is defined in Fig. 5.3(d).) The dashed line shows that the coefficient B_v decreases with increasing axial load in order to maintain the displacement f_{s0} . It decreases to zero and thereafter becomes negative. Zero lateral load shear is the failure criterion for an elastic column that is free to sway. Negative values of B_v mean that the shear must change direction to support the column in the displaced position. The required negative lateral load shear must be provided by the rest of the structure to maintain the equilibrium of the column as well as the whole frame. In short, when B_v is positive, the column is a supporting sway column (as defined previously), and when B_v is negative, the column is a supported sway column.

The coefficient B_1 for the moment at the end with the more flexible restraint initially remains quite stationary with increasing axial load, although it finally increases indefinitely as the non-sway critical load is approached. The coefficient B_2 , however, decreases continuously as the load level increases. At a certain load level, B_2 changes direction and finally approaches infinity in the new direction at the non-sway critical load. The coefficient

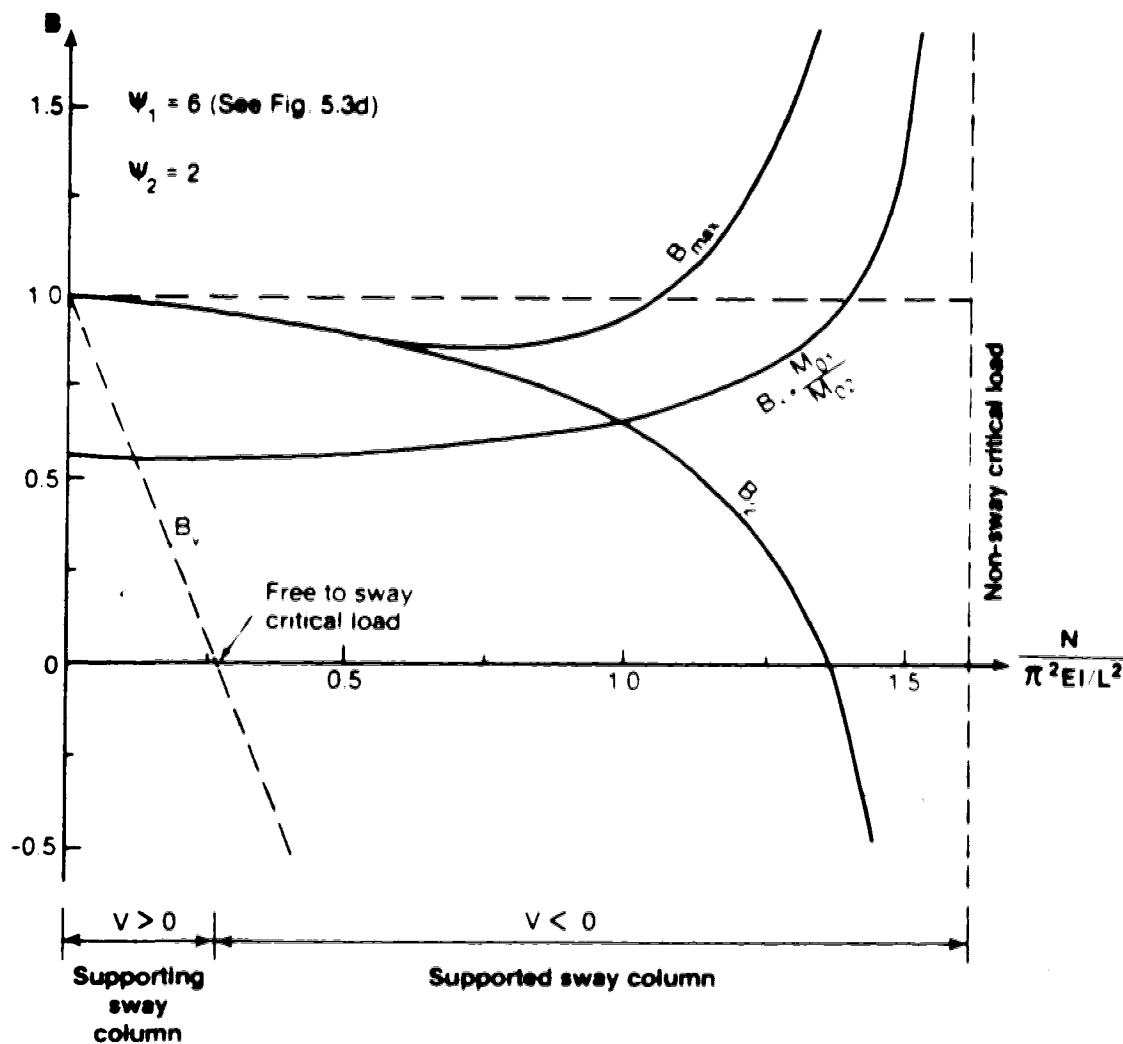


Fig. 5.4 Variation in B values with axial loads for a column with flexible restraints

B_{\max} for the maximum moment in the column initially equals B_2 , i.e., the maximum moment occurs at the end. At a certain load level, B_{\max} becomes greater than B_2 and later rises as the axial load increases further. This occurs when the maximum moment moves away from the end of the column. This, however, happens after the column has become a supported sway column (Hellesland and MacGregor, 1982). At a rather high axial load, B_{\max} even exceeds 1.0. The bending moment diagrams corresponding to different load levels are similar to those shown in Figs. 3.7(b) and (c) except that M_0 in Fig. 3.7 should be replaced by $f_s M_0$.

Figure 5.4 has illustrated the case with initial moments M_{01} and M_{02} which are quite different. When the magnitudes of the two end-restraints are close, or when the more flexible restraint (ϕ_1) is in fact considerably stiffer than the column, the initial moments are nearly equal. This is demonstrated in Fig. 5.5 by a column with stiffer restraints than in Fig. 5.4. Although the end-restraints are quite different, the initial moments are very close. Compared to Fig. 5.4, the value of B_{\max} in Fig. 5.5 drops more severely before it increases. In addition, B_1 follows B_2 quite closely until the non-sway critical load is approached, when it reverses the trend and increases rapidly.

In summary, the value of B_2 is reduced by increasing axial load, and B_{\max} is equal to B_2 when the column is a supporting sway column. In the range of a supported sway

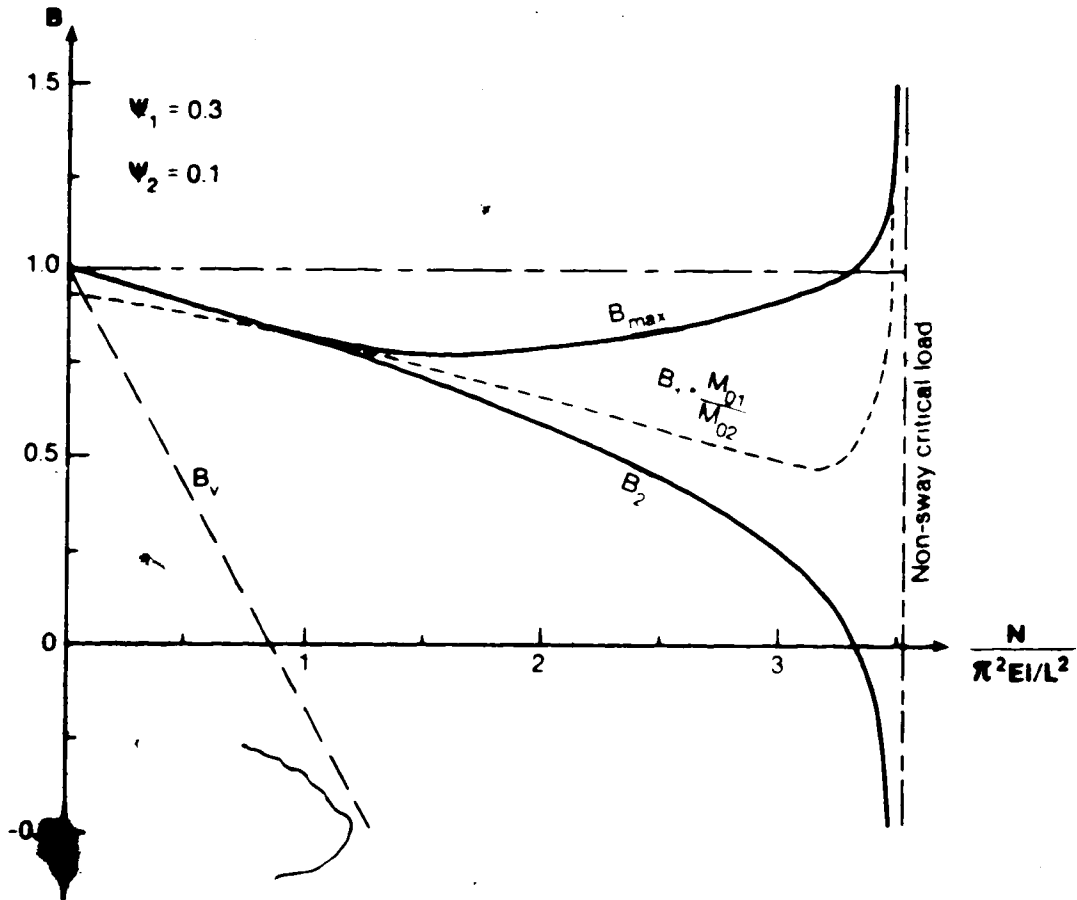


Fig. 5.5 Variation in B values with axial loads for a column with stiff restraints

column, B_{\max} may be greater than B_2 or even greater than 1.0, but for this to happen, the column must be able to sustain a very high axial load. For a column with flexible restraints, B_1 is quite insensitive to the axial loads except at high load levels. For stiff restraints, B_1 is decreased by axial loads until rather high axial loads are reached.

The validity for the assumption of constant end-restraints has been indirectly discussed for non-sway frames in Section 3.4. In particular, Fig. 3.12 is representative for this case since the beams of a laterally deformed non-sway frame with rigid joints always bend into double curvatures. The observations from Fig. 3.12 are therefore applicable here. In other words, the assumption is reasonable even for a frame with mixed strong and weak columns except when the non-sway elastic failure load is approached. In the case of a particularly heavily axially loaded column (which must be sufficiently braced), the assumption of constant end-restraints will underestimate the change of the B values, as indicated by Fig. 3.12, but the trend is correctly estimated.

5.3 Multi-storey frames

The horizontal interaction between columns has been studied in the previous sections. An attempt is made in this section to illustrate the vertical interaction between columns due to the geometric action. In the same manner as

before, the N-a effects and the C and S effects are dealt with separately.

The vertical interaction due to the N-a effects is explained with the aid of Fig. 5.6. A two-storey frame with a completely rigid beam connecting the two storeys is shown in Fig. 5.6(a). Only the bottom storey is loaded. It can be seen that the N-a effects are localized to the bottom storey and do not affect the upper storey. In Fig. 5.6(b) another extreme case is represented by a completely flexible beam (pin-ended) connecting the two storeys. Again, only the bottom storey is loaded, but in this case the N-a effects obviously increase the deformation in the upper storey. In fact, the N-a effects in the bottom storey are also affected by the lateral stiffness of the upper storey. If the top beam were made stiffer, for example, the deformation in the bottom storey would also be reduced. These effects suggest that the storeys tend to assist each other to resist the geometric effects.

The observations made in Section 3.5 with regard to the C and S effects for non-sway frames are also applicable here. The variables involved are the stiffnesses of the beams that connect the storeys and the relative stiffness of the upper and lower columns. In Section 3.5 it was observed that when the beams are rigid, the C and S effects are localized, and when the beams are more flexible, the stronger columns tend to assist the weaker columns. This is the same observation made in Fig. 5.6 for the N-a effects.

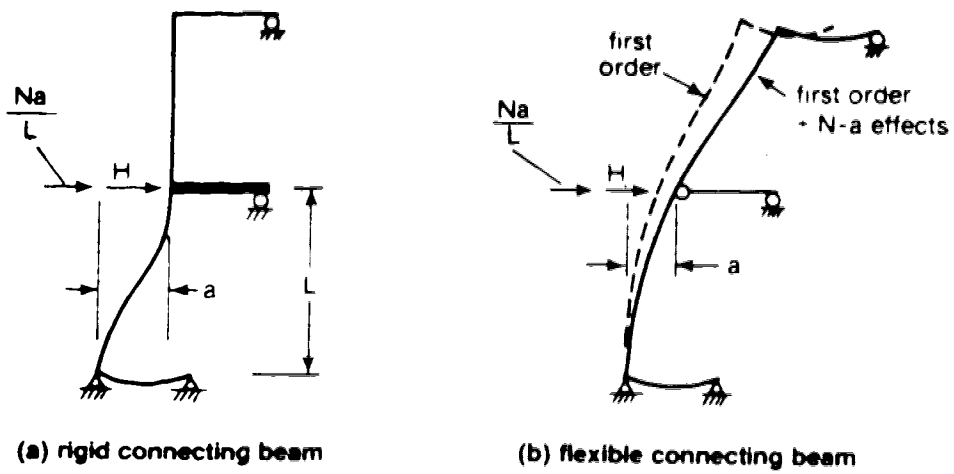


Fig. 5.6 Vertical interaction due to N-a effects

In summary, when the beams that connect the storeys are stiff, the geometric behavior in one storey is independent of the behavior in other storeys. However, when the beams are flexible, the storeys tend to interact with each other.

5.4 Summary

The geometric effects in a sway frame can be decomposed into two types: (a) the N-a effects which cause an increase in the lateral deflection and overturning moment in a storey, and (b) the C and S effects which reduce the lateral stiffness of a storey and cause a redistribution of end-moments and total shears (lateral load shears plus the N-a shears) in that storey. A single-storey frame has been used to illustrate these two types of effects.

The geometric effects in an individual column in a single-storey frame have been expressed as the product of a coefficient B and the deflection magnifier f_s (Eqs. 5.1-5.4). The deflection magnifier $f_s = a/a_0$, constant for all columns in a single-storey frame, is a function of the total vertical load and the lateral stiffness of the frame. The coefficient B is primarily a function of N/N_{ns} of a given column, reflecting the redistribution of end-moments or shear in that column due to the C and S effects. The properties of the B coefficients have been described.

In a multistorey frame with stiff beams between storeys, the geometric effects in one storey will not influence other storeys. However, when the beams are

flexible, the storeys tend to interact with each other to resist the geometric effects.

6. APPROXIMATE SECOND-ORDER ANALYSIS OF ELASTIC SWAY FRAMES

Various methods of approximate second-order analysis of elastic sway frames are reviewed in this chapter. Although most methods presented are based on the work of others, the derivations of the various methods presented in this chapter differ in one way or another from the original presentation. In particular, all the necessary assumptions in each method are explicitly stated. In many cases this is not clearly done elsewhere. It is believed the presentation provides insight into the validity of different methods. Finally, most of the methods of analysis are improved, and extended to more general types of frames than originally intended.

6.1 Iterative method

This method of second-order analysis, often referred to as the P-Delta analysis, is the most well known. It will be first developed for frames consisting of only vertical and horizontal members, where all the columns in the same storey are of equal height. It is then extended to a frame with different column heights in the bottom storey. Finally it is also extended to a frame with inclined bracing elements in any storey.

As mentioned in Chapter 5, the first-order analysis neglects the N-a and the C and S effects. The iterative method modifies the first-order analysis to include the N-a

effects but neglects the C and S effects. According to Fig. 5.1, an equivalent shear $N \cdot a/L$ is added at the end of each column to represent the N-a effects. For a storey with identical column heights, the total additional storey shears become $(\Sigma N) \cdot a/L$. The symbols L and a are the storey height and the relative storey deflection (the deflection of the top of the storey relative to the bottom of the storey), respectively. The summation term ΣN is the sum of the column axial loads in that storey. To produce the required N-a shears $(\Sigma N) \cdot a/L$ in each storey of a multistorey frame, fictitious lateral loads, commonly called sway forces, are added to the lateral loads. The sway force at a given floor level is equal to the algebraic sum of the N-a shears from the columns above and below the floor, as shown in Fig. 6.1. The frame subjected to the lateral loads and the sway forces is then analyzed according to the first-order theory.

Since the lateral deflections are not known in advance, the deflections from the analysis without the sway forces (first-order deflections) are used as starting values. The analysis is then iterated until convergence is achieved. Generally one or two cycles of iteration are adequate for frames of practical stiffnesses. It should be noted that the analysis using the sway forces gives a column shear equal to the sum of lateral load shear plus the N-a shear. The lateral load shear in a column can be obtained by subtracting the N-a shear of that column from the total shear, as illustrated in Sect. 5.2.1.

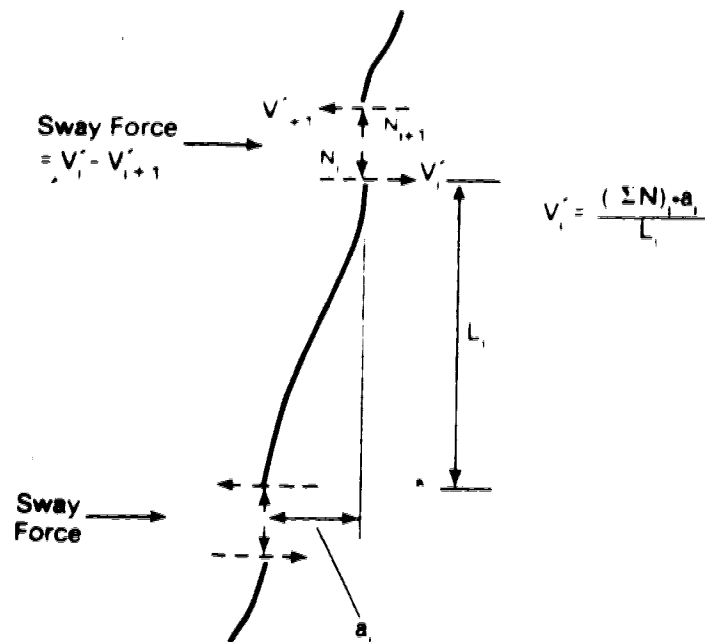


Fig. 6.1 Sway Forces in Iterative Method

The procedure of the iterative analysis has been presented by Iffland (1972) and Adams(1972). The application of this method to the design of steel frames has been studied by Springfield and Adams (1972), Wood, Beaulieu and Adams (1976a), and Wood (1978a). This method is also recommended in the Canadian Code for steel design (CSA, 1974). MacGregor and Hage (1977) and Furlong (1979) also suggested the use of this method for the design and analysis of reinforced concrete frames.

In the case of a frame with different column heights in the bottom storey (Fig. 6.2(a)) or a single-storey frame of unequal column heights, as often occur in bridges (Fig. 6.2(b)), the iterative method can also be used with some modification. Since the N-a shear for each column is equal to N_a/L , with different column heights in the bottom storey, the sum of N-a shears in the bottom storey becomes $(\sum N/L) \cdot a$. Because the axial load N in a given column should not differ significantly from the first-order axial load N_0 which is obtained from the first-order analysis of the frame subjected to both gravity and lateral loads, it is reasonable to assume N equal to N_0 to simplify the calculation. Corrections, however, can be made successively during the iterative analysis, if found necessary.

In the case that a frame includes inclined bracing members, which are assumed pin-ended, the same methodology can be used, as shown schematically in Fig. 6.3. It can be seen that the 'N-a' shear for the inclined member is also

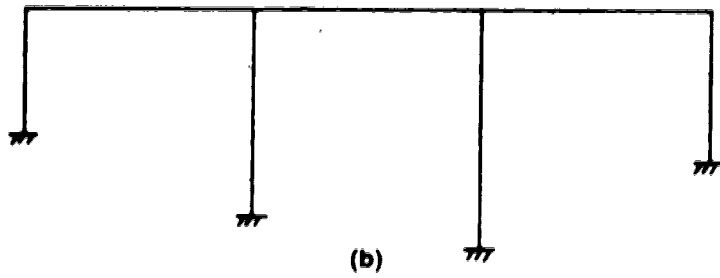
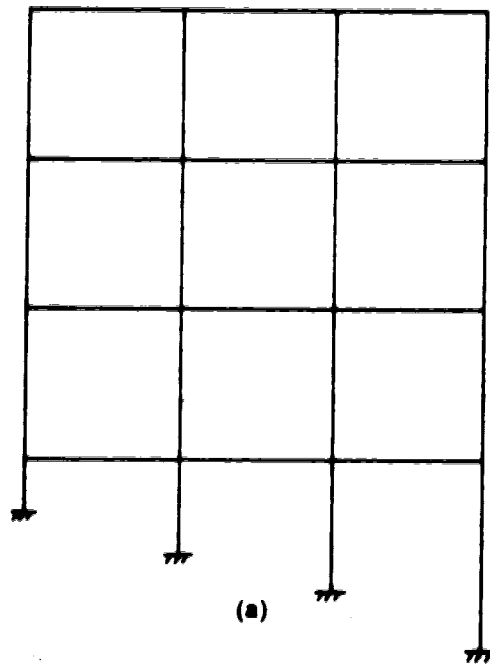


Fig. 6.2 A frame with different column heights in the bottom storey

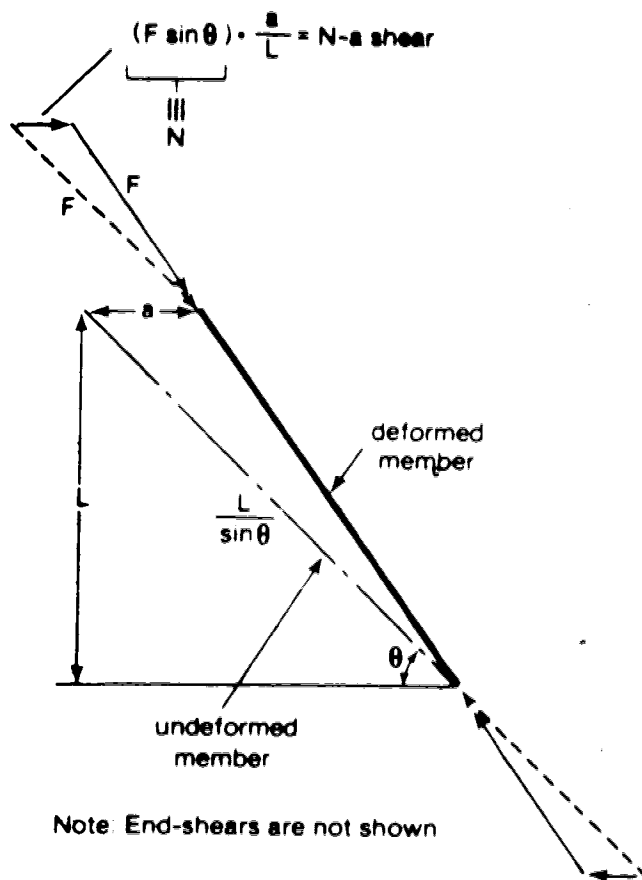


Fig. 6.3 N-a shear of an inclined bracing member

equal to $N \cdot a/L$, but N is redefined as the vertical force component of the axial force in the member and L the vertical projection of the member length. (Note that N is positive for compression in the bracing member.) When the entire storey is considered, it can be seen that ΣN is generally defined as the total vertical load in a storey regardless of the existence of any inclined bracing elements. The exception occurs for a storey of unequal column heights with or without inclined bracing members. Here the value of N must be known for each member, and it can be reasonably assumed to be equal to N_0 , as mentioned before.

6.2 Modified iterative method

Section 5.2.1 has shown that neglecting the C and S effects will result in underestimating the lateral deflections. The sum of column end-moments in a storey and the bracing forces for the bracing members (if any) obtained from the iterative method are also underestimated. In other words, the method is unconservative. A modified iterative method which is more accurate than the iterative method described in Sect. 6.1 is presented in this section. In subsequent discussions the iterative method will not be considered any more. As before, the modified iterative method is first developed for regular rectangular multistorey frames before it is extended to those frames with unequal column heights in the bottom storey. Finally,

it is also extended to a frame with inclined bracing members in any of the storeys.

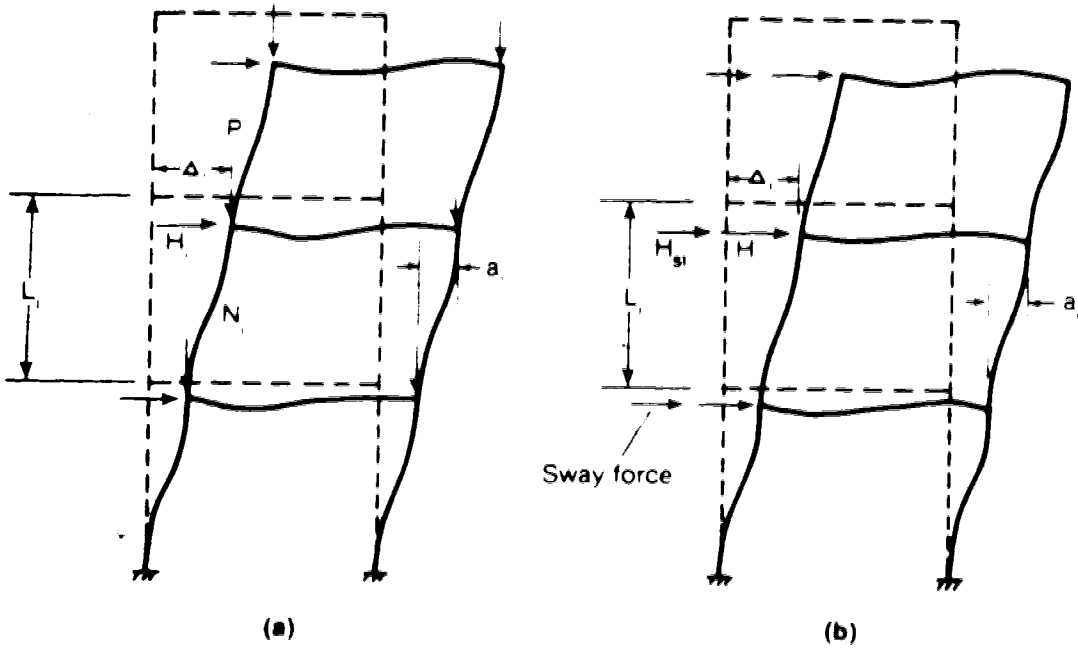
6.2.1 The method

Figure 6.4(a) shows a rectangular multistorey frame subjected to lateral loads H and vertical loads P at the joints. Figure 6.4(b) shows the same frame subjected to the same lateral loads H plus the sway forces H_s , which together produce the same lateral deflections as occur under the actual loading shown in Fig. 6.4(a). The total potential energy in the two systems will be examined in the following, restricting the consideration to the strain energy due to the bending moments and the potential energy of the lateral loads and the column axial forces.

The total potential energy Π_a of the system in Fig. 6.4(a) is equal to the sum of the strain energy U_a and the potential energy of the lateral and vertical loads:

$$\Pi_a = U_a - \sum_{i=1}^n (\Sigma V)_i a_i - \sum_{i=1}^n \left(\sum_{j=1}^m N_j e_j \right)_i \quad (6.1)$$

where m denotes the total number of columns in any storey i , and n is the total number of storeys. The term $(\Sigma V)_i$ represents the sum of lateral load shears in storey i , N_j is the axial compressive force in column j in storey i , and e_j is the amount by which the upper end of column j descends relative to the lower end due to the flexural shortening of



(a)
Deformed shape due to lateral and vertical loads

(b)
Deformed shape due to lateral loads plus sway forces

6.4 Assumption in the modified iterative method

column j . Note that the last term in the above equation results from the consideration of geometric effects.

Estimates of e are obtained by considering the deflected shape of the columns. It is written in the form:

$$e = \gamma e_r \quad (6.2)$$

where e_r is the vertical displacement of a rigid column or a pin-ended column due to the rigid body rotation of the column length (Fig. 6.5(a)). The term γ is referred to as the flexibility factor because it accounts for the actual curved deflected shape of a column, i.e., the flexibility of the column (Fig. 6.5(b)). The factor ranges from 1.0 to 1.22 and will be examined in the next section. The factor e_r can be obtained from simple trigonometry, and e can also be written as:

$$e_j = 0.5 \frac{a_i^2}{L_i} \gamma_j \quad (6.3)$$

which is then substituted into Eq. 6.1.

For the system shown in Fig. 6.4(b), the total potential energy Π_b is equal to the sum of the strain energy U_b and the potential energy of the lateral loads H and the sway forces H_s :

$$\Pi_b = U_b - \sum_{i=1}^n (H_i + H_{si}) \Delta_i \quad (6.4)$$

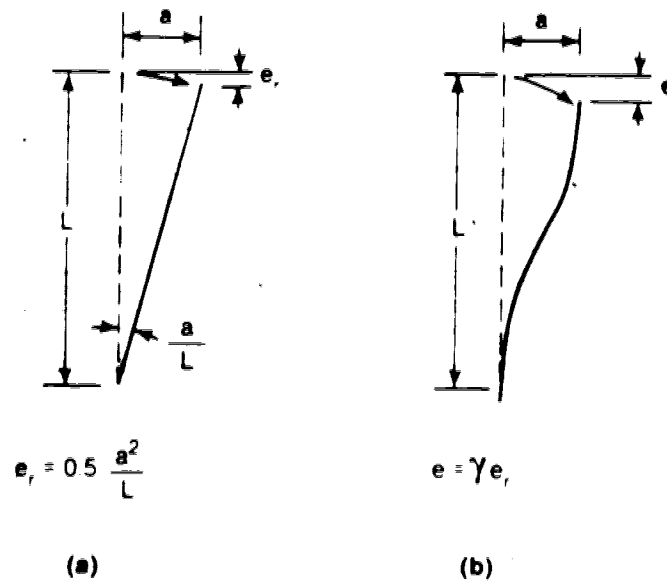


Fig. 6.5 Vertical displacement of column distortion

where Δ_i is the horizontal displacement of floor i from the original position. An alternative form of the equation is:

$$\Pi_b = U_b - \sum_{i=1}^n (\Sigma V)_i a_i - \sum_{i=1}^n (\Sigma \bar{V}_s)_i a_i \quad (6.5)$$

where $(\Sigma V)_i$ is the sum of storey shears in storey i due to lateral loads H , and therefore identical with the term $(\Sigma V)_i$ in Eq. 6.1. The term $(\Sigma \bar{V}_s)_i$ is the sum of storey shears in storey i due to the sway forces H_s .

It is assumed that the deformed shape in both systems is equal, and as a result U_a is equal to U_b . According to the principle of minimum total potential energy (i.e., $\delta \Pi_a = 0$ and $\delta \Pi_b = 0$) and equating both Eqs. 6.1 and 6.5 after performing the differentiation, the sway shear $(\Sigma \bar{V}_s)_i$ is obtained:

$$(\Sigma \bar{V}_s)_i = (\Sigma \gamma N)_i \frac{a_i}{L_i} \quad (6.6)$$

which differs from the former N-a shears by introducing the flexibility factor. (Note that the subscript j is discarded in the above equation for simplicity.) The sway shear defined by the above equation is termed the modified N-a shear. The sway force becomes the algebraic sum of the modified N-a shears from the columns above and below, and the analysis is iterative as discussed before. The method based on the modified N-a shears is referred to as the modified iterative method. The column axial force N in

Eq. 6.6 can be reasonably assumed equal to N_0 to simplify the calculation. This will not introduce any significant errors since the summation sign will offset the errors. Here, as in the conventional iterative method, the lateral load shear in a column is obtained by subtracting the modified N-a shear of that column from the shear obtained from the analysis.

The introduction of the flexibility factor into the conventional N-a shears was suggested by Rubin (1973) (see also p. 248 of ECCS Manual, 1976), but the derivation of the method and the assumptions involved were not shown in the paper.

It will be shown in Sect. 6.2.3 that an average flexibility factor $\bar{\gamma}$ for a storey or an entire frame may be used in order to considerably simplify the calculation. The modified N-a shear can be written as:

$$\Sigma \bar{V}_s = \bar{\gamma} (\Sigma N) \frac{a}{L} \quad (6.7)$$

and the value of ΣN for any storey can be easily obtained.

The modified iterative method can be extended to a frame with different column heights in the bottom storey (Fig. 6.2). Following the same derivation as before except that the storey height L_1 in Eq. 6.3 is replaced by individual column heights L_j , the modified N-a shear in the bottom storey becomes:

$$\Sigma \bar{V}_s = \left(\Sigma \frac{Y^N}{L} \right) a \quad (6.8)$$

The method can also be extended to a frame including inclined bracing elements. First, the work due to the axial deformation of the bracing elements must be included. As demonstrated previously in Fig. 6.3, the axial force in the bracing member can be resolved into two components which are also shown in Fig. 6.6. The potential energy V_b of these two force components is equal to:

$$V_b = -F(a \cdot \cos \theta) - \frac{1}{2} (F \cdot \sin \theta) \frac{a^2}{L} \quad (6.9)$$

where F is the axial force in the bracing member (positive for compression). The derivation of the above equation is obvious from the geometry shown in Fig. 6.6. The symbols are also defined in the figure. Note that when the member is inclined in the other direction, the same equation will result as long as the sign convention is followed.

The first term in Eq. 6.9 is the potential energy due to the axial deformation of the member, and in effect is the potential energy of the horizontal component of the member axial force. Since the term $(\Sigma V)_i$ in Eq. 6.1 or 6.5 is defined as the sum of lateral load shears in storey i , i.e., equal to $\sum_i^n H_i$, the potential energy of this type of load effects for all bracing members in storey i will be included automatically.

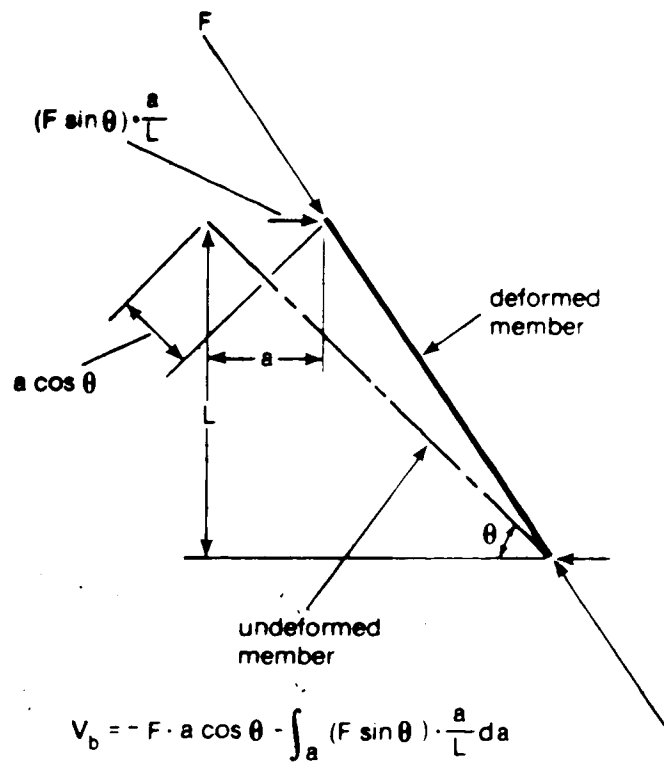


Fig. 6.6 The potential energy in a deformed bracing member

The second term in Eq. 6.9 results from the consideration of geometric effects. The potential energy of this type of load effects will also be included in Eq. 6.1 (after Eq. 6.3 has been substituted) if the term N includes the vertical component of the axial force F , L is the vertical projection of the member length, and γ is equal to 1.0 for the bracing member.

Consequently, the modified iterative method is also applicable for a frame with inclined bracing members in any storey by noting the definition of the terms N and L , and using γ equal to 1.0 for those members.

In deriving the modified iterative method, the deformed shape of the frame is assumed equal to that produced by horizontal loads (Fig. 6.4). It follows that the prediction of storey deflections from this method would be as accurate as the assumption itself. In other words, when there is only a small error in the assumption (as is generally the case), the errors in the computed storey deflections are also small. On the other hand, this may not be the case for the bending moments in the columns. Because the bending moment at any section of the column is a function of the second derivative of the deflection curve ($M = EIy''$), the moments are relatively sensitive to any error in the assumption of the deflected shape. As a result, the column end-moments from the modified iterative method may not be as accurate as the deflections.

The above phenomenon can be better understood by explaining the physical significance of introducing the flexibility factor into the N-a shears. As discussed in Chapter 5, the C and S effects produce two consequences: further increasing the lateral deflections, and redistributing the total shears or the storey moments. The former is artificially looked after by the introduction of the flexibility factor. (Note that $\gamma = 1.0$ if C and S effects were neglected.) The latter, however, is not directly taken into account and is a source of possible errors in the moments. These will be dealt with in Sect. 6.8. On the other hand the flexibility factor can serve the intent as stated above, provided the basic assumption that the deflected shape under lateral and gravity loads can be represented by the deflected shape due to lateral loads plus sway forces is reasonably valid. The validity of this basic assumption will be examined in Sect. 7.2.1.

6.2.2 Flexibility factor

In Fig. 6.5 the vertical displacement of a bent column is related to that of a rigid column by the flexibility factor γ . This factor accounts for the effects of bending between the ends of the column.

The lower limit on the flexibility factor is 1.0 if the column remains straight, as shown in Fig. 6.5(a). The upper limit is derived in the following. If the basic assumption in the modified iterative method that the deflected shape of

a frame under vertical and lateral loads can be represented by the deflected shape produced by horizontal loads only (i.e., first-order deflected shape) is followed, a column is most deflected or the vertical displacement e is maximum when the attached beams are completely rigid, as shown in Fig. 6.7(a).

If a first-order deflected shape is assumed for the column, the flexibility factor is the ratio of e_1 in Fig. 6.7(a) to e_r in Fig. 6.5(a) or 1.20. If a sine curve is assumed for the column corresponding to the deflected shape of a column when the axial load is equal to N_e , the flexibility factor becomes 1.2337. The two values differ only by 2.7%, indicating the similarity of the two deflected shapes. Therefore, the flexibility factor is assumed to vary from 1.0 to 1.22 which is the average of the above two values. It is emphasized here that the upper limit as well as the formulae developed later are effective only within the bounds of the validity of the assumption behind the modified iterative method.

In the case of a supported sway column (Sect. 5.2), which may deflect in a mode as shown in Fig. 6.7(b), the value of e may be larger than the rigid-beam case. This case, however, is outside the assumption behind the modified iterative method since this 'supported-sway' mode is considerably different from the first-order deflected shape. Therefore, it will not be discussed in determining the flexibility factor, but it will be studied in Sect.

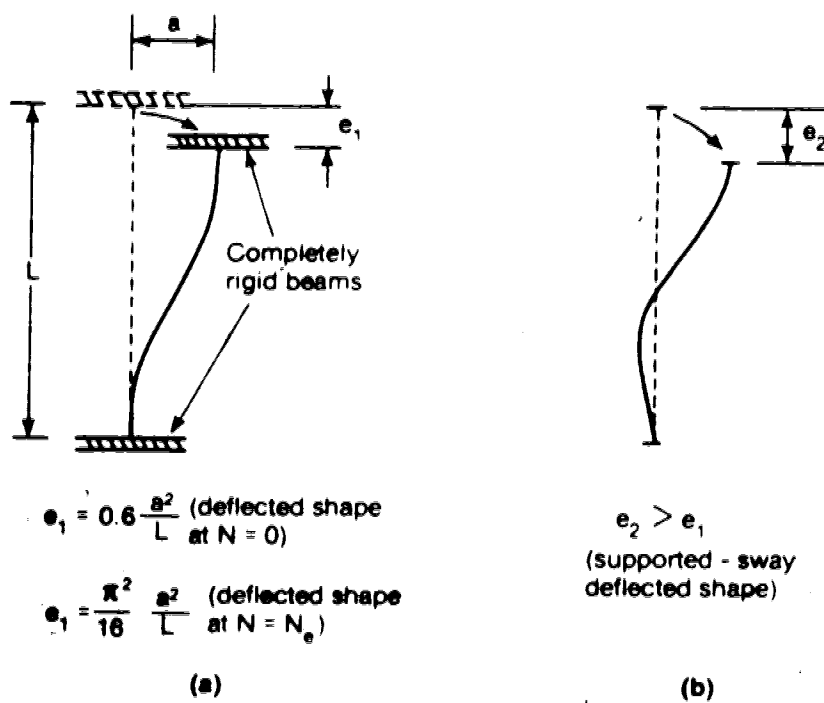


Fig. 6.7 Upper limit of the flexibility factor

7.2.1 to examine the bounds of the validity of this assumption.

A general expression for the flexibility factor is derived in the following by assuming a first-order deflected shape for the column. The deflection is therefore given by:

$$y = \frac{1}{EI} \left[(M_1 + M_2) \frac{x^3}{6L} - M_1 \frac{x^2}{2} + (2M_1 - M_2) \frac{xL}{6} \right] + \frac{ax}{L} \quad (6.10)$$

The symbols are defined in Fig. 6.8. The vertical displacement e can be found by (Timoshenko and Gere, 1961):

$$e = \frac{1}{2} \int_0^L \left(\frac{dy}{dx} \right)^2 dx \quad (6.11)$$

The flexibility factor is defined by (Fig. 6.5(b)):

$$\gamma = \frac{e}{e_r} \quad (6.12)$$

where e_r is equal to $0.5 a^2/L$ (Fig. 6.5(a)). Hence from Eqs. 6.10, 6.11 and 6.12, γ can be expressed as:

$$\gamma = 1 + \frac{1}{180} \left(\frac{L^2}{aEI} \right)^2 [4 (M_2 - M_1)^2 + M_1 M_2] \quad (6.13)$$

The above formula is the same as the one given by Rubin (1973) (see also Massonnet, 1978).

Since M and a in Eq. 6.13 are the final results of the modified iterative analysis, the calculation of γ based on Eq. 6.13 becomes also iterative. By making the following

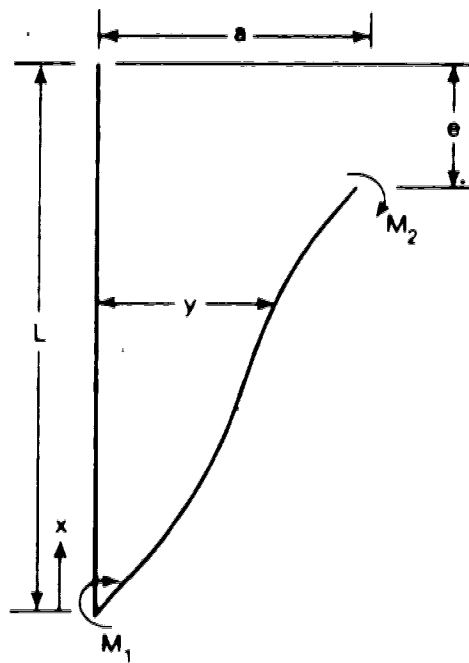


Fig. 6.8 Column bent by end moments

assumption:

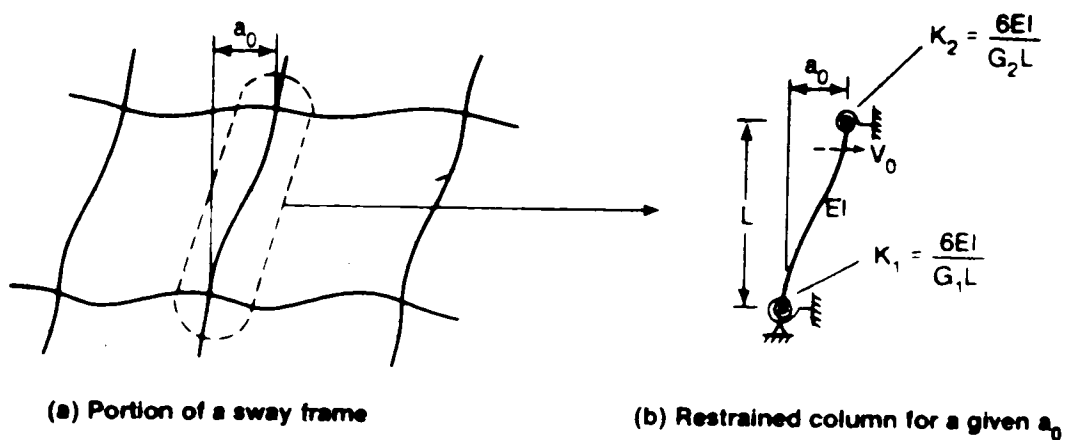
$$\frac{M_1}{M_{01}} = \frac{M_2}{M_{02}} = \frac{a}{a_0} \quad (6.14)$$

Eq. 6.13 can be rewritten as:

$$\gamma = 1 + \frac{1}{180} \left(\frac{L^2}{a_0 EI} \right)^2 [4 (M_{02} - M_{01})^2 + M_{01} M_{02}] \quad (6.15)$$

which can be readily obtained from the results of a first-order analysis. Because of the small range of variation in the flexibility factor, the assumption given by Eq. 6.14 is considered reasonable. Note that this assumption is exact for a single storey frame subjected to a lateral load plus the sway force.

Based on Eq. 6.15, the flexibility factor can also be more conveniently expressed as a function of end-restraints with the aid of the assumptions that (a) the end-rotational beam stiffness is equal to $6 \cdot EI_B / L_B$, and (b) the column end-moments at the joints are distributed between the column above and the column below in the ratio of the EI/L values of the two columns. These assumptions will be discussed later and they will be considered reasonable as far as the flexibility factor is concerned. As a result of these assumptions, any storey can be separated from the frame and the end-rotational restraints of any column in the storey will become a function of G_1 and G_2 as shown in Fig. 6.9(b). The stiffness ratio G_1 at one end of the column is



$$\text{Note } G = \frac{(\sum EI/L)_{\text{column}}}{(\sum EI_B/L_B)_{\text{beam}}}$$

Fig. 6.9 A column isolated from the frame

defined by:

$$G_1 = \frac{(\Sigma \frac{EI}{L})_{\text{col}}}{(\Sigma \frac{EI}{L_B})_{\text{beam}}} \quad (6.16)$$

where Σ denotes summation of columns or beams rigidly connected to the joint, and similarly for G_2 at the other end. For a given end-displacement a_0 (Fig. 6.9(b)), the end-moments M_{01} and M_{02} can be calculated as a function of G_1 and G_2 . The expressions of M_{01} and M_{02} are substituted into Eq. 6.15. After a_0 and other terms are cancelled out, the flexibility factor becomes:

$$\gamma = 1 + 0.2 \left\{ \frac{4 (G_1 - G_2)^2 + (G_1 + 3)(G_2 + 3)}{[(G_1 + 2)(G_2 + 2) - 1]^2} \right\} \quad (6.17)$$

which can be assessed directly from the properties of the frame.

The upper limit of γ given by Eq. 6.17 is 1.20 when $G_1 = G_2 = 0$ (rigid beams) or $G_1 = \infty$ (hinged) and $G_2 = 0$. The same limits are implied by Eq. 6.15. To increase the upper limit to the value of 1.22 obtained previously, the factor 0.2 in Eq. 6.17 is changed to 0.22, that is,

$$\gamma = 1 + 0.22 \left\{ \frac{4 (G_1 - G_2)^2 + (G_1 + 3)(G_2 + 3)}{[(G_1 + 2)(G_2 + 2) - 1]^2} \right\} \quad (6.18)$$

If the column is hinged at both ends ($G_1 = G_2 = \infty$), either Eq. 6.17 or 6.18 gives $\gamma = 1.0$. For the special case of a column with equal end-restraints ($G_1 = G_2 = G$), Eq. 6.18 is

simplified:

$$\gamma = 1 + \frac{0.22}{(1 + G)^2} \quad (6.19)$$

For a column restrained at one end and hinged at the other end ($G_1 = \infty$):

$$\gamma = 1 + \frac{0.22}{\left(1 + \frac{G^2}{2}\right)} \quad (6.20)$$

The flexibility factor can also be determined from the following method. In addition to the previous assumptions, it is assumed that the axial force in a column is equal to its free-to-sway critical load N_{fs} . As indicated earlier in this section, the flexibility factor is quite independent of the axial force in the column. Therefore, this assumption is only for the sake of obtaining a means to determine the flexibility factor, and the solution should not be restricted to this assumption. For an isolated storey (according to the previous assumptions) subjected to the lateral load shears plus the modified N-a shears, the shear in a column is equal to $(a/a_0) \cdot V_0$ where V_0 is the first-order shear of the column. When a column is sustaining its free-to-sway critical load N_{fs} , the lateral load shear of that column must be equal to zero. Therefore, the following relation results:

$$\frac{a}{a_0} V_0 - \gamma \frac{N_{fs} a}{L} = 0 \quad (6.21)$$

which can be simplified to:

$$\gamma = \frac{V_0 L}{N_{fs} a_0} \quad (6.22)$$

For given values of G_1 and G_2 , the relationship between V_0 and a_0 (Fig. 6.9(b)) can be obtained from a first-order analysis. Hence, Eq. 6.22 can be expressed as:

$$\gamma = \left(\frac{k_{fs}}{\pi} \right)^2 \left[\frac{6 (G_1 + G_2) + 36}{2 (G_1 + G_2) + G_1 G_2 + 3} \right] \quad (6.23)$$

where k_{fs} is the effective length factor defined by:

$$N_{fs} = \frac{\pi^2 EI}{(k_{fs} L)^2} \quad (6.24)$$

The value of k_{fs} is only a function of G_1 and G_2 , and can be obtained from the conventional effective length factor alignment chart which is available in many textbooks or commentaries to the design codes.

LeMessurier (1977) also developed Eq. 6.23 in yet another way. He presented a chart for the values of $(\gamma - 1)$ as a function of G_1 and G_2 . The values of γ given by Eq. 6.23 ranges from 1.0 to 1.22, the same range as given by Eq. 6.18. The comparison of the γ values given by Eq. 6.18 with those given by Eq. 6.23 (with the aid of LeMessurier's chart) shows the difference is never greater than 0.5%.

Prior to LeMessurier, Helleland in 1976 developed a graph of γ as a function of end-restraints based on Eq. 6.22

with additional simplifying assumptions in calculating N_{fs} . The values of γ obtained from Hellesland's chart are close to those from LeMessurier's (1977).

Hellesland and MacGregor (1982) also suggest the following equation:

$$\gamma = 1 + \frac{0.108 [1 + (1 - 0.5 G_l^p)^3]}{(1 + 0.5 G_s)^2} \quad (6.25)$$

where the power $p = 1$ for $G_l < 2$ and $p = -1$ for $G_l > 2$. The terms G_l and G_s refer to the larger and smaller values of G , respectively. Equation 6.25 is an empirical approximation for the values of γ given by Eq. 6.23. The errors in Eq. 6.25 are at most -2.5% when compared to the exact values given by Eq. 6.23. The different expressions for the flexibility factor are summarized in Table 6.1.

The above formulae of the flexibility factor as a function of G_1 and G_2 are based on the two assumptions mentioned previously. The assumption of mid-span inflection points is reasonable for beams with both ends rigidly connected to columns which undergo similar deformations. In the case that the far end of a beam that is rigidly connected to the column under consideration is hinged, the beam length should be multiplied by 2 when calculating the corresponding value of G before substituting into the equation. For a beam with far end fixed against rotation, the beam length should be multiplied by 1.5.

Table 6.1 Formulae for the flexibility factor

| Formulae for γ | Eq. No. |
|---|---------|
| $1 + \frac{1}{180} \left(\frac{L^2}{a_0 EI} \right)^2 [4 (M_{02} - M_{01})^2 + M_{01} M_{02}]$ | 6.15 |
| $1 + 0.22 \left\{ \frac{4 (G_1 - G_2)^2 + (G_1 + 3)(G_2 + 3)}{[(G_1 + 2)(G_2 + 2) - 1]^2} \right\}$ | 6.18 |
| $\left(\frac{k_{fs}}{\pi} \right)^2 \left[\frac{6 (G_1 + G_2) + 36}{2 (G_1 + G_2) + G_1 G_2 + 3} \right]$ | 6.23 |
| $1 + \frac{0.108 [1 + (1 - 0.5 G_\lambda^p)^3]}{(1 + 0.5 G_s)^2}$ | 6.25 |
| where $p = 1$ for $G_\lambda < 2$ $p = -1$ for $G_\lambda > 2$ $G_\lambda > G_s$ | |

The second assumption regarding the relationship between storeys is reasonable for stiff beams with relative storey deflections between the upper and the lower storey about the same. This is easily observed from the slope-deflection equation (Eq. 2.3). For a multistorey frame with stiff beams where the lateral stiffness and loading of a given storey do not differ significantly from the storey above or below, this assumption should be considered reasonable. In other words, this assumption is most valid for the values of the flexibility factor close to the upper limit. For a frame with flexible beams, this assumption is susceptible to violation, but its effect is proportionally reduced since the values of the flexibility factor become smaller. This offsetting effect is best reflected by the extreme case of a shear wall. For a shear wall, the assumption completely breaks down but for G approaching zero, Eq. 6.18, 6.23 or 6.25 gives $\gamma = 1.0$. This is a reasonable answer since a shear wall within a storey deflects in a very similar manner to a rigid column. Therefore, it can be seen that this assumption leads to reasonable values of γ although it may not represent the actual behavior in the case of flexible beams.

6.2.3 Average flexibility factor

All the equations developed in the previous section require the evaluation of the flexibility factor for each column. This would be laborious for a large multistorey

frame. In recognition of the small range of the values of the flexibility factor, it may be preferable to use a single value of γ for the entire frame or a storey, when a precise calculation is deemed unnecessary. Based on Eq. 6.18 (or LeMessurier's chart), Table 6.2 shows the range of the values of the flexibility factor corresponding to a given range of G_s (G_s is the smaller value of G for a given column). The range of G from 0.1 to 10 is believed to include most common cases. Thus, for example, AISC permits a hinge to be approximated by $G = 10$. An average flexibility factor $\bar{\gamma}$ which tends to be on the conservative side is also suggested for a given range of the values of G_s . From the table, the average flexibility factor can be roughly estimated for a storey or the entire frame. Since G_s will rarely be less than 0.1 in practical frames, a conservative value of $\bar{\gamma} = 1.15$ can be used for any frame and considerable simplicity in the calculation will be achieved.

6.3 Modified negative brace method

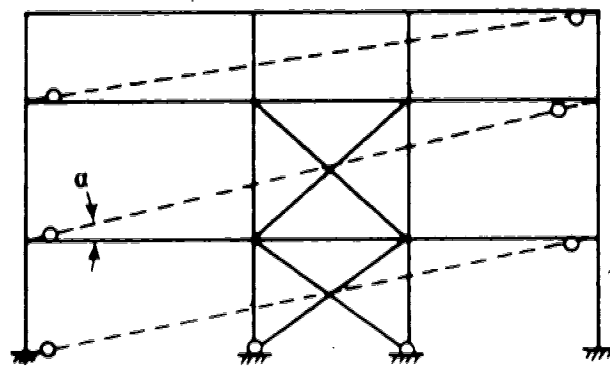
This method is essentially the same as the modified iterative method but it allows a direct calculation of the results without any iteration. A fictitious pin-ended bracing member with a negative value of AE is inserted in each storey as shown in Fig. 6.10. The negative value of AE implies that the bracing member will lengthen under compression or shorten under tension. When a frame including the negative braces is analyzed for the lateral

Table 6.2 Suggested values for the average flexibility factor

| G_s | 0.1-0.4 | 0.4-1.0 | 1.0-10 |
|----------------|------------|------------|-----------|
| γ | 1.09-1.18* | 1.05-1.12* | 1.0-1.07* |
| $\bar{\gamma}$ | 1.15 | 1.10 | 1.05 |

* The highest γ value corresponds to the minimum value in the range of G_s .

Note: $0.1 < G < 10$ is the range of G considered and G_s is the smaller value of G for a given column.



----- Negative bracing members

Fig. 6.10 Modified negative brace method

loads acting alone (i.e., a first-order analysis), the results are very close to those from the modified iterative analysis. The values of AE required for the negative braces are derived as follow:

If the negative brace elongates under lateral loads, the horizontal component of the compressive force F (tensile force if it shortens) in the brace is set equal to $(\Sigma \gamma N) \cdot a/L$ in order that the total shears in that storey become equal to the lateral load shears plus the modified N-a shears. Hence,

$$F \cdot \cos \alpha = (\Sigma \gamma N) \cdot \frac{a}{L} \quad (6.26)$$

where α is the angle of elevation (Fig. 6.10). From the geometric relationships,

$$\frac{FL_b}{AE} = a \cdot \cos \alpha \quad (6.27)$$

where L_b is the length of the negative brace. Equating Eqs. 6.26 and 6.27 gives:

$$AE = - \frac{(\Sigma \gamma N) \cdot L_b}{L \cdot \cos^2 \alpha} \quad (6.28)$$

which is the value of AE required for the negative brace in a storey.

For a frame with unequal column heights in the bottom storey (Fig. 6.2), the term $(\Sigma \gamma N)/L$ in Eq. 6.26 should be

replaced by $\Sigma(\gamma N/L)$ where L is the individual column height. Therefore, the value of AE for the negative brace in the bottom storey becomes:

$$AE = - \frac{(\Sigma \gamma N/L) \cdot L_D}{\cos^2 \alpha} \quad (6.29)$$

Note that the calculation of AE (Eq. 6.28 or 6.29) can be simplified by using an average flexibility factor (Sect. 6.2.3)†

The concept of negative bracing members originated with Nixon et al. (1975) who derived Eq. 6.28 using a different analysis neglecting the flexibility factor.

A frame analysis using negative braces gives slightly incorrect axial forces in the columns due to the vertical force components of the negative braces. For this reason this method gives slightly different results from the modified iterative method when the effects of the axial deformations of the column are also considered. The difference, however, is trivial, and the error of the axial forces in the columns can be minimized by using a maximum member length for the negative brace, as illustrated in Fig. 6.10.

6.4 Storey magnifier method

This method is a further simplification of the modified iterative method based on the additional assumption that a storey can behave independently of other storeys. This is a

reasonable assumption for a frame with stiff beams but may not be valid for flexible beams (Sect. 5.3). As a result of this assumption, any storey in a frame which is subjected to lateral loads plus the sway forces can be treated like a single-storey frame subjected to lateral load shears ΣV plus the modified N-a shears of that storey. Because the deflection of a single-storey sway frame under horizontal forces only is directly proportional to the applied horizontal force, the following relation is obtained:

$$\frac{a}{a_0} = \frac{\Sigma V + (\Sigma \gamma N) \cdot a/L}{\Sigma V} \quad (6.30)$$

where a_0 is the first-order deflection of the storey. After rearranging the terms in the above equation, the deflection magnifier f_s , which is defined as a/a_0 , is equal to:

$$f_s = \frac{1}{1 - \frac{(\Sigma \gamma N) a_0}{(\Sigma V) L}} \quad (6.31)$$

Because the moments in a single-storey frame subjected to horizontal forces are directly proportional to the deflection, the column end-moments M are equal to:

$$M = f_s M_0 \quad (6.32)$$

Similarly, if there are any inclined bracing members, the first-order axial forces in the bracing members are also magnified by f_s .

The deflection magnifier given by Eq. 6.31, which can be calculated directly from the first-order results, needs to be evaluated for each storey. After the column end-moments are magnified by the corresponding f_s , the beam moments should also be increased properly to equilibrate the column end-moments. The lateral load shear in a column can be obtained by subtracting the modified N-a shear ($\gamma Na/L$) of that column from $f_s V_0$ where V_0 is the first-order shear in that column. If an average flexibility factor (Sect. 6.2.3) is used in Eq. 6.31, the calculation of f_s will be further simplified.

In the case of a frame with unequal column heights in the bottom storey (Fig. 6.2), the deflection magnifier for the bottom storey becomes:

$$f_s = \frac{1}{1 - \frac{(E\gamma N/L)a_0}{EV}} \quad (6.33)$$

The above equation is obtained using the modified N-a shears for such a case (Sect. 6.2.1).

The approximate method based on Eq. 6.31 or 6.33 is referred to as the 'storey magnifier method'. Rosenblueth (1965) and Fey (1966) each derived an expression similar to Eq. 6.31 in a way different from the one presented here. Neglecting the flexibility factor, Parme (1966) and Goldberg (1973) also developed a similar expression. Hellesland (1976) developed the more general Eq. 6.33 in a different way. Similar method was proposed by LeMessurier (1977) for

the design of steel frames. MacGregor and Hage (1977) also suggested this method for the design of reinforced concrete frames.

It has been discussed in Sect. 6.2.1 that the modified iterative method is more accurate in predicting the deflections than the moments. Since the derivation of the storey magnifier method is based on the modified iterative method, the same situation will result. This is why f_s is termed the deflection magnifier rather than the moment magnifier. The accuracy of the storey magnifier method, however, is also subject to the additional assumption that a storey can be treated independently of other storeys. The accuracy of this method will be examined in Chapter 7.

6.5 Overturning moment method

This method is a further simplification of the modified iterative method by introducing an additional assumption: the horizontal displacement at any floor of a structure is assumed to be directly proportional to the sum of the overturning moments of the horizontal loads about the base of the structure. In other words, horizontal loads with different force distributions produce the same displacement at any floor, provided the overturning moments about the base are the same. It follows that a single deflection magnifier f_s for the entire structure can be obtained:

$$f_s = \frac{1}{1 - \frac{\sum M_s}{\sum M_H}} \quad (6.34)$$

in which ΣM_H is the sum of the overturning moments of the lateral loads H about the base of the structure, and ΣM_s is the sum of the overturning moments of the sway forces which are calculated using the first-order deflections (i.e., the deflections due to H acting alone). Note that the above equation is the same as Eq. 6.31 for a single-storey frame. Since the deflection is increased by the same ratio in every storey, the column end-moments, beam end-moments, and the axial forces in the inclined bracing elements (if any) are also magnified by the value of f_s given by Eq. 6.34. The analysis based on Eq. 6.34 is referred to as the 'overturning moment method'. Unlike the modified iterative method, this method cannot be applied to frames with unequal column heights in the bottom storey. The simplifying assumption for this method will be explained later.

This method can be further simplified when an average flexibility factor (Sect. 6.2.3) is used for the entire structure. Then Eq. 6.34 can be rewritten in an alternate form:

$$f_s = \frac{1}{1 - \frac{\bar{\gamma} \sum_{i=1}^n (\Sigma P)_i \Delta_{0i}}{\Sigma M_H}} \quad (6.35)$$

in which Δ_{0i} is the first-order horizontal displacement of floor i from the original position (Fig. 6.4), $(\Sigma P)_i$ is the

sum of floor loads on floor i (Fig. 6.4), and n is the total number of storeys.

To avoid complex equations, only the derivation of Eq. 6.35 is shown here although the general equation (Eq. 6.34) can be derived in a similar way. The derivation basically follows an iterative method. The total displacement Δ_{ki} at any floor i in iteration k due to the lateral loads plus the sway forces which are calculated using the displacements $\Delta_{(k-1)i}$ from the iteration $k-1$ is given by:

$$\Delta_{ki} = \Delta_{0i} + \frac{\Delta_{0i}}{\Sigma M_H} \bar{\gamma} \sum_{i=1}^n [(\Sigma P)_i \Delta_{(k-1)i}] \quad (6.36)$$

The second term in the above equation calculates the additional displacement due to the sway forces, which are functions of the total displacements, according to the previous assumption about displacements being proportional to the overturning moment at the base of the structure. In the first iteration, i.e., $k = 1$, $\Delta_{(k-1)i}$ is equal to Δ_{0i} and therefore the final displacement Δ_i corresponding to $k = \infty$ can be obtained by successive iteration, which results in an infinite geometric series of Δ_{0i} . The infinite series can be condensed to Eq. 6.35 when f_s is also defined as Δ_i/Δ_{0i} .

The assumption relating displacements to the overturning moment originated by Perez-V (1977). Perez-V (1977) developed Eq. 6.35 in a somewhat different way and did not consider the flexibility factor in his derivation.

His underlying assumption was drawn from observations about the first-order elastic deflections of idealized structures and loadings shown in Fig. 6.11. A cantilever shear beam which undergoes shear deformation and no bending deformation (Fig. 6.11) represents a structure with rigid beams relative to the columns. A cantilever bending beam (Fig. 6.11), neglecting the shear deformation, represents a structure with very flexible beams. Uniform stiffness and linearly varying stiffness (zero stiffness at the top) of the beams were considered. Because the foregoing assumption was found valid within small limits for each of these models and loadings, it was extrapolated to real structures, as used in the overturning moment method.

This method gives an overall magnifier for the entire structure. This may be reasonable for a structure with flexible beams in which the storeys tend to assist each other to resist the geometric effects (Sect. 5.3). This, however, needs to be proven and will be examined in Chapter 7. Although the shear beam used in developing the assumption for this method was meant to represent a real structure with stiff beams, the points along the shear beam are interrelated and hence this model is not able to represent a real structure with stiff beams in which the behavior of one storey can be independent of other storeys (Sect. 5.3). In other words, if the magnification due to geometric effects in one storey can be very much different from that in the other storeys, especially far away storeys,

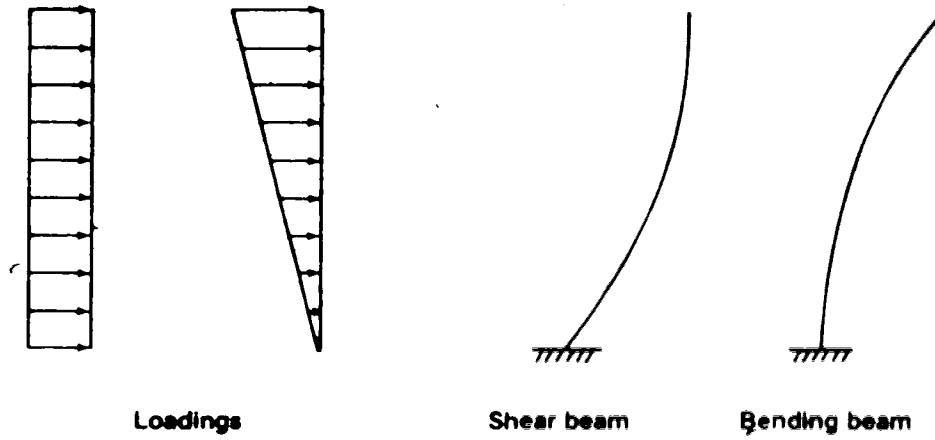


Fig. 6.11 Loadings and deformation of a shear beam and a bending beam

this method will be inaccurate. This will also be shown in Chapter 7.

6.6 Frame magnifier method

This method is a further simplification of the modified iterative method in which the additional assumption is made that the ratio a/a_0 is equal for all the storeys of the frame subjected to lateral loads H plus sway forces. In other words, the total lateral deflections of the frame are those produced by the lateral loads $f_s H$, where $f_s = a/a_0$. As a result, the energy stored in the structure due to the lateral loads plus the sway forces is identical with the energy resulting from the lateral loads $f_s H$. This is expressed as:

$$\sum_{i=1}^n \left[\sum (\gamma N)_i \frac{a_i^2}{L_i} + (\Sigma V)_i a_i \right] = f_s \sum_{i=1}^n [(\Sigma V)_i a_i] \quad (6.37)$$

By setting a_i equal to $f_s \cdot a_{0i}$, the above equation can be rearranged to give the deflection magnifier f_s equal to:

$$f_s = \frac{1}{1 - \frac{\sum_{i=1}^n (\Sigma \gamma N)_i \cdot a_{0i}^2 / L_i}{\sum_{i=1}^n (\Sigma V)_i a_{0i}}} \quad (6.38)$$

In the case of a bottom storey with unequal column heights, the deflection magnifier is equal to:

$$f_s = \frac{1}{1 - \frac{\sum_{i=1}^n (\Sigma \gamma N/L)_i a_{0i}^2}{\sum_{i=1}^n (\Sigma V)_i a_{0i}}} \quad (6.39)$$

If an average flexibility factor is used, the above equations can be further simplified. Since all the deflections are increased by the same ratio, and since this method is based on the modified iterative method, the column end-moments are equal to $f_s M_0$. Note that this method gives the same equation as the other methods presented earlier for a single-storey frame.

The critical load factor implied by Eq. 6.38 (i.e., when $f_s = \infty$) is similar to the one presented by Stevens (1967) although derived in a different manner.

Although this method and the overturning moment method both give a single magnifier for the entire structure, the derivation of this method is based on a more direct assumption. The overturning moment method implies the same assumption but it requires the additional assumption that the deflections are proportional to the overturning moments at the base (Sect. 6.5). Hence if the assumption that an overall magnifier can be used is valid (the condition that this assumption may or may not be valid has been mentioned in Sect. 6.5), the frame magnifier method gives the same or better results than the overturning moment method, as demonstrated in Chapter 7.

6.7 ACI method

The following is an attempt to formulate rationally the current ACI (1987) method for sway frames although the original derivation was semi-empirical (MacGregor et al., 1970). This method can be considered a further simplification of the modified iterative method, but it has the restriction that the frame to be considered cannot include any distinct bracing elements such as shear walls or inclined bracing members. This will be shown when developing the method.

The simplifying assumptions required for this method (in addition to the assumption that the deformed shape of the structure under lateral and vertical loads can be represented by the deformed shape under lateral loads plus sway forces made in the modified iterative method) are introduced as follows:

1. The end-rotational stiffness of each beam is equal to $6 \cdot EI_B / L_B$ for that beam.
2. The restraining moments provided by the beams at one end of a column are distributed between the column above and the column below in proportion to the EI/L value of the two columns.

Assumption 2 precludes the existence of any shear walls in a structure. The above two assumptions will be discussed later. These two assumptions permit a storey to be isolated from the frame with the column end-rotational restraints expressed as a function of G_1 and G_2 as shown in Fig. 6.12.

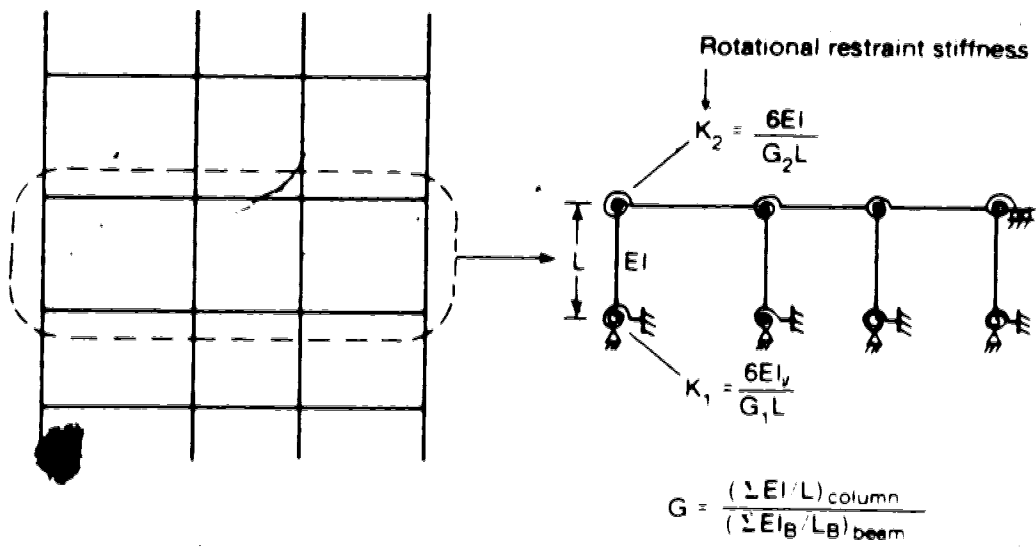


Fig. 6.12 A storey isolated from the frame (ACI method)

For an isolated single-storey frame (Fig. 6.12), the modified iterative method is simplified to Eq. 6.31 stated in Section 6.4. The deflection magnifier given by Eq. 6.31 is rewritten as follows:

$$f_s = \frac{1}{1 - Q} \quad (6.40)$$

where

$$Q = \frac{\sum_{j=1}^m \gamma_j N_j}{\sum_{j=1}^m V_{0j} L/a_0} \quad (6.41)$$

where V_{0j} is the first-order end-shear in column j , and m is the number of columns in the storey. It is tacitly assumed that there are no inclined bracing elements in the storey. The free-to-sway critical load N_{fs} of a column, from Eq. 6.22 (Sect. 6.2.2), is equal to:

$$N_{fs} = \frac{V_0 L}{\gamma a_0} \quad (6.42)$$

By substituting Eq. 6.42 into Eq. 6.41, Eq. 6.41 becomes:

$$Q = \frac{\sum \gamma N}{\sum \gamma N_{fs}} \quad (6.43)$$

Note that the subscript j is discarded for simplicity.

Therefore the deflection magnifier is also equal to:

$$f_s = \frac{1}{1 - \frac{\sum \gamma N}{\sum \gamma N_{fs}}} \quad (6.44)$$

and the end-moments of any column in the storey is equal to $f_s M_0$ (Sect. 6.4). If it is assumed that the flexibility factor f_s is equal for all columns in the storey, it can be cancelled out in the above equation and Eq. 6.44 is simplified to:

$$f_s = \frac{1}{1 - \frac{\sum N}{\sum N f_s}} \quad (6.45)$$

which is the form of equation given in the ACI Code (1977). Due to the small range in the values of the flexibility factor, the assumption of a constant γ is relatively minor, and the consequence of errors introduced by this assumption should be considered insignificant.

The free-to-sway effective length factor k_{fs} , which is a function of G_1 and G_2 only, can be obtained from an effective length factor alignment chart given in the ACI Commentary (1977). Approximate formulae to determine k_{fs} are also given in the ACI Commentary. The approximate second-order analysis based on Eq. 6.45 and the alignment chart is referred to as the ACI method. Note that f_s needs to be evaluated for each storey.

The ACI method can be modified to be applied to the type of frames with different column heights in the bottom storey. According to Eq. 6.33 (Sect. 6.4), Eq. 6.41 is rewritten as:

$$Q = \frac{\sum \left(\gamma \frac{N}{L} \right)}{\sum \left(\frac{V_0 L}{a_0} \cdot \frac{1}{L} \right)} \quad (6.46)$$

By substituting Eq. 6.42 into the above equation and making the assumption that γ can be cancelled out, the deflection magnifier for the bottom storey becomes:

$$\underline{f_s} = \frac{1}{1 - \frac{\sum N/L}{\sum N_{fs}/L}} \quad (6.47)$$

The above equation was given by Hellesland (1976) but the derivation was not shown in his paper.

The two assumptions stated previously are examined in the following. Assumption 1 is reasonable for beams rigidly connected to columns. In fact, the summation of N_{fs} for all columns in a storey offsets some of the error resulting from the inflection points not occurring exactly in mid-span of the beams. This will be demonstrated in Sect. 7.2.2. In the case that the far end of a beam framed into the column under consideration is hinged or fixed, the beam length should be multiplied by 2 or 1.5, respectively when calculating the corresponding value of G , in order to obtain the correct value of k_{fs} from the alignment chart. This, however, is not mentioned in the ACI Commentary (1977).

The second assumption, which permits a storey to be separated from the frame, has been discussed when deriving the flexibility factor in Sect. 6.2.2 where it was shown that this is a reasonable assumption for a regular

multistorey frame with stiff beams and regular loading. It should be noted, however, that the significance of the errors in the assumption in evaluating the deflection magnifier given by the ACI method is much greater than when evaluating the flexibility factor (Sect. 6.2.2), since the free-to-sway effective length factor can vary from 1.0 to ∞ while the flexibility factor varies from 1.0 to 1.22. This is clearly reflected by the case of a shear wall or stiff column which bends into single curvature within a storey. The value of N_{fs} for the shear wall with G approaching infinity is very small, and therefore the very substantial lateral resistance offered by the shear wall is neglected. The errors resulting from this assumption will be demonstrated in Chapter 7.

Although the storey magnifier method is based on a similar assumption that a storey can be treated like a single-storey frame, the ACI method requires the additional assumption of idealized end-restraints for each column. Hence the ACI method is less accurate than the storey magnifier method, as will be shown in Chapter 7.

Alternative ACI method

The ACI Code appears to permit replacement of the term ϵN_{fs} in Eq. 6.45 by ϵN_c , i.e.,

$$f_s = \frac{1}{1 - \frac{\epsilon N}{\epsilon N_c}} \quad (6.48)$$

in which N_c is the exact elastic critical load of a column. In other words, a designer may perform a rigorous stability analysis to calculate the exact critical load for each column (strictly speaking, a critical load factor λ_c for the entire frame), and substitute the values into the above equation. Of course, one would not do this in practice since a stability analysis is generally more complicated than an exact second-order analysis.

Nevertheless, it is still of interest to examine this alternative because the question is often asked whether an 'exact' effective length factor (which results in an exact critical load) is better than the 'approximate' value obtained from the conventional alignment chart. Discussion of this also entails another question about what values of the axial forces should be used (i.e., what values of the vertical loads should be applied at the joints) when the load factor λ is equal to 1.0. Because the ACI Code or Commentary (1977) is not specific in this respect, the following is a reasonable attempt to discuss this approach.

The alternative ACI method can be derived on the basis of Eqs. 2.10 and 2.11 developed in Sect. 2.5. Consider a multistorey frame subjected to lateral and vertical loads applied at the joints. Assume that the first-order deflection y_0 can be adequately represented by the lowest sidesway critical mode \bar{y} with the critical load factor λ_c , while the other critical modes in Eq. 2.10 are negligible. Then according to Eq. 2.11, the total deflection y due to

the action of vertical and lateral loads is found to be:

$$y = \frac{y_0}{1 - \frac{1}{\lambda_c}} \quad (6.49)$$

It follows that a single deflection magnifier f_s for the entire frame is also equal to:

$$f_s = \frac{1}{1 - \frac{1}{\lambda_c}} \quad (6.50)$$

In determining the critical load factor λ_c , the effects of the axial forces in the beams are assumed to be neglected. Consequently, when calculating λ_c , the frame is only subjected to vertical loads at the joints such that the only internal forces acting are the column axial forces (Sect. 2.5). According to the derivation of Eq. 2.11, from which Eq. 6.50 was derived, the axial forces N in the columns for $\lambda = 1.0$ are equal to those from the original state of loading, i.e., gravity and lateral loads acting together (Fig. 2.8). Thus, when N_c in Eq. 6.48 is written as $\lambda_c N$, Eq. 6.48 becomes identical with Eq. 6.50. It is also apparent that the summation sign in Eq. 6.48 is not necessary since λ_c is constant for each column. As a result, the alternative ACI method in fact implies a single magnifier for the entire structure given by Eq. 6.50.

Although the validity of the assumption made for Eq. 6.50 that the deformed shape due to lateral loads can be represented by the sidesway critical deflection mode is

uncertain, it is certain that an overall magnifier is not valid for the case where a storey is not sensitive to the behavior of other storeys as discussed before in Sect. 6.5. In fact it will be shown in Chapter 7 that if a frames does not have any distinct shear walls (as implied in the ACI Code for 'unbraced' frames), an overall magnifier is not justified. Hence, it can be seen that the exact determination of the effective length factors may not guarantee any better results (in fact, may be worse) than the use of the effective length factors from the conventional alignment chart in the case of approximate second-order analysis.

6.8 Moment-correction factors

6.8.1 Introductory remarks

In Sect. 6.2.1 it was mentioned that the modified iterative method is more accurate in predicting the deflections than moments. This is because the redistribution of end-moments for individual columns due to the C and S effects (Chapter 5) has not been considered. An attempt is made in this section to rectify this error by introducing moment-correction factors. The derivation of these factors is based on the assumption that the lateral deflections are exactly determined.

Since each of the other approximate methods of second-order analysis discussed in this chapter is derived from the modified iterative method, the above error exists in all of

these methods. The additional assumptions made in these methods of second-order analysis are assumed valid in order that the moment-correction factors can also be applied. In other words, the deflections determined from these methods are also assumed to be exact. The validity of the additional assumptions in each of these methods will be examined in Chapter 7.

The moment-correction factor implied in the AISC (1978) approach for sway frames will be discussed first to illustrate the problem and to show the limitations in this procedure. The Hellesland and MacGregor approach (1982) which is developed on the basis of single-storey frames is used here and extended to multistorey frames. It should be noted that except for the ACI method, all the methods converge to the same method for single-storey frames as indicated in the development of the methods.

6.8.2 AISC approach

The AISC Commentary (1978) suggests a correction factor B_{\max} (the original text uses C_m) to modify the deflection magnifier f_s such that

$$M_{\max} = B_{\max} f_s M_{02} \quad (6.51)$$

where

$$B_{\max} = 1 - 0.18 \frac{N}{N_{fs}} \quad (6.52)$$

The free-to-sway critical load N_{fs} is a function of G_1 and G_2 , the same as in the ACI method. According to the AISC Commentary, under the combination of compression stress and bending stress most affected by the moment magnifier $B_{max} \cdot f_s$, a value of 0.15 can be substituted for the latter term in Eq. 6.52, giving a constant value of $B_{max} = 0.85$. This, however, is questionable, since the value of 0.85 corresponds to $N = 0.83 N_{fs}$ which is a very high axial load for a beam-column.

Equation 6.52 is obtained by considering a single free-to-sway column with an infinitely rigid beam at one end (Fig. 6.13(a)). The maximum moment occurs at the end attached to the rigid beam. In the derivation the column is replaced, as shown in Fig. 6.13, by an equivalent pin-ended beam-column subjected to the lateral load and the axial load equal to those of the original column. The equivalent beam-column has a length equal to the free-to-sway effective length $k_{fs}L$ of the column. It has been assumed that the deflected shape of the column due to the lateral load acting alone and the deflected shape due to the lateral load and the axial load acting together are both the same type of curve as the buckled shape of the column. Since the beam in Fig. 6.13(a) is rigid and therefore the slope of the deflected shape is zero at the column end, the lateral load acts at mid-span of the beam-column in Fig. 6.13(b). Based on the assumption that the final deflected shape is a sine

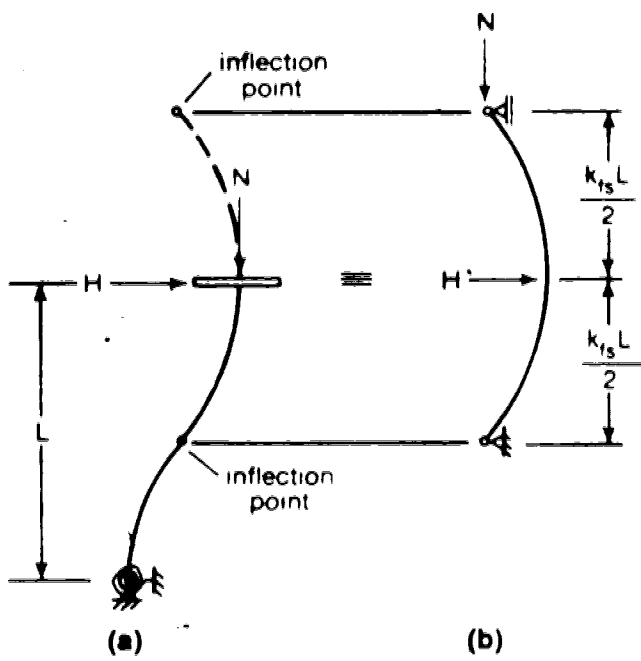


Fig. 6.13 Concept in AISC approach for B_{max}

curve, the bending moment at mid-span of the beam-column which corresponds to the maximum moment in the actual column is found as given by Eqs. 6.51 and 6.52. A complete derivation for the beam-column in Fig. 6.13(b) is given by Wang and Salmon (1973).

It is apparent that the moment-correction factor B_{\max} given by Eq. 6.52 is only applicable to a free-to-sway column attached to an infinitely rigid beam, but this is not explicitly stated in the AISC Commentary. In fact, the next section will show that this approach and particularly the constant value of 0.85 is unconservative in most other cases.

6.8.3 Hellesland and MacGregor approach (for single-storey frames)

Hellesland and MacGregor (1982) propose the following equations of B_{\max} which are developed on the basis of single-storey frames:

$$B_{\max} = 1 - g_2 \alpha_{fs} \quad \text{for } \alpha_{fs} < 1.0 \quad (6.53)$$

$$B_{\max} = 1 - g_2 \quad \text{for } \alpha_{fs} > 1.0 \quad (6.54)$$

except that when $\alpha_{fs} < 0.5$ the value of B_{\max} given by Eq. 6.54 and Eq. 6.55 is used.

where

$$g_2 = \frac{0.24}{0.24 + (1 + 0.75 \phi_2)^2} \quad (6.56)$$

The load indices α_{fs} and α_{ns} are defined by N/N_{fs} and N/N_{ns} , respectively, where the critical loads N_{fs} and N_{ns} are determined on the basis of the first-order inflection points of the beams (first-order end-restraints) rigidly connected to the column under consideration. The moment gradient r_0 has been defined previously as $-M_{01}/M_{02}$. The stiffness ratio ϕ_2 at joint 2 of the column (note $\phi_2 < \phi_1$) is defined as $\frac{EI/L}{\sum EI_B/2\bar{L}_B}$ where \bar{L}_B is the distance from the joint to the first-order inflection point in the beam (see Figs. 5.3(c) and (d)). After B_{max} is determined for the column in question, the maximum moment in the column can be calculated according to Eq. 6.51, in which f_B can be obtained from any of the approximate methods discussed previously.

The equations for B_{max} were based on the observation that the geometric effects in a single-storey frame can be quantified by the product of the B coefficients and the deflection magnifier f_B as indicated previously by Eqs. 5.1 and 5.4. It is assumed that f_B can be exactly determined, and therefore the B coefficients are estimated using a laterally deformed non-sway column (Fig. 5.3(d)).

Chesland and MacGregor (1982) have observed that the size

with increasing axial load until fairly high axial loads are reached. Since, by definition of elastic sway buckling, B_v is equal to zero when $\alpha_{fs} = 1.0$ (Fig. 5.4), B_v can be reasonably approximated by:

$$B_v = 1 - \alpha_{fs} \quad (6.57)$$

The linear approximation of B_v is very good for $\alpha_{fs} < 1.0$.

For $\alpha_{fs} > 1.0$, the error increases although Eq. 6.57 remains conservative. The total end moment, $\Sigma M = M_1 + M_2$, of a column is equal to:

$$\Sigma M = - B_v f_s V_0 L - N f_s a_0 \quad (6.58)$$

Substituting Eq. 6.57 into Eq. 6.58 and noting $\Sigma M_0 = - V_0 L$ gives

$$\Sigma M = (1 - g \alpha_{fs}) f_s \Sigma M_0 \quad (6.59)$$

where

$$g = 1 - \frac{N f_s a_0}{V_0 L} \quad (6.60)$$

Using Eq. 6.22 for the flexibility factor γ (Sect. 6.2.2), Eq. 6.60 can also be expressed as:

$$g = 1 - \frac{1}{\gamma} \quad (6.61)$$

The coefficient g varies from zero for $\gamma = 1.0$ to 0.18 for $\gamma = 1.22$. For the case of equal end-restraints, i.e., $\phi_1 = \phi_2$ (and $M_1 = M_2$, $M_{01} = M_{02}$), M_2 (or M_1) is given by:

$$M_2 = (1 - g_2 \alpha_{fs}) f_s M_{02} \quad (6.62)$$

where

$$g_2 = \frac{0.22}{0.22 (1 + \phi_2)^2} \quad (6.63)$$

which are obtained by substituting Eq. 6.19 (the equation of γ for equal end-restraints) into Eq. 6.61. (Note that if \bar{L}_B is equal to half of the beam length, then ϕ is equal to the term G defined by Eq. 6.16). If a column is restrained at one end and hinged at the other end ($\phi_1 = 0$), Eq. 6.62 is also derived with g_2 given by:

$$g_2 = \frac{0.22}{0.22 + (1 + \frac{\phi_2}{2})^2} \quad (6.64)$$

obtained by substituting Eq. 6.20 into Eq. 6.61. Hellesland and MacGregor (1982) replaced the term in brackets in Eq. 6.62 with:

$$B_2 = 1 - g_2 \alpha_{fs} \quad (6.65)$$

They also observed that the lower limit of g_2 at $\alpha_{fs} = 1.0$

is defined by Eq. 6.63 and the upper limit is closely defined by Eq. 6.64. Since the difference in the values of g_2 computed from Eqs. 6.63 and 6.64 was not significant for practical values of ϕ , Eq. 6.56 was determined as an average of the two limiting equations and the error at $\alpha_{fs} = 1.0$ was found to be within $\pm 2.5\%$ for practical values of ϕ . Apparently the expression of g_2 given by Eq. 6.56 was derived on the basis of $\alpha_{fs} = 1.0$. From Figs. 5.4 and 5.5, it can be seen that B_2 decreases almost linearly for $\alpha_{fs} < 1.0$ and the linear approximation of B_2 given by Eqs. 6.65 and 6.56 is accurate for $\alpha_{fs} < 1.0$. For $\alpha_{fs} > 1.0$, the error increases on the conservative side.

For a supporting sway column the maximum moment always occurs at the end (Sect. 5.2.2), and therefore B_{max} is equal to B_2 (by definition $M_{O2} > M_{O1}$), as indicated by Eq. 6.53. For a supported sway column ($\alpha_{fs} > 1.0$), the maximum moment may occur away from the end and initially B_{max} can be assumed to be constant with the axial load, as given by Eq. 6.54 (Fig. 6.14, to follow). For a very high axial load ($N > 0.5 N_{ns}$ as suggested by Hellesland and MacGregor, 1982), M_{max} can be found by the conventional ACI method for a non-sway column (Sect. 4.3) except that the limits in the original equation (Eq. 4.20) are discarded as shown by Eq. 6.55.

Equations 6.63 and 6.64 indicate that except for $\phi_2 = 0.0$, g_2 is less than 0.18. As a result, Eq. 6.53 suggested by the AISC Commentary (1978) is unconservative except for

the rigid-beam case. The values of B_{max} from Eqs. 6.53 to 6.56 are compared to the exact solution for a typical laterally deformed non-sway column in Fig. 6.14. The values of B_{max} implied by the AISC Code (1978) and the ACI Code (1977) are superimposed. As far as B_{max} is concerned (i.e., assuming that f_s is exactly determined), the ACI procedure is conservative in the load range of most practical interests. The AISC procedure, however, is unconservative in the load range of a supporting sway column which is the most common design situation.

In addition to the maximum column moment needed to proportion the column, the column end-moments M_1 and M_2 are needed to determine the moments required in the attached beams. The coefficient B_2 has been defined by Eq. 6.65 with g_2 given by Eq. 6.56, also illustrated in Fig. 6.14. Hellesland and MacGregor (1982) have observed that B_1 stays almost stationary with increasing axial load for a column with flexible restraints (as illustrated by Fig. 5.4), but follows C_2 for stiff restraints (Fig. 5.5). Therefore B_1 is approximated by:

$$B_1 = 1 - g_1 \alpha f_s \quad (6.66)$$

where

$$\bullet g_1 = 0.0$$

$$\text{for } \phi_1 > 1.0$$

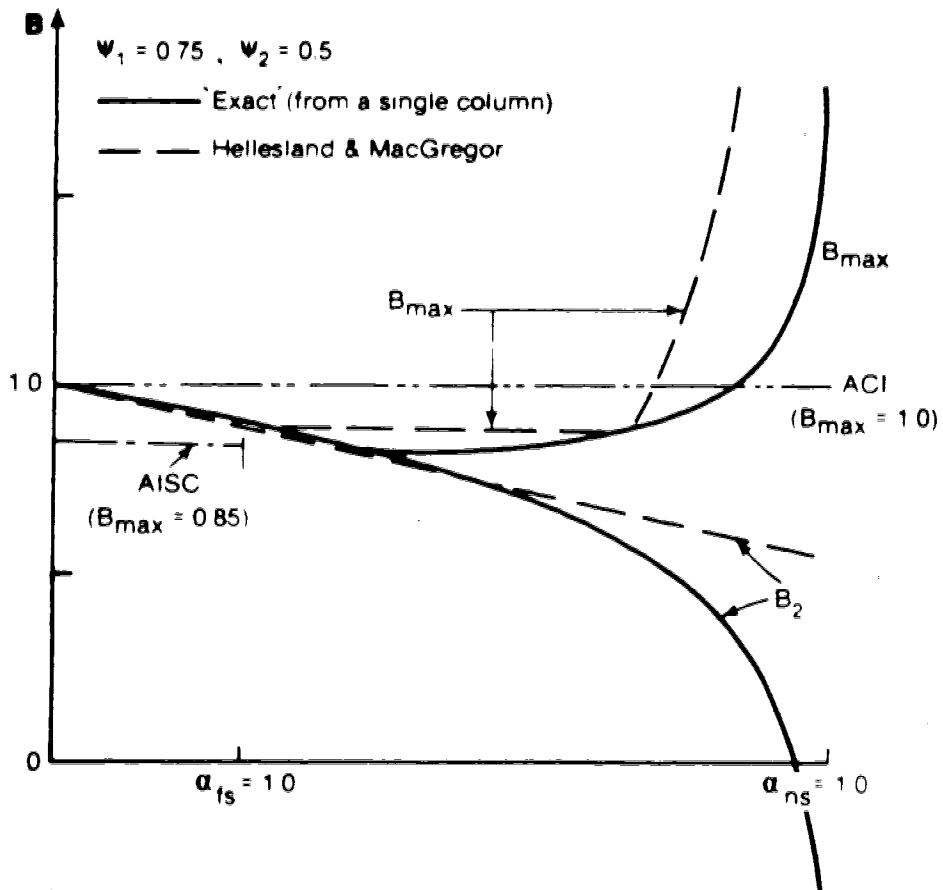


Fig. 6.14 Approximate values for B_{max} and B_2

$$g_1 = \frac{0.22}{0.22 + (1 + \phi_1)^2} \quad \text{for } \phi_1 < 1.0$$

Note that the above equation for g_1 is similar to Eq. 6.63.

Hellesland and MacGregor method can be simplified as regards the calculation of ϕ_1 and ϕ_2 by making the conventional assumption that the inflection points occur in mid-span of the beams that are rigidly connected to columns. When this is done, the values of N_{fs} and N_{ns} can also be directly obtained from the effective length factor alignment chart given in the ACI Commentary by noting that $G = \phi$ (for N_{fs}) and $G = \phi/3$ (for N_{ns}). In fact, it will be suggested in Sect. 6.8.4 that $G = \phi$ for calculating N_{ns} .

6.8.4 Moment-correction factors for multistorey frames

This section attempts to extend Hellesland and MacGregor's method to multistorey frames and to discuss the assumptions involved.

Figure 6.15(a) shows a multistorey frame which is braced at the joints against sidesway with imposed lateral deformations equal to the exact displacements produced by the combined action of the vertical and lateral loads. Holding forces R are required to hold the frame in the deformed shape. The moments in the laterally deformed columns are denoted as M_d . According to the assumption made in Sect. 6.8.1 that the deflections are exactly determined, the values of M_d are equal to those from the approximate methods of second-order analysis. In the case of

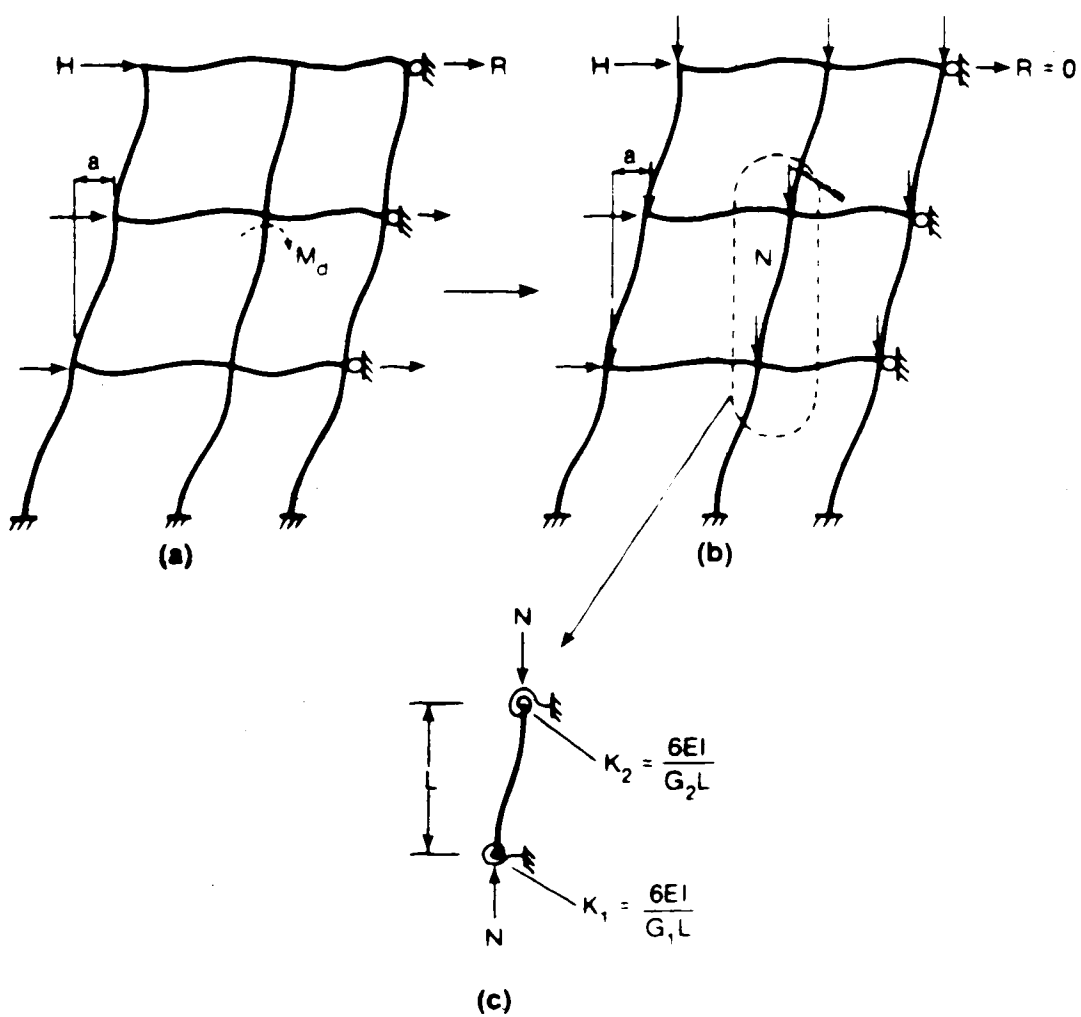


Fig. 6.15 A laterally deformed non-sway multistorey frame

modified iterative method or modified negative brace method, M_d can be directly obtained from the analysis. For the other methods which give the deflection magnifier f_s , M_d is assumed equal to $f_s M_0$. Note that this assumption is based on the assumption that a storey behaves independently of other storeys (stiff beams) or the ratio a/a_0 is equal in all the storeys. Obviously, these are the same assumptions made in deriving the various deflection magnifiers.

The vertical loads are then applied to the deformed non-sway frame as shown in Fig. 6.15(b). The resulting load effects are identical with those from the original state of loading. By making the same assumptions as for the ACI method (assumptions 1 and 2 in Sect. 6.7), any column in the frame can be isolated from the frame with end-restraints as a function of G_1 and G_2 , as shown in Fig. 6.15(c). These assumptions will be discussed later. It is apparent that the whole process is conceptually the same as the previous case for a single-storey frame (Fig. 5.3) except that $f_s M_0$ is being replaced by a more general term M_d . Therefore, Hellesland and MacGregor method is also applicable for multi-storey frames with $f_s M_0$ replaced by M_d , ϕ replaced by G , and the values of N_{fs} and N_{ns} calculated accordingly.

The assumption of mid-span inflection points in the beams has been discussed before. The major problem lies in the assumption regarding the relationship between storeys. Sections 6.2.2 and 6.7 have shown that this assumption is reasonable for a frame with stiff beams, and this will be

demonstrated in the next chapter. For flexible beams, this assumption can be violated. Nevertheless, Hellesland and MacGregor's equations indicate that the moment-correction factors are only significant for stiff beams (i.e., for low values of ϕ_2 in Eq. 6.56). For more flexible beams, the correction factors become closer to 1.0 and therefore the consequence of the assumption becomes less significant. In other words, although the assumption is less valid for more flexible beams, its effect is proportionally reduced. For example, this assumption breaks down for a shear wall with G_2 approaching infinity but the values of the correction factors approach 1.0, which is a reasonable answer.

For a very heavily loaded column, it has been shown that B_{\max} may be greater than 1.0. Equation 6.55 suggested by Hellesland and MacGregor may be unconservative in this range because the effective stiffness of the end-restraints may be decreased drastically by a shift in the point of inflection in the beam at high axial loads as discussed in Sect. 5.2.2. It would seem prudent to base the calculation of N_{ns} on the assumption that the end-rotational stiffness of the beam is equal to $2EI_B/L_B$ rather than on the first-order inflection point or $6EI_B/L_B$. In addition, B_{\max} may exceed 1.0 for a column attached to weak beams. Due to the uncertainty of the validity of the assumption concerning the relationship between storeys in frames with weak beams as mentioned earlier (Sect. 6.2.2), a conservative estimate

would seem more appropriate. This suggestion will be explicitly stated in Chapter 8.

6.9 Summary

Various approximate methods of second-order analysis for elastic sway frames have been reviewed in this Chapter. The major assumptions in each method are summarized in Fig. 6.16. Note that all approximate methods are shown to grow out of the modified iterative method. In terms of accuracy, the modified iterative method and the modified negative brace method are obviously the best. However, in terms of simplicity the other methods (not including the iterative method) are more appealing.

The frame magnifier method and the overturning moment method, both of which give an overall magnifier for the entire structure, appear to be valid for a frame with flexible beams relative to columns. The storey magnifier method, which gives a magnifier for each storey, is most valid for a frame with stiff beams. The ACI method, which also gives a magnifier for each storey, is the only method which cannot be applied to a frame with bracing elements. The ACI method is most valid for a frame with stiff beams but it is less accurate than the storey magnifier method because of additional assumptions required in the ACI method (Fig. 6.16). In short, the validity of the four approximate methods, which are simplifications of the modified iterative method, appears to depend on the stiffnesses of the beams

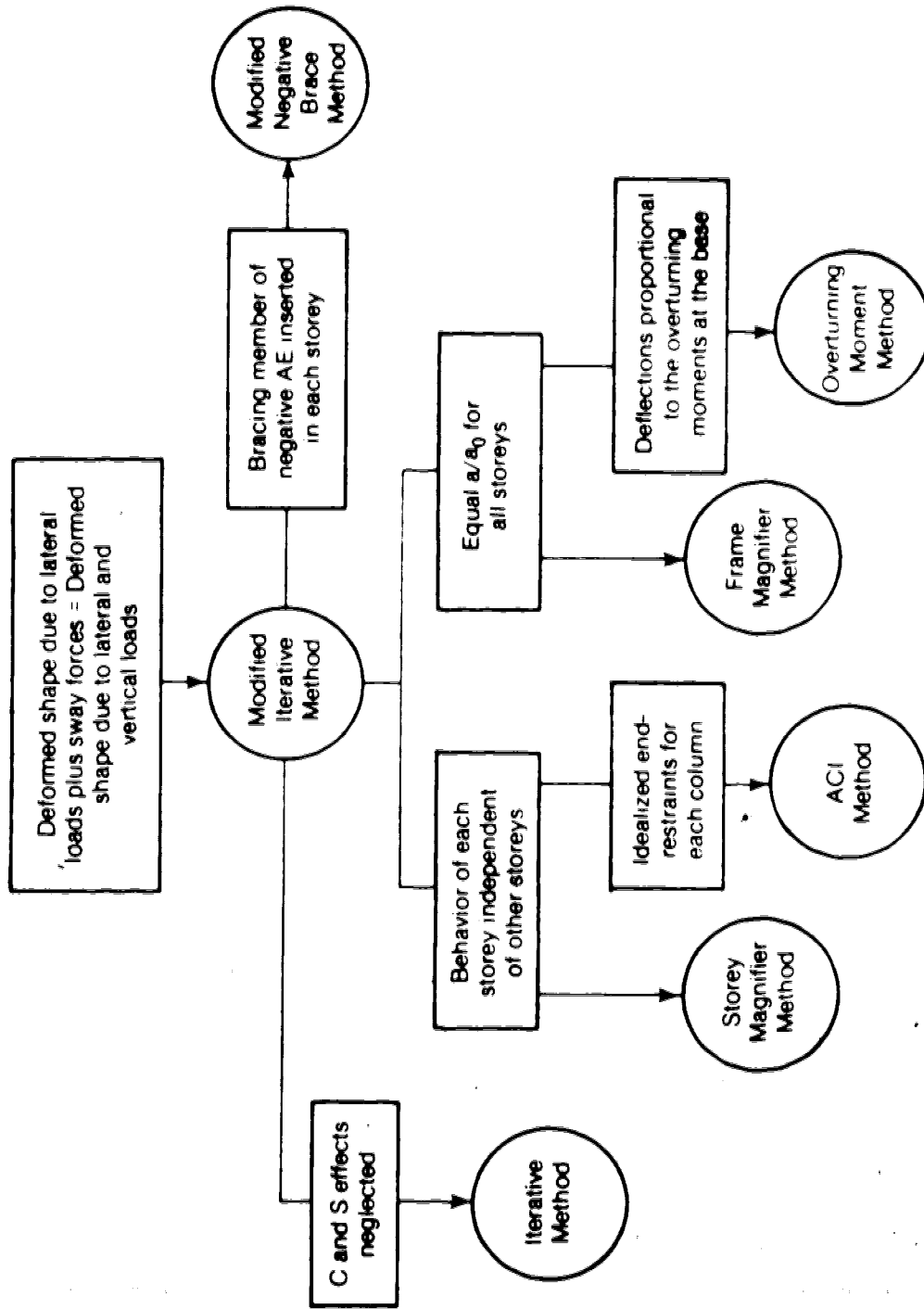


Fig. 6.16 Major assumptions in the approximate methods of second order analysis for sway frames

relative to the columns. These will be evaluated in the next chapter.

The basic error (resulting from the assumption stated at the top of Fig. 6.16) in all the approximate methods in estimating the column moments is rectified by introducing the moment-correction factors. The other sources of errors inherent in some of the methods as discussed in the above paragraph, however, still limit their applicability. This will be examined in the next chapter.

7. EVALUATION OF THE APPROXIMATE METHODS FOR SWAY FRAMES

7.1 Introduction

7.1.1 Problem statement

The approximate methods of second-order analysis of elastic sway frames, including the moment-correction factors B (Sect. 6.8.4), are as follows: In the modified iterative method or the modified negative brace method, the deflections are obtained directly from the analysis, but the column moments are obtained by multiplying the column end-moments from the analysis by the corresponding moment-correction factors. In the other methods, namely, the storey magnifier, frame magnifier, overturning moment and ACI methods, which give deflection magnifiers f_s , the deflections and column moments are given by:

$$a = f_s \cdot a_0 \quad (7.1)$$

$$M = B \cdot f_s \cdot M_0 \quad (7.2)$$

7.1.2 Method of evaluation

The errors in the approximate methods are due to the errors of the assumptions involved. The major sources of errors are derived from:

- The basic assumption that the deformed shape of the frame subjected to lateral loads and vertical loads can be represented by the deformed shape due to lateral loads plus sway forces (see Fig. 6.16).
- The major additional assumption required in each of the methods which are simplified from the modified iterative method (see Fig. 6.16).
- The assumptions of mid-span inflection points and idealized vertical relationship between continuous columns made in the moment-correction factors (Sect. 6.8.4).

Note that the last source of errors is relatively minor, as discussed in Sect. 6.8.4. An attempt is made in the following sections to determine the limits and conditions for which the errors resulting from the above assumptions are acceptable. In effect, the applicability of different methods are also compared.

First, the assumption about the deformed shape will be examined in Sect. 7.2.1 with the aid of a supported sway frame. The assumption of mid-span inflection points made in the M1 method and in the derivation of the moment-correction factors will be examined using a similar frame.

magnifier, overturning moment, and ACI methods all require assumptions to idealize the vertical relationship between storeys (the second source of errors as stated previously). Similarly, the moment-correction factors also require an assumption as regards the vertical relationship between storeys. This type of assumption will be checked with multistorey structures, first with low-rise structures in Sect. 7.3, and then with high-rise structures in Sect. 7.4. Finally, in Sect. 7.5, recommended methods of second-order analysis of sway frames will be proposed.

7.2 Single-storey structures

7.2.1 Supported sway columns

The basic assumption of all the approximate methods developed in Chapter 6 is that the deformed shape of the structure due to vertical and lateral loads is equal to that due to the lateral loads plus sway forces (see Fig. 6.16). The validity of this assumption is uncertain in the case of supported sway columns, as mentioned in Sect. 6.2.2. This problem is examined with the aid of a simple elastic frame shown in the inset to Fig. 7.1(b). The frame consists of a column carrying an axial force and a much stiffer column carrying no axial force. In the approach of the elastic analysis of the frame, the weak column will deflect in a shape considerably different from the assumption as shown

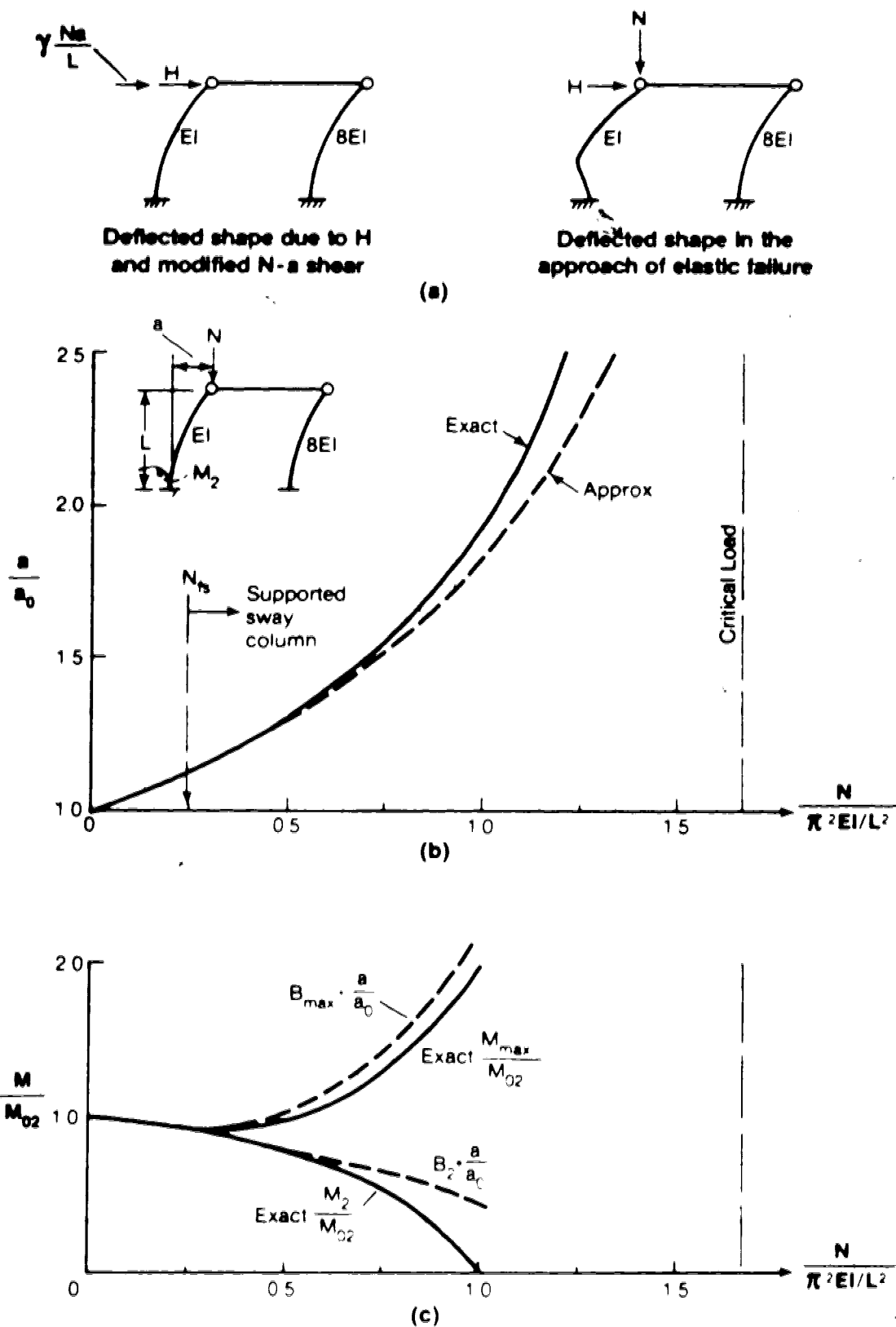


Fig. 7.1 Supported sway column

the extent to which the basic assumption can be considered valid.

In Fig. 7.1(b), the exact ratio a/a_0 is compared with the deflection magnifier from the approximate method. Note that all approximate methods give the same results for this particular case when $\gamma = 1.22$ is used. The two curves agree reasonably well far beyond the stage when the weak column has become a supported sway column. When the weak column reaches a deflected shape very different from the assumption, e.g., at $N > N_e$, the approximate curve becomes less accurate. The figure, however, indicates that for $f_g < 1.5$, which is considered a very large value in practice, the two curves are almost indistinguishable. This indicates that the approximate methods are not sensitive to the basic assumption in the practical ranges of f_g values.

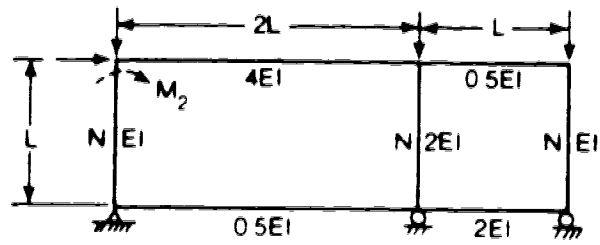
In Fig. 7.1(c), the end-moment and the maximum moment in the weak column are compared with those based on the moment-correction factors and the exact a/a_0 . The two sets of curves agree reasonably well. The approximate curve for M_2 tends to be conservative because of the linear approximation of B_2 (Sect. 6.8.3). This figure also demonstrates the previous discussion (Sect. 6.2.1) that the deflection magnifier is better in estimating the deflections than the column moments. The moment-correction factors are shown to rectify the error.

The above illustration is believed to represent a typical case for the assumption examined because the

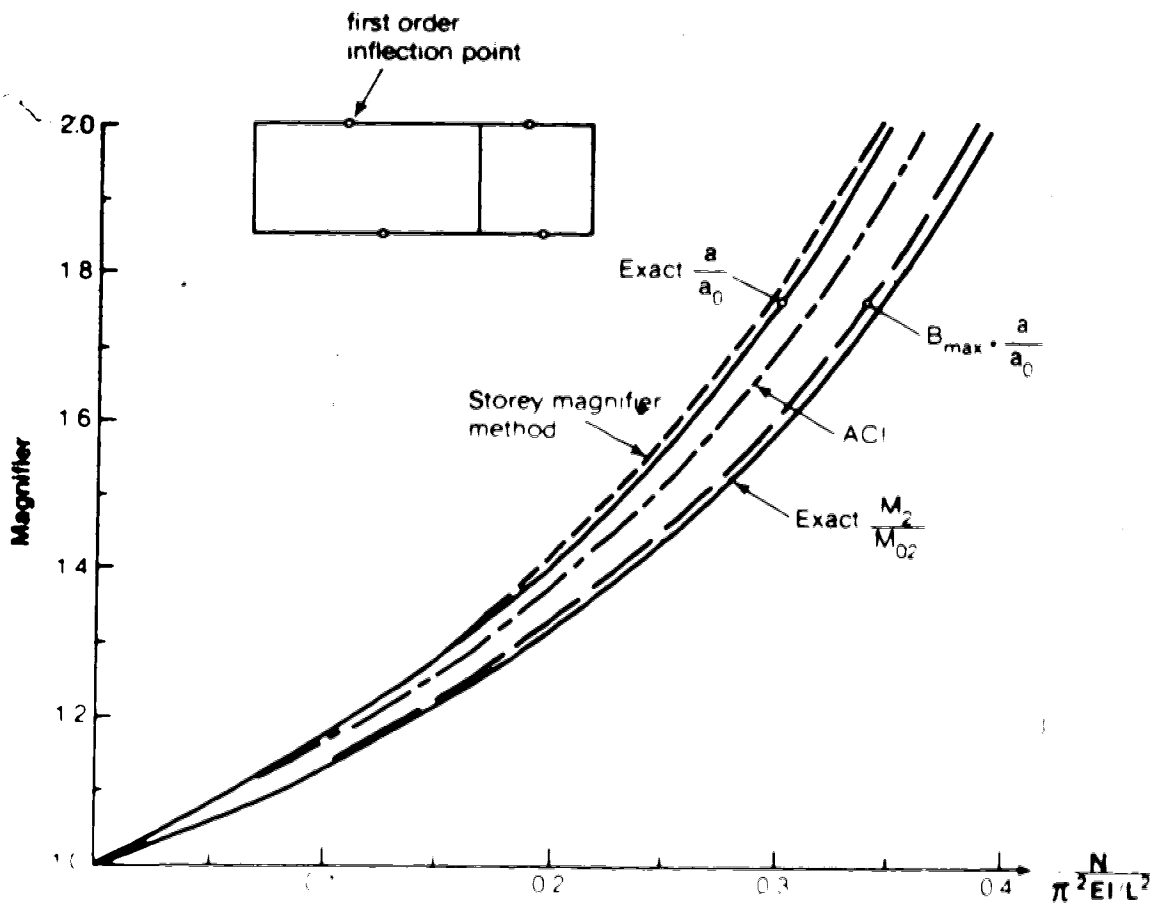
increase in the deflection of the frame is solely produced by the axial force in the weak column. If the stiff column also carried a vertical load, the agreement between the deflection magnifier and the exact a/a_0 would be very good up to f_s greater than 1.5. In the case of a multistorey multi-bay frame, it is likely that the majority of the columns are supporting sway columns, and the limit of the accuracy of f_s should be far greater than 1.5. In short, the basic assumption of the approximate methods is considered valid in the case of supported sway columns when f_s is less than about 1.5. For multistorey multibay frames where most columns are supporting sway columns, this limit is likely to be much higher.

7.2.2 Assumption concerning inflection points

In the alignment chart used to calculate the effective length factors for use in the ACI method (Sect. 6.7), the inflection points in the beams are assumed to occur at mid-span. As mentioned in Sect. 6.7, the deflection magnifier (Eq. 6.45) given by the ACI method should not be sensitive to this assumption because the summation of N_{fs} for all columns in a storey tends to offset the errors. This is illustrated using a frame shown in Fig. 7.2(a). Since the inflection point in a beam is a function of the relative stiffnesses of the adjacent columns and the stiffness of the beam relative to the columns, the middle column of the frame was chosen to be twice as stiff as the other two columns.



(a) Single-storey structure



(b) Approximate vs. exact results

Fig 7.2 Evaluation of the approximate methods for a single-storey structure

while the stiffnesses of the beams are arbitrarily chosen to introduce irregularity. In Fig. 7.2(b), the magnifier from the ACI method is compared with the exact a/a_0 . The agreement is good and for $f_g < 1.5$, the difference is not greater than 3%.

The assumption of mid-span inflection points is also made in determining the moment-correction factors. This is also evaluated in Fig. 7.2(b) by comparing the ratio M_2/M_{02} in the end column with $B_{\max} \cdot a/a_0$ based on the exact a/a_0 values. Note that the maximum moment occurs at the end of the column, i.e., $M_2 = M_{\max}$ and $B_{\max} = B_2$ because the column is a supporting sway column. The difference is minimal, suggesting that the moment-correction factor B_{\max} is insensitive to the assumption of mid-span inflection points. In fact, this should have been expected because in the case of a supporting sway column, the moment-correction factors only vary in a small range of 0.81 to 1.0 (Sect. 6.8.3).

The deflection magnifier obtained from the storey magnifier method (Eq. 6.31) is also compared with the exact a/a_0 in Fig. 7.2(b). Although an average flexibility factor of 1.10, which is roughly estimated from Table 6.2, is used in the storey magnifier method, the difference from the exact a/a_0 is very small. If an individual flexibility factor were used for each column, the two curves would be indistinguishable. In fact, this demonstrates the accuracy

certainly valid for supporting sway columns, as implied by the conclusion in the preceding section.

7.3 Low-rise multistorey structures

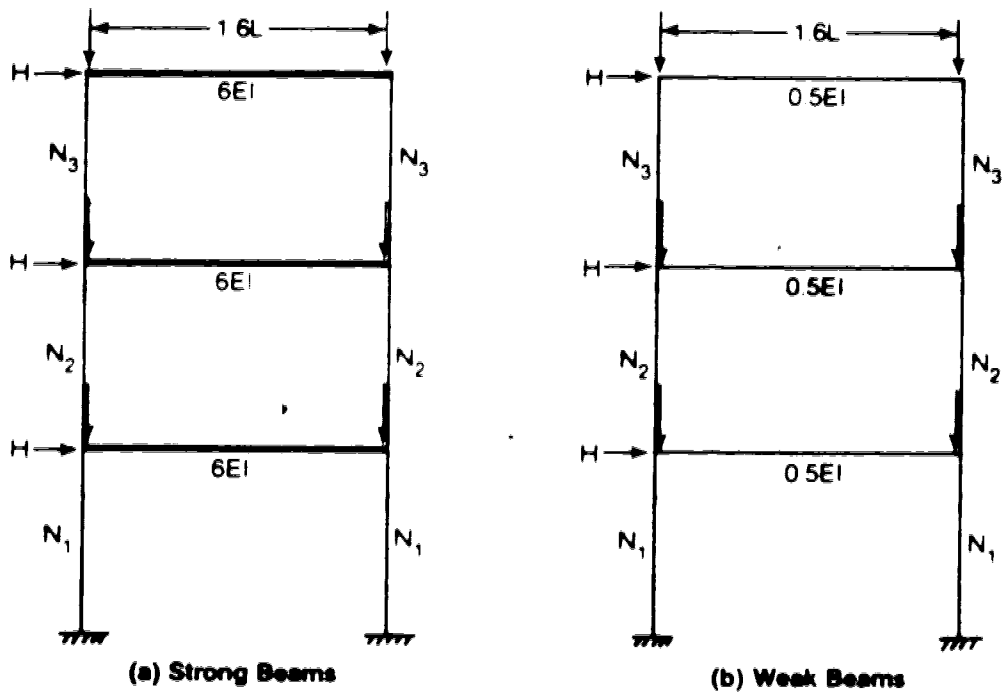
7.3.1 Problems

The storey magnifier, frame magnifier, overturning moment, and ACI methods are evaluated in this section. The most significant assumption in each of these methods concerns the vertical relationship between storeys. (Note that the other assumptions have been shown to be valid within practical values of f_g in previous sections.) The errors resulting from this type of assumption are examined in the following paragraphs for each method in the realm of low-rise structures. An attempt will also be made to determine the applicability of each method.

As part of the investigation, the assumption concerning the vertical relationship made in the moment-correction factors will also be examined.

7.3.2 Structures studied

The multi-storey structures shown in Fig. 7.3 are used in attempting to solve the problems stated in the preceding section. The structure in Fig. 7.3(a) has stiff beams. The shear wall structure shown in Fig. 7.3(c) represents an extreme case of completely flexible beams. The shear walls are assumed to rotate rigidly with the slab at every floor level. At



Note All columns have the same EI and L
and $N_1 : N_2 : N_3 = 3 : 2 : 1$

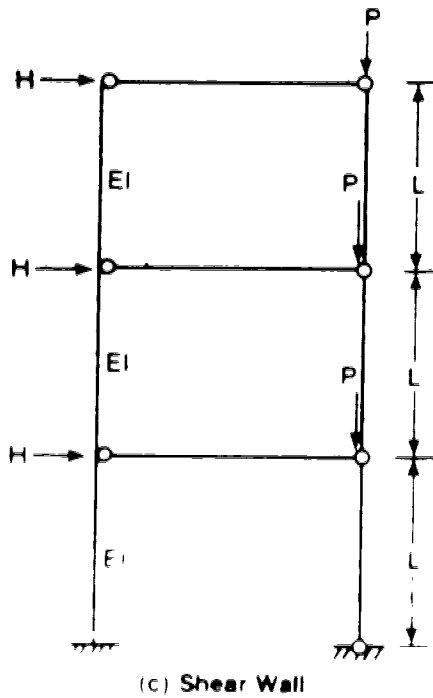


Fig. 3.1.3. Low rise structures studied

Fig. 7.3(b), where the beams are weak relative to the columns.

The loadings in each structure are also shown in Fig. 7.3. The ratios of the axial forces in the columns are kept constant during loading.

7.3.3 Results

(a) Strong beams

In Fig. 7.4, the deflection magnifiers obtained from the approximate methods for the structure with the strong beams (Fig. 7.3(a)) are compared with the exact values of a/a_0 in each storey. The results are plotted as a function of the axial forces in the columns. Since the axial loads are in a constant ratio, points corresponding to a given stage in the loading history plot on the same vertical line in all three parts of Fig. 7.4. An average flexibility factor of 1.15, which is estimated from Table 6.2, was used in the approximate analyses. The exact curves indicate that the ratio a/a_0 in one storey is markedly different from that in the other storeys, and therefore the overall magnifier given by the frame magnifier or overturning moment method fails to give generally good results. The storey magnifier method has the best agreement with the exact solutions. If it is assumed that the maximum value of f_g should not be greater than 1.5 in any storey of the structure, the agreement is excellent. The ACI method is not as good as the storey magnifier method but it gives reasonably good

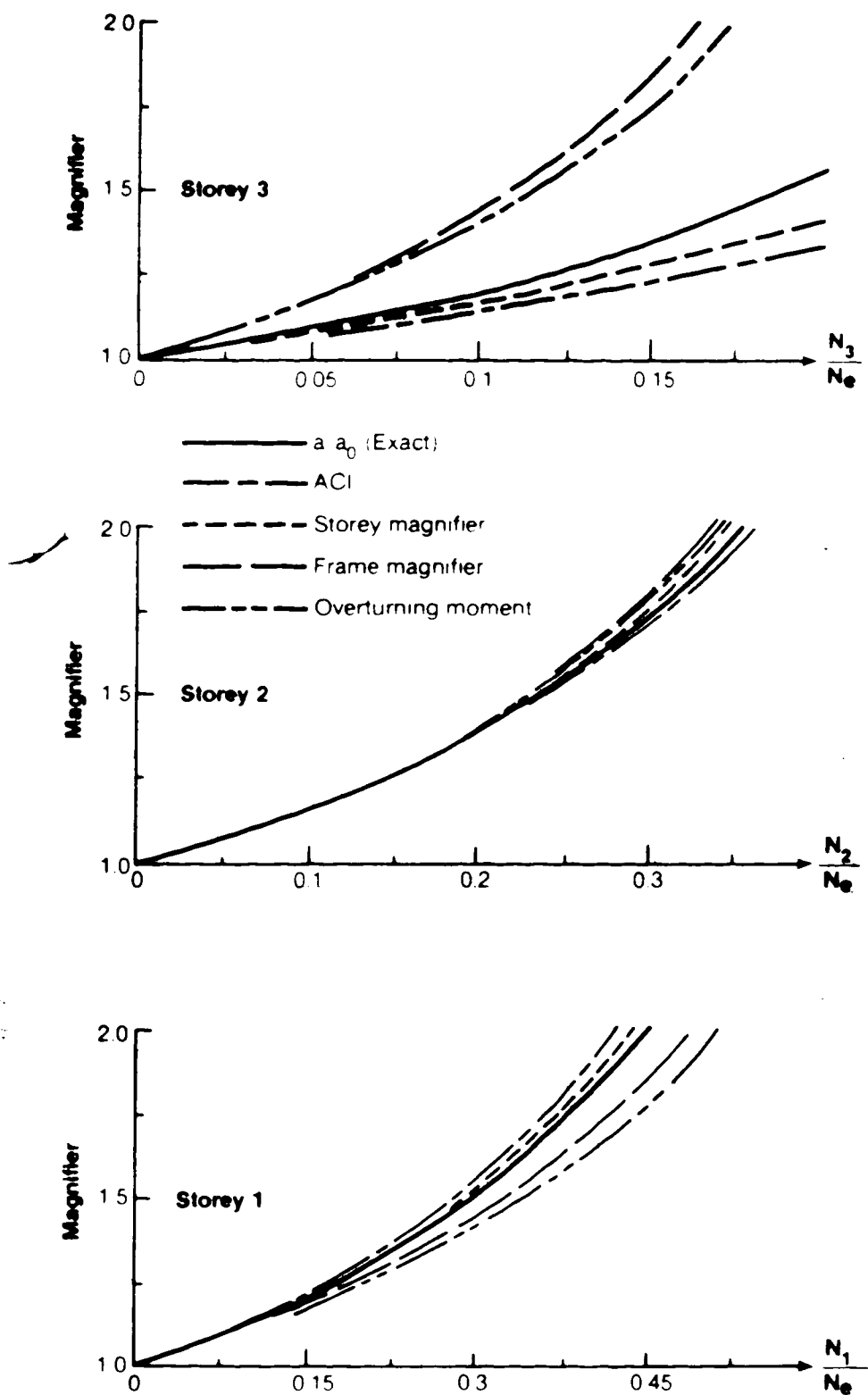


Fig. 7.4 Approximate vs. exact results for a low-rise structure with strong beams

results. The above situation occurs because each storey of the structure behaves quite independently of other storeys due to the strong beams. The lateral stiffness of each storey is essentially the same as the other storeys, but the total vertical load changes from storey to storey. Consequently, the geometric effects in each storey are different from other storeys.

In Fig. 7.5, the column maximum moments, which occur at the ends of the columns, are compared with the values of $B_{\max} \cdot a/a_0$ based on exact a/a_0 . The agreement is good. This indicates that the assumption regarding the vertical relationship made in the moment-correction factor B_{\max} is valid for the structure with stiff beams. In effect, this demonstrates the discussion made in Sect. 6.8.4 concerning the assumptions concerned. The same conclusion can be drawn for M_1 (the smaller end-moment in a column) although it is not shown in Fig. 7.5.

(b) Weak beams

In Fig. 7.6, the deflection magnifiers from the approximate methods for the structure with weak beams (Fig. 7.3(b)) are compared with the exact values of a/a_0 . An average flexibility factor of 1.05 (Table 6.2) was used in the approximate analyses. (In the storey magnifier method, $\gamma = 1.20$ was used for the bottom storey.) It is shown that at a given stage in the loading of the frame, the ratio a/a_0 in one storey is very close to that of other storeys. The

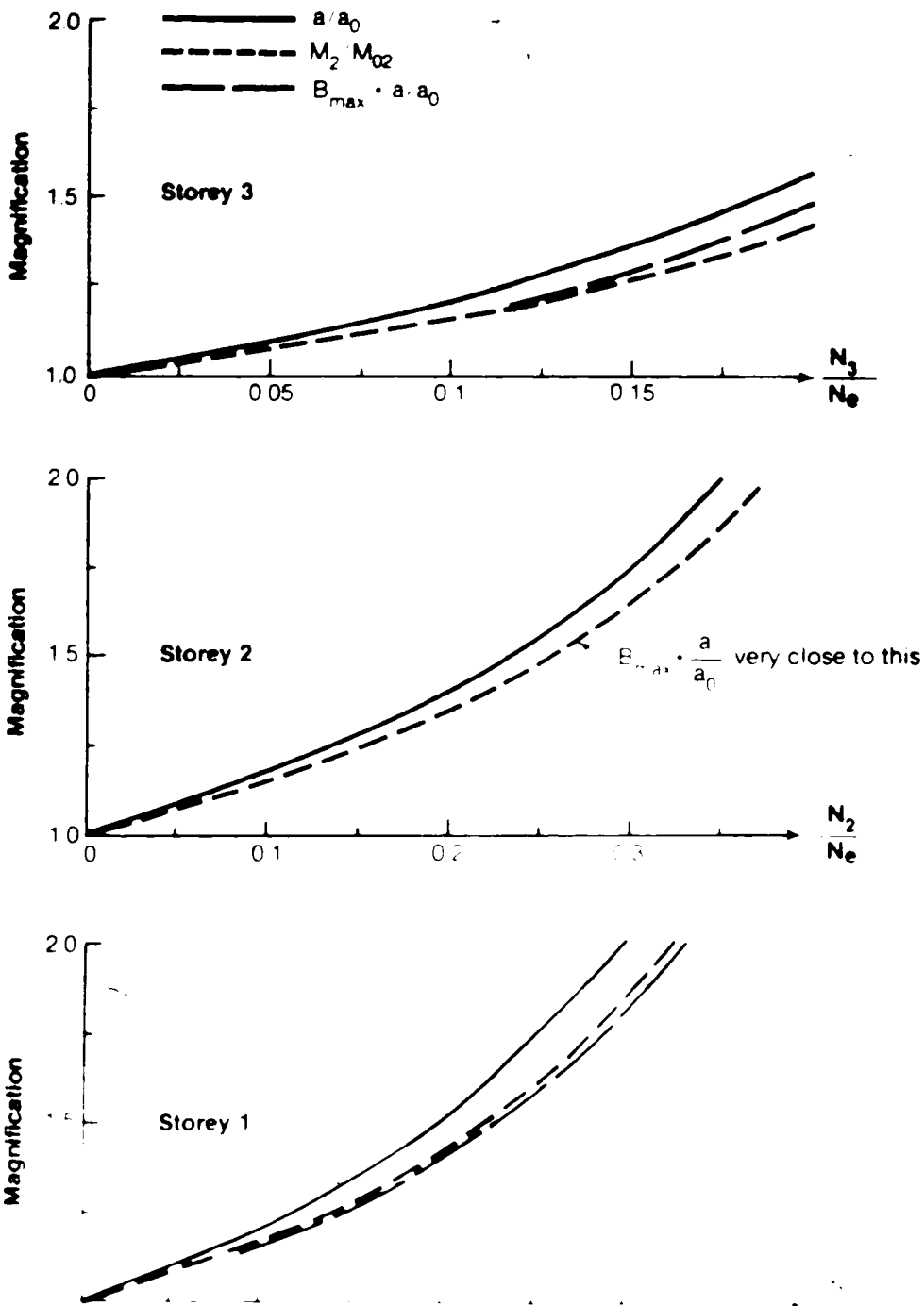


Fig. 7.5 Evaluation of the moment correction factor for a three-storey frame with strong beams

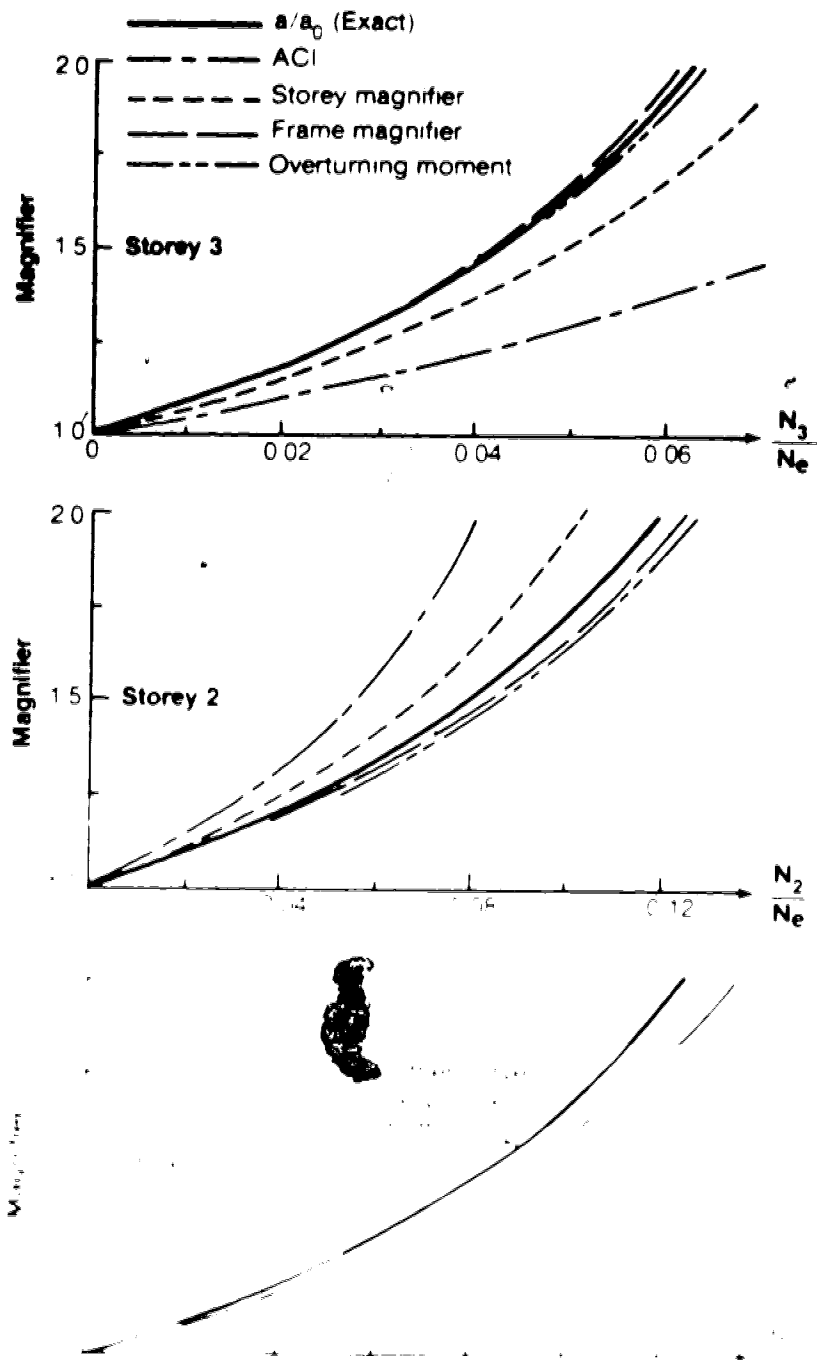


Fig. 7.6. Approximate vs. exact results for a low aspect ratio with wide beams.

overall magnifiers given by the frame magnifier method or the overturning moment method agree closely with the exact values of a/a_0 . The storey magnifier method is generally less accurate. The ACI method is shown to be the worst and the errors are considerable. The above situation results from the occurrence of vertical interaction (Sect. 5.3) in which the laterally stiffer storey (storey 3) assists the weaker storey (storey 2).

It is of interest to compare the storey magnifier method and the ACI method. Although both methods are inclined to be accurate for frames with stiff beams, the storey magnifier method is shown to behave much better than the ACI method in this case of weak beams. This is because the ACI method requires the additional assumption of idealized end-restraints for each column, as mentioned in Sect. 6.7 (see Fig. 6.16). For f_g (from the exact a/a_0) less than 1.5, the errors of the values from the storey magnifier method are shown to be less than 7%, which may be considered acceptable in many cases. The errors of the ACI method, however, are considerably larger than those in the storey magnifier method.

In Fig. 7.7, the exact values of a/a_0 , M_1/M_{01} and M_2/M_{02} are plotted for each storey. In the bottom storey (storey 1), the maximum moment which in this case is equal to M_{01} is very accurately predicted by $k_1 \gamma a/a_0$ (see Sect. 6.7). In the top two storeys, the maximum moment is

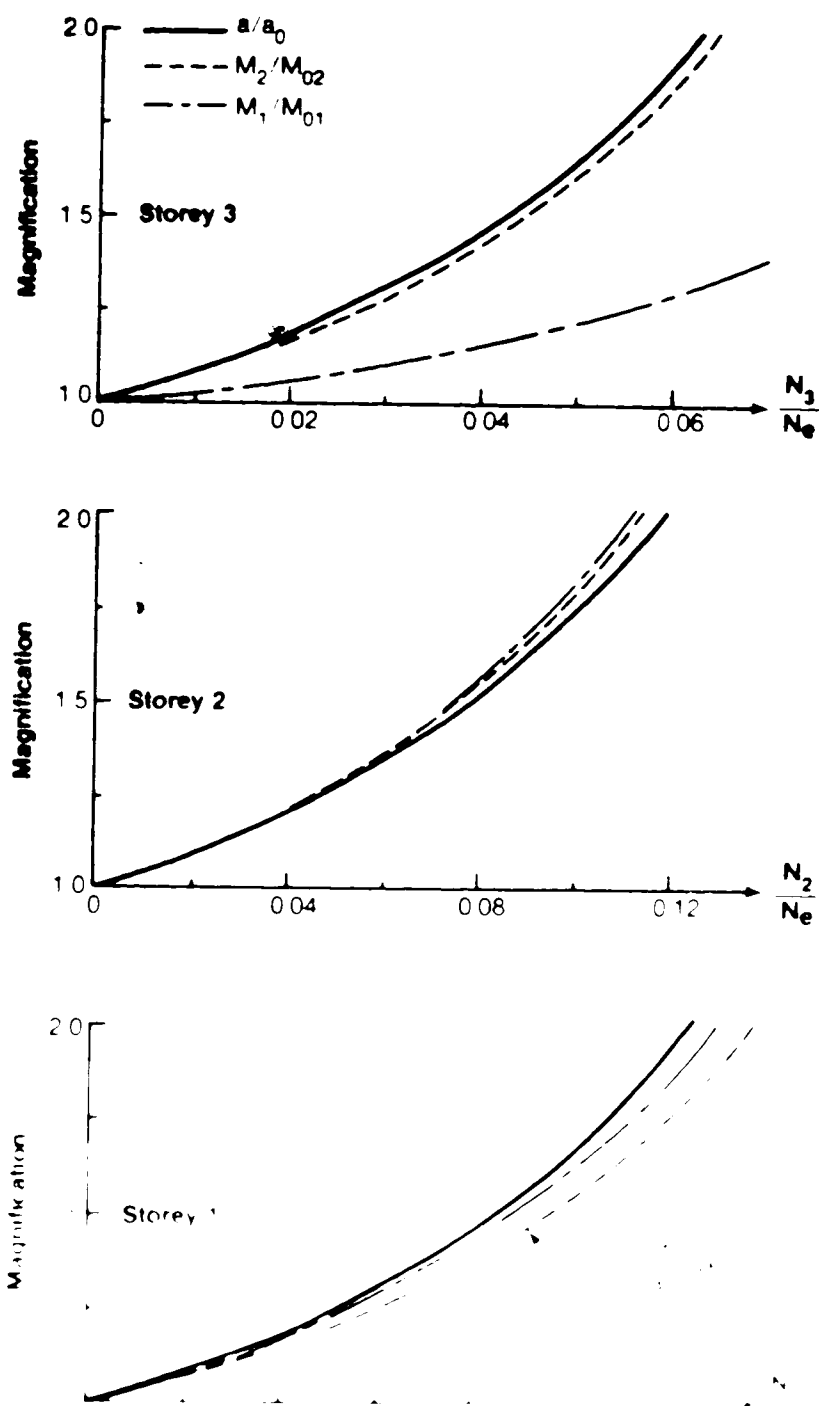


Fig. 12 Deflection and moment magnification curves for a frame with weak beams

$B_{\max} \cdot a/a_0$ approximation can be seen by comparing the a/a_0 curves with those for M_2/M_{02} and M_1/M_{01} . The end-moments in the top two storeys are very close to a/a_0 as predicted except M_1/M_{01} in the top storey. To explain the discrepancy of the exceptional case, the assumption of $M_d = f_s M_0$ (Fig. 6.15) made in Sect. 6.8.4 needs to be recalled. Although the assumption that the ratio a/a_0 is equal in all the storeys is fairly well satisfied in this case, the small value of M_1 in the top storey, which is about 1/4 of the moment M_2 at the other end, is relatively sensitive to the deviation from this assumption. The small value of M_1 , however, plays a much less significant part in the design of the column since the maximum moment in the column will dominate the design.

(c) Completely weak beams

In Fig. 7.8, the deflection magnifiers from the approximate methods for the shear-wall structure (Fig. 7.3(c)) are compared with the exact values of a/a_0 and M_1/M_2 . The symbols P and EI (implied in N_e) in Fig. 7.8 refer to those in Fig. 7.3(c). An average flexibility factor of 1.0 was used. The ACI method is unable to handle this type of structure, and therefore it is not shown in the figure. Note that this structure (Fig. 7.3(c)) can be easily analyzed using the modified iterative method

described in Sect. 7.9. The results are shown in Fig. 7.8.

It is seen that the ACI method is not applicable to this case.

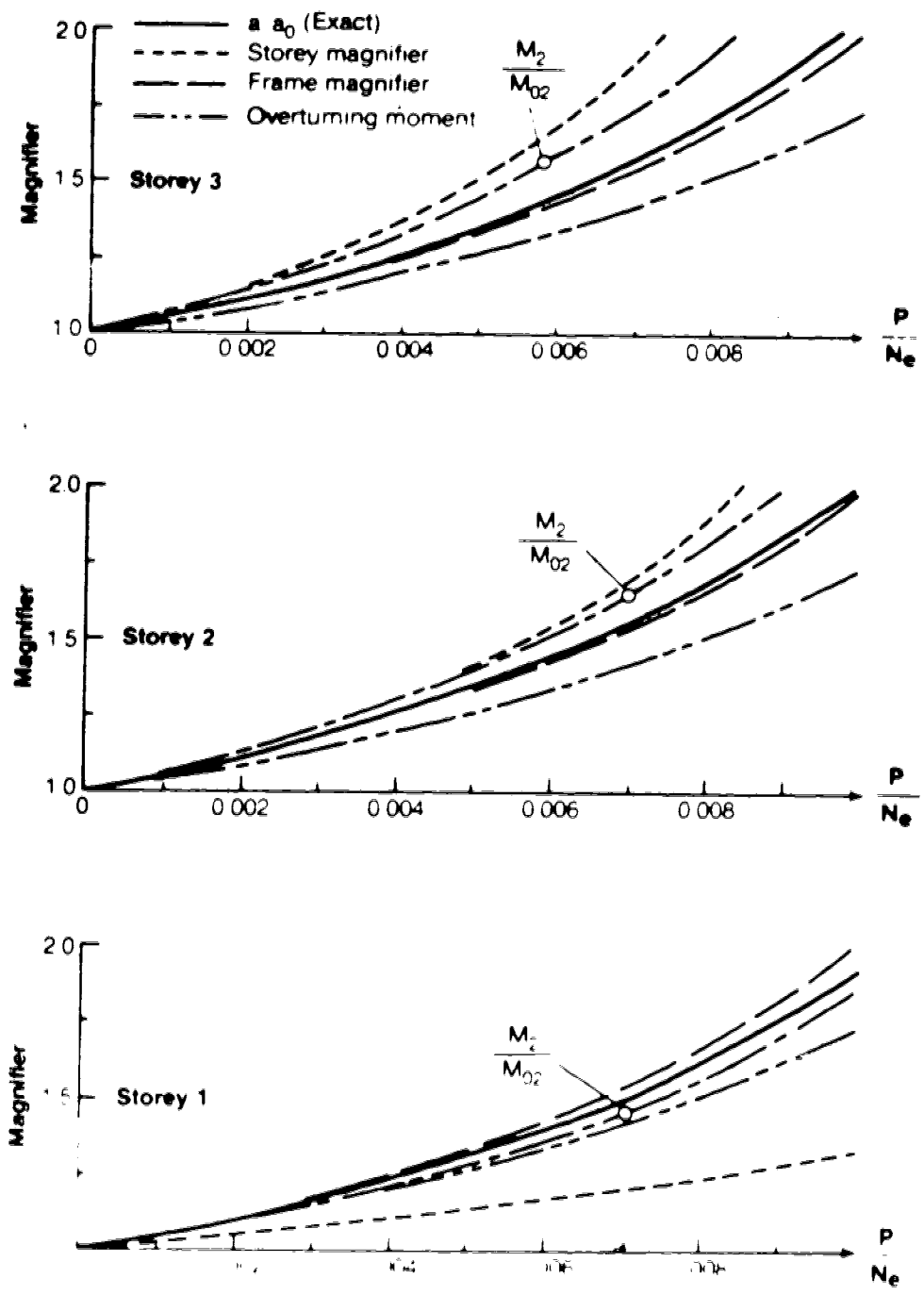


Fig 7.8 Approximate vs exact results for a low-rise shear wall

deflection magnifiers given by the frame magnifier method agree very well with the exact values of a/a_0 , while those given by the overturning moment method are less accurate. This is because the overturning moment method involves more assumptions than the frame magnifier method, as mentioned in Sect. 6.6 (see Fig. 6.16). The storey magnifier method is not acceptable in this case.

The values of the moment-correction factors are equal to 1.0 for this case, and therefore the column moments are assumed equal to $f_g M_0$. As explained in the previous case (Fig. 7.7), the smaller values of moments are less accurate. The largest error occurs at the top storey in which M_2 is about 1/6 of the moment at the base. Nevertheless, for $f_g < 1.5$, the error is less than 8% which may be considered acceptable due to its small value relative to the bottom moment in the case of a shear wall.

7.3.4 Concluding remarks

Several conclusions can be drawn from the above investigation for the low-rise structures studied:

1. When the beams become more flexible, the values of a/a_0 in all the storeys tend to be closer.
2. For a structure without any distinct shear walls, the storey magnifier method may be used with an accuracy of f_g not greater than 1.5.

3. For a structure with distinct shear walls, the frame magnifier method may be used with sufficient accuracy if f_g is limited to be less than 1.5.

7.4 High-rise multistorey structures

7.4.1 Problems and structures studied

This section extends the investigation stated in Sect. 7.3.1 into the realm of high-rise structures. It is apparent that there is little need for further study on structures with strong beams which can be handled effectively by the storey magnifier method or the ACI method. Therefore, the emphasis in this section is given to structures with weak beams. The following five structures are considered:

Structure A (Fig. 7.9) - This 24-storey frame is characterized by a constant beam size throughout the height. As a result the relative stiffness of the beams is smallest in the lower storeys. The exterior columns in the bottom storey are bent into single curvature.

Structure B (Fig. 7.10) - The 24-storey frame is attached to a shear wall of constant stiffness. It is of interest to observe the effect of the shear wall-frame interaction, and therefore the shear wall is made quite flexible. It carries about 50% of the lateral loads.

Structure C (Fig. 7.11) - The 24-storey frame is attached to a flexible shear wall of two storeys.

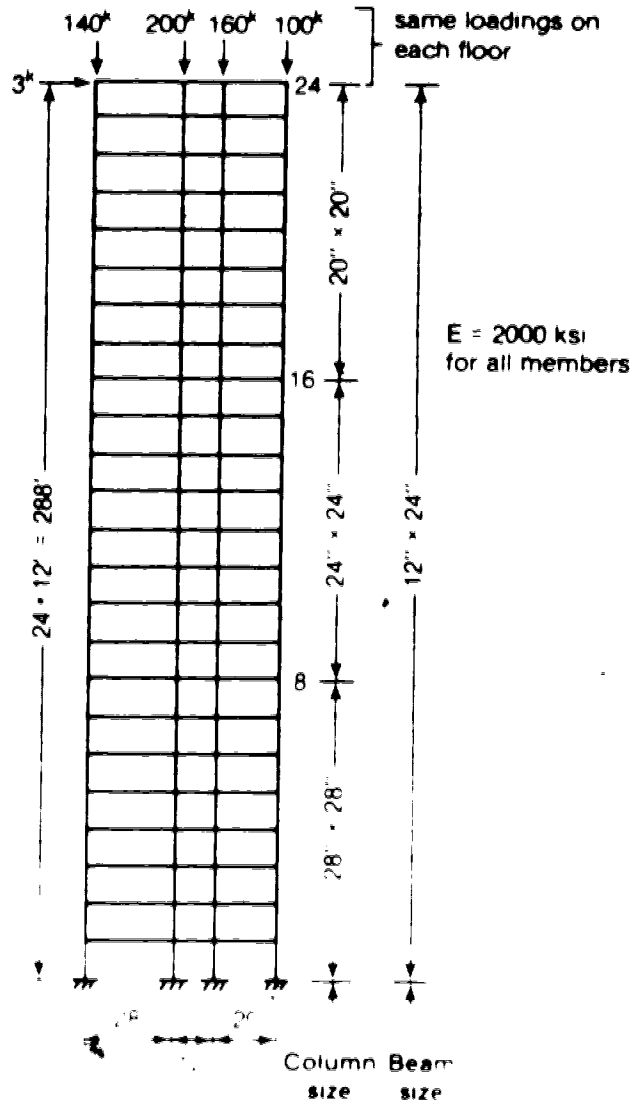
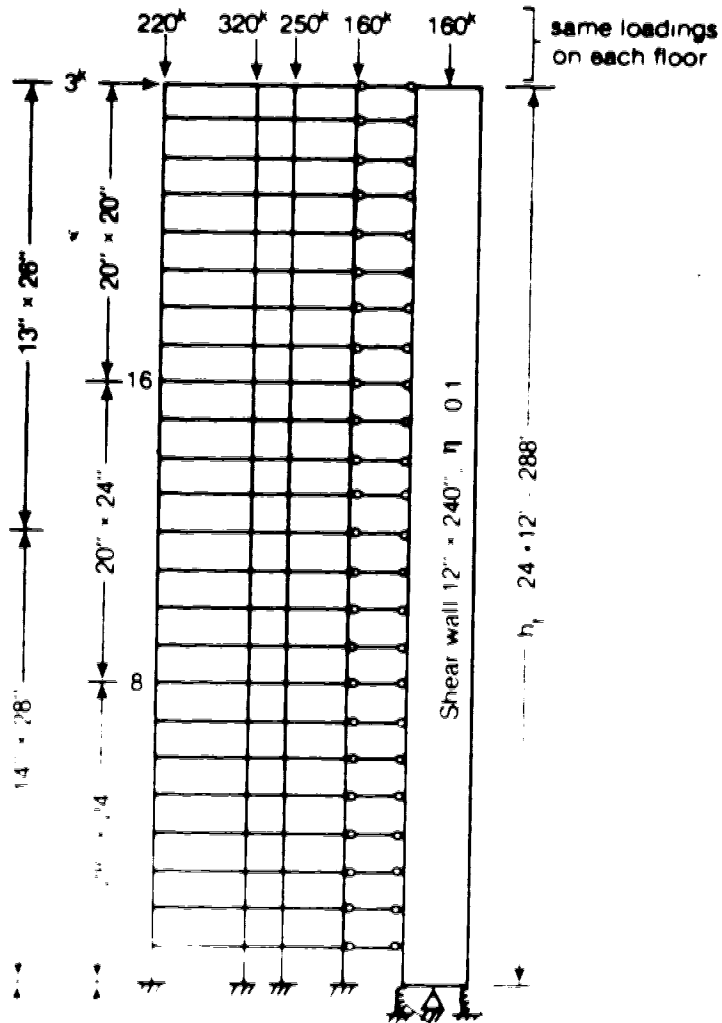
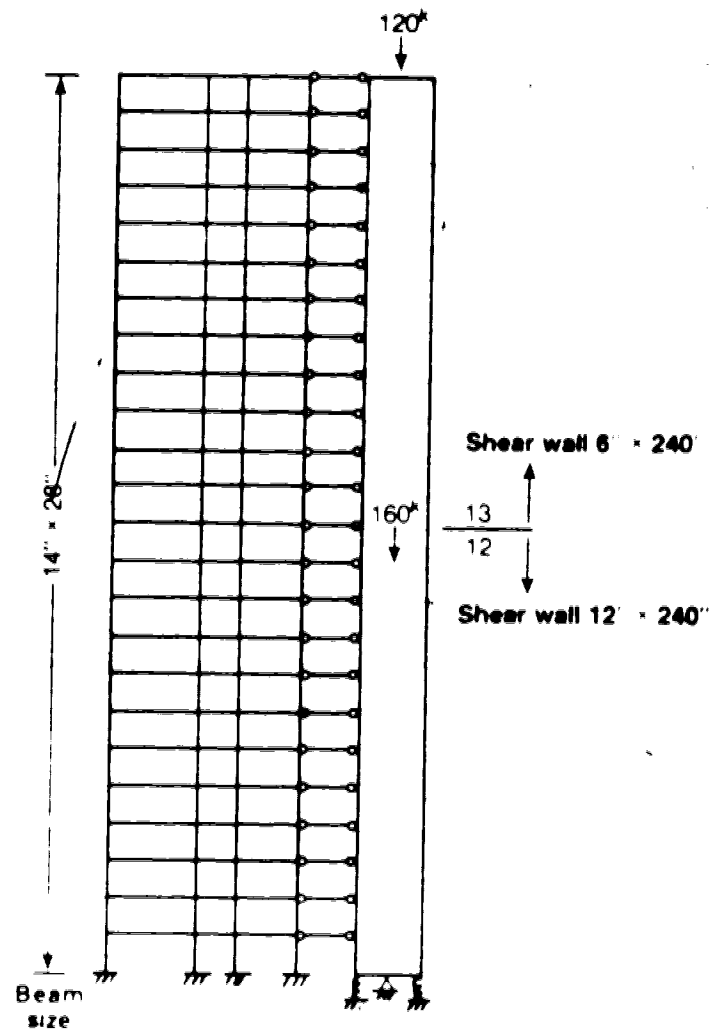


Figure 10.10. Structure A: A frame with weak beams at the bottom





1. The dimensions and loads are the same as in Fig. 7.10.

Fig. 7.11 Structure C: A frame with a flexible shear wall of two discrete stiffnesses

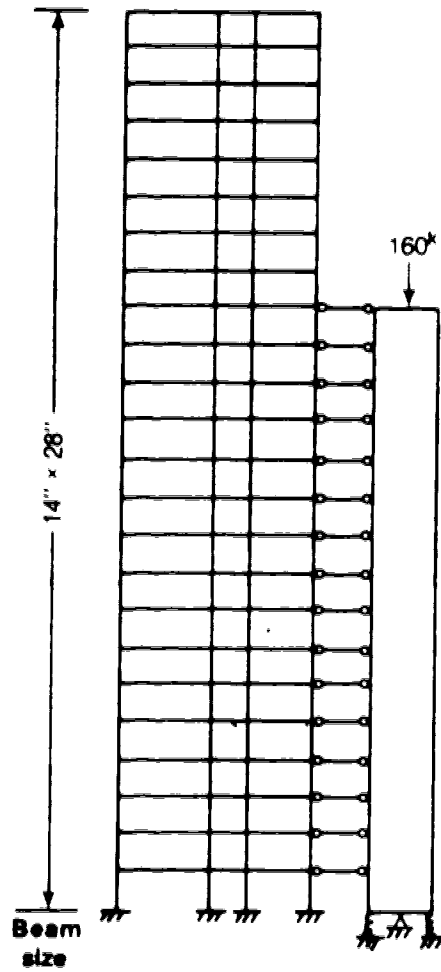
half of that for the lower half of the shear wall.

Structure D (Fig. 7.12) - The 24-storey frame is attached to a discontinuous flexible shear-wall. The upper eight storeys are not attached to the shear wall.

Structure E (Fig. 7.13) - This 24-storey frame is characterized by very strong columns (or very weak beams) in the lower storeys. The columns in the four bottom storeys are bent into single curvature as shown by the first-order bending moment diagram in Fig. 7.13. In the region of the lower storeys, the strong columns are essentially indistinguishable from a shear wall.

In the analysis of the above structures, the effects of the joint width of the shear wall were neglected by the use of hinged link beams. This assumption does not introduce serious errors because the load effects will be non-dimensionalized by dividing by the first-order load effects. As a result, the errors due to neglecting the joint-widths in both load effects are offset.

Since a limit of $f_s < 1.5$ was established in the previous section, the loadings were selected so that the largest values of f_s would be in the vicinity of 1.5. For the structures and the loading selected, all the columns are strong sway columns, and therefore the maximum moment in each column occurs at the end, i.e., $M_{\max} = M_2$. In all cases the moment-correction factors for the structures studied were 1.0, and therefore the column moments in the ultimate analyses have been assumed to be equal to $f_s M_0$.



Note Other dimensions and loadings are the same as those of Structure B

Fig. 7.12 Structure D: A frame with a flexible discontinuous shear wall

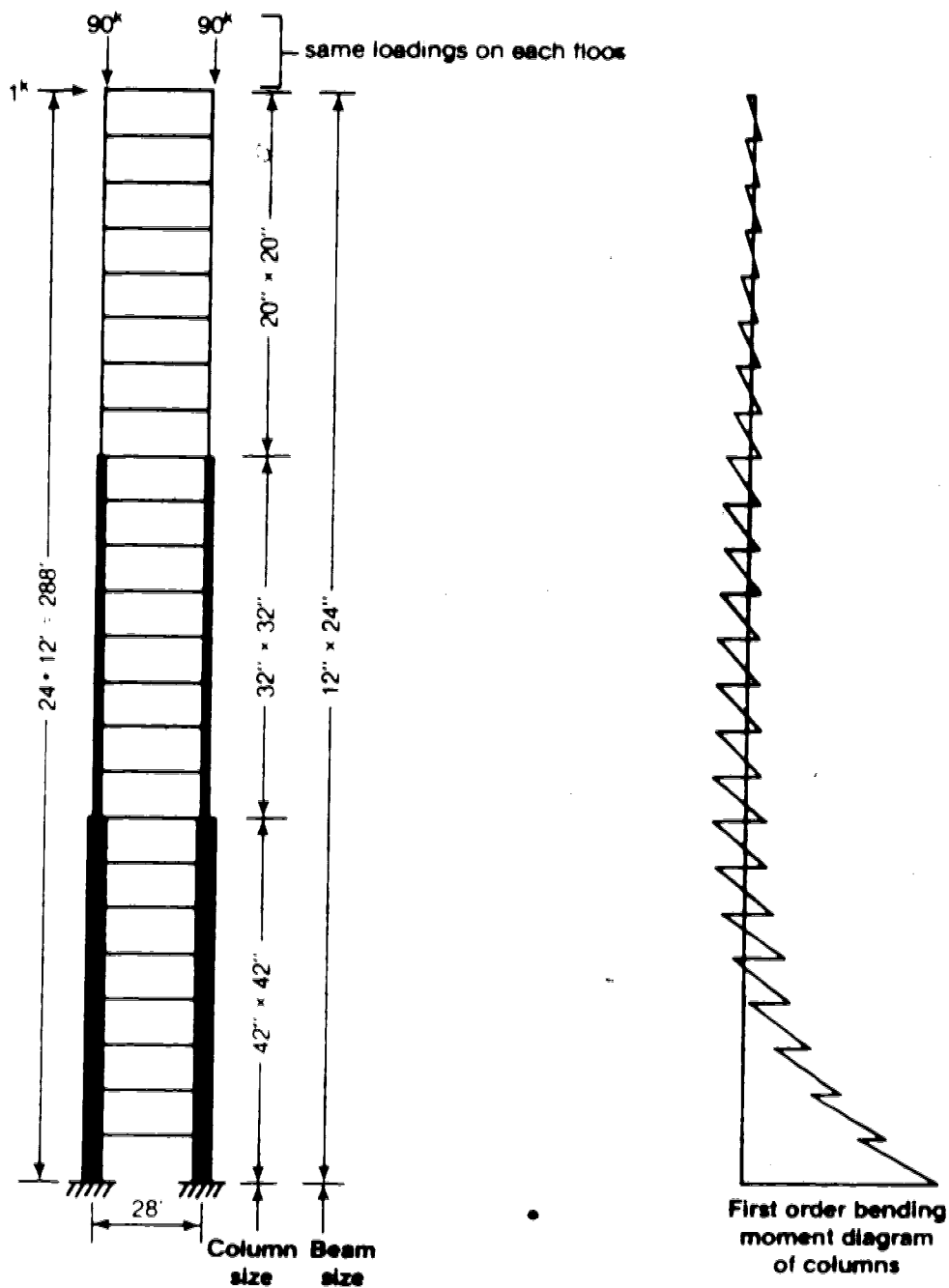


Fig. 7.13 Structure E: A frame with very strong columns (weak beams) at the bottom

7.4.2 Results

In all cases the average flexibility factor $\bar{\gamma}$ has been taken equal to 1.05 in the approximate methods in these comparisons, except that $\bar{\gamma} = 1.20$ was used in the bottom storey in the storey magnifier method to recognize the fixed base of the columns.

The results for structure A are shown in Fig. 7.14. The bounds of M_1/M_{01} , which are not shown in the figure, are similar to those of M_2/M_{02} shown in the figure. Similarly, a/a_0 also follows closely with M_2/M_{02} . It is apparent from Fig. 7.14 that the storey magnifier method produces very good results. The ACI method also gives good results except at discontinuities such as at the bottom storey, and at the storeys where the column stiffness changes abruptly. The discrepancies, obviously, are due to violation of the assumption regarding the vertical relationship made in the ACI method. The frame magnifier and overturning moment methods are unacceptable in this case.

The results for the frame in structure B are shown in Fig. 7.15. The values of M_1/M_{01} , which are not shown in the figure, are similar to those of M_2/M_{02} . From Fig. 7.15 it can be seen that the values of a/a_0 are very close in all the storeys. The overall magnifier given by the frame magnifier method or the overturning moment method agree very well with the exact solutions. The storey magnifier method does not give good results. The ACI procedure

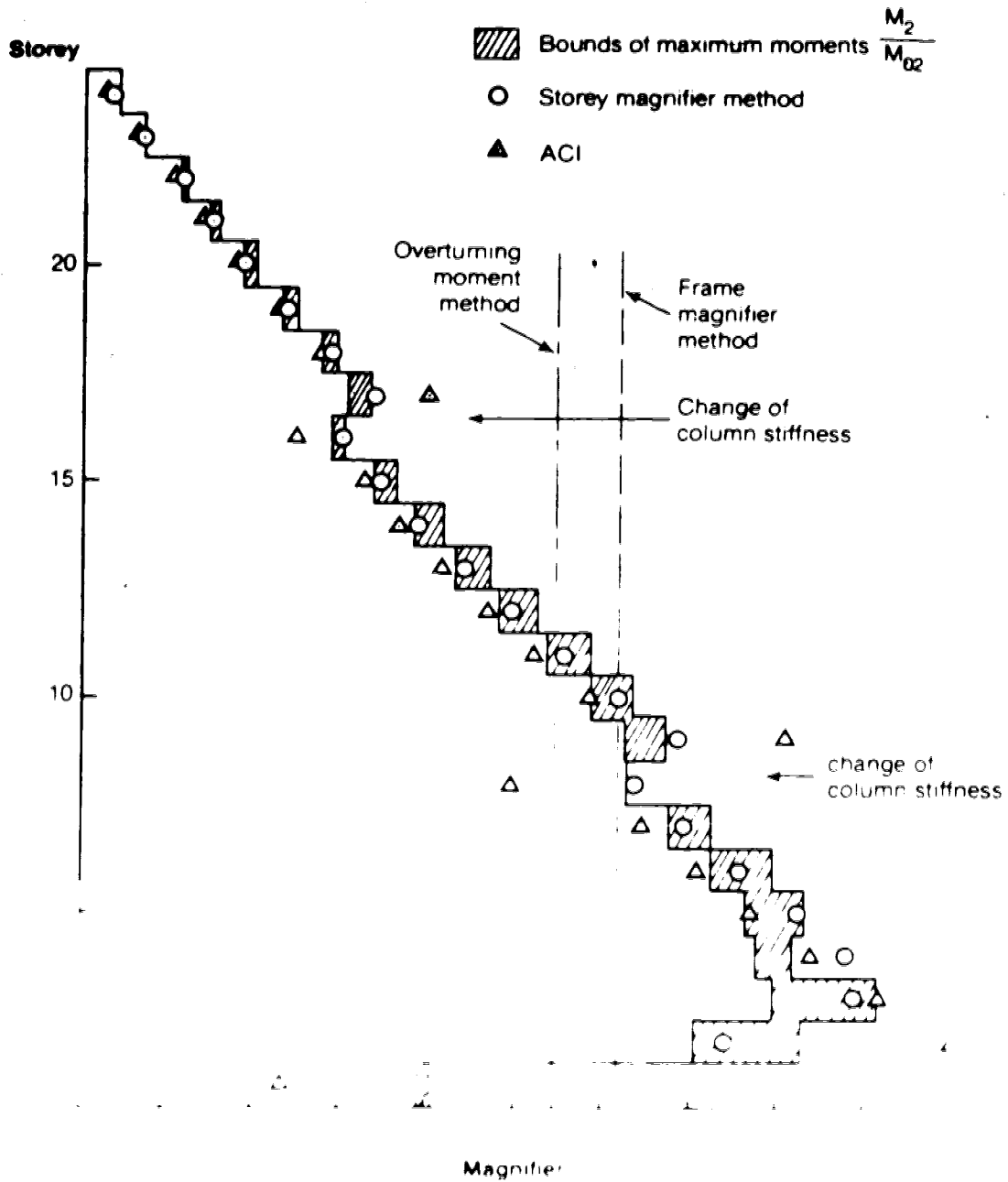


Fig. 11.4 Approximate vs. exact solution for storey magnifier

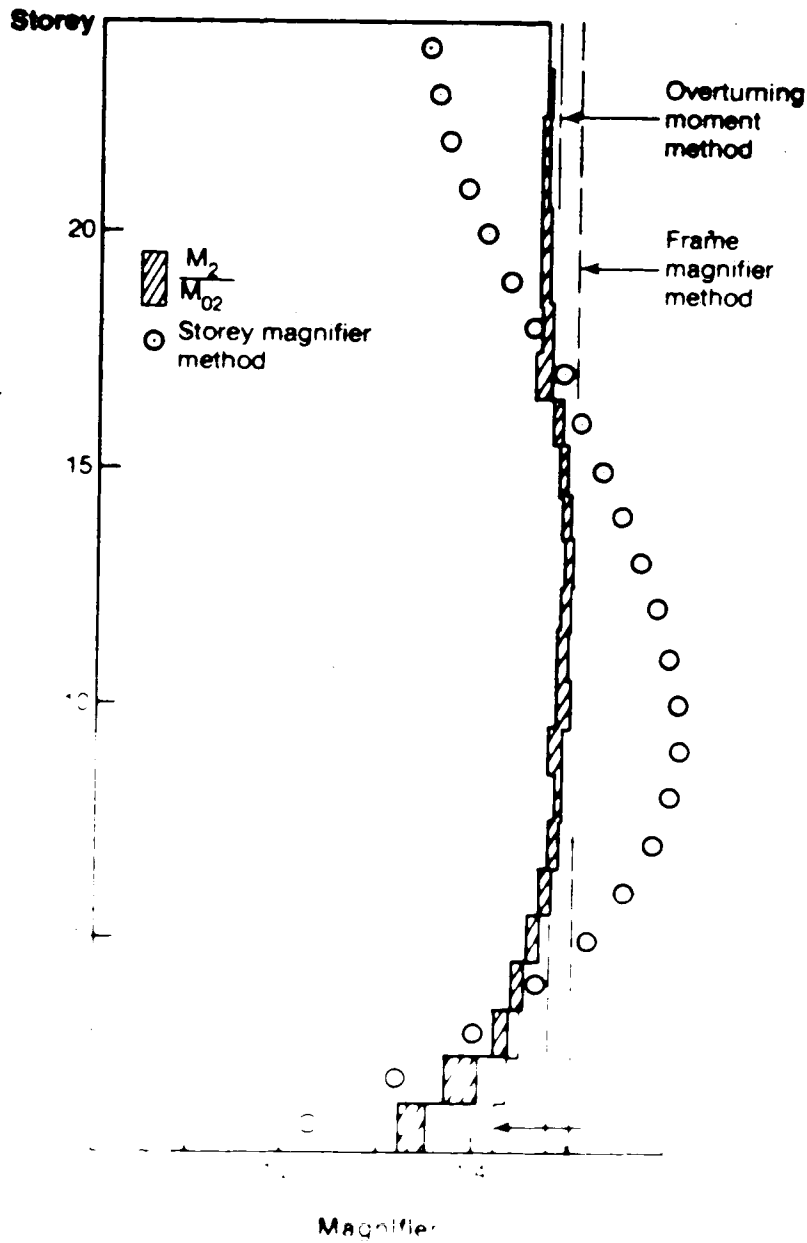


Fig. 15 Approximate vs. exact solutions for the frame magnifier method. Structure B.

The bending moments in the shear wall of structure B are shown in Fig. 7.16. In this figure ΣM_H is the sum of the overturning moments of the lateral loads about the base of the structure. The results predicted by the frame magnifier method (or the overturning moment method) agree sufficiently well with the exact solutions. The accuracy of the storey magnifier method is good except at the bottom levels at which the bending moments are largest.

For structure C, the results from the approximate analyses are compared with the exact a/a_0 in Fig. 7.17. The values of a/a_0 are also considered representative of the moments in the columns and in the shear wall. Similar to the observations for structure B, the frame magnifier method or the overturning moment method gives acceptable results, while the storey magnifier method gives less accurate results.

The results for structure D are shown in Fig. 7.18. For the upper part of the structure which does not have the shear wall, the storey magnifier method gives very good results. For the lower part which is attached to the shear wall, the frame magnifier or overturning moment method gives better estimates.

The results for structure E are shown in Fig. 7.19. For the upper storeys where the columns are bent in single curvature, the storey magnifier method is quite accurate. For the lower part where the columns are bent in double curvature, the frame magnifier method gives better estimates.

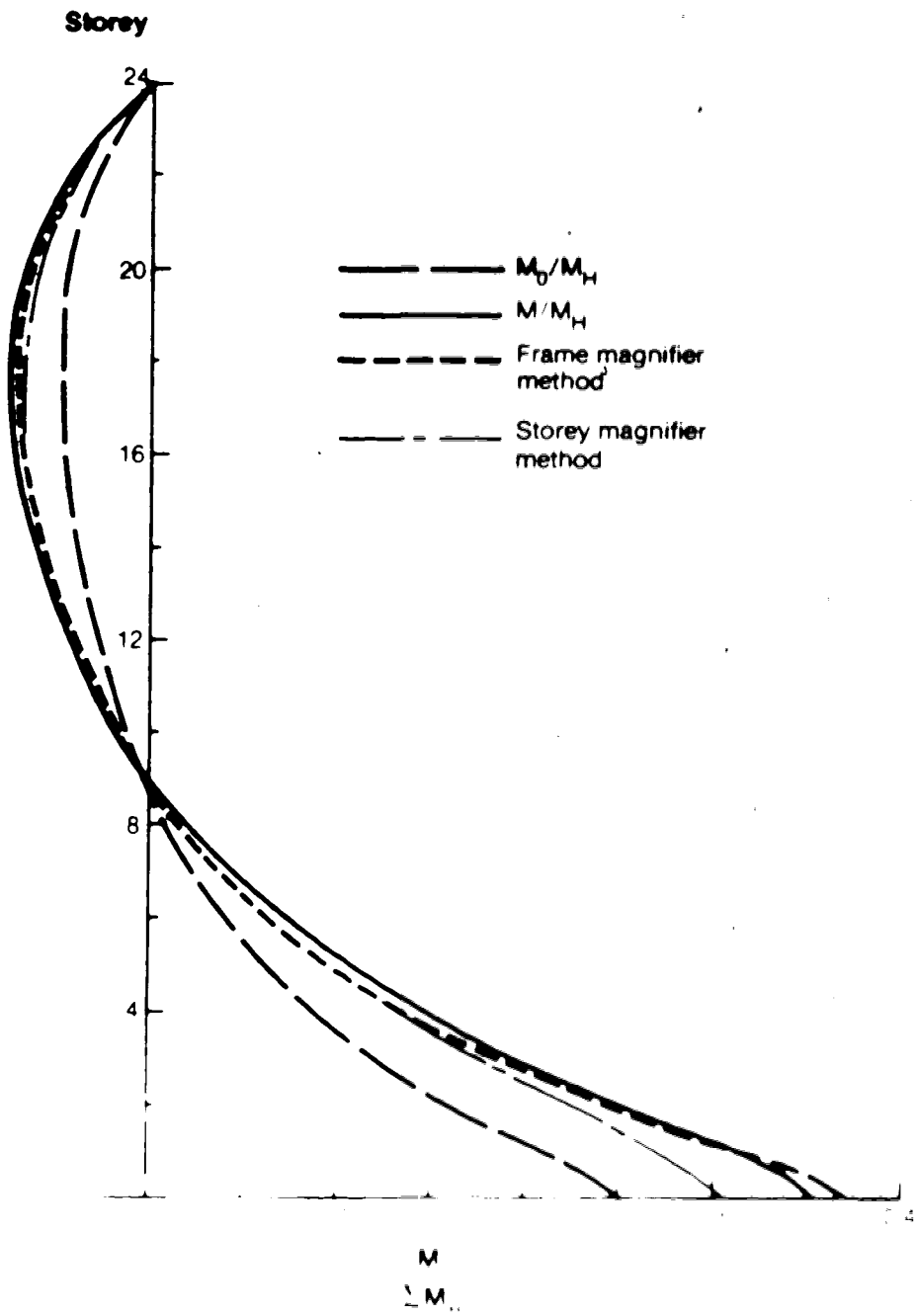


Fig. 10. Bending moments in the steel wall of structure B

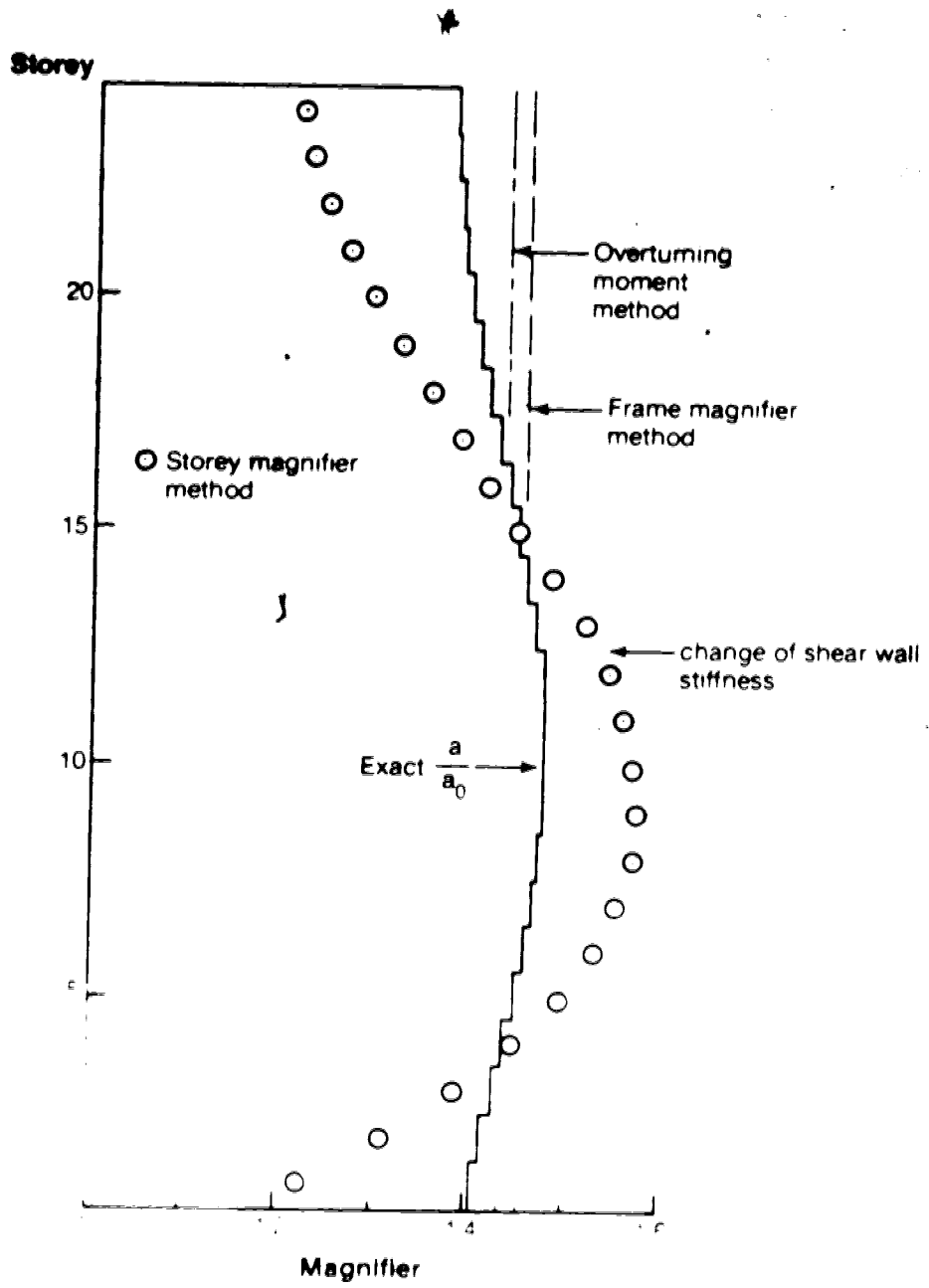


Fig. 7.17 Approximate vs. exact solutions for Structure

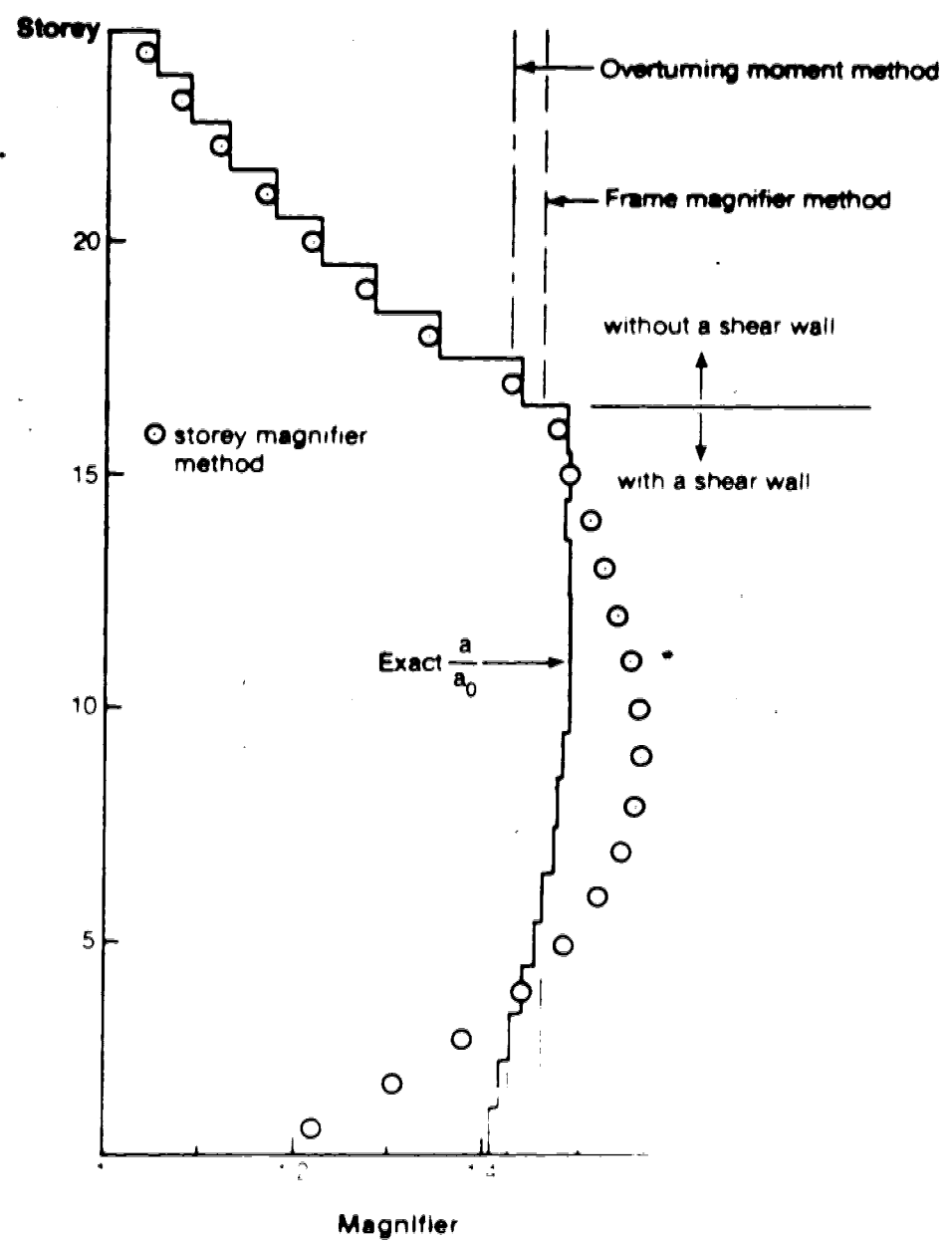


Fig. 7.18 Approximate vs. exact solutions for structures

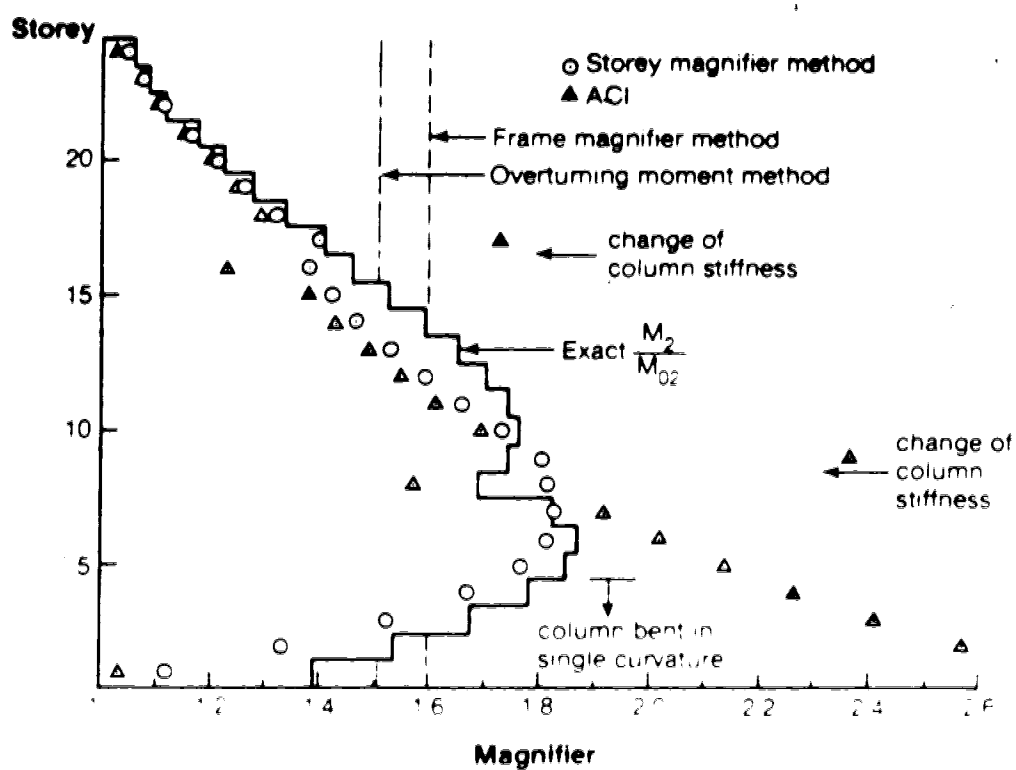


Fig 7.19 Approximate vs. exact solutions for Structure E

points occur within each storey, the storey magnifier method gives reasonable results. The ACI method errs considerably at the storeys where the column stiffness changes. The frame magnifier or overturning moment method is not acceptable for this case.

7.4.3 Concluding remarks

Two specific conclusions can be drawn from the above study for high-rise structures subject to $f_g < 1.5$:

1. If an inflection point exists at or between the ends of each column in a given storey, the storey magnifier method may be used for that storey.
2. For a structure with a distinct shear wall extending from the base to the top of the structure, the frame magnifier method or the overturning moment method may be used.

It is apparent that the above two conclusions are very similar to those made in Sect. 7.3.4 for low-rise structures.

The term 'distinct shear wall' is mentioned above in Sect. 7.3.4. A distinct shear wall is defined here as a vertical element which has only one point of contraflexure (Fig. 7.16). It also includes the case where there is no point of contraflexure (Fig. 7.3(c)). The term 'distinct shear wall' is not related to the storey

magnifier, frame magnifier, overturning moment and ACI methods can give generally good results.

7.5 Proposed methods

The proposed methods and the corresponding conditions are as follows:

1. If an inflection point occurs at or between the ends of each column in every storey of the structure, the storey magnifier method may be used provided the maximum value of f_g in the structure is less than 1.5.
2. For a structure with a distinct shear wall extending from the base to the top of the structure, the frame magnifier may be used provided f_g is less than 1.5.
3. For conditions different from the above, the modified iterative method or modified negative trace method should be used.

It is noted that the moment-correction factors are included in the methods. The reasons that the frame magnifier method, rather than the overturning moment method, is suggested to be used are the wider applicability of the frame magnifier method, the overturning moment method can be applied only to structures with unequal column heights and the latter method is generally better accurate.

chapter, the storey magnifier method can also be used for this type of structures provided the conditions stated in the above point 1 plus the condition that the sway deflections due to the axial deformations of the columns are insignificant relative to the flexural deflections are satisfied. In the case that the sway deflections induced by axial deformations of the columns are dominant (commonly called cantilever action), the storey magnifier method, which assumes that each storey behaves independently of other storeys, may not be applicable because the increase in the axial forces in the bracing elements in one storey due to the geometric effects will increase the axial deformations of the columns in the other storeys. If cantilever action dominates, the modified iterative method or modified negative brace method should be used and the effect of axial deformations should be included in the analysis.

8. PROCEDURES FOR SECOND-ORDER ELASTIC ANALYSIS

8.1 Introduction

Once sway moments and non-sway moments have been computed in a frame, they must be combined before the columns can be designed. The major difficulty arises from the fact that the column end-moments in the non-sway frame are not exactly known (Sect. 4.5.3). A rational method, which is more accurate than the current design approaches, will be proposed in this chapter. The effects of deflections due to gravity load moments and out-of-plumb construction will be included in the second-order analysis in a practical way. The balance of this chapter summarizes the findings and observations from this study in the form of step-by-step procedures for second-order analysis, and proposes modifications to the current ACI Code (1977) procedure if the current effective length approach is desired to be retained.

8.2 Combination of non-sway and sway moments

8.2.1 Current approaches

Basically, there are three current approaches of combining the non-sway and sway moments. The first approach is the one recommended in the current ACI (1977) or AISI code. The maximum moment, M_{max} , in a column is

$$M_{\max} = f_s \cdot (M_{0ns} + M_{0s})_2 \quad (8.1)$$

where f_s is the sway magnifier, M_{0ns} is the first-order end-moment of the column from the non-sway analysis, and M_{0s} is the first-order end-moment from the sway analysis. Note that the summation of the two end-moments is performed at each end of the column and the numerically larger value of the two ends, denoted by the subscript 2, is used. This, obviously, is not a rational approach because the sway magnifier is only applicable for M_{0s} (Chap. 6).

The second approach, suggested by Gouwens (1976), is to combine directly the non-sway maximum moment, $M_{ns,max}$, and the sway maximum moment, $M_{s,max}$, of a given column, namely:

$$M_{\max} = M_{ns,max} + M_{s,max} \quad (8.2)$$

This is a conservative approach since the summation of the two maximum values must be greater than or equal to the actual maximum moment. The same approach is suggested by Ford, et al. (1981) for reinforced concrete columns. This approach, however, may be overconservative in certain cases when the two maximum moments occur in different sections and the two values are comparable. This will be demonstrated in Sect. 8.2.2.

The third approach is based on the assumption that C and S effects can be neglected. As a result of this assumption, the non-sway end-moments are equal to the first-

order values. The sway end-moments can be obtained from the approximate methods of sway analysis by considering the flexibility factor and the moment-correction factors all equal to 1.0. This simplification is consistent with the assumption that the C and S effects can be neglected. Consequently, the end-moments of the non-sway and sway frames can be added algebraically at each end of the column. Once this is done, the maximum moment in the column with the known end-moments can be determined as in a pin-ended column (Sect. 4.5.2). This approach can be expressed as:

$$M_{\max} = \delta \cdot (M_{0ns} + f_{s1} M_{0s})^2 \quad (8.3)$$

where $f_{s1} M_{0s}$ is the end-moment from the approximate method of second-order analysis for sway frames and the subscript 1 refers to $\gamma = 1.0$. The term δ is the moment magnifier for a pin-ended column, and can be determined according to Eq. 4.2 with M_0 equal to the sum of M_{0ns} and $f_{s1} M_{0s}$. This approach appears to be first mentioned by Iffland (1972) for use with the iterative method (Sect. 6.1). MacGregor and Hage (1977) also adopted this approach for use with other approximate methods of second-order analysis.

According to the principle of superposition that the load effects should be superimposed at the same section, the third approach (Eq. 8.3) is more rational than the second one (Eq. 8.2). Nevertheless, the second approach can take

into account the C and S effects, which the third approach cannot. The approach proposed in the next section is similar to the third one, satisfying the principle of superposition, while an attempt will be made to include the C and S effects.

8.2.2 Proposed approach

A method of combining the non-sway and sway moments is developed schematically in Fig. 8.1. This procedure is conceptually similar to that shown in Fig. 6.15 in deriving the moment-correction factors. A frame subjected to external moments, lateral loads and column axial forces is shown in Fig. 8.1(a). In Fig. 8.1(b) the same frame, subjected to external moments only, is braced against sway with lateral deformations, a , equal to those in the original state of loading (Fig. 8.1(a)). This frame can be decomposed into a non-sway frame subjected to external moments and a laterally deformed non-sway frame with forced deformations a , as shown in Fig. 8.1(c). Therefore, it can be seen that the column end-moment of the frame in Fig. 8.1(b) is equal to the sum of M_{0ns} and M_d . The term M_d is the same as in Fig. 6.15, and therefore it can be obtained from the modified iterative method or the modified negative moment method. For other second-order analysis methods which use the deflection magnifier f_s , M_d is assumed equal to $f_s M_{0ns}$. See Fig. 8.4. Since the frame in Fig. 8.1(b) is

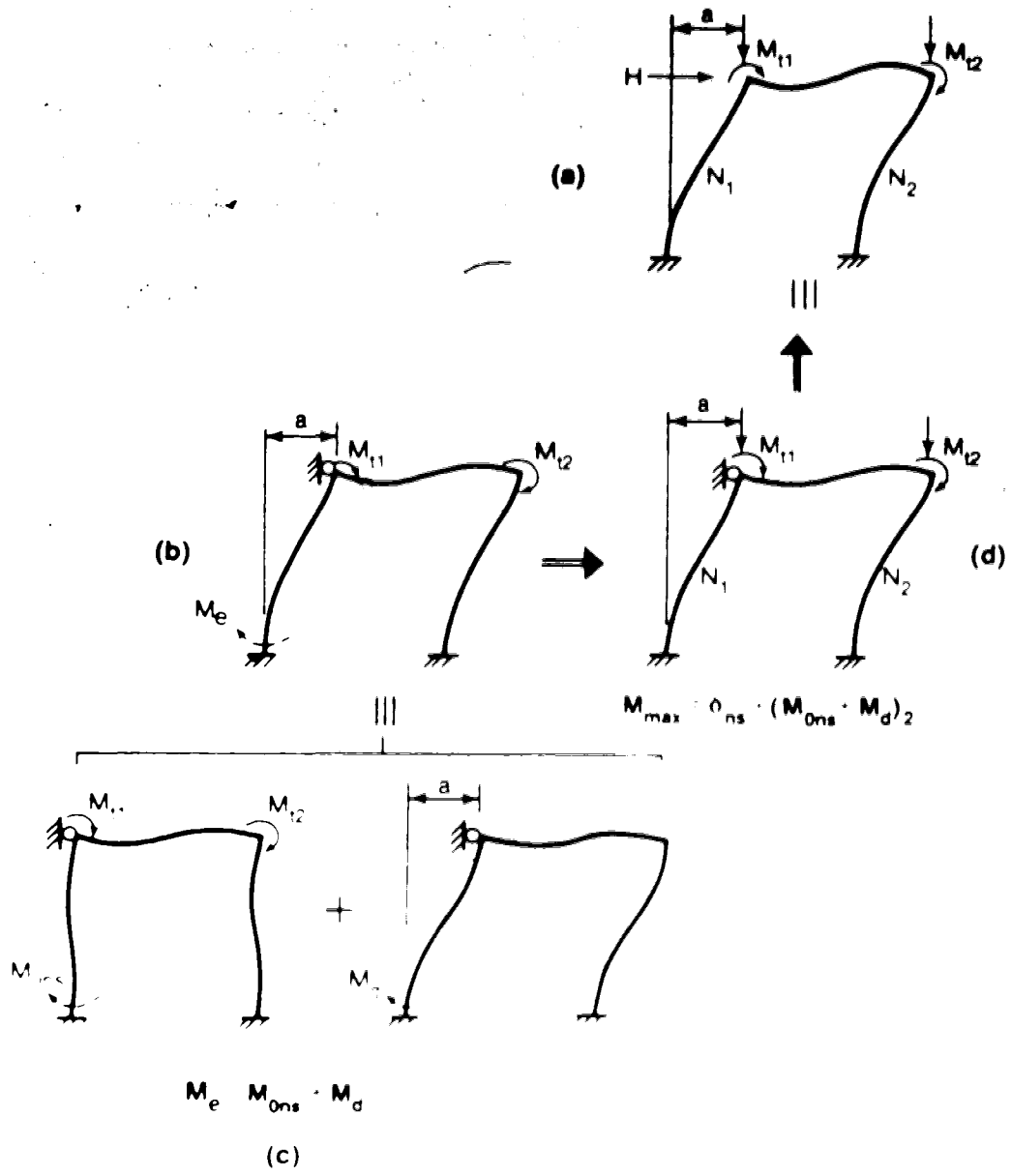


Fig. 8.1 Schematic development of the proposed approach for combining the non-sway and sway moments

7.5), the general term M_0 will be replaced by $f_s M_0$ which corresponds to the definition of the moments from the modified iterative method or negative brace method. When the frame in Fig. 8.1(b) is subjected to the column axial forces (Fig. 8.1(d)), the resulting load effects are identical with those in the original state of loading. Therefore, it can be seen that the maximum moment M_{\max} in a column can be given by:

$$M_{\max} = \delta_{ns} \cdot (M_{0ns} + f_s M_{0s})_2 \quad (8.4)$$

where δ_{ns} is the moment magnifier for the restrained non-sway column with given first-order end-moments. The approximate formula for δ_{ns} suggested in Sect. 4.5.4 (Eq. 4.27) is used here with M_0 equal to the sum of M_{0ns} and $f_s M_{0s}$. Note that the summation is performed separately at each end of the column and the numerically larger value for the two ends (denoted by the subscript 2 in Eq. 8.4) is multiplied by δ_{ns} .

Retically, the approach developed in the above is no assumptions other than those required in the approximate methods for the analysis of non-sway and sway frames. In other words, if δ_{ns} and $f_s M_{0s}$ were exact in non-sway and sway analysis, respectively, the value of M_{\max} given by Eq. 8.4 would also be exact. From Chapter 4, it is known that the proposed method for the analysis of non-sway and sway frames is an approximate analysis. As a result, the value of M_{\max} given by Eq. 8.4 is also an approximate value.

conservative. This is the major source of errors in this approach, and will be discussed in the following paragraphs for two cases. First, the limiting case of M_{0ns} equal to zero is considered. Second, an intermediate case with M_{0ns} equal to M_{0s} is studied. It should be noted that the limiting case of M_{0s} equal to zero has been discussed in detail in Chapters 3 and 4.

When M_{0ns} is equal to zero, δ_{ns} theoretically should be equal to the moment-correction factor B_{max} defined in Sect. 6.8.3. Compared with B_{max} given by Eqs. 6.53 to 6.56, δ_{ns} errs on the conservative side because δ_{ns} is always equal to or greater than 1.0 while B_{max} is less than 1.0 in some cases. On the other hand, δ_{ns} is simpler to calculate than B_{max} . In the same manner as B_{max} , δ_{ns} takes into account the possibility that the maximum moment may occur away from the end for a heavily loaded column. Note that end-rotational restraints of the beams implied in δ_{ns} is $2EI_B/L_B$. This has been shown to be a desirable assumption for a heavily loaded column in Sect. 6.8.4.

For the case of M_{0ns} equal to M_{0s} , the proposed approach is examined with the help of an example shown in Fig. 6.17. The example is intended to represent a typical interior column in a large multistorey frame. The column is symmetrically restrained with end-restraints defined by $3EI_B/L_B$ in the non-sway analysis and $6EI_B/L_B$ in the sway analysis. The column is loaded in the z -direction. The non-sway analysis is based on the usual structural analysis method. The sway analysis is based on the usual structural analysis method. The column is

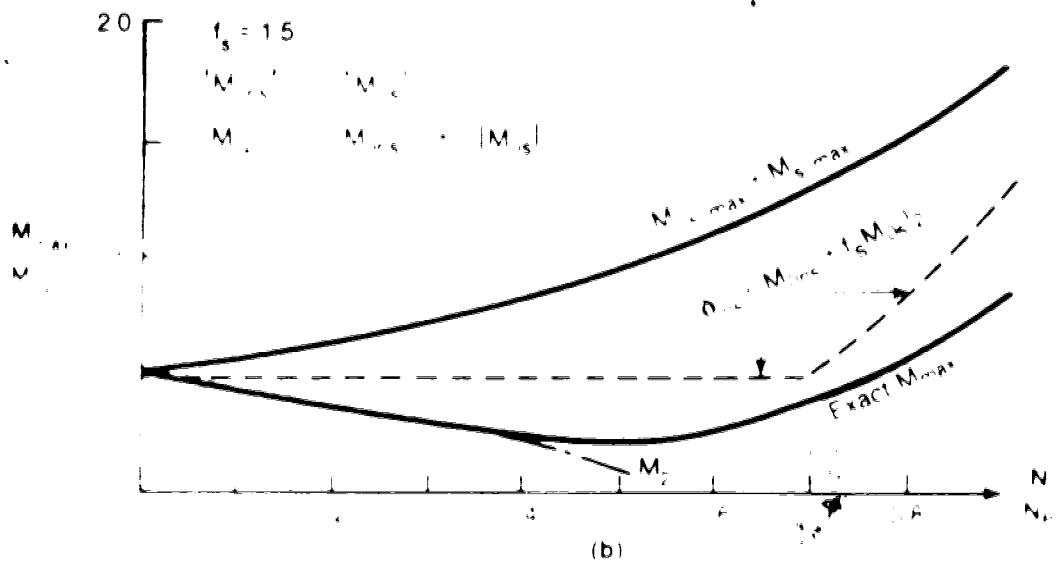
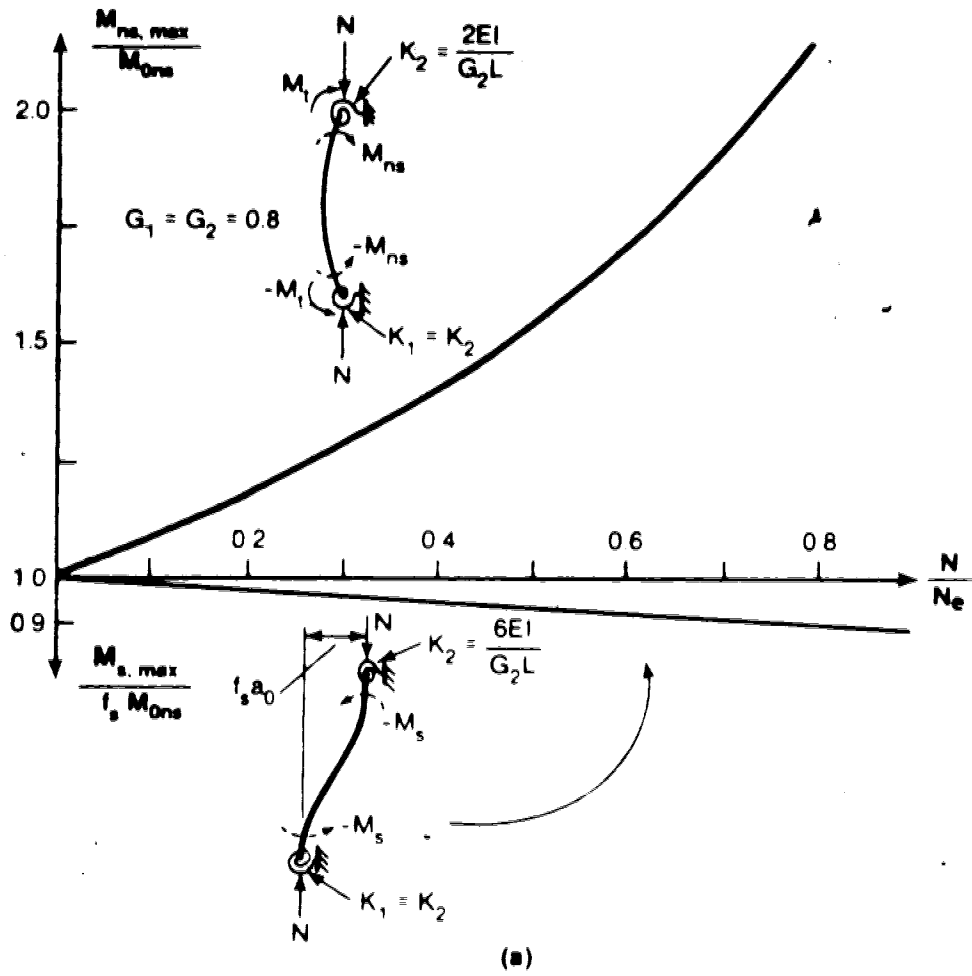


Fig 8.2 Combination of the non sway and sway moments

moments, and therefore the maximum non-sway moment always occurs at mid-height. The maximum non-sway moment $M_{ns,max}$, which is non-dimensionalized by dividing by the first-order end-moment M_{0ns} , is plotted in Fig. 8.2(a) as a function of the column axial force. Using the same concept as in the moment-correction factors (Sect. 6.8.3), the ratio $M_{s,max}/f_s M_{0s}$ for the sway column is also shown in Fig. 8.2(a). For the range of axial forces considered, the maximum moment $M_{s,max}$ occurs at the end.

In Fig. 8.2(b), the results of combining the non-sway and sway moments are presented for $M_{0ns} = M_{0s}$. The sway magnifier f_s is kept equal to a constant value of 1.5 as the axial force increases. This implies that the column sway deflection is held constant as N/N_e varies as was done in Sect. 5.2.2. From Fig. 8.2(a), it can be seen that the non-sway moment magnification ranges from 1.0 to about 2.5. The results from the direct combination of the non-sway and sway maximum moments (Eq. 8.2) and the proposed approach (Eq. 8.4) are compared with the exact maximum of the combined moments, M_{max} , in Fig. 8.2(b). Initially, the maximum moment decreases as the axial force increases although the non-sway maximum moment increases from the outset. This is because the maximum of the combined moment still occurs at the end, even though the non-sway end-moment M_{ns} is diminished by the axial force. With further increase in the axial force, the maximum moment shifts to the increase in the axial force, the maximum moment is found to be $M_{max} = M_{0ns} + M_{0s}$.

shown in Fig. 8.2(b) where M_{\max} departs from M_2 . Thereafter, the maximum moment increases. This whole process is completely ignored by the direct combination of the non-sway and sway maximum moments, which is extremely conservative for this case. The proposed approach, which theoretically takes into account this process, gives much better results, although it too tends to be conservative at certain values of the axial force.

As a conclusion, it may be stated that although the proposed approach gives somewhat conservative results, it is more rational and more accurate than the current approaches (Sect. 8.2.2).

8.3 Deflections due to gravity load moments

In Sect. 2.6, where the principle of superposition was discussed, it was shown that the holding forces resulting from the gravity load moments in the non-sway frame (Fig. 2.9) must be added to the actual lateral loads when the sway frame is analyzed. The holding forces are assumed herein to be equal to those from a first-order analysis of the non-sway frame, thereby neglecting the C and S effects. This assumption is based on the normal condition that the internal moments resulting from the holding forces are small compared to the lateral load moments or the gravity load moments. As a result, the error resulting from

Frequently, it is more convenient to perform a first-order analysis for gravity loads without bracing the structure against sidesway. The results of such an analysis can be used in the load superposition by following the procedure described below. For simplicity, this procedure is derived using a single-storey frame, but it can be generalized to apply to multistorey frames.

A single-storey frame, subjected to external moments only, displaces a distance a_{0g} . It is then braced against further sway while the column axial forces are applied, as shown in Fig. 8.3(a). The first-order moments in the resulting non-sway frame are those obtained from a first-order gravity load analysis of the frame without bracing the structure against sway. This frame can be decomposed into the two frames shown in Figs. 8.3(b) and (c). The frame in Fig. 8.3(b) is a non-sway frame, subjected to external moments and column axial forces, with a zero displacement at the joint. The holding force in this frame is denoted by V_1 . The frame in Fig. 8.3(c) is a non-sway frame, subjected to column axial forces, with an imposed displacement of a_{0g} at the joint. The holding force is denoted by \bar{V} . In this way, the holding force V_1 in the original frame (Fig. 8.3(a)) is equal to

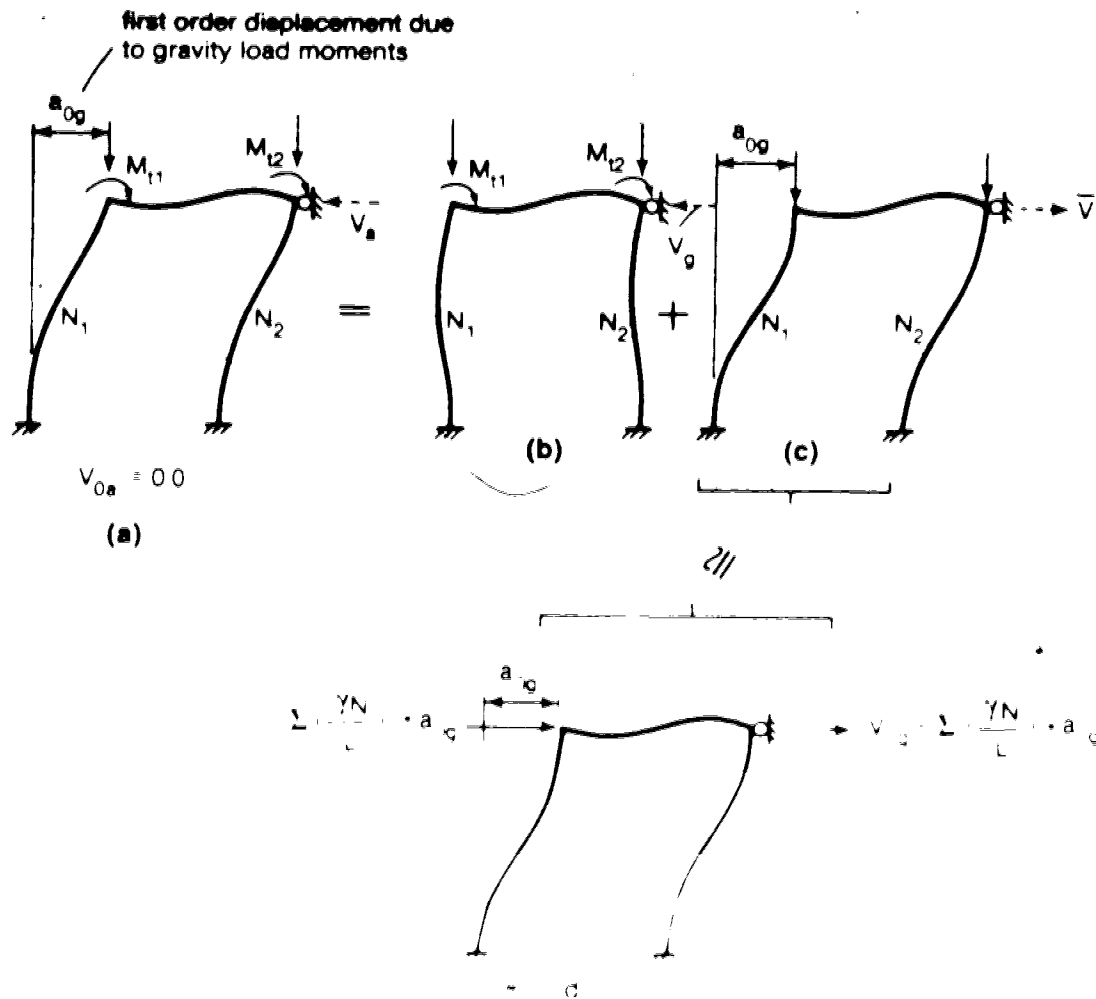


Fig. 4.3. Hiding shears in a non-sway frame with imposed displacements

For the frame shown in Fig. 8.3(c), the column axial forces are assumed to be replaced by a horizontal load equal to $(\Sigma \gamma N/L) a_{0g}$ (Fig. 8.3(d)) where Σ denotes summation for all the columns in the storey. This can be derived based on the same assumption and method as in the modified iterative method (Sect. 6.2) except that a is replaced by a_{0g} . Consequently, the holding force \bar{V} (Fig. 8.3(c)) is assumed equal to:

$$\bar{V} = V_{0g} - \left(\Sigma \frac{\gamma N}{L} \right) a_{0g} \quad (8.6)$$

where V_{0g} is the first-order value of V_g (Fig. 8.3(b)). By substituting Eq. 8.6 into Eq. 8.5 and making the assumption that $V_g = V_{0g}$ as discussed before, V_a is therefore equal to:

$$V_a = \Sigma \frac{\gamma N}{L} a_{0g} \quad (8.7)$$

which is the horizontal force which must be added to the actual lateral loads in the sway analysis. To apply Eq. 8.7 to a multistorey frame, the holding force V_a should be treated as holding shear which is added to the lateral load at the storey in the sway analysis. In other words, the total lateral load at a given floor level is equal to the actual lateral load plus the algebraic sum of the holding shear from the storey above and below the floor. The

In the modified iterative method (Sect. 6.2), the holding shears can be included more conveniently by writing the modified N-a shear $\Sigma \bar{V}_s$ (Eq. 6.8) as:

$$\Sigma \bar{V}_s = \left(\Sigma \gamma \frac{N}{L} \right) \cdot (a + a_{0g}) \quad (8.8)$$

Note that the term 'a' still represents the final value of the deflection of the structure.

In the storey magnifier method (Sect. 6.4), the procedure can be simplified. For a single-storey frame subjected to the lateral load shear plus the modified N-a shear as assumed in the storey magnifier method, the deflection is directly proportional to the horizontal load applied at the joint. Noting this condition, the following relation, based on Eq. 6.33, can be derived:

$$\frac{1}{\Sigma \bar{V}_s} = f_{sH} + (f_{sH} - 1) \frac{a_{0g}}{a} \quad (8.9)$$

$$\frac{1}{\Sigma \bar{V}_s} = \frac{1}{\Sigma V_H} + \frac{1}{\Sigma V_H} (f_{sH} - 1) \frac{a_{0g}}{a}$$

where ΣV_H and $\Sigma \bar{V}_s$ represent the total storey shear and the total storey shear, respectively, caused by the actual lateral loads H only. Similarly, ΣV_H and $\Sigma \bar{V}_s$ in the analysis for the sway frame subjected to the lateral loads H only.

to:

$$f_s M_{Os} = \left[f_{sH} + (f_{sH} - 1) \frac{a_{Og}}{a_{OH}} \right] M_{OH} \quad (8.11)$$

where M_{OH} is the moment from a first-order analysis of the frame subjected to the actual lateral loads H only.

Equation 8.11 is also applicable for the ACI method (Sect. 6.7) except that f_{sH} is equal to f_s given by Eq. 6.45 (or Eq. 6.47).

8.4 Out-of-plumbs

In real structures, the centroid of the top of a column frequently is not directly over the centroid at the other end due to construction errors. In other words, columns are frequently 'out-of-plumb'. As a result, the gravity loads acting through the initially inclined columns generate additional forces within the structure. Although the current ACI Code (1977) does not require consideration of this effect, other design regulations do. Beaulieu and Adams (1977) have done an extensive review and investigation of this area. Based on their work and limited measurement of concrete structures, MacGregor (1979) has proposed a simple design formula for the magnitude of the out-of-plumbs of concrete structures.

For design purposes, all columns in the same storey are normally assumed to lean in the same direction with the same magnitude. Based on this assumption, the

inclusion of the effect of out-of-plumbs in the second-order analysis is derived in the following paragraph.

Assume that fictitious external moments acting at the joints of a structure can produce the prescribed initial out-of-plumbs. It is understood that the first-order moments caused by these fictitious external moments do not exist, and therefore only those caused by the column axial forces acting through the out-of-plumbs are considered. The methodology follows the one for the gravity load deflections (Sect. 8.3). In Fig. 8.3, the term a_{0g} is replaced by a_{0p} which denotes the initial out-of-plumb for any storey. Consequently, the holding shear, which should be added to the lateral load shear in the sway analysis of an initially undeformed structure, is equal to $(\Sigma \gamma N/L)a_{0p}$ for a storey. Note that the real first-order moments in the non-sway frame (Fig. 8.3(a)) with the lateral displacement equal to a_{0p} are equal to zero. The additional moments caused by the column axial forces in the non-sway frame are assumed negligible.

In short, the out-of-plumbs are included in the analysis in the same way as the gravity load deflections. In other words, the term a_{0g} in Sect. 8.3 is simply replaced by $(a_{0g} + a_{0p})$ in the sway analysis.

8.5 Summary of the proposed procedures for second-order analysis

8.5.1 Introductory remarks

This section summarizes the proposed procedures for the second-order analysis of an elastic structure subjected to gravity loads and wind loads. The essential equations will also be repeated. While the approximate second-order analysis is based on the modifications to the first-order analysis, the first-order analysis should include the effects of axial deformations of columns, foundation deformations and where necessary, finite joint widths. The resistance factors (ϕ factors) will not be mentioned in the following procedures, but the ϕ factors should be included in design according to the design regulations.

8.5.2 Storey magnifier method

The storey magnifier method is used subject to two conditions:

1. An inflection point occurs at or between the ends of each column in every storey of the structure when it is subjected to lateral loads.
2. The maximum value of the sway magnifier f_s in the structure is less than 1.5. For this case, f_s is equivalent to f_{sw} which will be defined later.

A second-order analysis based on the storey magnifier involves the following steps:

1. Analyze the structure for gravity loads to compute column end-moments M_{0g} , column axial forces N_{0g} , and relative deflections a_{0g} in each storey.

2. Analyze the structure for wind loads to compute column end-moments M_{0w} , column axial forces N_{0w} , relative deflection a_{0w} in each storey, and the storey shear ΣV_w .
3. Determine the out-of-plumb a_{0p} for each storey.
4. Estimate the deflection magnifier f_{sw} for each storey:

$$f_{sw} = \frac{1}{1 - \frac{(\Sigma \gamma N/L) a_{0w}}{\Sigma V_w}} \quad (8.12)$$

where γ can be conservatively taken as 1.15 or roughly estimated from Table 6.2. If a more precise calculation is necessary, any of the formulae in Table 6.1 can be used. Note that in the case of an inclined bracing element, N is the vertical force component of the axial force in the bracing element (positive for compression), L is the vertical projection of the member length, and γ is equal to 1 for the bracing member. The same definitions are used in the modified iterative method or the modified negative brace method for inclined bracing members.

5. Determine the modified deflection magnifier \bar{f}_s for each storey:

$$\bar{f}_s = f_{sw} + (f_{sw} - 1) \frac{a_{0g} + a_{0p}}{a_{0w}} \quad (8.13)$$

6. Determine the column axial forces N :

$$N = N_{0g} + \bar{F}_s N_{0w} \quad (8.14)$$

If the values of N given by Eq. 8.14 are too different from the estimates of N in the deflection magnifier f_{sw} (Eq. 8.12), go back to step 4 and iterate.

7. Determine the maximum moment M_{max} in each column.

First, by defining:

$$M_{e1} = (M_{0g} + \bar{F}_s M_{0w})_1 \quad (8.15)$$

$$M_{e2} = (M_{0g} + \bar{F}_s M_{0w})_2 \quad (8.16)$$

where subscripts 1 and 2 refer to the individual ends of a column, and M_{e2} is numerically larger than M_{e1} . The maximum moment is then given by:

$$M_{max} = \delta_{ns} M_{e2} \quad (8.17)$$

where

$$\delta_{ns} = \frac{1 + 0.25\alpha_{ns}}{1 - \alpha_{ns}} C_m > 1.0 \quad (8.18)$$

$$C_m = 0.6 + 0.4 r_e > 0.4 \quad (8.19)$$

$$r_e = - \frac{M_{e1}}{M_{e2}}$$

$$\alpha_{ns} = \frac{N}{N_{ns}}$$

$$N_{ns} = \frac{\pi^2 EI}{(k_{ns} L)^2}$$

and the effective length factor k_{ns} is the lesser of:

$$k_{ns} = 0.7 + 0.05 (G_1 + G_2) < 1.0 \quad (8.20)$$

$$k_{ns} = 0.85 + 0.05 G_s < 1.0$$

where G_s is the smaller of G_1 and G_2 . Note that if the far end of the beam that is framed into the column under consideration is hinged or fixed, the beam length should be multiplied by 2/3 or 0.5, respectively, when calculating the corresponding value of G .

8. Magnify the wind load moments in the beams to equilibrate the column end-moments, M_s , given by:

$$M_{s1} = B_1 \bar{F}_s M_{Ow1} \quad (8.21)$$

$$M_{s2} = B_2 \bar{F}_s M_{Ow2} \quad (8.22)$$

where B_1 and B_2 can be conservatively taken as 1.0

or the values given by Eq. 6.65 (with g_2 given by Eq. 6.56) and Eq. 6.66, respectively, with ϕ replaced by G . Note that M_{0w2} is numerically larger than M_{0w1} for a given column.

9. The relative deflection, a , of any storey is equal to:

$$a = a_{0g} + \bar{f}_s a_{0w} \quad (8.23)$$

10. If the structure includes inclined bracing elements, the axial force F in a given bracing element is equal to:

$$F = F_{0g} + \bar{f}_s F_{0w} \quad (8.24)$$

where F_{0g} and F_{0w} are the values from the gravity load analysis (step 1) and wind load analysis (step 2), respectively.

11. Because of different load factors, it is often necessary to consider the loading case involving gravity loads only. With due attention to the difference in load factors, the steps in this case follow essentially the same as above, except the modified deflection magnifier \bar{f}_s which should be written as:

$$\bar{f}_s = (f_{sw} - 1) \frac{a_{0g} + a_{0p}}{a_{0w}} \quad (8.25)$$

Note that the wind load effects, M_{0w} , ΣV_w and a_{0w} , which are available from the wind load analysis (step 2), are fictitious for this case.

8.5.3 Frame magnifier method

The frame magnifier method is used subject to two conditions:

1. The structure includes a distinct shear wall extending from the base to the top of the structure.
2. The sway magnifier f_s is less than 1.5.

A second-order analysis based on the frame magnifier method involves the following steps:

1. Follow steps 1 and 3 in the storey magnifier method.
2. Analyze the structure for wind loads plus the horizontal forces H_a given by:

$$H_{ai} = V_{a,i} - V_{a,i+1} \quad (8.26)$$

where

$$V_a = \left(\Sigma \frac{YN}{L} \right) (a_{0g} + a_{0p})$$

The subscript i refers to floor level for H_a and storey level for V_a . The storey below floor i is storey i . From this analysis, the column end-

moments M_{0s} , column axial forces N_{0s} , relative deflections a_{0s} in each storey, and the storey shear ΣV_s can be obtained.

3. Estimate the overall magnifier f_s :

$$f_s = \frac{1}{1 - \frac{\sum_{i=1}^n (\Sigma \gamma N/L)_i a_{0si}^2}{\sum_{i=1}^n (\Sigma V_s)_i a_{0si}}} \quad (8.27)$$

where n is the total number of storeys in the structure.

4. Follow steps 6, 7, 8 and 9 in the storey magnifier method with \bar{f}_s replaced by f_s and subscript w replaced by s . Note that in step 8, the wind load moments should be replaced by the lateral load moments.
5. For the loading case involving gravity loads only, follow the same procedure as above except that the wind loads are neglected in step 2.

8.5.4 Modified iterative method

The modified iterative method (or the modified negative brace method, which gives essentially the same results) is recommended, when the structure cannot be handled by the storey magnifier method or the frame magnifier method.

A second-order analysis based on the modified iterative method involves the following steps:

1. Follow steps 1 and 3 in the storey magnifier method.
2. Analyze the structures for wind loads plus the sway forces H_s given by:

$$H_{si} = \bar{V}_{s,i} - \bar{V}_{s,i+1} \quad (8.28)$$

where

$$\bar{V}_s = \left(\sum \frac{YN}{L} \right) (a_s + a_{0g} + a_{0p})$$

where a_s is the storey deflection from the previous iteration. In the first iteration, a_s is equal to a_{0s} which is the storey deflection produced by the wind loads plus the sway forces H_s (Eq. 8.28) in which the values of a_s are equal to zero. The analysis is iterative until the values of a_s are converged. From the final iteration, the column end-moments M_d , the column axial forces N_s and others can be obtained.

3. Follow steps 6 and 7 in the storey magnifier method with $\bar{F}_s N_{0w}$ replaced by N_s , and $\bar{F}_s M_{0w}$ replaced by M_d .
4. The column end-moments in the sway frame are equal to:

$$M_{s1} = B_1 M_{d1} \quad (8.29)$$

$$M_{s2} = B_2 M_{d2} \quad (8.30)$$

which are basically the same as Eqs. 8.21 and 8.22. If B_1 and B_2 are taken as 1.0, the end-moments in the beams are equal to those from the analysis in step 2. If more economical values of B_1 and B_2 are used (Eqs. 6.65 and 6.66), the moments in the beams (from step 2) can be reduced accordingly.

5. The deflections of the structure and the axial forces in the inclined bracing elements (if any) can be obtained from the direct superposition of values from the gravity load analysis and the horizontal load analysis in step 2.
6. For the loading case involving gravity loads only, follow the same steps as above except that the wind loads are neglected in step 2.

8.5.5 Modified negative brace method

The modified negative brace method is an alternative to the modified iterative method. A second-order analysis based on this method follows the same steps as given for the modified iterative method except step 2 which should be changed to:

2. Analyze the structure with an inserted diagonal brace of negative AE given by Eq. 6.29 (Sect. 6.5) in each storey for wind loads plus the horizontal

forces H_a given by Eq. 8.26. The column end-moments M_d , the column axial forces N_g and others are obtained from the analysis.

8.6 Proposed modifications to the ACI method

If the effective length approach for the design of slender columns is retained, the modifications to the current ACI Code (1977) procedure proposed in this section are desirable. In addition, the definitions of 'braced' frames and 'unbraced' frames, necessary in the effective length approach, will be discussed. The resistance factors for slender columns will not be considered here but they should be included properly in design.

8.6.1 Modified formulae

The maximum moment M_{max} in a column is determined by:

$$M_{max} = \delta_{ns} M_{e2} \quad (8.31)$$

where δ_{ns} is a function of M_{e1} , M_{e2} and others, as given by Eqs. 8.18 to 8.20, and

$$M_{e1} = (M_{0g} + \bar{F}_s M_{OH})_1 \quad (8.32)$$

$$M_{e2} = (M_{0g} + \bar{F}_s M_{OH})_2 \quad (8.33)$$

The term M_{0g} is the first-order column end-moment due to

gravity loads, and M_{OH} is the first-order column end-moment due to applied lateral loads such as wind loads. The subscripts 1 and 2 refer to the individual ends of the column. In other words, in each case the summation is carried out at the same section of the column. Note that by definition M_{e2} is numerically larger than M_{e1} .

For a 'braced' frame, defined later, the value of \bar{f}_s is assumed equal to 1.0. In most cases, M_{OH} is assumed negligible for the 'slender columns in the analysis of a braced frame, but this is not necessarily so.

For an 'unbraced' frame, defined later, the value of \bar{f}_s should be determined by:

$$\bar{f}_s = f_s + (f_s - 1) \frac{a_{0g} + a_{0p}}{a_{0H}} \quad (8.34)$$

where

$$f_s = \frac{1}{1 - \frac{\Sigma N}{\Sigma N_{fs}}} \quad (8.35)$$

and k_{fs} is the free-to-sway effective length factor, which is a function of G_1 and G_2 , available from the conventional alignment chart in the ACI Commentary. The approximate formulae for k_{fs} given in the ACI Commentary (1977) can also be used. If the far end of a beam framed into the column

under consideration is hinged or fixed, the beam length should be multiplied by 2 or 1.5, respectively, when calculating the corresponding value of G . The sign Σ denotes summation for all columns in a storey. The term a_{0g} is the first-order relative lateral deflection of the storey due to the gravity loads, a_{0p} is the assumed initial out-of-plumb of the storey, and a_{0H} is the first-order relative lateral deflection of the storey due to the applied lateral loads. Frequently, the second term in Eq. 8.34 is small enough to be neglected when compared to the first term, and therefore \bar{f}_s can be assumed equal to f_s . Nevertheless, it is felt that such simplification should be left to the designer's judgement.

In the case of a structure with different column heights in the bottom storey, the value of f_s for the bottom storey should be determined by:

$$f_s = \frac{1}{1 - \frac{\Sigma N/L}{\Sigma N_{f_s}/L}} \quad (8.36)$$

For the loading case involving gravity loads only, the value of \bar{f}_s given by Eq. 8.34 becomes:

$$\bar{f}_s = (f_s - 1) \frac{a_{0g} + a_{0p}}{a_{0H}} \quad (8.37)$$

Note that the wind load effects, M_{0H} and a_{0H} , which can be obtained from the routine lateral load analysis, are not included here.

8.6.2 Definitions of braced frames and unbraced frames

In the effective length approach for sway frames (Eq. 8.35) it is necessary to be able to distinguish between 'braced' frames and 'unbraced' frames. This is elaborated in the following.

Braced frames

Literally, a braced frame must include some type of bracing elements. As indicated in Sect. 6.7, the effective length approach for sway frames is inadequate to handle a frame with bracing elements. Consequently, for this type of frame, it is necessary that the sway deflections due to the geometric effects are negligible. In other words, the deflection magnifier f_g must be close to 1.0. It should be noted that f_g can never be equal to 1.0 except when the structure cannot sway under the action of external loads, or when the columns do not carry any loads. These cases, of course, rarely occur in actual structures. Nevertheless, it is a common practice that a 5% tolerance in moments is acceptable, and based on this a structure is assumed to be a 'braced' structure when f_g is less than 1.05.

Two types of bracing elements are considered separately to derive a parameter that is used to limit $f_g < 1.05$. The first type is a distinct shear wall extending from the base to the top of the structure. The second type is truss elements which are assumed pin-ended. Based on the frame magnifier method (Eq. 8.27), which is applicable for a

structure with a shear wall, a stability index Q_s for a shear-wall structure is defined:

$$Q_s = \frac{\sum_{i=1}^n (\Sigma N/L)_i a_{OH_i}^2}{\sum_{i=1}^n (\Sigma V_H)_i a_{OH_i}} \quad (8.38)$$

where a_{OH_i} is the first-order relative lateral deflection of storey i , and ΣV_H is the total storey shear, both due to the applied lateral loads. By assuming an average flexibility factor $\bar{\gamma}$ equal to 1.15 (Sect. 6.2.3), f_s will be less than 1.05 when $Q_s < 0.043$. This can be rounded off to 0.04. It has been tacitly assumed that the second-order sway deflections due to the gravity load moments and out-of-plumbs are negligible. In short, a shear-wall structure is considered braced when $Q_s < 0.04$.

For a structure with truss elements or inclined bracing elements, it is assumed (as discussed in Sect. 7.5) that the storey magnifier method can be applied. By defining the stability index Q_t for a storey with truss elements,

$$Q_t = \frac{(\Sigma N/L) a_{OH}}{\Sigma V_H} \quad (8.39)$$

and applying the assumptions similar to the above for shear-wall structure, f_s is less than 1.05 when $Q_t < 0.04$. In other words, a storey with truss elements is considered braced when $Q_t < 0.04$.

The stability index Q_t and the limit of 0.04 are recommended in the ACI Commentary (1977) but Q_t is also recommended for shear-wall structures. As shown from studies in Chapter 7, the parameter Q_t is not suitable for a shear-wall structure and the parameter Q_s given by Eq. 8.38 is preferred.

Unbraced frames

Literally, an unbraced frame must not include any bracing elements. Sometimes, it is, however, difficult to distinguish a shear wall from a column. Hence, a more specific definition of unbraced frames is suggested as follows: A storey, without any inclined bracing elements, is considered 'unbraced' if an inflection point occurs at the end or between the ends of every column in the storey when the structure is subjected to lateral loads only. Obviously, this is similar to the condition specified for the storey magnifier method (Sect. 8.5.2). It should be noted that this definition of unbraced frames does not guarantee consistently good results from the effective length approach, as demonstrated in Chapter 7. Nevertheless, this test indicates that if a storey is not 'unbraced', the effective length approach for sway frames will give very poor results.

9. SUMMARY

The primary objective of this investigation was to develop approximate methods for the second-order elastic analysis of multistorey frames. The basis of the study was an examination of geometric effects on the behavior of elastic multistorey frames subjected to gravity and lateral loads. Because a frame under gravity and lateral loads can be analyzed separately as a non-sway frame and a sway frame with the final force resultants obtained by superposition, this study was divided into three distinct parts: (a) non-sway frames, (b) sway frames and (c) combination of load effects from non-sway and sway frames.

The behavior of pin-ended columns and restrained non-sway columns was examined to show how the geometric non-linearity affects deformations, end-moments and maximum moments, and to analyze the factors concerned. The horizontal and vertical interaction of geometric effects in adjacent bays or storeys of non-sway multistorey frames were also discussed.

Approximate formulae for calculating the maximum moment in a pin-ended column were derived and the effective length design method was evaluated. In the effective length method a restrained non-sway column is replaced by a pin-ended column with its length equal to the effective length of the actual restrained column. This pin-ended column is subjected to the first-order end-moments of the actual

restrained column. Based on these two separate studies, the ACI design method for predicting the maximum moments in single restrained non-sway columns was examined. The assumptions required to extend the ACI method, originally developed for single columns, to non-sway multistorey frames and the problems involved in this method were also discussed. Finally, modifications to the present ACI design method for non-sway columns are suggested.

The geometric effects in a sway frame can be separated into two types: (a) the N-a ($P\Delta$) effects which cause an increase in the lateral deflection and overturning moment in a storey, and (b) the C and S effects which reduce the lateral stiffness of a storey and cause a redistribution of internal forces. A single-storey frame was used to illustrate these two types of effects. In particular the redistribution of internal forces due to the C and S effects was examined using a laterally deformed non-sway column. The vertical interaction between columns in successive storeys was also discussed.

Various approximate methods of second-order analysis for sway frames were derived and the assumptions in each of the methods were discussed. According to the assumptions involved, the accuracy of approximate methods was evaluated using single-storey frames, low-rise multistorey frames and high-rise multistorey frames. Based on these studies, certain calculation procedures are recommended and the conditions limiting the use of these procedures are stated.

A rational method for combining the non-sway and sway moments is proposed. This method is more accurate than the current design approaches. The proposed method entails no assumptions other than those required in the approximate methods for the second-order analysis of non-sway and sway frames. A practical method of including the effects of sway deflections due to gravity load moments and out-of-plumb construction in the approximate second-order analysis was derived. As a conclusion the recommended methods of approximate second-order elastic analysis of frames subjected to both gravity and lateral loads or gravity loads only are summarized in the form of step-by-step procedures, and the modifications to the present ACI Code (1977) procedure are suggested if it is decided that the current effective length approach for sway frames should be retained.

References

1. Aas-Jakobsen, K. (1973),
"Design of Slender Reinforced Concrete Frames",
Report No. 48 Institut Für Baustatik ETH Zurich,
November.
2. ACI Code (1977),
"Building Code Requirements for Reinforced Concrete
(ACI-318-77)", American Concrete Institute,
Detroit.
3. ACI Commentary (1977),
"Commentary on Building Code Requirements for
Reinforced Concrete (ACI-318-77)", American
Concrete Institute, Detroit.
4. Adams, P.F. (1972),
"Design of Steel Beam-Columns", Proceedings,
Canadian Structural Engineering Conference,
Montreal, Canada.
5. AISC Code (1978),
"Specifications for the Design, Fabrication and
Erection of Structural Steel for Buildings",
American Institute of Steel Construction, New York.
6. AISC Commentary (1978),
"Commentary on the Specifications for the Design,
Fabrication and Erection of Structural Steel for
Buildings", American Institute of Steel
Construction, New York.
7. Austin, W.J. (1961),
"Strength and Design of Metal Beam-Columns",
Proceedings, ASCE, Vol. 87, ST4, April, p. 1.
8. Baker, J.F., Horne, M.R. and Heyman, J. (1956),
"The Steel Skeleton", Vol. II, University Press,
Cambridge.
9. Beaulieu, D. and Adams, P.F. (1977),
"The Destabilizing Forces Caused by Gravity Loads
Acting on Initially Out-of-Plumb Members in
Structures", Structural Engineering Report No. 59,
Department of Civil Engineering, University of
Alberta, Edmonton, Canada.
10. Bijlaard, P.P., Fisher, G.P. and Winter, G. (1953),
"Strength of Columns Elastically Restrained and
Eccentrically Loaded", Proceedings, ASCE, Separate
No. 292, October.

11. Bleich, F. (1952),
"Buckling Strength of Metal Structures", McGraw-Hill, New York.
12. BS 449,
"The Use of Structural Steel in Buildings", British Standard.
13. Chen, W.-F. and Atsuta, T. (1976),
"Theory of Beam-Columns", Vol. 1, McGraw-Hill, New York.
14. CP 110 (1972),
"The Structural Use of Concrete", British Standards Institution, London.
15. Cranston, W.B. (1972),
"Analysis and Design of Reinforced Concrete Columns", Research Report No. 20, Cement and Concrete Association.
16. CSA (1974),
"Steel Structures for Buildings - Limit States Design", CSA Standard S16.1-1974, Canadian Standards Association, Ottawa.
17. ECCS Manual (1976),
"Stability of Steel Structures", Introductory Report of the Second International Colloquium on Stability, European Convention for Construction Steel Work.
18. EL-Zanaty, M.H. and Murray, D.W. (1980),
"Finite Element Programs for Frame Analysis", Structural Engineering Report No. 84, Department of Civil Engineering, University of Alberta, Edmonton, Canada.
19. Fey, T. (1966),
"Approximate Second-Order Analysis of Reinforced Concrete Frames", (In German), Bauingenieur, Berlin, Germany, June.
20. Ford, J.S., Chang, D.C. and Breen, J.E. (1981),
"Design Indications from Tests of Unbraced Multipanel Concrete Frames", Concrete International - Design and Construction, Vol. 3, No. 3, March, p. 37.
21. Furlong, R.W. (1979),
"Rational Analysis of Stability of Reinforced Concrete Frames", Proceedings of Symposium on Non-linear Design of Concrete Structures, University of Waterloo, Waterloo, Canada.

22. Galambos, T.V. (1968),
"Structural Members and Frames", Prentice-Hall, New York.
23. Goldberg, J.E. (1973),
"Approximate Methods for Stability and Frequency Analysis of Tall Buildings", Proceedings, Conferencia Regional Sobre Edificios de Altura, Madrid, Spain, September, p. 123.
24. Gouwens, A.J. (1976),
"Discussion of 'Column Design by the P-Delta Method', Wood, B.R. et al.", Proceedings, ASCE, Vol. 102, ST10, October, p. 2099.
25. Hage, S.E. (1974),
"The Second-Order Analysis of Reinforced Concrete Frames", M.Sc. Thesis, Department of Civil Engineering, University of Alberta, Edmonton, Canada.
26. Hellesland, J. (1976),
"Approximate Second-Order Analysis of Unbraced Frames", Internal Report, Dr. Ing. Aas-Jakobsen, A/S, Oslo, Norway.
27. Hellesland, J. and MacGregor, J.G. (1982),
"Mechanics and Design of Columns in Sway Frames", Proceedings, ASCE (In Press).
28. Horne, M.R. (1956),
"The Stanchion Problems in Frame Structures Designed According to Ultimate Carrying Capacity", Proceedings, ICE (London), Vol. 5, Part 3, p. 105.
29. Horne, M.R. (1962),
"The Effect of Finite Deformations in the Elastic Stability of Plane Frames", Proceedings, Royal Society of London, Series A, Vol. 266, p. 47.
30. Horne, M.R. and Merchant, W. (1965),
"The Stability of Frames", Pergamon Press, London, England.
31. Iffland, J.S.B. (1972),
"Design for Stability in High-Rise Buildings", Proceedings, International Conference on Planning and Design of Tall Buildings, Vol. II, Lehigh University, Bethlehem, Pennsylvania, p. 445.
32. Johnston, B.G., Ed. (1976),
"Guide to Stability Design Criteria for Metal Structures", Structural Stability Research Council, Third Edition, John Wiley & Sons, New York.

33. Ketter, R.L. (1961),
"Further Studies of the Strength of Beam-Columns",
Proceedings, ASCE, ST6, August, p. 135.
34. Kordina, K. (1972),
"Discussion No. 3 - Cracking and Crack Control",
Proceedings, International Conference on Planning
and Design of Tall Buildings, Vol. III, Lehigh
University, Bethlehem, Pennsylvania, p. 721.
35. Lee, A.Y.-W. (1949),
"A Study on Column Analysis", Ph.D. Dissertation,
Cornell University, New York.
36. LeMessurier, W.J. (1977),
"A Practical Method of Second-Order Analysis, Part
2 - Rigid Frames", AISC Engineering Journal, Vol.
14, No. 2, Second Quarter, p. 49.
37. Lu, L.-W. (1961),
"Stability of Frames Under Primary Bending
Moments", Proceedings, ASCE, S3, June, p. 35.
38. MacGregor, J.G. (1972),
"Discussion No. 5 - Flexural Stiffness",
Proceedings, International Conference on Planning
and Design of Tall Buildings, Vol. III, Lehigh
University, Bethlehem, Pa., 1972, p. 724.
39. MacGregor, J.G. (1979),
"Out-of-Plumb Columns in Concrete Structures",
Concrete International - Design and Construction,
Vol. 1, No. 6, June, p. 26.
40. MacGregor, J.G. and Barter, S.L. (1966),
"Long Eccentrically Loaded Concrete Columns Bent in
Double Curvature", Symposium on Reinforced Concrete
Columns, Publication SP-13, American Concrete
Institute, Detroit, p. 139.
41. MacGregor, J.G., Breen, J.E. and Pfrang, E.O. (1970),
"Design of Slender Concrete Columns", ACI Journal,
Vol. 67, No. 1, January, p. 6.
42. MacGregor, J.G. and Hage, S.E. (1977),
"Stability Analysis and Design of Concrete Frames",
Proceedings, ASCE, Vol. 103, ST10, October, p.
1953.
43. MacGregor, J.G., Oelhafen, U.H. and Hage, S.E. (1975),
"A Re-examination of the EI Value for Slender
Columns", Reinforced Concrete Columns, Publication
SP-50, American Concrete Institute, Detroit, p. 1.

44. Martin, I. and Olivieri, E. (1966),
"Tests of Slender Reinforced Concrete Columns Bent in Double Curvature", Symposium on Reinforced Concrete Columns, Publication SP-13, American Concrete Institute, Detroit, p. 121.
45. Massonnet, C.E. (1959),
"Stability Considerations in the Design of Steel Columns", Proceedings, ASCE, Vol. 85, ST7, September, p. 75.
46. Massonnet, C.E. (1978),
"European Approaches to the P- Δ Method of Design", Proceedings, ASCE, ST1, Technical Notes, January, p. 193.
47. Masur, E.F., Chang, I.C. and Donnel, L.H. (1961),
"Stability of Frames in the Presence of Primary Bending Moments", Proceedings, ASCE, EM4, August, p. 19.
48. McGuire, W. (1968),
"Steel Structures", Prentice-Hall, New Jersey.
49. Nixon, D., Beaulieu, D. and Adams, P.F. (1975),
"Simplified Second-Order Frame Analysis", Canadian Journal of Civil Engineering, Vol. 2, No. 4, December, p. 602.
50. Parme, A.L. (1966),
"Capacity of Restrained Eccentrically Loaded Long Columns", Symposium on Reinforced Concrete Columns, Publication SP-13, American Concrete Institute, Detroit, p. 355.
51. Perez-V., F.J. (1977),
"Stability Problems of Tall Buildings", Proceedings of Annual Conference on Reinforced Concrete Design, Institute of Cement Producers of Columbia, Bogota.
52. Roberts, E.H. and Yam, L.C.P. (1981),
"Column Design in the U.K.: Steel Columns, Reinforced Concrete Columns, Composite Steel-Concrete Columns", ACI 1981 Fall Convention.
53. Rosenblueth, E. (1965),
"Slenderness Effects in Buildings", Proceedings, ASCE, Vol. 91, ST1, February, p. 229.
54. Rubin, H. (1973),
"The Q- Δ Procedure for Simplified Computation of Sway Frames According to the Second-Order Plastic Design Theory", (In German) Der Gauingenieur, Vol.

- 48, p. 275.
55. Salvadori, M.G. (1956),
"Lateral Buckling of Eccentrically Loaded I-Columns", Transactions, ASCE, Vol. 121, p. 1163.
 56. Springfield, J. and Adams, P.F. (1972),
"Aspects of Column Design in Tall Steel Buildings", Proceedings, ASCE, Vol. 98, ST5, May, p. 1069.
 57. Stevens, L.K. (1967),
"Elastic Stability of Practical Multistorey Frames", Proceedings, ICE (London), Vol. 36, p. 99.
 58. Timoshenko, S.P. and Gere, J.M. (1961),
"Theory of Elastic Stability", McGraw-Hill, New York.
 59. Wang, C.-K. and Salmon, C.G. (1973),
"Reinforced Concrete Design", Intext Educational Publishers, New York.
 60. Winter, G. (1954),
"Compression Members in Trusses and Frames", The Philosophy of Column Design, Proc. of the Fourth Tech. Session, Column Research Council.
 61. Wood, R.H. (1953),
"A Derivation of Maximum Stanchion Moments in Multistorey Frames by Means of Nomograms", The Structural Engineer, Vol. 31, No. 11, p. 316.
 62. Wood, R.H. (1958),
"The Stability of Tall Buildings", Proceedings, ICE (London), Vol. 11, p. 69.
 63. Wood, R.H. (1974),
"Effective Length of Columns in Multistorey Buildings", The Structural Engineer, Vol. 52, No. 7, July, No. 8, August, No. 9, September, p. 235, 295, 341.
 64. Wood, R.H. and Shaw, M.R. (1979),
"Developments in the Variable-Stiffness Approach to Reinforced Concrete Column Design", Magazine of Concrete Research, Vol. 31, No. 108, September, p. 127.
 65. Wood, B.R. (1978a),
"The Design of Tall Steel Building Frames for Stability", Ph.D. Dissertation, Department of Civil Engineering, University of Alberta, Edmonton, Canada.

66. Wood, B.R., Beaulieu, D. and Adams, P.F. (1976a),
"Column Design by P-Delta Method", Proceedings,
ASCE, Vol. 102, ST2, February, p. 411.
67. Wood, B.R., Beaulieu, D. and Adams, P.F. (1976a),
"Further Aspects of Design by P-Delta Method",
Proceedings, ASCE, Vol. 102, ST3, March, p. 487.

APPENDIX A

DERIVATION OF AN ELEMENT STIFFNESS MATRIX

Let u and v be the displacements parallel and perpendicular to an element, respectively. The virtual work equation for the element shown at the top of Fig. 2.5 can be written as:

$$\int_L (EAu'\delta u' + EIV''\delta v'')dx - \int_L Nv'\delta v'dx - \langle Q \rangle \{\delta q\} = 0 \quad (A.1)$$

Note that the second term in the above equation accounts for the effect of geometry on the external work done by the axial force N .

The displacements u and v may be approximated in terms of the nodal displacements $\langle q \rangle$ as

$$u = \langle \bar{\phi} \rangle \langle q_1, q_4 \rangle^T \quad (A.2)$$

and

$$v = \langle \phi \rangle \langle q_2, q_3, q_5, q_6 \rangle^T \quad (A.3)$$

Standard linear shape functions are used for $\langle \bar{\phi} \rangle$ and cubic shape functions for $\langle \phi \rangle$. The shape functions are expressed in terms of the non-dimensional coordinate ξ which is defined as $\xi = 2 \frac{x}{L} - 1$. The shape functions are:

$$\langle \bar{\phi} \rangle = \langle -\frac{1}{2} (\xi-1), \frac{1}{2} (\xi+1) \rangle \quad (\text{A.4})$$

and

$$\begin{aligned} \langle \phi \rangle = \langle & \frac{1}{4} (\xi+2)(\xi-1)^2, \frac{L}{8} (\xi+1)(\xi-1)^2, \\ & \frac{1}{4} (2-\xi)(\xi+1)^2, \frac{L}{8} (\xi-1)(\xi+1)^2 \rangle \quad (\text{A.5}) \end{aligned}$$

By differentiating the above shape functions, the derivatives of Eqs. A.2 and A.3 are obtained, before they are substituted into the virtual work equation (Eq. A.1). After carrying out the integration and cancelling (δq) , Eq. A.1 can be written as

$$[K] \{q\} = \{Q\}$$

where the element stiffness matrix $[K]$ is given in Fig. 2.6. The geometric stiffness matrix $[K_g]$ results from the second term in Eq. A.1.

APPENDIX B

DERIVATION OF EQUATION 2.11 IN SECTION 2.5

The following derivation is drawn heavily from the work of Horne (1962). Let u and v be the displacements parallel and perpendicular to any member respectively, and subscript 0 denotes a corresponding first-order quantity. The displacements can be expressed in terms of the critical modes \bar{u}_i, \bar{v}_i corresponding to the modified state of loading shown in Fig. 2.8(b):

$$u_0 = \sum_{i=1}^{\infty} C_{0i} \bar{u}_i \quad (B.1)$$

$$v_0 = \sum_{i=1}^{\infty} C_{0i} \bar{v}_i \quad (B.2)$$

$$u = \sum_{i=1}^{\infty} C_i \bar{u}_i \quad (B.3)$$

$$v = \sum_{i=1}^{\infty} C_i \bar{v}_i \quad (B.4)$$

where C_{0i} and C_i are magnitudes of the critical modes. The orthogonal relations of the critical modes developed by Horne (1962) are stated as follows: For $i \neq j$,

$$\sum_m \int_L \bar{u}_i' \bar{u}_j' dx = 0 \quad (B.5)$$

$$\sum_m \int_L EI \bar{u}_i'' \bar{u}_j'' dx = 0 \quad (B.6)$$

and similarly for \bar{v} . The symbol Σ denotes summation for all members, and L is the length of any member.

(a) Buckling of the frame shown in Fig. 2.8(b)

The strain energy U_b during buckling in the i^{th} mode is equal to:

$$U_b = \Sigma_m \frac{1}{2} \int_L EI (\bar{v}_i'')^2 dx \quad (\text{B.7})$$

The work W_b done by the axial loads during buckling is given by:

$$W_b = \Sigma_m \frac{1}{2} \int_L \lambda_{ci} N (\bar{v}_i')^2 dx \quad (\text{B.8})$$

By putting $U_b = W_b$,

$$\int_L N (\bar{v}_i')^2 dx = \frac{f_i}{\lambda_{ci}} \quad (\text{B.9})$$

where

$$f_i = \int_L EI (\bar{v}_i'')^2 dx \quad (\text{B.10})$$

(b) Work done by the first-order load effects

Let any external load P (Fig. 2.8(a)) be divided into components S parallel and T perpendicular to the member. Where a load is applied at a joint, it may be considered as applied to the end of a particular member at that joint.

The strain energy U_0 produced by first-order load effects is equal to:

$$U_0 = \sum_m \frac{1}{2} \int_L EI (v_0'')^2 dx \quad (B.11)$$

and the work W_0 done by the external loads is:

$$W_0 = \sum_l S_l (u_0)_l + \sum_l T_l (v_0)_l \quad (B.12)$$

where \sum_l denotes summation for all loading points. The total potential energy Π_0 is given by:

$$\Pi_0 = U_0 - W_0 \quad (B.13)$$

Equation B.2 is substituted into Eq. B.11, and the orthogonal relation B.6 is needed to simplify the equation. Then Eqs. B.1 and B.2 are substituted into Eq. B.12, and finally Eqs. B.11 and B.12 into Eq. B.13. According to the principle of minimum potential energy,

$$\frac{\delta \Pi_0}{\delta C_{0i}} = 0 \quad (B.14)$$

Eq. B.15 results:

$$\sum_l S_l (\bar{u}_i)_l + \sum_l T_l (\bar{v}_i)_l = \sum_m C_{0i} f_i \quad (B.15)$$

where f_i is given by Eq. B.10, and subscript i denotes the

i^{th} critical mode.

(c) Work done by the total load effects

Similarly to Part (b),

$$U = \sum_m \frac{1}{2} \int_L EI (v'')^2 dx \quad (\text{B.16})$$

$$W = \sum_l S_l (u)_l + \sum_l T_l (v)_l + \sum_m \frac{1}{2} \int_L N (v')^2 dx \quad (\text{B.17})$$

The effect of geometry (flexural shortening) on the work done by the axial force N introduces the last term in Eq. B.17.

$$\Pi = U - W \quad (\text{B.18})$$

$$\frac{\delta \Pi}{\delta C_i} = 0 \quad (\text{B.19})$$

By substituting the related equations into the above formulae and applying both orthogonal relations B.5 and B.6, the following equation is obtained:

$$\sum_m C_i f_i - \left[\sum_l S_l (\bar{u}_i)_l + \sum_l T_l (\bar{v}_i)_l \right] - \sum_m C_i \int_L N (\bar{v}_i')^2 dx = 0 \quad (\text{B.20})$$

By substituting Eqs. B.9 and B.15 into Eq. B.20 and rearranging the terms, the final result is derived, i.e.,

$$C_i = \frac{C_{0i}}{1 - \frac{I}{\lambda C_i}} \quad (\text{B.21})$$

VITA

NAME: Lai, Shu-Ming Albert

PLACE OF BIRTH: Hong Kong

DATE OF BIRTH: August 7, 1956

EDUCATION:

1963-69, Tsung Tsin School, Hong Kong

1969-74, St. Francis Xavier's College, Hong Kong

1975, Alberta College, Edmonton, Canada

1975-79, University of Alberta, Edmonton, Canada
B.Sc. with Distinction - Civil Engineering

1979-81, University of Alberta, Edmonton, Canada
M.Sc. - Civil Engineering
Thesis - "Monte Carlo Study of Pattern Loadings on
Continuous Beams and Slabs"

1981-82, University of Alberta, Edmonton, Canada
Ph.D. - Civil Engineering

AWARDS:

Underwood McLelland & Associates Ltd. Scholarship
University of Alberta, 1978

Teaching Assistantship
University of Alberta, 1979-82

NSERC Research Assistantship
University of Alberta, 1981-82